

**GUT MICROBIAL METABOLOME:
REGULATION OF HOST METABOLISM
BY SCFAs**

Thesis submitted by

MOHD BADRIN HANIZAM BIN ABDUL RAHIM

For the degree of Doctor in Philosophy (PhD) of Imperial College London and
the Diploma of Imperial College London (DIC).

Primary supervisor: Dr Marc E Dumas

Secondary supervisor: Professor Nigel J Gooderham

Computational and System Biology

Department of Surgery and Cancer

Faculty of Medicine

2016

ABSTRACT

There is increasing evidence demonstrating a determinant role of gut microbiota in host health, and one underlying mechanism is *via* gut-microbial metabolites-host interaction in modulating host's cellular functions. SCFAs, main fermentation products of dietary fibres by gut microbiota in GI tract, are considered to be generally beneficial to the host. It has been shown that SCFAs act as substrates for energy metabolism, receptor agonists, and as histone deacetylase (HDAC) inhibitors. However, there are still gaps in the knowledge of their biological effects. It has been hypothesised that SCFAs may act as substrate for energy metabolism as well as ligand for several GPCRs, thus play roles in many cellular functions. Combining ^1H nuclear magnetic resonance (NMR) spectroscopy with multivariate statistical analysis of the effect of SCFAs on the hepatic cancer metabolic network identified a metabolic signature associated dose- and time- related SCFA exposure. TCA cycle intermediate, α -keto- β -methylvalerate was strongly correlated with the treatment of SCFAs suggesting the preferential of the cells to SCFAs for energy production. This signature further confirms that SCFAs play direct role in host energy metabolism. Having implemented a harmonised pharmacological assessment of a comprehensive SCFA panel on FFAR2, FFAR3, and GPR109A, this study is the first to reveal that isobutyrate and isovalerate are novel partial agonists for GPR109A. Furthermore, niacin, a classical agonist for GPR109A also has been shown to activate FFAR2 and FFAR3 but with much lower affinity. In another study, the effect of SCFAs on 3T3-L1 adipogenesis and adipocytes lipolysis has been characterised. Dosing the 3T3-L1 cells with isobutyrate, valerate, and isovalerate significantly induce the adipogenesis of the cells. In contrast, other SCFAs have no effect of the 3T3-L1 cell differentiation. Subsequent study focused on the effect of SCFAs on basal adipocyte lipolysis. Mature adipocytes were treated with 100 μM of SCFAs for 3hr and glycerol release was measured. This study revealed the anti-lipolytic property of propionate, butyrate, and valerate by significantly inhibits lipolysis in mature 3T3-L1 adipocytes. Thus, the role of SCFAs in regulating adipocytes functions may be particular important and beneficial in regulating plasma lipid profile and possibly aspects of metabolic syndrome. Together, these data enhance our understanding on the role of SCFAs on important metabolic tissues, which are hepatocyte and adipocyte.

STATEMENT OF ORIGINALITY

I certify that this thesis, and the research to which it refers, are the product of my own work, conducted during my PhD years. Any ideas or quotations from the work of other people, published or otherwise, are fully acknowledged in accordance with the standard referencing practices of the discipline.

COPYRIGHT DECLARATION

“The copyright of this thesis rests with the author and is made available under a Creative Commons Attribution Non-Commercial No Derivatives licence. Researchers are free to copy, distribute, or transmit the thesis on the condition that they attribute it, that they do not use it for commercial purposes and that they do not alter, transform, or build upon it. For any reuse or redistribution, researchers must make clear to others the licence terms of this work”

To my beloved family ~

Mak, ayah, my amazing wife Liyana, my super cute son Ryan, my brother Aizat, and my sister Atikah ~ Thanks for your endless love, sacrifices, prayers, supports, and advices. Without these I would not be where I am today.

This thesis is proudly dedicated to you.

ACKNOWLEDGEMENTS

First and foremost, I would like to thank Dr. Marc E Dumas and Prof. Nigel J Gooderham for the incredible opportunity, help, guidance, and reassurance throughout the course of this PhD. A special thanks to Marc for the critical reading of this thesis and advice throughout writing it.

A special thanks to MARA, a Malaysian government agency for funding my PhD and giving me the opportunity to gain this valuable experience.

Thank you to the past and present members of CSM who contributed to the success of this PhD, and with whom I have had interesting conversations with, both work and non-work related. Special thanks to Dr. Julien Chilloux who taught me a lot of experimental techniques in the lab and gave me a valuable advices during my PhD. To all the previous and current lab members: Dr. Anthony Dona, Dr. Quan Gu, Dr. Rhiannon David, Dr. Claire Boulange, Dr. Ana Luisa Neves, Dr. Abdullah Alkandari, Magali Sarafian, Andrea Rodriguez Martinez, Michael Osborne, Dr. Saroor Patel, Durr Malik Shahwar, Mariana Flores Torres, Yang Tianlai, Oliver Graham, and Richmond Bergner a big thank you must be extended.

I would like to thank my family in Malaysia, especially my mom and dad, as well as my in-laws family for their unwavering support and their confidence in me. I am grateful for my other-half Liyana, for all the support she has given me through all these years and for always been beside me on this amazing journey. I can't thank you enough for all that you have done for me. Finally, to Ryan Haris, my precious little angel, thank you for making this journey more special.

TABLE OF CONTENTS

ABSTRACT	2
STATEMENT OF ORIGINALITY.....	3
COPYRIGHT DECLARATION	4
ACKNOWLEDGEMENTS.....	6
TABLE OF CONTENTS	7
TABLE OF FIGURES.....	13
LIST OF TABLES	16
ABBREVIATIONS	18
1. CHAPTER 1: INTRODUCTION	21
1.1 Obesity	21
1.1.1 Definition of obesity and metabolic syndrome.	22
1.1.2 Aetiology of obesity and metabolic syndrome	22
1.1.3 Adipocytes dysfunction and obesity.	24
1.1.4 Free FAs and insulin resistance.	25
1.2 Obesity and energy homeostasis.....	26
1.2.1 Amino acid metabolism.....	29
1.3 Host-gut microbiota interactions.	31
1.3.1 Gut microbial ecology.	32
1.3.2 Roles of the gut microbiota in host physiology and health.	33
1.4 Production of SCFAs from fermentable substrates.....	35
1.4.1 Acetate	38
1.4.2 Propionate.....	39
1.4.3 Butyrate.....	40
1.4.4 Other fermentation products.....	41
1.5 Transport of SCFAs.....	42
1.6 SCFAs are G-protein coupled receptor (GPCR) agonists.	43
1.6.1 FFAR2.....	43
1.6.2 FFAR3.....	46

1.6.3 GPR109A.....	47
1.7 SCFAs in human health and disease	50
1.8 Overview of metabonomics	52
1.8.1 Analytical strategies in metabonomics	53
1.9 Hypothesis and aims.....	54
2. CHAPTER 2: GENERAL METHODOLOGY.....	55
2.1 Analytical strategy	55
2.2 Nuclear Magnetic Resonance (NMR) Spectroscopy.....	56
2.2.1 Principles of NMR spectroscopy	56
2.3 Statistical analysis.....	61
2.3.1 Unsupervised method: Principal Component Analysis (PCA)	62
2.3.2 Supervised methods.....	64
2.4 Cell culture	68
2.4.1 HepG2 cell line	68
2.4.2 HepaRG™ cell line	68
2.4.3 3T3-L1 cell line.....	69
2.4.4 CHO-K1 cell line	69
2.4.5 Justification of the cell line used for chapter 3 and chapter 4.....	70
2.5 Biological assays	70
2.5.1 Cell viability	70
2.5.2 Lipid staining (Oil Red-O).....	72
2.5.3 Lipolysis assay.....	73
3. CHAPTER 3: METHODOLOGICAL OPTIMISATION OF NEGATIVE CONTROL GROUPS: THE EFFECT OF SODIUM CHLORIDE (NaCl) TREATMENT ON HEPG2 CELLS GROWTH AND METABOLISM.	74
3.1 INTRODUCTION.....	74
3.2 MATERIALS AND METHODS.....	75
3.2.1 Cell culture	75
3.2.2 Cell thawing and seeding	76
3.2.3 Cell maintenance and passaging.....	77

3.2.4	Cell count.....	77
3.2.5	Cell freezing.....	78
3.2.6	Cell proliferation assay- PrestoBlue®	78
3.2.7	pH optimisation of the culture media.....	79
3.2.8	Cell culture preparation for ¹ H NMR study.....	79
3.2.9	Sample preparation for ¹ H-NMR cell supernatant analysis.....	80
3.2.10	Metabolic profiling by ¹ H-NMR spectroscopy.....	80
3.2.11	Data processing and multivariate data analysis.....	81
3.2.12	Metabolite-Set Enrichment Analysis (MSEA).....	81
3.3	RESULTS	82
3.3.1	Complete growth media is able to maintain its pH after the addition of different types of sodium salts.....	82
3.3.2	The effect of different sodium chloride (NaCl) doses on the growth of HepG2 cells.....	83
3.3.3	¹ H NMR cell media supernatant metabolic profiling of sodium chloride (NaCl) treatment on HepG2 cells.	85
3.3.4	Metabolite-Set Enrichment Analysis of the list of significant metabolites revealed a significant enrichment in the BCAA degradation pathway. .	94
3.4	DISCUSSION	95
3.4.1	The addition of sodium salt did not alter the pH of the growth media.	95
3.4.2	Exposure to NaCl at different doses and time points did not affect HepG2 cell viability.....	96
3.4.3	NaCl does not possess significant effect on HepG2 cells metabolism at...	97
3.5	CONCLUSION	98
4. CHAPTER 4: THE EFFECT OF SHORT-CHAIN FATTY ACIDS; PROPIONATE AND BUTYRATE ON HEPG2 CELL METABOLISM.		99
4.1	INTRODUCTION.....	99
4.2	MATERIALS AND METHODS.....	101
4.2.1	Preliminary cell viability test (toxicity test).....	101

4.2.2	Detection of FFAR2 and FFAR3 expression in HepG2 cell line using Western blot analysis.	101
4.2.3	Cell culture preparation for ¹ H NMR analysis.	102
4.2.4	Sample preparation and ¹ H NMR spectroscopy.	103
4.2.5	¹ H NMR spectra pre-processing, ¹ H NMR data processing, and multivariate data analysis.	103
4.2.6	Pathways-specific analysis using univariate analysis.	103
4.3	RESULTS	104
4.3.1	Optimisation of the pharmacological concentrations of SCFA; propionate and butyrate on HepG2 cell viability.	104
4.3.2	Investigating the expression of free fatty acids receptor 2 (FFAR2) and free fatty acid receptor 3 (FFAR3) in HepG2 cells.	108
4.3.3	Characterisation of ¹ H NMR metabolic profiles of HepG2 cell media.	109
4.3.4	¹ H NMR cell media metabolic profiling of propionate-treated HepG2 cells identifies constant metabolic signature associated to isoleucine metabolism.	112
4.3.5	HepG2 cells treated with butyrate have an increase rate in nutrient consumption and nutrient uptake related to energy metabolism pathways.	122
4.5	DISCUSSION	133
4.5.1	SCFA: propionate and butyrate demonstrate growth inhibition in HepG2 cells at dose above 10 mM.	133
4.5.2	Accumulation of α -keto- β -methylvalerate associated to modulation of BCAA isoleucine metabolism in propionate-treated HepG2 cells.	134
4.5.3	Butyrate changes HepG2 cells energy metabolism by modulating BCAA metabolism.	136
4.6	CONCLUSION	139

5. CHAPTER 5: PHARMACOLOGICAL EFFECT OF SHORT-CHAIN FATTY ACIDS IN RECEPTOR ACTIVATION: GPR109A (HYDROXYCARBOXYLIC ACID RECEPTOR 2 OR HCAR2), FREE FATTY ACID RECEPTOR 2 (FFAR2/GPR43), AND FREE FATTY ACID RECEPTOR 3 (FFAR3/GPR41).....	140
5.1 INTRODUCTION.....	140
5.2 MATERIALS AND METHODS.....	143
5.2.1 GPR109A activation assay.....	143
5.2.2 Free fatty acid receptor 3 (FFAR3) activation assay.....	144
5.2.3 Free fatty acid receptor 2 (FFAR2) activation assay.....	144
5.3 RESULTS	145
5.3.1 SCFAs: C ₄ and C ₅ SCFAs as well as niacin, induced activation of GPR109A.	145
5.3.2 SCFAs and niacin –induced activation of FFAR3.	147
5.3.3 SCFAs and niacin –induced activation of FFAR2.	149
5.4 DISCUSSION	153
5.4.1 Butyrate and valerate are full agonists of G-protein coupled receptor 109A (GPR109A) whereas isobutyrate and isovalerate are partial agonists.....	153
5.4.2 SCFAs 3 to 5 carbons are stronger FFAR3 agonists.....	155
5.4.3 SCFAs with 2 to 4 carbons are stronger FFAR2 agonists.....	156
5.5 CONCLUSION	158
6. CHAPTER 6: EFFECTS OF SHORT-CHAIN FATTY ACIDS ON 3T3-L1 DIFFERENTIATION AND 3T3-L1 ADIPOCYTE LIPOLYSIS.....	159
6.1 INTRODUCTION.....	159
6.2 MATERIALS AND METHODS.....	161
6.2.1 Cell culture	161
6.2.2 Differentiation to adipocytes.....	161
6.2.3 Cell viability assay.....	162
6.2.4 Adipogenesis assay.....	162
6.2.5 Lipolysis assay.....	162
6.2.6 RNA extraction and quantification.....	163

6.2.7 Reverse transcription.....	163
6.2.8 Quantitative polymerase chain reaction (q-PCR).....	165
6.2.9 Statistical analysis.....	165
6.3 RESULTS	166
6.3.1 Validation of GPR41/ <i>Ffar3</i> , GPR43/ <i>Ffar2</i> , and GPR109A/ <i>Hcar2</i> expression in 3T3-L1.....	166
6.3.2 The effect of SCFA on 3T3-L1 differentiation and functions.....	168
6.4 DISCUSSION	176
6.4.1 Valerate, isobutyrate, and isovalerate (100 μ M) stimulate 3T3-L1 differentiation.	177
6.4.2 Adipogenic genes expression was not affected by the treatment of SCFAs on 3T3-L1 cells.....	178
6.4.3 Single dose (100 μ M) of propionate, butyrate, and valerate decrease basal level of lipolysis in 3T3-L1 adipocytes.....	181
6.5 CONCLUSION	182
7. CHAPTER 7: GENERAL DISCUSSION AND CONCLUSION	184
7.1 Key findings	184
Future research.....	191
Conclusion.....	192
REFERENCES	193
APPENDIX:	217

TABLE OF FIGURES

Figure 1.1: Amino acid catabolism showing the fate of carbon skeletons and how they enter the TCA cycle..	28
Figure 1.2: Microbial numbers and composition in the gastrointestinal tract.	33
Figure 1.3: Gut microbiota and host symbiosis.	35
Figure 1.4: Functional/phylogenetic groups involved with the formation and conversion of SCFA in the human large intestine.	37
Figure 1.5: Acrylate pathway of propionate formation from lactate..	39
Figure 1.6: Role of butyrate in colonocytes metabolism and schematic overview of receptors activation by short-chain fatty acids (SCFA)..	45
Figure 1.7: Roles of gut microbial metabolites (SCFAs) in human.	52
Figure 2.1: Theory of NMR spectroscopy.	58
Figure 2.2: Standard one pulse sequence	60
Figure 2.3: General scheme for 2D NMR spectroscopy.	61
Figure 2.4: Diagrammatic representation of PCA.	63
Figure 2.5: PLS schematic.	65
Figure 2.6: Comparison between PCA, PLS-DA, and O-PLS-DA.	66
Figure 2.7: A 7-fold cross validation.	67
Figure 2.8: Reduction of resazurin to resorufin in living cells.	71
Figure 2.9: Chemical structure of crystal violet.	71
Figure 2.10: Chemical structure of Oil Red-O	72
Figure 3.1: Experimental design for the exposure of HepG2 cell to the NaCl treatment...	80
Figure 3.2: pH of growth media. NaCl, NaOH, and NaHCO ₃ were individually added to the complete growth media at different final doses and the pH of the media was read using bench top pH reader to see any change in the pH.	83
Figure 3.3: Proliferation of HepG2 cells in growth media containing various doses of NaCl.	84

Figure 3.4: OPLS-DA score and validation plots separating the control group and the treatment groups (NaCl) as well as separating between the treatments groups themselves..	87
Figure 3.5: OPLS- regression models predicting the dose-related response of NaCl treatment on HepG2 cells..	90
Figure 3.6: Loadings plots of OPLS-regression models showing the quantitative dose-response of NaCl on HepG2 cells culture media samples at (A) 24-hr, (B) 48-hr, and (C) 72-hr exposure.....	91
Figure 4.1: Experimental design for the exposure of HepG2 cells to the SCFAs treatment.	103
Figure 4.2: The effect of propionate on HepG2 cell viability.	106
Figure 4.3: The effect of butyrate on HepG2 cell viability.	107
Figure 4.4: Examining the expression of free fatty acid receptor (FFAR2 and FFAR3) in HepG2 cell.....	108
Figure 4.5: Mean of ¹ H NMR spectra of cell media from SCFA-treated HepG2 cells at 24 hours exposure measured by 600-MHz ¹ H NMR spectroscopy.	110
Figure 4.6: OPLS-DA score and validation plots separating the control group and the treatment groups (propionate) as well as separating between the treatment groups themselves.....	113
Figure 4.7: OPLS- regression models predicting the dose-related response of propionate treatment on HepG2 cells.	115
Figure 4.8: Loadings plots of OPLS-regression models showing the quantitative dose-response of propionate on HepG2 cells culture media samples at (A) 24, (B) 48, and (C) 72 hours of exposure.....	116
Figure 4.9: Mapping of HepG2 cells medium metabolites accumulation and consumption pattern involved in BCAAs metabolism, amino acids metabolism, TCA cycle, and gluconeogenesis for propionate experiment..	120
Figure 4.10: OPLS-DA score and validation plots separating the control group and the treatment groups (butyrate) as well as separating between the treatments groups themselves.....	123
Figure 4.11: OPLS regression models predicting the dose-related response of butyrate treatment on HepG2 cells.	125
Figure 4.12: Loadings plots of OPLS-regression models showing the quantitative dose-response of butyrate on HepG2 cells culture media samples at (A) 24, (B) 48, and (C) 72 hours exposure.	128

Figure 4.13: Mapping of HepG2 cells medium metabolites accumulation and consumption pattern involved in BCAAs metabolism, amino acids metabolism, TCA cycle, and gluconeogenesis for propionate experiment.	131
Figure 5.1: Biosynthesis of niacin from essential amino acid tryptophan.....	142
Figure 5.2: Pharmacology of GPR109A in a cAMP accumulation assay.....	146
Figure 5.3: Pharmacology of FFAR3 in a cAMP accumulation assay.....	148
Figure 5.4: Short-chain fatty acids (SCFA) activate FFAR2. SCFA, from 1 to 5 carbons, and niacin were screened on FFAR2 activation using cAMP accumulation assay.	150
Figure 6.1: The levels of <i>Hcar2</i> , <i>Ffar2</i> , and <i>Pparg</i> mRNA during differentiation of 3T3-L1 adipocytes.....	167
Figure 6.2: Isobutyrate, but not other tested SCFAs, increases 3T3-L1 adipocytes cell viability at 100 μ M dose.	169
Figure 6.3: Functional role of selected compounds on differentiation of 3T3-L1 cells....	171
Figure 6.4: Isobutyrate, valerate, and isovalerate stimulate <i>de novo</i> lipogenesis in 3T3-L1 adipocytes.....	172
Figure 6.5: RT-qPCR analysis of the gene expression during 3T3-L1 cell differentiation.	174
Figure 6.6: Propionate, butyrate, and valerate inhibit lipolysis in 3T3-L1 adipocytes.	176
Figure S.1: Valerate, isobutyrate, and isovalerate at 100 μ M dose increase lipogenesis in 3T3-L1 cells.	219
Figure S.2: RT-qPCR analysis of the gene expression during 3T3-L1 cell differentiation..	220

LIST OF TABLES

Table 1.1: Amino acids in human	30
Table 1.2: The chemical formula for the main SCFAs produced from the fermentation of dietary fibres by gut microbiota.	41
Table 1.3: Summary of the GPCRs activation, including its ligands, expression, and functions	49
Table 3.1: Value of Q^2Y , R^2Y , and validation of OPLS-DA models.	86
Table 3.2: Goodness of fit (R^2Y), prediction (Q^2Y) and validation values for OPLS regression models of NaCl-treated vs control.	89
Table 3.3: List of metabolites assigned in the loadings plots of OPLS-regression models shown in	92
Table 3.4: Result from Over Representation Analysis (ORA) of MSEA based on the set of significant metabolites.	94
Table 4.1: 1H NMR chemical shifts from metabolites assigned of cell media obtained from SCFA-treated HepG2 cells measured by 600-MHz 1H NMR spectroscopy.....	111
Table 4.2: Value of Q^2Y , R^2Y , and validation of OPLS-DA models for propionate experiment.	112
Table 4.3: Goodness of fit (R^2Y), prediction (Q^2Y) and validation values for OPLS regression models of propionate -treated vs control.	114
Table 4.4: List of metabolites assigned in the loadings plots of OPLS-regression models for propionate experiment (shown in Figure 4.8).	117
Table 4.5: Result from Over Representation Analysis (ORA) of MSEA based on the set of significant metabolites.	121
Table 4.6 : Value of Q^2Y , R^2Y , and validation of OPLS-DA models for butyrate experiment.	122
Table 4.7: Goodness of fit (R^2Y), prediction (Q^2Y) and validation values for OPLS regression models of butyrate -treated vs control.	124

Table 4.8: List of metabolites assigned in the loadings plots of OPLS-regression models for butyrate experiment (shown in Figure 4.11).	129
Table 4.9: Metabolic pathway enrichment analysis of the set of metabolites that positively correlate with the treatment of butyrate in HepG2 cells.	132
Table 5.1: EC ₅₀ values of SCFAs and related molecule for GPR109A.	151
Table 5.2: EC ₅₀ values of SCFAs and related molecule for FFAR3	151
Table 5.3: EC ₅₀ values of SCFAs and related molecule for FFAR2.	152
Table 6.1: Calculation of sample preparation for reverse transcription.	164
Table 6.2: Preparation of MasterMix.	164
Table S.1: List of <i>p value</i> obtained from pair-wise comparison between propionate-treated and control group at 24-, 48-, and 72-hr time points using non parametric Wilcoxon-Mann-Whitney test.	217
Table S.2: List of <i>p value</i> obtained from pair-wise comparison between butyrate-treated and control group at 24-, 48-, and 72-hr time points using non parametric Wilcoxon-Mann-Whitney test.	218
Table S.3: <i>p</i> -values for the slope coefficient comparison between SCFAs-treated and control groups on the gene expression analysis.	221
Table S.4: Minimum Essential Medium (MEM) formulation (ThermoFisher Scientific)...	222

ABBREVIATIONS

7TM	Seven transmembrane protein
AC	Adenylate cyclase
ADP	Adenosine diphosphate
ATP	Adenosine Tri-Phosphate
BCAA	Branched Chain Amino Acid
BCAT	Branched Chain Aminotransferase
BCKDH	Branched-Chain Keto Acid Dehydrogenase
BMI	Body Mass Index
BSA	Bovine serum albumin
BW	Body Weight
cAMP	Cyclic adenosine monophosphate
CNS	Central nervous system
CPMG	Carr-Purcell-Meilboom-Gill
CREB	cAMP response element binding protein
CT	Cycle threshold
CV	Cross Validation
CVD	Cardiovascular Disease
DAG	Diacylglycerol
DMEM	Dulbecco's Modified Eagle's Medium
DMSO	Dimethyl sulfoxide
DNA	Deoxy ribonucleic acid
DNAse	Deoxyribonuclease
DNTP	Deoxynucleotide Tri-Phosphate
DTT	Dithiothreitol
EC50	Effective concentration 50
EDTA	Ethylenediaminetetraacetic acid
ERK	Extracellular Signal Kinase
FA	Fatty Acid
FAD	Flavin adenine dinucleotide

FASN	Fatty Acid Synthase
FBS	Foetal bovine serum
FFA	Free fatty acid
FFAR	Free fatty acid receptor
FID	Free Induction Decay
FT	Fourier Transform
GC	Gas Chromatography
GDP	Guanidine diphosphate
GF	Germ Free
GLP-1	Glucagon like peptide-1
GLUT4	Glucose transporter 4
GPCR	G-Coupled Receptor
GSIS	Glucose-stimulated insulin secretion
GTP	Guanidine triphosphate
HCAR2	Hydroxycarboxylic Acid Receptor 2
HDAC	Histone Deacetylase
HDL	High Density Lipoprotein
HF	High Fat
IBMX	Isobutylmethylxanthine
IDL	Intermediate Density Lipoprotein
IL	Interleukin
IR	Insulin Resistance
IRS	Insulin Receptor Substrate
KEGG	Kyoto encyclopaedia of genes and genomes
KO	Knockout
Lp(a)	Lipoprotein-A
LPL	Lipoprotein Lipase
LPS	Lipopolysaccharide
MAG	Monoacylglycerol
MEM	Minimum Essential Media
mRNA	Messenger ribonucleic acid

MS	Mass Spectrometry
MSEA	Metabolite set enrichment analysis
NAD	Nicotinamide adenine nicotinamide
NAFLD	Non-alcoholic fatty acid liver disease
NEAA	Non-essential amino acids
NEFA	Non-esterified fatty acids
NMR	Nuclear Magnetic Resonance Spectroscopy
OD	Optical density
ORO	Oil Red-O
OSC	Orthogonal Signal Correlation
PBS	Phosphate buffer saline
PC	Principal Component
PCA	Principal Component Analysis
PCR	Polymerase Chain Reaction
PDK 1	Phosphoinositide-dependent Kinase 1
PI3-K	Phosphoinositol-3-OH-Kinase
PKA	Protein kinase A
PLS	Partial Least Squares
PPAR γ	Peroxisome Proliferator Activated Receptor Gamma
RNA	Ribonucleic acid
ROS	Reactive Oxygen Species
RT	Reverse Transcriptase
SEM	Standard error mean
SCFA	Short-Chain Fatty Acid
SR	Strong Responder
T2D	Type II Diabetes
TCA	Tricarboxylic
TG	Triglyceride
TNF- α	Tumor Necrosis Factor- α
VLDL	Very Low Density Lipoprotein
WHO	World Health Organisation

CHAPTER 1

1. INTRODUCTION

1.1 Obesity

Obesity is one of the most important health problems in the world right now. The worldwide prevalence of obesity has increased drastically since 1980, and according to the data from World Health Organisation (WHO) in 2014, there are more than 1.9 billion overweight adults with 600 million classified as clinically obese. Overall, approximately 13% of the adult population in the world were obese (11% of men and 15% of women). Children are not excluded from this problem with 42 million children under the age of 5 were obese or overweight in 2013 (WHO, 2015). The occurrence of obesity in developed countries to increase in part due to inactive lifestyle.

Obesity is the results of a long-term imbalance between energy intake and expenditure, which is regulated by a number of pathways involving metabolites and hormones (Greenwood *et al.*, 2011). In addition, its development also depends on genetic and environmental factors. Moreover, this epidemic also increases the chance of having other health problems including type 2 diabetes, hypertension, respiratory problems, cardiovascular diseases (CVDs), and cancer (van Greevenbroek *et al.*, 2013; Liu *et al.*, 2010; Wildman *et al.*, 2011). The healthcare cost for obesity costs the world economy around \$2 trillion in economic burden (Dobbs and Manyika, 2015). Therefore, reversing the obesity trend is crucial as it could greatly save world economy.

1.1.1 Definition of obesity and metabolic syndrome.

Obesity is a medical condition characterised by an accumulation of excess body fat to the magnitude that it may affect health. A person is considered obese when having body mass index (BMI) of 30 or more (<http://www.who.int/topics/obesity/en/>). However, BMI cannot be used as the only method to definitively diagnose obesity. A very muscular person for example, can have a high BMI without having an excess of body fat, and can easily be misclassified (Seidell and Flegal, 1997). Therefore, a waist circumference measurement is a better method to define obesity as it measures the proportion of abdominal fat.

Obesity is commonly associated with an array of additional chronic metabolic problems, including hyperglycaemia, hypertriglyceridemia, low high-density lipoprotein cholesterol (HDL), and high blood pressure (Alberti *et al.*, 2005). The epidemiological clustering of these conditions led to the introduction of the 'metabolic syndrome' concept, defined by the presence of three or more of these conditions (Alberti *et al.*, 2005). Metabolic syndrome is a strong predictor of the development and progression of CVDs, the leading cause of mortality and morbidity worldwide (Després and Lemieux, 2006; Kim and Reaven, 2004).

1.1.2 Aetiology of obesity and metabolic syndrome

Despite a growing knowledge on the signalling pathways involved in obesity and metabolic syndrome, their causes and regulatory checkpoints remain unclear. Most of the evidence suggests that the aetiology for obesity as well as metabolic syndrome is resulted from complex interaction between genetic and environmental factors (Bleich *et al.*, 2008).

Factors, such as eating habits, genetics, environment, metabolism, and lifestyle play an important role in the development of obesity. Obesity is a highly heritable trait. Studies focusing on the inheritance pattern rather than on the specific genes have demonstrated that child from obese parents has ~70% chances to get obese compared to the child of normal weight parents (Barsh *et al.*, 2000).

However, over 90% of obesity cases are still of uncertain origin and less than 10% are associated with genetic and hormonal causes (Xu and Xue, 2015). For instance, a study performed to characterise causative genes for obesity and metabolic syndrome has demonstrated that the obese (*ob*) gene in C57BL/6 mouse model and its product, leptin, regulate both food intake and energy expenditure (Zhang *et al.*, 1994). However, the frequency of this mutation on human obese gene is very rare, and the obesity pandemic in human is not primarily caused by dysregulation of leptin production (Pi-Sunyer *et al.*, 1999).

In the Western world, as well as in developing countries, sedentary lifestyles and high-carbohydrate and high-fat diets frequently lead to obesity as a consequences of the imbalance between energy intake and energy expenditure. Environmental stimuli, such as diet or stress, can trigger epigenetic mechanisms (e.g. histone acetylation, DNA methylation) that regulate the expression of several genes involved in cell differentiation and energy homeostasis (Musri and Párrizas, 2012; Pjetri *et al.*, 2012). An animal study showed that high fat diet (HF) causes DNA methylation of gene promoters in specific brain areas, thus decreasing gene expression in the reward-related brain regions (Pjetri *et al.*, 2012).

There is growing evidence that the gut microbiota can also play a role in systemic metabolism, making the host more prone or resistant to obesity and its related diseases. It has been shown that mammalian host-gut microbiota interaction plays an important role in the host's physiological processes such as in nutrients digestion and absorption, increase energy harvest, and can play a pivotal role in the development of metabolic diseases (Holmes *et al.*, 2011). Previously, a study has revealed that obesity is associated with changes in the composition of specific gut microbiota and their activity, which cause an increase in efficiency to extract energy from the diet (Turnbaugh *et al.*, 2006). These results highlight that the gut microbiota could play a significant factors in the development of obesity.

1.1.3 Adipocytes dysfunction and obesity.

Energy balance or homeostasis can be explained by the energy equation. Under normal conditions in which there is sufficient energy availability, the amount of energy intake is equal with energy expenditure. Thus, the amount of energy stored in the form of adipose tissues remains constant. The maintenance of energy balance requires complex communication between central nervous system (CNS) and other tissues. This takes place through a number of mechanisms, including hormonal control, neural, and nutritional signals. Obesity develops as a result of a long-term imbalance in these processes. It is characterised by an increase in the accumulation of triglyceride (TG) storage in adipose tissues and peripheral tissues. Adipogenesis is a tightly regulated process in which preadipocytes are differentiated into mature adipocytes and become highly specialised cells. Mature adipocytes are spherical cells with the majority cellular component being lipid droplet. Normal adipocytes are metabolically active and dynamic in response to different hormones (Kersten, 2001). Adipose tissue is a site where excess energy is stored in the form of TGs, and when needed somewhere else in the body, the TGs are then mobilised and then hydrolysed to generate fatty acids (FAs), which is subsequently transported into mitochondria to undergo β -oxidation (Duncan *et al.*, 2007a). During development of obesity, there is an accumulation of fat mass attributed to both adipocyte hypertrophy and hyperplasia, usually concomitant with increased angiogenesis and macrophage infiltration into adipose tissue as well as an altered secretory profile (Bourlier *et al.*, 2008).

As a physiological response to chronic nutrient surplus, hyperinsulinemia promotes enlargement of the adipocyte by increasing the expression of lipogenic enzymes while reducing lipolysis. As adipocytes are full with lipids, if there is an inadequate proliferation and differentiation of adipocyte to cope the energy excess, for example due to genetically defect in adipocyte differentiation, the upper limit of lipid storage will be reached. This results in an increase in the size of adipocyte, resulting in hypertrophic adipocytes (Jankovic *et al.*, 2015). Hypertrophic adipocytes are typically seen in obese individuals. These are characterised by having elevated circulating level of pro-inflammatory cytokines (e.g. IL-6 and TNF- α), an altered adipokine secretion profile, and increased lipolytic capacity (Hauner, 2005; Laurencikiene *et al.*, 2011; Skurk *et al.*, 2007). These types of adipocytes

have been suggested to decrease sensitivity to insulin and impair the insulin-mediated effect in adipose tissue, including its anti-lipolytic regulation (Jankovic *et al.*, 2015). Impairment of lipolysis regulation results in the increase of free fatty acids (FFAs) and glycerol release, which further cause an elevation level of plasma non-esterified fatty acids (NEFA). An increase in adipocyte lipolysis in hypertrophic adipocytes causes elevation in plasma FFAs, which promotes ectopic fat deposition in non-adipose tissues, including liver, pancreas, skeletal muscle, and heart (Snel *et al.*, 2012). Lipid accumulation in these tissues impairs insulin sensitivity and cell functions (Snel *et al.*, 2012).

1.1.4 Free FAs and insulin resistance.

The clinical definition of insulin resistance (IR) is “the inability of a known quantity of exogenous or endogenous insulin to increase glucose uptake and utilisation in an individual as much as it does in normal population” (Lebovitz, 2001). During fasting, lipids, stored in the form of TGs in adipocytes and hepatocytes are broken down and hydrolysed into glycerol and free FAs via a process called lipolysis. The resulting free FAs then enter blood circulation, bind with serum albumin and are then transported to peripheral tissues, such as muscle and kidney for energy production. Disruption of lipolysis causes excess of free FAs in circulation, the medical condition known as hyperlipidaemia. There is growing evidence demonstrating the deteriorated effects of excess free FAs on both insulin sensitivity and insulin secretion, which lead to the development of IR. In a study of non-obese, normal glucose-tolerant persons with genetic predispositions to type 2 diabetes (T2D), prolonged lipid infusion for more than 24 hours to a level that is similar to the plasma free FAs level in obese individuals, led to impaired glucose-stimulated insulin secretion (GSIS) by pancreatic β -cells, and caused hepatic insulin resistance (Kashyap *et al.*, 2003).

Skeletal muscle has been identified as an important endocrine organ that produces and releases cytokines, which are called “myokines” (Pedersen and Febbraio, 2008). A study conducted on lean and healthy individuals without history of T2D in family has demonstrated that a prolonged physiological increase in plasma free FAs to the same level as can be found in obese person impairs the insulin sensitivity (Kashyap *et al.*, 2004). In

different study, increase in plasma free FAs causes a dose-dependent inhibition of insulin-mediated glucose uptake by skeletal muscle and insulin signalling cascade (Belfort *et al.*, 2005). Moreover, lean glucose tolerant individuals showed a decrease in insulin sensitivity as well as impaired mitochondrial inner membrane potential after short-term increase in plasma free FAs levels (Chavez *et al.*, 2010).

The impairment of insulin action by hyperlipidaemia often associated with other disorders such as dyslipidaemia, hypertension, and fat accumulation in adipose tissues. This causes deterioration in insulin signalling thus promoting the development of insulin resistance (IR) (Delarue and Magnan, 2007; Saltiel and Kahn, 2001). The deterioration in insulin signalling has been shown to affect important cellular pathways that are crucial in maintaining energy homeostasis (Sharma *et al.*, 2008).

1.2 Obesity and energy homeostasis.

As mentioned previously, obesity is characterised by increased TG in adipose tissue and non-adipose tissues. This condition is a result of an imbalance between energy intake and energy expenditure. In order to carry out their functions, all cells require energy. Energy can be obtained from diets or in the event of low nutrient supply, it can be obtained from source stored within the cell (TGs). The main source of energy substrate for most organisms is glucose. It is the key energy source for human body. Besides glucose, our body also capable of utilising FAs, and amino acids for fuel as well as for carrying out many cellular processes. The right combination of these nutrients allows the body to function well and remain healthy. Metabolic pathway is a series of biochemical reactions in a cell that build or breakdown molecules for cellular processes. The energy pathways involving glucose, FAs, and amino acids are connected due to having many common intermediate metabolites which subsequently feed into tricarboxylic acid cycle (TCA cycle) to generate ATP (Ramsey Bronk, 1999).

Plasma glucose concentration is determined by the rate of glucose entering the circulation and the rate of glucose utilisation (Aronoff *et al.*, 2004). It requires a precise matching of these two processes in order to maintain the normal plasma glucose

concentration (Giugliano *et al.*, 2008). Circulating glucose is obtained from three sources; 1) intestinal absorption during the state of digestion of dietary carbohydrate; 2) glycogenolysis; 3) and via gluconeogenesis. There is a potential of brain damage due to low circulating blood glucose or severe hypoglycaemia, while chronically high glucose levels in the circulation (hyperglycaemia) is toxic and has been shown to cause organ damage (Adler, 2002). Following high carbohydrate diets, human body stores glucose in the liver and the skeletal muscle in the form of glycogen. When glucose is not being used for energy, it is converted into glycogen by the process called glycogenesis. Glycogen acts as the secondary energy storage, fat being the body's primary energy storage in adipose tissue. In addition, the catabolism of glucose produces acetyl-CoA, an intermediate metabolite. Acetyl-CoA is used for FA synthesis, the process known as lipogenesis. Lipogenesis includes both the synthesis of FA and TG synthesis, where the latter is produced by the esterification of glycerol and FAs (Kersten, 2001).

During starvation or low energy levels, human body undergoes glycogenolysis and lipolysis, breaking down glycogen and TGs to generate glucose and free FAs, respectively which supply energy for other tissues. The glucose produced in this manner is then metabolised to produce pyruvate via glycolysis, while the FAs undergo β -oxidation forming acetyl-CoA. Moreover, amino acids, produced from the catabolism of proteins also can generate intermediate metabolites for TCA cycle and generate energy for the cell. The human body can also undergo gluconeogenesis, a metabolic process that can generate glucose from non-carbohydrate carbon substrate such as pyruvate, glycerol, and glucogenic amino acids. In humans, only two organs have sufficient gluconeogenic enzymes activity and glucose-6-phosphatase (G6Pase) activity, which are the liver and the kidney. These two enzymes allow them to release glucose into the bloodstream as a result of gluconeogenesis (Gerich *et al.*, 2001).

Pyruvate, acetyl-CoA, and other intermediate metabolites produced in the manners explain above will then use to generate energy via incorporating in the TCA cycle. The series of reactions of the TCA cycle generate reduced coenzymes (3 NADH and 1 FADH₂), which will then use by the oxidative phosphorylation to form energy-rich adenosine triphosphate (ATP). Energy homeostasis is largely controlled by hormonal excretion. In human body, the glucoregulatory hormones are responsible in maintaining normal circulation of glucose. In

particular, insulin is the main glucoregulatory hormone (Giugliano *et al.*, 2008). Ingestion of carbohydrate causes a rise in insulin secretion and stimulates glucose uptake by the cell. It also increases glycogenesis and FAs synthesis activity, while at the same time inhibiting protein degradation. In the fasting state, insulin secretion is reduced and simultaneously increased the secretion of glucagon from α -cells of the islets of Langerhans of the pancreas. Glucagon increases circulating glucose by promoting glycogenolysis and gluconeogenesis. In this condition, lipolysis activity is also increased while decreasing the lipogenesis.

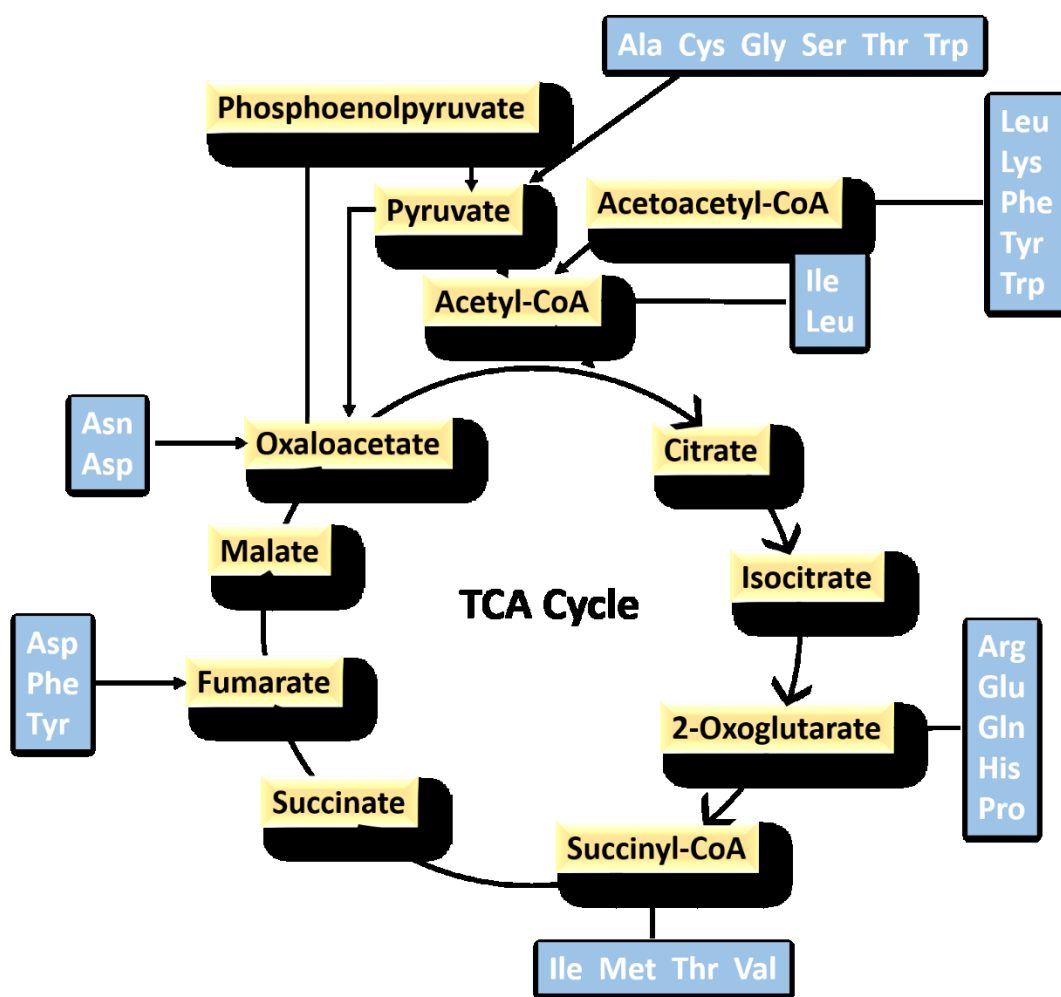


Figure 1.1: Amino acid catabolism showing the fate of carbon skeletons and how they enter the TCA cycle. Figure was adapted from Ramsey Bronk, (1999).

1.2.1 Amino acid metabolism.

Proteins are an integral part of the human body and are involved in many of the biosynthetic pathways. A number of evidences show that amino acids directly involve in cell-specific nutrient metabolism (Jobgen *et al.*, 2006), cell signalling (Marc Rhoads and Wu, 2009), oxidative defence (Wu *et al.*, 2004), as well as increase the efficiency of utilising dietary proteins (Wang *et al.*, 2008). Dietary proteins and amino acids are essential nutrients as they supply the nitrogen source for the synthesis of nitrogenous compounds (protein, amino acids, and nucleic acids) for cells. Due to the needs for nitrogen balance and cell growth, amino acids can be supplied from diet. They are classified in two main groups; 1) nutritionally essential, and 2) non-essential (Wu, 2009). Essential amino acids (EAAs) are amino acids that cannot be synthesised by body and must be supplied from the diet, while non-essential amino acids (NEAAs) can be synthesized *de novo* from a non-amino acid source of nitrogen (**Table 1.1**).

Protein and amino acid degradation can produce intermediate metabolites for energy production. The catabolism of amino acids provides up to 15% of the human body's energy requirement. Dietary protein digestion in the stomach occurs through the action of pepsins, and continues within the lumen of duodenum. There are two main pancreatic enzymes responsible in the digestion of protein in small intestine, which are trypsin and chymotrypsin (Rawlings and Barrett, 1994; Wilcox, 1970). Protein breakdown, or proteolysis, generates amino acids and peptides, which are then absorbed by enterocytes via peptide transporters (PepT1). Inside the enterocyte, the peptides are further hydrolysed into amino acids by the action of cytoplasmic peptidase. The resulting amino acids are then shuffled across intestinal mucosa by basolateral amino acids transporter and enter the blood circulation (Ramsey Bronk, 1999). Amino acids are distributed into other tissues where they can have a number of fates; 1) to synthesise new amino acids, 2) used for protein biosynthesis, or 3) degraded to provide nitrogen. In the organism, amino acids catabolism is strongly regulated in order to maintain the balance between nitrogen intake and nitrogen excretion levels. The balance between nitrogen intake and excretion is strictly controlled to keep a constant nitrogen level in the organism.

Table 1.1: Amino acids in human

Essential amino acids	Non-essential amino acids
Histidine*	Alanine
Isoleucine	Arginine*
Leucine	Aspartic acid
Lysine	Cysteine
Methionine	Glutamic acid
Phenylalanine	Glutamine
Threonine	Glycine
Tryptophan	Proline
Valine	Serine
	Tyrosine
	Asparagine

(*) Essential in certain cases. (Fürst and Stehle, 2004; Reeds, 2000; Wu, 2009).

The initial stage in the catabolism of many amino acids (phenylalanine, tyrosine, leucine, isoleucine, valine) is transamination. Transamination is a process in which α -keto acids are converted into 2-oxo acids by the action of aminotransferase enzymes (Ramsey Bronk, 1999). In this process, α -amino groups are transferred to either oxaloacetate or 2-oxoglutarate producing aspartate or glutamate, respectively. These two amino acids then participate in urea cycle. Glutamate needs to be deaminated by glutamate dehydrogenase

to provide ammonia, which is used to synthesize another urea cycle intermediate, citrulline. On the other hand, aspartate participates directly in urea synthesis (Ramsey Bronk, 1999). For other amino acids (such as arginine, lysine, proline, threonine, and tryptophan), there is no transamination reaction process for during their catabolism process. Instead, the major pathway for the degradation of these amino acids involves the conversion into different amino acids.

Following nitrogen removal, most of the carbon atoms from amino acid carbon skeletons are degraded to TCA cycle intermediates, pyruvate, and acetyl-CoA which are used to generate ATP and CO₂ (**Figure 1.1**). Amino acids can form glucose via pyruvate in tissues capable of gluconeogenesis and can be converted into FAs or ketone bodies via acetyl-CoA production. However, leucine and lysine do not form glucose as they are exclusively ketogenic and can only yield acetyl-CoA (Ramsey Bronk, 1999; Wu, 2009). Although protein is not the primary energy source for human body, it is still important to consider the dietary significance of proteins in the energy supply. The balance of nitrogen in the body is tightly regulated by the rate of protein turnover and the production of urea. Due to this reason, a diet high in protein can promote amino acid degradation, which can cause excess in FAs synthesis, increase TGs storage, and thus promote obesity.

1.3 Host-gut microbiota interactions.

The human body is a habitat for diverse microbial organisms. These microbial organisms live at various sites all over the human body (Camp *et al.*, 2009; Eckburg *et al.*, 2005). The major site where the most microbial populations reside is at the human intestinal tract, where the population is up to 100 trillion bacteria, far more than all other microbial population in body's surface (Bäckhed *et al.*, 2005). The human gut microbiome is considered as a microbial organ inside the host. It is a collection of different cell lineages that are capable of communicating with each other and the host, and has an ability to undergo self-replication for its repair and maintenance. Moreover, it also consumes, stores, and redistributes energy, as well as regulating many important physiological

processes (Bäckhed *et al.*, 2005). The human gut microbiota may contain approximately 100 times as many genes as the host's genome (Bäckhed *et al.*, 2005).

1.3.1 Gut microbial ecology.

There are more than 800 different species of bacteria incorporated in human gut, with the highest number of bacteria can be found in the colon (up to 10^{12} cells/gram of faeces) (Eckburg *et al.*, 2005). The composition and number of the bacteria reside along the GI tract is increase from the stomach to the colon (**Figure 1.2**). There is growing evidence that suggest the colonisation of human gut starts before birth. After birth, at first the infant's microbiota shows low diversity and stability, but increase and converges towards an adult-type microbiota by the end of the first 36-60 months of life (Rodríguez *et al.*, 2015). The establishment of the microbiota is strongly dependent on external factors (DiBaise *et al.*, 2008). In the first month of life, *Bifidobacterium* is the main genus especially in breast-fed infants (up to 90% of total faecal bacteria), while more diverse bacteria are found in formula-fed infant as well as in weaning children (Laparra and Sanz, 2010). Moreover, metagenomic analysis of human faecal samples show that in adults and weaned children, the major constituents of colonic microbiota are Bacteroides, followed by several genera from the *Firmicutes*, such as *Eubacterium*, *Ruminococcus*, and *Clostridium*, and the genus *Bifidobacterium*. In contrast, in the infants, *Bifidobacterium* and/or a few genera from the family *Enterobacteriaceae*, such as *Escherichia*, *Raoultella*, and *Klebsiella* are predominant (Kurokawa *et al.*, 2007). The changes of this bacterial ecosystem occur throughout an individual's lifetime through the influence of several factors including diet, environmental, and disease conditions, and led to the alteration of bacterial-host symbiosis (Nazli *et al.*, 2004; Xu *et al.*, 2007).

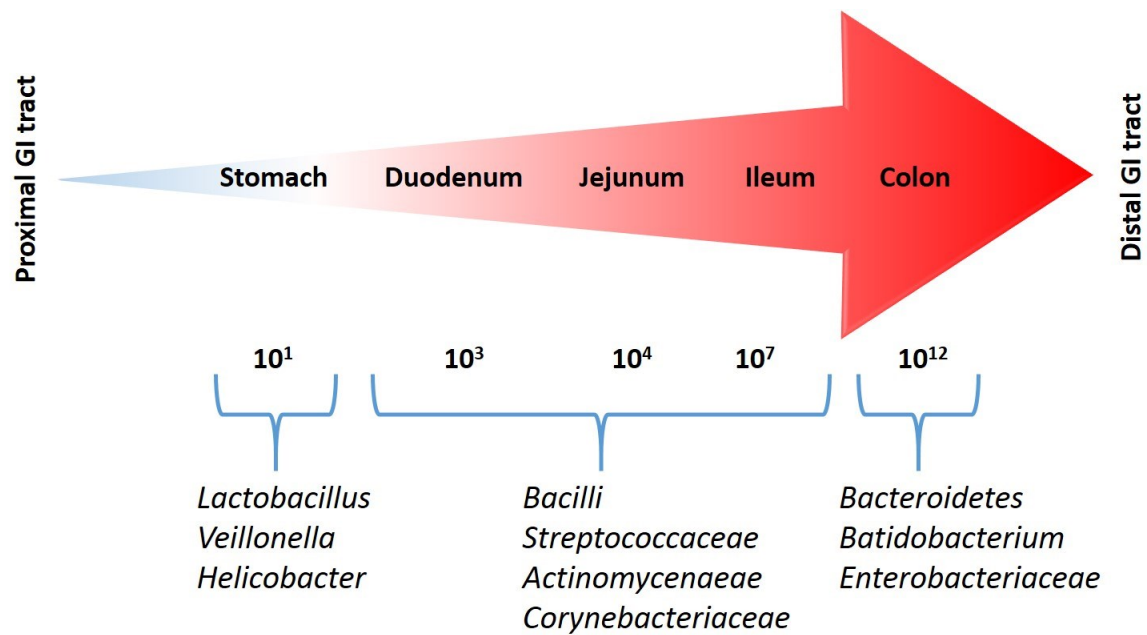


Figure 1.2: Microbial numbers and composition in the gastrointestinal tract. Information taken from Sartor, (2008) and Sekirov *et al.*, (2010).

1.3.2 Roles of the gut microbiota in host physiology and health.

The human intestinal tract provides the trillions of bacteria with a nutrient-rich environment for them to live and in exchange the host benefits from them as the gut microbiota help process nutrients for our body needs. This relationship between the human intestinal tract and its gut microbiota is often described as mutualism interaction, as both the bacteria and the host benefit from the interaction (*Figure 1.3*). For example, a highly-adaptive glycopile, *Bacteroides thetaiotaomicron*, is one of the most common known microbes in human intestine, capable of degrading the indigestible dietary polysaccharides that serve the host with 10-15% of their calorific requirement (Bäckhed *et al.*, 2005).

Gut microbiota is involved in the development of intestinal mucosa and systemic immune system throughout the life of the host (Macpherson and Harris, 2004). Studies conducted on Germ Free (GF) animals revealed that gut microbiota plays an important role in regulating physiological, biochemical, and immunological development of the host. GF animals have abnormal numbers of immune cell types and immune products. Moreover,

in GF animals, the formation of the spleens and lymph nodes are also impaired, with poorly formed B- and T-cell zones (Bauer *et al.*, 1963). The GF mice also have a lower levels of serum immunoglobulin (IgG₂ and IgG₁) compared to holoxenic mice (Benveniste *et al.*, 1971). Reduction in the efficiency of the immune system and in inflammatory responses also observed in GF animals (Berg, 1996). Furthermore, commensal bacterium are also involved in many important intestinal functions by modulating the gene-expression profile of the intestinal epithelial-cell layer (Hooper, 2001). Therefore, the presence of gut microbial community is vital to the host as it helps in maintaining the gut formation and assisting in pathogen colonisation resistance (Nicholson *et al.*, 2005).

A large number of the microbiota cell metabolic processes beneficial to the host are involved in the digestion and degradation of indigestible dietary fibres. A number of gut microbiota species have been shown to involve in the metabolism of dietary fibres to short-chain fatty acids (SCFAs), generating energy substrates for the host. Interestingly, the metabolism of nutrients by the bacteria is not only for the host's benefit, but also benefit the microbiota itself, to maintain its population and activity. In addition, resident microbes also regulate fat storage by modulate the uptake of dietary lipids. It has been demonstrated that gut microbiota promotes de novo lipogenesis by increasing the activity of lipoprotein lipase (LPL) in adipose tissue, leading to an increase of hepatic triglyceride production. Previous study by Bäckhed *et al* found that conventionalisation of GF mice with normal mice cecal microbiota, produces a 60% increase in total body fat content even with reduced food intake (Bäckhed *et al.*, 2004). As the gut microbiota is involved in many processes in host growth and development, the imbalance in its composition and number may lead to many diseases and dysfunctional in human body. Therefore, the balance of the microbiota species is very important and can determine the health of the host.

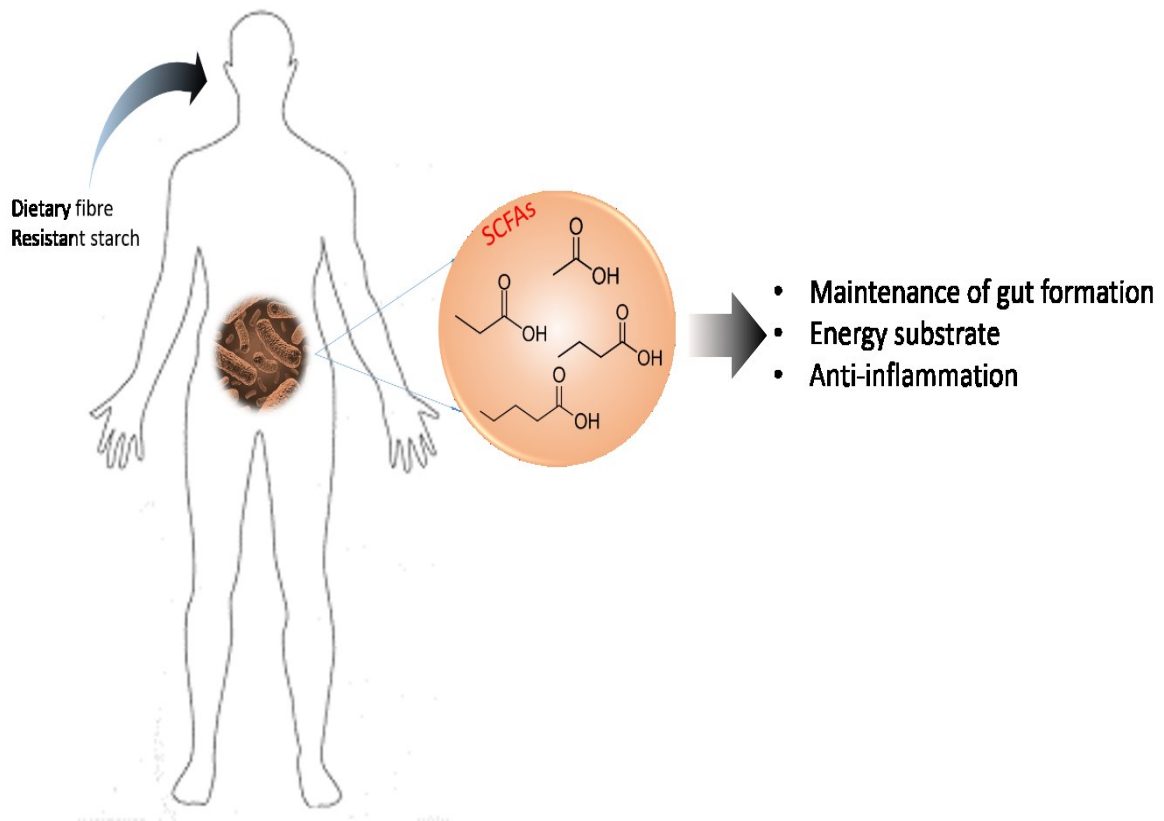


Figure 1.3: Gut microbiota and host symbiosis. Constructed based on idea taken from Neves *et al.*, (2015).

1.4 Production of SCFAs from fermentable substrates.

Dietary fibres are defined as non-digestible carbohydrates and lignin that are intrinsic and intact in plant (IOM (Institute of Medicine), 2002). This means almost 100% of dietary fibres escape the digestion in the small intestine and reach the colon relatively intact, making them the main fermentable substrate available to the gut microbiota. Fermentation of the dietary fibres occurs predominantly in the proximal colon where substrate availability and bacterial activity are the highest. Toward the distal colon, substrate availability is limited and diffusion of substrates and microbial fermentation products is reduced because of the extraction of free water (den Besten *et al.*, 2014). The main by-products of the microbial fermentation of carbohydrate including CO_2 , CH_4 , H_2 , SCFAs, bacterial cell mass, and heat (Cummings *et al.*, 2001; Topping and Clifton, 2001).

Polysaccharides that enter the large intestine contain insoluble fibres of plant-wall polysaccharides, resistant starch, inulin, and oligosaccharides. It is estimated that approximately 10% of human caloric requirements are derived from the fermentation of dietary fibres by gut microbiota (Bergman, 1990a). SCFAs are organic acids with 1 to 6 carbon atoms, and are the principal anions produced from this fermentation process along with the gasses H₂, CH₂, and CH₄ (Cummings, 1981; Macfarlane and Gibson, 1995). The main SCFAs produced are acetate, propionate, and butyrate. Being the major SCFAs produced in this manner, they are released at high concentrations in ascending colon (70-140 mM), while their concentration are declining in the transverse colon (20-70 mM) and in the descending colon (20-40 mM)(Topping and Clifton, 2001). The molar ratio of acetate, propionate, and butyrate production in the colonic lumen is 60:25:15, respectively (Tazoe *et al.*, 2008). However, this ratio can change depending on several factors such as diet, microbial composition, and the site of fermentation (Fredstrom *et al.*, 1994). The pathway of SCFAs production by anaerobic system are summarised in **Figure 1.4** and the chemical formula for the main SCFAs is presented in **Table 1.2**.

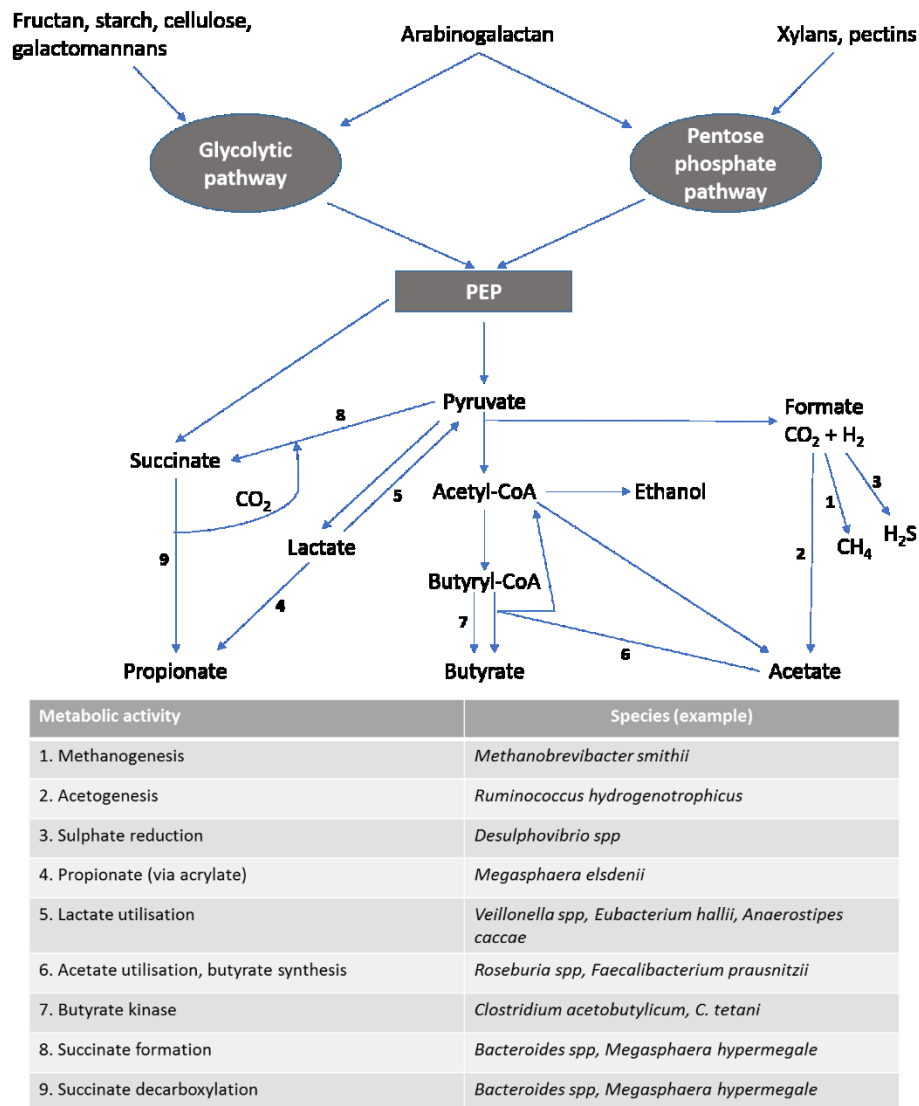


Figure 1.4: Functional/phylogenetic groups involved with the formation and conversion of SCFA in the human large intestine. Diagram above simplified the main routes of carbohydrate fermentation in the human large intestine. Two distinct cross-feeding mechanisms operate in the GI tract: (1) due to the consumption of fermentation end-products (lactate and acetate), and (2) due to cross-feeding of partial breakdown products from complex substrates (Belenguer *et al.*, 2007; Falony *et al.*, 2006). Both mechanisms contribute to the production of butyrate. Adapted from Macfarlane and Macfarlane (2003) and Flint (2006). PEP, Phosphoenolpyruvate.

1.4.1 Acetate

Endogenous production of acetate in human body originates from the cells producing and utilising SCFAs (Pouteau *et al.*, 2003). Under fasting condition, endogenous acetate contributes approximately 6.5% of resting energy expenditure in human (Pouteau *et al.*, 2003). Colonic production of acetate (exogenous) is the major source of circulating SCFAs in human, accounting 60-70% of total SCFAs produced from carbohydrate fermentation (Pouteau *et al.*, 2003). This is also the principal route by which the body obtains energy from carbohydrate that escapes digestion in small intestine ($6.3-8.4 \text{ kJ g}^{-1}$, $1.5-2 \text{ kcal g}^{-1}$) (Livesey, 1990; Roberfroid *et al.*, 1993). Moreover, in animal studies, it has been demonstrated that acetate is secreted by the liver when the portal blood levels fall below a critical level (Salminen *et al.*, 1998).

Almost all heterotrophic anaerobic gut bacteria are able to produce acetate. However, up to one-third of all acetate in the large intestine can come from reductive acetogenesis (Miller and Wolin, 1996). Hydrogen produced during the fermentation process of the fibre is either released as gas or used by hydrogen-utilising species including methanogenic archaea, sulphate reducers, and acetogens (Macfarlane and Gibson, 1995). Species such as *Ruminococcus productus* and *Rumminococcus hydrogenotrophicus* are able produce acetate from H_2 and CO_2 (Bernalier *et al.*, 1996; Ohashi *et al.*, 2007) (**Figure 1.4**). Apart from being taken up by colonic mucosa, butyrate-producing bacteria found in the human colon can be net utilisers of acetate. In particular, bacteria such as *Anaerostipes caccae*, *Roseburia intestinalis*, *Roseburia* sp. A2-181, *Roseburia* sp. A2-183, *Coprococcus* sp. Strain L2-50, and *Faecalibacterium prausnitzii* are able to produce butyrate from acetate (Duncan *et al.*, 2002, 2004a; Falony *et al.*, 2006). *Roseburia intestinalis*, *Faecalibacterium prausnitzii*, and *Eubacterium hallii* are the most abundant butyrate-producing bacteria in human colon with a mean populations of 2.3, 3.8, and 0.6%, of faecal microbiota, respectively. Among this, *Faecalibacterium prausnitzii* and *Roseburia* spp. generate much of their butyrate carbon from exogenously derived acetate via the action of butyryl-CoA:acetyl-CoA transferase (Duncan *et al.*, 2002). Formation of acetate benefits bacteria because it produces ATP via substrate-level phosphorylation (Macfarlane and Gibson, 1997).

1.4.2 Propionate

Intestinal bacteria produce propionate through two major routes; the first is directly from sugar in a single species, while the second route is indirect formation by cross-feeding from succinate and lactate producers. It has been suggested that there are two main metabolic pathways of propionate production; the 'randomising' pathway via succinate and the acrylate pathway. Belenguer *et al* (2007) established that the dominant route of propionate formation was via the acrylate pathway, by which lactate was converted to propionate, so presumably the same applies for propionate formation via conversation of sugars (Belenguer *et al.*, 2007) (**Figure 1.5**). If this assumption is correct, based on the process in rumen, the main species responsible for the formation of propionate from sugars and lactate would probably be *Megasphaera elsdenii* (Counotte *et al.*, 1981). Furthermore, members of the *Clostridium* cluster IX such as *Selenomonas*, *Megasphaera*, and *Veillonella* spp. are capable of producing propionate through decarboxylation succinate (Flint, 2006).

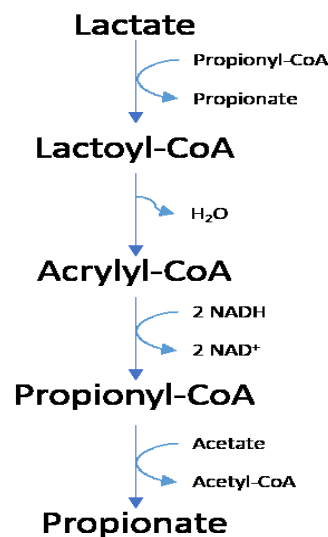


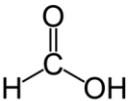
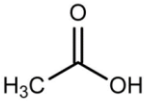
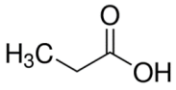
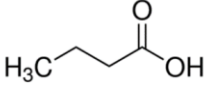
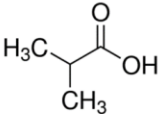
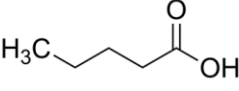
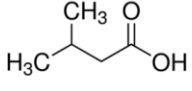
Figure 1.5: Acrylate pathway of propionate formation from lactate. Gut microbiota can increase the production of propionate via this pathway based from the *in vitro* fermentations of human faeces in the presence of lactate and the absence of carbohydrate. Information taken from Belenguer *et al.*, (2007).

1.4.3 Butyrate

Roseburia spp. and *Faecalibacterium prausnitzii* are the two most abundant groups of butyrate-producing bacteria isolated from human faecal samples (Duncan *et al.*, 2006; Flint, 2006; Walker *et al.*, 2005). As discussed earlier (**section 1.4.1**), butyrate is also produced by acetate-utilising bacteria. In addition, it has been reported that a significant amount of lactate can be converted into butyrate in the human colon by the action of lactate-utilising bacteria, *Eubacterium hallii* and *Anaerostipes caccae* (Duncan *et al.*, 2004b). There are two metabolic routes in which gut microbiota can produce butyrate. The first one is the conversion of butyryl-CoA to butyrate via butyrate kinase, and the second one is via acetyl-CoA transferase (Duncan *et al.*, 2002; Louis *et al.*, 2004). It has been suggested that the supply of butyrate in the colon can be influenced by diet and variations in the dominant metabolic type of butyrate-producer among individuals (Duncan *et al.*, 2004b). Duncan *et al.*, (2007) further validated this hypothesis in relation to dietary variations, which shows a significant decrease in members from *Clostridium* cluster XIVa (*Roseburia* spp. and *Eubacterium rectale*) that associated with butyrate production, caused by the decreasing of dietary carbohydrate intake.

Despite producing acetate, propionate, and butyrate as its main fermentation products, gut-microbial fermentation of dietary fibres also resulted in the production of several other metabolites but in much lower amounts.

Table 1.2: The chemical formula for the main SCFAs produced from the fermentation of dietary fibres by gut microbiota.

Short-chain fatty acids	Number of carbon	Chemical formula
Formate	1	
Acetate	2	
Propionate	3	
Butyrate	4	
Isobutyrate	4	
Valerate	5	
Isovalerate	6	

1.4.4 Other fermentation products

As mentioned previously, acetate, propionate and butyrate are the three major SCFAs produced by gut microbiota fermentation of dietary fibres. Other SCFAs also present, but in much lower amounts including formate, valerate, caproate, and branched chain fatty acids (BCFAs) 2-methylbutyrate, isobutyrate, and isovalerate. It has been shown that 2-methylbutyrate, isobutyrate, and isovalerate are formed by the fermentation of branched amino acids (BCAAs) (isoleucine, valine, and leucine, respectively) by the faecal microbiota (Macfarlane and Gibson, 1995). The levels of BCFAs are higher than other FAs

in the descending colon. This is caused by the higher rate of protein fermentation compared to carbohydrate fermentation due to substrates availability and increased of pH in this region (Cummings *et al.*, 1987). Higher level (25%) of BCFAs production was observed after inoculation with gut microbiota from individuals with inflammatory bowel disease (IBD) compared with inoculation with microbiota from healthy individuals (van Nuenen *et al.*, 2004). Based on this findings, high level of metabolites produced from proteolytic fermentation may play a role in the aetiology of IBD, but more data is needed to support this hypothesis.

While majority of SCFAs especially butyrate are being used in the gut, however there is still small amount of these SCFAs being transported from the intestinal lumen into the portal blood where they are taken up by organs.

1.5 Transport of SCFAs

As mentioned previously, while the majority of SCFAs produced is utilised within the gut, a small proportion of these SCFAs reached the liver and peripheral tissues where they can be used as substrates and/or signalling molecules. As small proportion of SCFAs present in the gut in unionised forms, they can cross the apical membrane through passive diffusion. However, the major part of SCFAs exists in an ionised form and transport across the intestinal mucosa is mediated by two main protein transporters: 1) monocarboxylate transporter 1 (MCT-1) (Hadjiagapiou *et al.*, 2000; Vidyasagar, 2005), and 2) sodium-coupled monocarboxylate transporter 1 (SMCT-1) (Gupta *et al.*, 2006; Takebe *et al.*, 2005). High expression of both transporters has been found on colonocytes (Takebe *et al.*, 2005; Teramae *et al.*, 2010). In addition, MCT-1 also expressed abundantly on lymphocytes (Halestrap and Meredith, 2004), while SMCT-1 is expressed in kidney and thyroid gland (Ganapathy *et al.*, 2005).

1.6 SCFAs are G-protein coupled receptor (GPCR) agonists.

Next to its role as substrate for energy production, previous studies indicate that SCFAs can act as signalling molecules through cell surface receptors known as G-protein coupled receptors (GPCRs). This group of protein receptors constitutes a large and diverse family of proteins that sense molecules outside the cell and activate intracellular signalling cascades. GPCRs are also known as seven-transmembrane (7TM) receptors with an extracellular N-terminus and an intracellular C-terminus (Palczewski *et al.*, 2000). Several endogenous ligands, such as hormones, peptides, protein, neurotransmitters, and fatty acids are able to activate GPCRs (Howard *et al.*, 2001; Kirkham *et al.*, 1992). Upon ligand binding, the structural changes within GPCRs allow the receptors to activate guanine-nucleotide binding protein (G protein) inside the cell. G protein is a heterotrimeric protein that made up of an alpha (α), beta (β), and gamma (γ) subunits (Hurowitz *et al.*, 2000), the activation of which regulates cellular responses via a variety of second messenger cascades (Lefkowitz, 2007; Oldham and Hamm, 2007; Wettschureck and Offermanns, 2005). In 2003, three independent groups have successfully deorphanised G-protein coupled receptor 41 (GPR41) and 43 (GPR43), and revealed that SCFAs act as a ligand for these receptors (Brown *et al.*, 2003; Le Poul *et al.*, 2003; Nilsson *et al.*, 2003). The receptors were later renamed to free-fatty acid receptor 2 (FFAR2) and 3 (FFAR3), for GPR43 and GPR41, respectively. These two receptors share 42% amino acid identity and belong to the same family (Brown *et al.*, 2003). Another type of GPCR, called GPR109A (also known as hydroxycarboxylic acid receptor 2 or HCA2) is a high affinity receptor for niacin which also can be activated by butyrate (Thangaraju *et al.*, 2009a).

1.6.1 FFAR2

FFAR2, also known as GPR43 is activated by high micromolar or millimolar concentrations of SCFAs, most notably acetate, propionate, and butyrate with varying potency. This receptor responds somewhat more strongly to shorter chain length SCFAs, while propionate was reported to be the most potent agonist, acetate is the most selective (Le Poul *et al.*, 2003). FFAR2 couples primarily to $G\alpha_i$ and $G\alpha_q$ proteins family (**Figure 1.6-**

B). FFAR2 activation following ligand binding activates a series of second messenger cascades regulating intracellular responses. $G\alpha_i$ family were first identified as the inhibitory G proteins (Bokoch *et al.*, 1984). Activation of $G\alpha_i$ protein subunit inhibits the production of cyclic adenosine monophosphate (cAMP)-dependent pathway by adenylate cyclase, resulting in the reduction in intracellular cAMP production from ATP (Birnbaumer, 2007; Le Poul *et al.*, 2003). As for the $G\alpha_q$, this protein family activates phospholipase C β (PLC β) isoforms. Activated PLC β then hydrolyses phosphatidylinositol 4,5 bisphosphate into 1,2 diacylglycerol (DAG) and inositol 1,4,5 triphosphate (IP $_3$). While DAG acts as a second messenger that activate protein kinase C (PKC), IP $_3$ binds to specific IP $_3$ receptor (calcium (Ca $^{2+}$) release channels in the endoplasmic reticulum, thus increase Ca $^{2+}$ release (Le Poul *et al.*, 2003).

FFAR2 was shown to be highly expressed in immune cells such as polymorphonuclear (PMN) cells and peripheral blood mononuclear (PBMC) cells, with high expression was observed in neutrophils (Brown *et al.*, 2003; Le Poul *et al.*, 2003; Nilsson *et al.*, 2003). A number of studies have demonstrated that FFAR2 acts as a chemoattractant receptor for SCFAs in neutrophils (Le Poul *et al.*, 2003; Maslowski *et al.*, 2009; Vinolo *et al.*, 2011). A study conducted by Maslowski *et al.*, (2009) demonstrated that FFAR2-deficient mice show exacerbated or unresolving inflammation in model of colitis, arthritis, and asthma. In addition, germ-free mice which are unable to produce SCFAs from fibre, display similar dysregulation of inflammatory responses, which suggests that SCFAs and FFAR2 are likely to have a molecular link between fibre-rich diet, gut microbial metabolism, and inflammatory immune responses (Maslowski *et al.*, 2009).

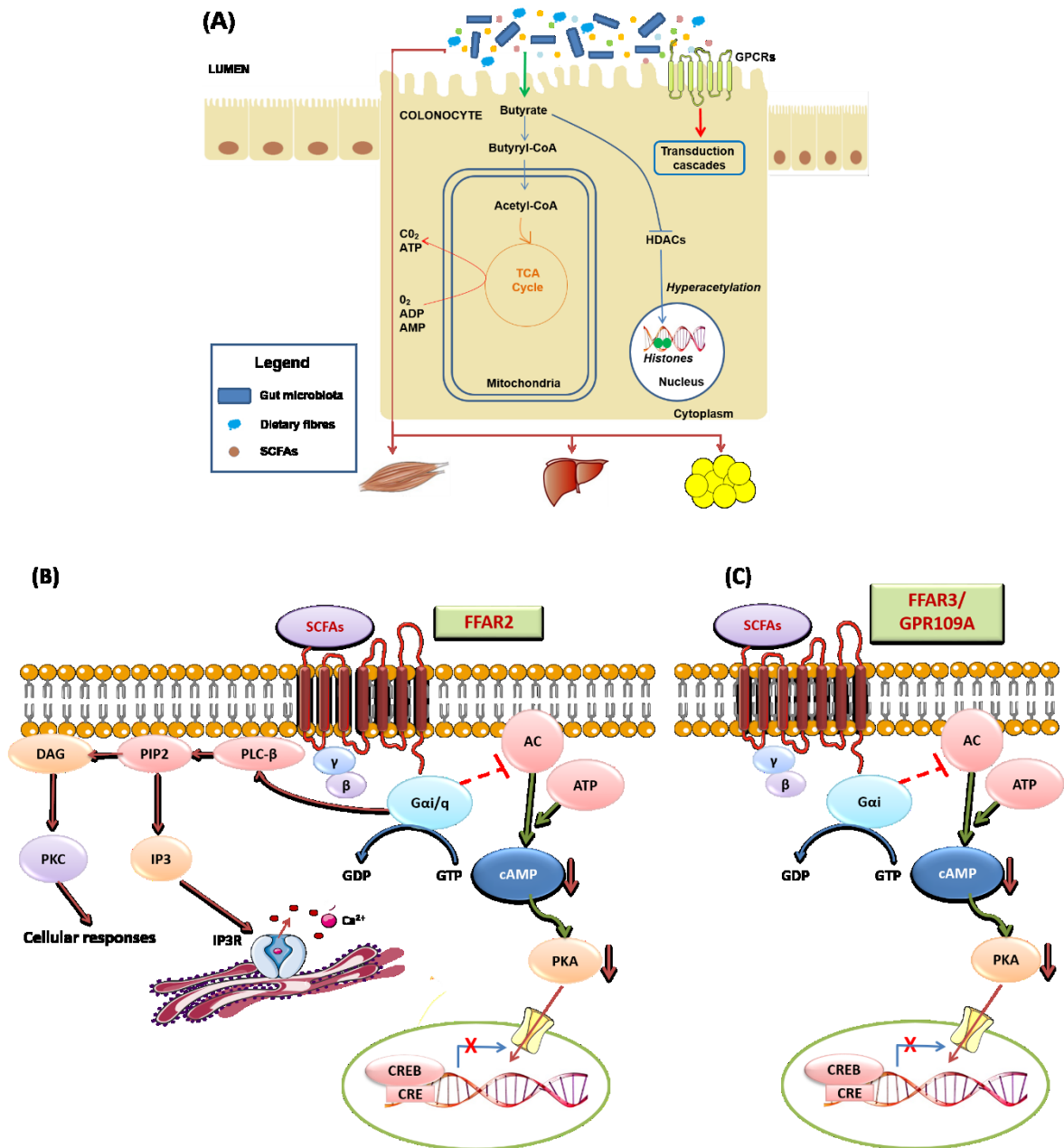


Figure 1.6: Role of butyrate in colonocytes metabolism and schematic overview of receptors activation by short-chain fatty acids (SCFA). (A) Fate of butyrate after being produced from microbial fermentation of dietary fibre. (B) FFAR2, and (C) FFAR3, and GPR109A signalling pathways. Part of illustrations was designed using Servier Medical Art used under CC BY 3.0. Adapted from Neves *et al.*, 2015).

It has been shown previously that SCFAs, in particular propionate and butyrate are able to inhibit the growth of colon cancer cells in *in vitro* model (Gamet *et al.*, 1992). More recently, a study shows that the expression of FFAR2 is frequently reduced or abolished in colon cancer cells, and that the restoration in the FFAR2 expression followed by propionate treatment induced G₀/G₁ cell cycle arrest and activated caspases, and increased apoptotic cell death (Tang *et al.*, 2011). Therefore, it is suggested that there is a possible link between the gut microbial fermentation products and FFAR2 in lowering colon cancer incidence. FFAR2 is also found to be expressed in peptide YY (PYY)-expressing enteroendocrine cells (L cells) (Karaki *et al.*, 2006). These cells produce glucagon like peptide (GLP-1), a hormone which regulates insulin secretion from pancreatic β -cells and increase insulin sensitivity in target tissue. A study using *in vitro colonic* cultures shows that the regulation of GLP-1 release by SCFAs is FFAR2 mediated (Tolhurst *et al.*, 2012). Hong *et al.*, (2005) reported FFAR2 expression in adipose tissue. The results of their study highlight the vital role of FFAR2 expression during the adipogenesis process and that acetate and propionate mediated differentiation of 3T3-L1 cells from preadipocytes into adipocytes. However, studies on human adipocyte differentiation were not able to draw a relationship between FFAR2 and human adipogenesis as its ligands were not able to induce differentiation of preadipocytes, unlike what was reported in mice (Dewulf *et al.*, 2013). SCFAs have previously been shown to inhibit lipolysis in human (Laurent *et al.*, 1995). In 3T3-L1 adipocytes, inhibition of lipolysis by SCFAs has been shown to be mediated by FFAR2 (Ge *et al.*, 2008). Based on this observation, this receptor could be used as a target for treatment of dyslipidaemia.

1.6.2 FFAR3

FFAR3 was orphanised at the same time as FFAR2 by two independent groups (Brown *et al.*, 2003; Le Poul *et al.*, 2003). FFAR3 is a receptor for SCFAs, particularly acetate, propionate, and butyrate, with propionate being the most potent agonist. This receptor also can be activated by other SCFAs including caproate and valerate, but to a lesser degree (Xiong *et al.*, 2004). FFAR3 couples to G_i protein pathway (Brown *et al.*, 2003; Le Poul *et al.*, 2003; Nilsson *et al.*, 2003) (**Figure 1.6-C**). This receptor has been shown to be expressed in

various tissues, including PBMC, spleen, adipose tissue, and pancreas (Brown *et al.*, 2003; Le Poul *et al.*, 2003). Stimulation of the anorexigenic hormone secretion, leptin, in adipocytes has been shown to be mediated by FFAR3 (Xiong *et al.*, 2004). Overexpression of FFAR3 in adipocytes increased SCFAs-mediated leptin secretion, while reduced secretion of leptin was observed in FFAR3-knockdown adipocytes. The expression of FFAR3 on adipocyte is still controversial as Hong *et al.*, (2005) and Frost *et al.*, (2014) were unable to detect FFAR3 expression in adipocytes, but high levels of FFAR2 were observed (Hong *et al.*, 2005). Another group was also not able to detect FFAR3 mRNA in mouse adipose tissue, which then observed consistent reduction on FFAR2 expression in adipose tissue of FFAR3-knockout mice compared to wild-type mice (Zaibi *et al.*, 2010). Furthermore, they also demonstrated that SCFAs promotes leptin secretion in wild-type mice, and found that the secretion was reduced in FFAR3-knockout mice, which then suggests that this effect may be associated with the down-regulation of FFAR2 in the FFAR3-knockout mice (Zaibi *et al.*, 2010). Similar to FFAR2, FFAR3 is also expressed in enteroendocrine cells secreting PYY hormone. The release of this satiety hormone may also be regulated by FFAR3 (Karaki *et al.*, 2006).

FFAR3 is highly expressed in sympathetic ganglia in both human and mouse (Kimura *et al.*, 2011). It has been demonstrated that SCFAs and ketone bodies were able to regulate the sympathetic nervous system (SNS) directly via FFAR3 at the sympathetic ganglion. Under fed conditions, propionate stimulates sympathetic ganglion through FFAR3 activation. However, β -hydroxybutyrate, a ketone body produced during starvation or diabetes, antagonised FFAR3 and suppressed the SNS activity (Kimura *et al.*, 2011). This finding suggests that FFAR3 could play an important role in maintaining energy balance, and that FFAR3 agonists could potentially be used for the treatment of obesity.

1.6.3 GPR109A

GPR109A (hydroxycarboxylic acid receptor 2 or HCA2), also known as Niacin receptor 1, is a high affinity niacin receptor. GPR109A is found to be expressed most abundantly in adipocytes of white and brown adipose tissue (Soga *et al.*, 2003; Tunaru *et al.*

al., 2003; Wise *et al.*, 2003). In addition, this receptor is also expressed in keratinocytes (Hanson *et al.*, 2010) and immune cells, including dendritic cells, macrophages, and neutrophils (Benyó *et al.*, 2005), but to a lesser degree. GPR109A couples to the G_{ai} protein pathway, the activation of which leads to an inhibition of adenylate cyclase, thus reducing the production of intracellular cAMP (Wise *et al.*, 2003) (**Figure 1.6-C**). The agonist activity of niacin on this receptor is really important as niacin has been used for more than half a century in treating dyslipidaemia (Knopp, 1999). While working on the lipid-lowering effect of niacin, two independent groups have discovered that the anti-lipolytic and lipid-lowering effects of niacin are mediated by GPR109A activation (Tunaru *et al.*, 2003; Wise *et al.*, 2003). The niacin-induced decrease in free fatty acids (FFAs) and plasma TG levels were abolished in GPR109A-deficient mice (Tunaru *et al.*, 2003).

GPR109A is expressed in the lumen-facing apical membrane of colonic and intestinal epithelial cells. Recently, it has been shown that this receptor also can be activated by butyrate (Thangaraju *et al.*, 2009b). A previous study has shown that the expression of GPR109A is abolished in colon cancer in human and mouse model, as well as in colon cancer cell lines. In the presence of its ligands, butyrate and niacin, the re-expression of this receptor has been shown to induce apoptosis in colon cancer (Thangaraju *et al.*, 2009b). Another study by the same group further demonstrated that the activation of GPR109A by butyrate promotes anti-inflammatory responses in colonic macrophages and dendritic cells. This resulted in the differentiation of Treg cells and IL-10-producing T cells, thus suppressing colonic inflammation and carcinogenesis (Singh *et al.*, 2014a). More recently, it has been reported that the beneficial effects of high-fibre diet involves the activation of GPR109A and GPR43 in the gut epithelium, which promote gut epithelium homeostasis via inflammasome pathway (Macia *et al.*, 2015).

Present evidence indicates that GPR109A activation by its ligands acts on multiple sites to modulate anti-inflammatory responses and lipid profile. However, as this receptor is also involved in a niacin-induced flushing effect (Benyó *et al.*, 2005), it is controversial as to whether the development of new agonists for GPR109A for treating atherosclerosis would be therapeutically important.

Table 1.3: Summary of the GPCRs activation, including its ligands, expression, and functions

GPCRs	Ligands	Expression	Roles
FFAR2 (GPR43)	SCFAs; Formate, acetate, propionate, butyrate, isobutyrate, valerate, isovalerate	Adipocytes Immune cells Gut epithelium Enteroendocrine L cells	Induce adipogenesis, lipolysis inhibition, anti-inflammatory, colon cancer suppression, anorexigenic effect via GLP-1 secretion, insulin sensitivity
FFAR3 (GPR41)	SCFAs; Acetate, propionate, butyrate, isobutyrate, valerate, isovalerate	Adipocytes Immune cells Enteroendocrine L cells	Anorexigenic hormone secretion (Leptin), regulation of sympathetic nervous system (SNS)
GPR109A	SCFAs; Butyrate Niacin	Adipocytes Immune cells Gut epithelium Intestinal cells Enteroendocrine L cells	Anti-lipolytic, anti- inflammatory responses, colon cancer suppression, Treg cells development

It has been shown that SCFAs play a crucial role in many physiological processes in humans, via acting as substrate for energy production, ligand for GPCRs activation, and as HDAC inhibitors (**Figure 1.7**). Thus these small metabolites are important in maintaining human health as well as might be associated in the development of some diseases.

1.7 SCFAs in human health and disease

Acetate is the principal SCFAs in the gut. Acetate, which is produced via the fermentation of carbohydrate by intestinal bacteria, is taken up by the gastrointestinal (GI) epithelium, appears in portal blood, and eventually passes through the liver to peripheral tissues where it is metabolised by muscle (Salminen *et al.*, 1998). After crossing the blood brain barrier, it has been shown that acetate modified acetyl-CoA carboxylase activation and expression of neuropeptides responsible for appetite suppression by suppressing appetite and inducing hypothalamic neuronal activation (Frost *et al.*, 2014b). Moreover, acetate has also been demonstrated as the primary substrate for cholesterol synthesis, and may interfere directly in lipid metabolism (Day and Fidge, 1964). High concentrations of acetate provide substrate for hepatic lipogenesis (Jenkins *et al.*, 1991).

In humans, propionate produced from the fermentation of carbohydrate is largely cleared by the liver (Salminen *et al.*, 1998). The liver clears majority of propionate and butyrate from the portal circulation to prevent high SCFAs concentrations in blood (Bloemen *et al.*, 2009). Propionate is a precursor for liver gluconeogenesis (Roy *et al.*, 2006). SCFAs, propionate in particular contributes about 80% of ruminants energy need. However it is unclear if the human uses propionate in a similar manner to ruminants (Bergman, 1990a). Propionate enters TCA cycle via the succinyl-CoA entry point. In brief, propionate is first converted into propionyl-CoA by propionyl-CoA synthetase. Propionyl-CoA is then converted to succinyl-CoA via three successive reactions. The resulting succinyl-CoA enters the TCA cycle and is converted to oxaloacetate, the gluconeogenesis precursor (Bloemen *et al.*, 2010). It has been shown that approximately 50% of propionate is used by humans as a substrate for hepatic gluconeogenesis (Reilly and Rombeau, 1993). Moreover, in another study, the concentrations of propionate in both portal blood and hepatic vein suggest the greater uptake of propionate by the liver (Cummings *et al.*, 1987). These accumulating evidences point out that the liver clears a large amount of propionate from the portal blood.

In human subjects, it has been shown that the effect of propionate on hepatic carbohydrate metabolism was mediated by its role in improving glucose tolerance and insulin sensitivity, as well as increasing high density lipoprotein (HDL)(Venter *et al.*, 1990).

Moreover, it has been demonstrated that propionate is converted into glucose by intestinal gluconeogenesis (IGN), thus improving energy homeostasis (De Vadder *et al.*, 2014). Moreover, another study shows that the consumption of propionate-enriched bread decreased high-density lipoprotein while increasing serum triglyceride and improving carbohydrate tolerance (Todesco *et al.*, 1991). The inhibitory effect of propionate on the synthesis of cholesterol is rather controversial. Demigné *et al.*, (1995) demonstrated that propionate (0.6 mmol/L) significantly inhibits cholesterol synthesis in isolated rat hepatocytes, but another study using a higher concentration (1 mmol/L) did not (Nishina and Freedland, 1990).

Of the SCFAs produced by gut microbiota in human intestine, butyrate has caught the most attention and has been studied extensively. Its involvement in suppressing colonic inflammation, causing cell cycle arrest, and apoptosis highlight its role in protecting against colon cancer and colitis (Ganapathy *et al.*, 2013; Roediger, 1990; Williams *et al.*, 2003). Butyrate is the principal substrate and energy source for colonocytes (Roediger, 1980a). It is estimated that butyrate provides at least 60-70% of colonic mucosa energy requirements essential for their proliferation and differentiation (Suzuki *et al.*, 2008). Butyrate is important in maintaining colonic epithelium formation, and plays role in lipid metabolism, as well as possessing an anti-tumorigenic effects on many cancer cell lines (Hamer *et al.*, 2008). At least part of its beneficial effects is due to its ability to inhibit histone deacetylases (HDACs) (Chen *et al.*, 2003). Millimolar concentrations of sodium butyrate have previously been shown to inhibit histone deacetylases both *in vivo* and *in vitro* and cause an accumulation of acetylated histone species (Candido, 1978).

Most of the butyrate in intestinal lumen present in anionic form. In this form, butyrate is transported across the intestinal epithelial via monocarboxylate transporter-1 (MCT1) and then metabolised by colonocytes (Hadjiagapiou *et al.*, 2000). Inside the cell, butyrate enters mitochondria in which it undergoes β -oxidation to acetyl-CoA and enters the tricarboxylic acid cycle (TCA cycle) for energy production (Allan *et al.*, 1996) (**Figure 1.6-A**). A study conducted by Donohoe *et al.*, (2011) shows that mitochondrial respiration is replenished on the addition of butyrate in colonocytes from germ-free mice culture medium, which then prevents autophagy. MCT1 mRNA and protein expression, and intracellular butyrate concentrations are significantly reduced during the progression from

normal to malign cell in the human colon (Lambert *et al.*, 2002). In addition, a reduction in MCT1-mediated butyrate uptake has also been associated with the deficiency in butyrate oxidation in colonocytes of inflamed intestine (Thibault *et al.*, 2007).

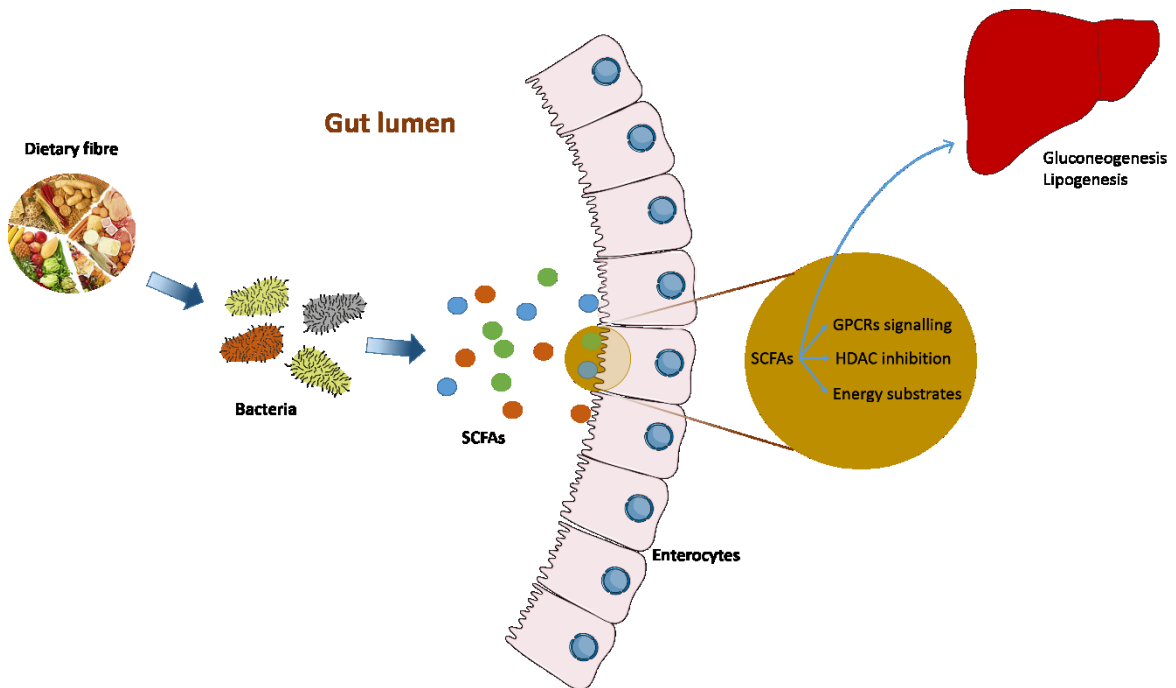


Figure 1.7: Roles of gut microbial metabolites (SCFAs) in human. Once absorbed in the colon, butyrate serves as energy substrates for colonocytes, and acetate and propionate reach liver and peripheral organs. In addition, SCFAs also act as HDAC inhibitor and regulate many physiological processes through signalling via GPCRs.

1.8 Overview of metabonomics

Metabonomics by definition is 'the quantitative measurement of the dynamic multiparametric metabolic response of living systems to pathophysiological stimulation or genetic modification' (Nicholson *et al.*, 1999). This technique examines metabolites within a biological samples including urine, plasma, faecal, or cell extracts. It is an important tool for studying the microbial-mammalian host metabolic axis and has been widely used in research (Nicholson *et al.*, 2002).

Metabolomics, which is the study of metabolic regulation and fluxes in a living system is closely related to metabonomics (Nicholson *et al.*, 1999, 2002). Metabolites

measured in biofluids reflect genetic and environmental interactions in the mammalian host and symbiosis microbiota. This metabolic profiling (metabonomics/metabolomics) technique is one such approach in analysing cellular pathway based on the untargeted analysis of the metabolite composition in a biological sample (Nicholson *et al.*, 1999). As a global untargeted approach, by using this technique, a high-density data is produced which can be analysed using a chemometric approach, multivariate statistical analysis, and pattern recognition (Nicholson *et al.*, 2002). Thus, this method serves as an attractive strategy in biomarker discovery (Smolinska *et al.*, 2012).

1.8.1 Analytical strategies in metabonomics

Proton Nuclear Magnetic Resonance (^1H NMR) and mass spectrometry (MS) are the two most popular tools for metabolic profiling (Dumas and Davidovic, 2013; Fonville *et al.*, 2010). ^1H NMR spectroscopy has been used widely in metabolic profiling as it is highly reproducible and requires a simple sample preparation method for liquid samples (e.g. biofluids) (Dumas and Davidovic, 2013). Mass spectrometry is a highly sensitive analytical technique and is able to detect and measure low concentration metabolites. Because NMR is relatively insensitive, NMR is normally used in conjunction with GC/MS or LC/MS to help in assigning metabolites in samples (Fonville *et al.*, 2010).

NMR-based metabonomics studies have been successfully used in identifying potential biomarkers that associate to a disease, drug toxicology, and genetic as well as environmental variation (Coen *et al.*, 2008). Metabonomics is suitable for investigating the microbiome-host interaction as the metabolic profiles provide information on the endogenous metabolites as well as the host-gut microbial co-metabolites (Holmes *et al.*, 2011). Moreover, metabonomics studies also have been successfully used in identifying the relationship between choline metabolism and the development of nonalcoholic fatty liver disease (NAFLD) and IR in rat model (Dumas *et al.*, 2006).

Therefore, in this project, ^1H -NMR-based metabolic profiling technique will be used alongside with the cell-based and molecular approaches in assessing the role of gut-microbial metabolites (SCFAs) in host metabolism.

1.9 Hypothesis and aims

Although SCFAs have been extensively characterised from a mechanistic point of view as fuel for the cell, GPCR agonists, and as HDAC inhibitors, there remains gaps in the knowledge. The overall hypothesis of this PhD is that SCFAs may play important role in hepatic cancer metabolism by acting as substrate for energy metabolism and may act as ligand by activating GPCRs, thus regulating adipocyte differentiation and function.

Towards this end, a set of project aims have been implemented.

- 1) Assessment of the effect of sodium as a SCFA counter ion on hepatocyte metabolotypes -> see Chapter 3
- 2) Characterisation of the hepatocyte metabolic signature of SCFA exposure -> see Chapter 4
- 3) Implementation of a harmonised pharmacological assessment of a comprehensive SCFA panel on their GPCRs, *i.e.*, FFAR2, FFAR3, GPR109A -> see Chapter 5
- 4) Systematic Characterisation of the role of a comprehensive SCFA panel on adipocyte differentiation and function *i.e.*, adipogenesis and lipolysis -> see Chapter 6

In order to develop this, ¹H NMR-based metabolic profiling technique is used to profile the HepG2 cell culture medium in identifying specific biomarkers related to the sodium treatment on the cells. Using the same approach, the effect of SCFAs (propionate and butyrate) on hepatic cancer metabolism is then investigated by identifying the hepatocytes metabolic signature of SCFAs exposure. As it has been reported on the activation of several GPCRs by SCFAs before, here an effort has been made in harmonising the pharmacological role of a comprehensive SCFA panel in activating their GPCRs (FFAR2, FFAR3, GPR109A) by measuring the accumulation of cellular cAMP. Finally, by combining cell-based and molecular approaches, the role of comprehensive SCFA panel on adipocyte functions is investigated.

CHAPTER 2

2. GENERAL METHODOLOGY

In this PhD, several approaches were applied in order to address the aims of the project. In chapter 3 and chapter 4, a ^1H NMR-based metabonomics technique was used to assess the effect of SCFAs on hepatic metabolic network. In chapter 5, the pharmacological assessment of a comprehensive SCFA panel on FFAR2, FFAR3, and GPR109A was carried out using kits provided by a service company (Discoveryx, USA). In chapter 6, the role of a comprehensive SCFA panel on adipocytes development and function was assessed by using a combination of a cell-based assays and molecular approaches.

2.1 Analytical strategy

Metabolic profiling can be applied for the analysis of complex biological samples such as biofluids and tissues. This technique is a unique strategy for analysing cellular pathways based on the untargeted profiling of the small metabolites present in a biological sample. It provides a powerful tool for obtaining insight into functional biology (Nicholson *et al.*, 1999). The combination of an *in vitro* cell model and metabolic profiling technique allows us to study the response of the cells to specific treatment or chemical exposure. It has been demonstrated previously that NMR-based approach can be used to profile and monitor the endogenous metabolome of an *in vitro* cell system under various biological and toxicological exposures (Ellis *et al.*, 2011; Shintu *et al.*, 2012).

2.2 Nuclear Magnetic Resonance (NMR) Spectroscopy

High resolution NMR spectroscopy is a quantitative, non-destructive, and reproducible technique that detects small molecular weight molecules within a complex biological matrix such as tissue extracts and biofluids (Beckonert *et al.*, 2007). NMR-based metabolic profiling is a robust and reliable method, thus suitable for metabonomics applications (Bales *et al.*, 1984; Nicholson *et al.*, 1983). This technique provides a metabolic 'snapshot' representative of the sample at a particular time point and requires only simple sample preparation steps (Nicholson *et al.*, 1999). With the improvement in spectral dispersion and sensitivity, the current version of high-field NMR spectrometer enables the detection of metabolites in the micromolar range in a short experiment time (Holmes *et al.*, 1997).

2.2.1 Principles of NMR spectroscopy

Nuclear magnetic resonance (NMR) spectroscopy is a powerful analytical tool. It detects the way in which electromagnetic radiation interacts with the spin of atomic nuclei. The spin is characterised by a nuclear spin quantum number (I), which is dependent on the number of protons (atomic number) and nucleons (atomic mass) present (Jardetzky and Roberts, 1981). Nuclei with $I=0$ are not observable by NMR. Nuclear isotopes with a nuclear spin of $\frac{1}{2}$, such as ^1H , ^{13}C , ^{15}N , and ^{31}P are preferably used in biological approaches. Among these, ^1H NMR spectroscopy is the most commonly used due to its natural abundance of 99.9% (Jardetzky and Roberts, 1981).

When magnetic field (B_0) is applied, the nuclei orientate themselves, and the number of possible orientation is given by the equation: $2I+1$. Therefore, if $I=1/2$ like ^1H , this will generate two spin states in a magnetic field. The spin corresponding to $\frac{1}{2}$ is the lower energy state, more stable, and aligned (parallel and same direction) with the applied magnetic field, B_0 (position α). On the other hand, the spin corresponds to $-\frac{1}{2}$ is the higher energy state, and oriented in the opposite direction to B_0 (position β). For both states, the spins move around the magnetic field with an angular frequency called the Larmor

precession (Keeler, 2002). The energy transition between both states is given by the Boltzmann equation:

$$\eta_{\beta}/\eta_{\alpha} = e^{\Delta E/kT}$$

Where η_{β} and η_{α} represent the number of nuclei in the upper or lower energy state. ΔE is the difference in energy between the two spin states, α and β . k is the Boltzmann constant (1.3805×10^{-23} J/Kelvin), while T is the temperature in Kelvin (K). ΔE can be calculated by the following equation:

$$\Delta E = \gamma h B_0 / 2\pi$$

Where γ is the magnetogyric ratio, h is the Planck's constant (6.626208×10^{-34} J S), and B_0 is the NMR magnetic field. The slight excess of spins in the lower energy state (parallel orientation, α) than the higher energy state (β) causes a net absorption of energy which results in an NMR signal. If the ΔE value is small, the population between the two spin states is correspondingly small, thus the NMR signal is relatively low (Jardetzky and Roberts, 1981; Keeler, 2002).

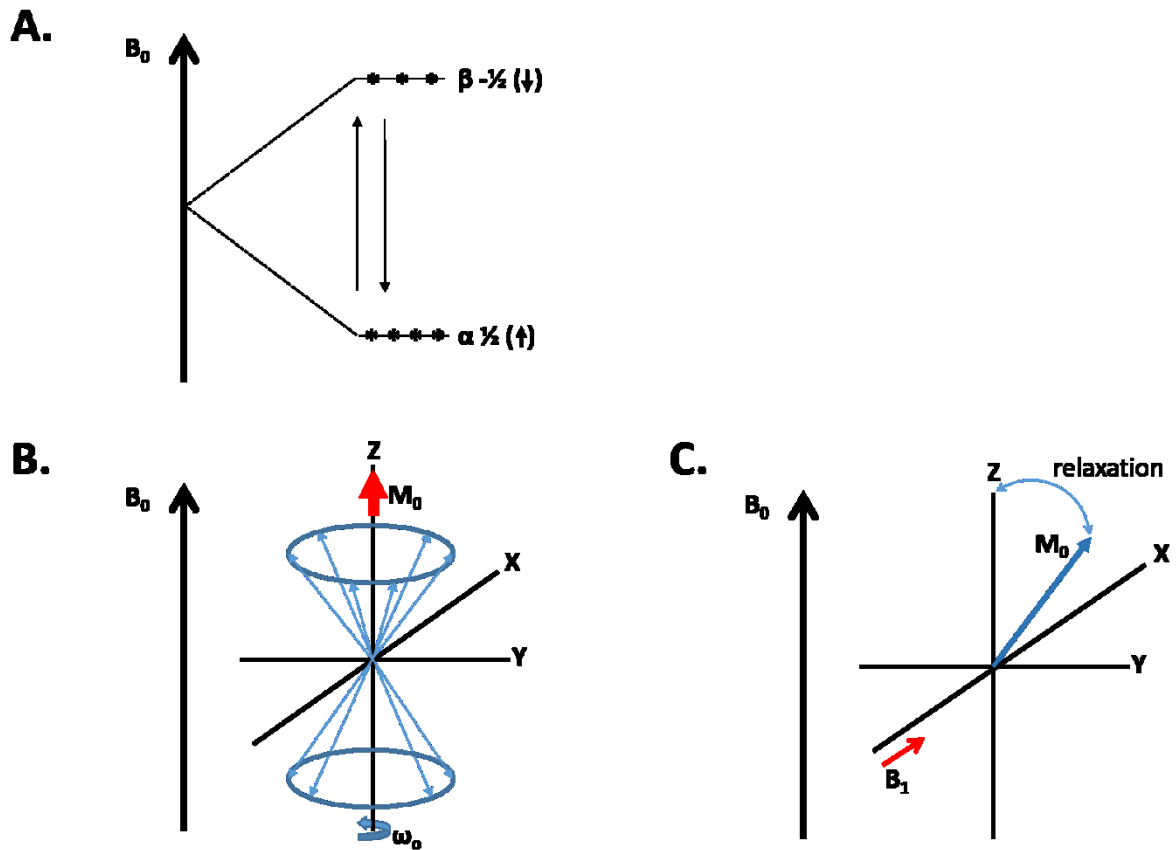


Figure 2.1: Theory of NMR spectroscopy. (A) Illustrates the nuclei distribution (*) in the two energy states when a magnetic field B_0 is applied. (B) Motion of net nuclei magnetisation which relaxes at the Larmor frequency in a magnetic field B_0 . (C) Effect of radio-frequency pulse B_1 on M_0 .

The difference between the two energy states results in the magnetisation vector M_0 lies along the direction of B_0 (along z axis). However, when a specific radio-frequency pulse is applied (B_1) at frequency ω , nuclear spins are excited to the higher frequency leading to a new orientation of M_0 . Once the pulse has stopped, the spins return back to equilibrium – a process known as relaxation. There are two major relaxation processes; the longitudinal (spin-lattice) relaxation and the transverse (spin-spin) relaxation. During the relaxation period, the NMR signal is detected as free induction decay (FID) and subsequently transformed to a NMR spectrum by mathematical process called a Fourier transform (Jardetzky and Roberts, 1981; Keeler, 2002).

The electric current around the nuclei produced a local magnetic field in the opposite direction to B_0 and shield it from the applied field. The magnetic field at the nuclei is not equal to the applied magnetic field. The difference between the applied field and the field at the nucleus is termed the nuclear shielding. The chemical shift is defined as the nuclear shielding divided by the applied magnetic field (Jardetzky and Roberts, 1981; Keeler, 2002).

Interaction between neighbouring groups produces splitting pattern of signals, which provides additional spectral information. This splitting pattern provides an idea about the connectivity of atoms within the molecule. Active nuclei that are close to another nuclei can influence each other's effective magnetic field. This is called spin-spin coupling or J-coupling. Spin-spin couplings from neighbouring groups within the molecule results in the splitting of NMR signals into two or more components. These components of the NMR signals are shifted from the original chemical shift (in ppm). The complexity of the splitting pattern is directly related to the number of neighbouring nuclei. The general rule of $n + 1$ is used for the multiplicity of splitting, where n is the number of protons on the adjacent atoms. For instance, a nucleus with two neighbouring protons will have their resonance signals split into three peaks called triplet. The two peaks in a multiplet are separated by a scalar coupling constant termed J-constant, and is independent of the external magnetic field (Keeler, 2002).

1.1.1 1D NMR spectroscopy

A 1D NMR uses a single pulse sequence that contains at least 3 parts: 1) the preparation time, also known as relaxation delay (in seconds), 2) the pulse width (in microseconds), and 3) the acquisition time (in seconds). The preparation time is the time in which the spins reach their equilibrium state. The pulse width is the length of time for a radio-frequency pulse to perturb the spin system. This is followed by the spins going back to their original state generating FID during the acquisition time (**Figure 2.2**). In order to increase signal to noise ratio, the radio-frequency pulse sequence is repeated multiple times to improve the signal to noise ratio. In metabonomics study of tissue extract and plasma metabolic profiles that contain a large amount of proteins and/or lipids, the high

molecular weight molecules typically produce broader resonances than the smaller metabolites. The Carr-Purcell-Meiboom-Gill (CPMG) is one of the examples for 1D NMR experiment. This experiment reduces the broad signals of macromolecules and allows a better observation of low molecular weight compounds.

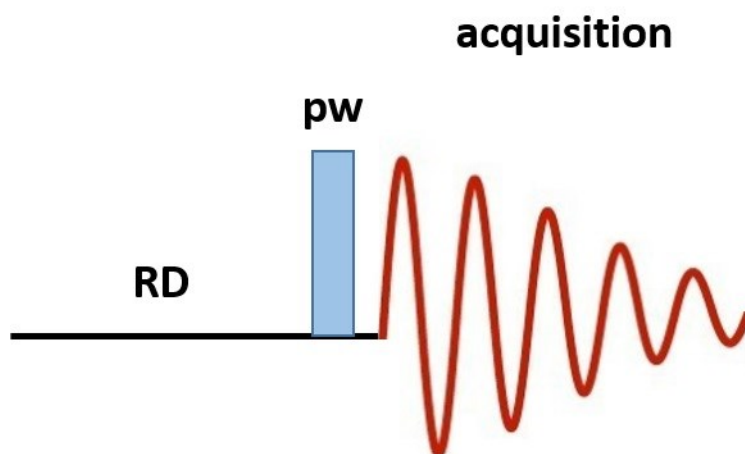


Figure 2.2: Standard one pulse sequence (RD: relaxation delay, pw: pulse width)

1.1.2 2D NMR spectroscopy

In 1D NMR metabolic profiles, large number of overlapped peaks makes the assignment work a tough challenge. Thus, it is important to perform 2D NMR experiment that can provide extra information about NMR peaks connectivity. This helps in the identification of unknown metabolites in the biological samples. In 2D NMR experiment, the signal is recorded on two time variables, t_1 and t_2 , and the resulting data Fourier Transformed twice to produce a spectrum with two frequency variables, F_1 and F_2 (Keeler, 2002). **Figure 2.3** presents the general scheme of 2D NMR spectroscopy.

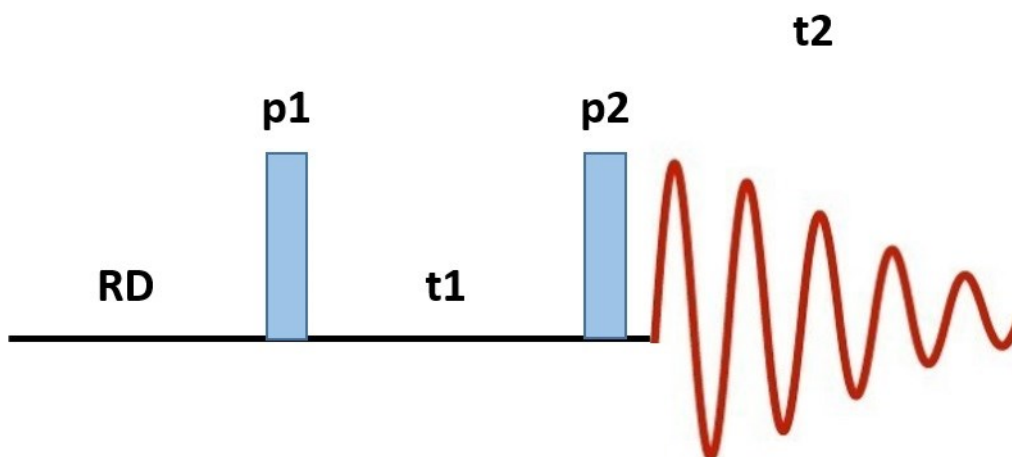


Figure 2.3: General scheme for 2D NMR spectroscopy. (RD: relaxation delay, p1: first pulse width to reach 90°, t1: evolution time, p2: second pulse width to reach 90°, t2: acquisition time)

In the first period, the spins are excited by several pulses. Then, the spin relaxation evolves for the first time period, t1. This follows by the second set of pulses during the mixing time. After this mixing period, the signal is recorded during the second time variable, t2. The signal is only recorded during the time t2 at the end of the sequence. The information present in the spectrum is determined by the nature and the time of pulse during the relaxation delay and mixing periods (Keeler, 2002). The example of 2D NMR experiments that normally used in metabonomics is the J-Resolved experiment (J-Res), the correlation spectroscopy (COSY), and the heteronuclear single quantum coherence (HSQC) experiments.

2.3 Statistical analysis

Metabolic profiling using NMR spectroscopy method produces high-density data sets. In order to analyse these huge data sets, the use of multivariate statistical analysis can be exploited. This statistical analysis method can be used to detect and visualise the main sources of variation as well as performing multivariate classification and discriminant

analysis. There are two types of pattern recognition methods that frequently being used, which are the unsupervised and supervised methods (Eriksson *et al.*, 2004; 2006).

2.3.1 Unsupervised method: Principal Component Analysis (PCA)

PCA is one of the simplest techniques that has been used widely in metabonomics (Nicholson *et al.*, 2007). It is a common unsupervised method used for which no 'prior' knowledge is required for the construction of the model. PCA is based on the representation of multivariate data comprising n rows (observation) and X columns (NMR variables). This method involves a mathematical procedure in which a number of variables (e.g. variables of NMR spectra), are transformed into a smaller number of components called principal components (PC). The first PC (PC1) accounts for the direction in the multidimensional space explaining the much of the variance in the data as possible. The second PC (PC2), which is orthogonal to the PC1 further improves the interpretation (**Figure 2.4**). PCs are constructed to give a low dimensionality representation of the data set. PCA is a common method in identifying outliers in large data sets (Trygg *et al.*, 2007; 2006).

Geometrically, one can imagine that NMR spectrum corresponds to a point in K – dimensional space, where K is the different variables. The scores plot (T) represents the point values of the observations in K -dimensional space, while loadings plot (P) describes the weight of variables in the model and identifies them (*i.e.* metabolites). Unexplained part of the matrix are referred to as residuals (E), that is defined by the distance between each observation and its projection on the PC space (Trygg *et al.*, 2007). Information from the PCA can be interpreted by both the scores plot and the loadings plot (**Figure 2.4**).

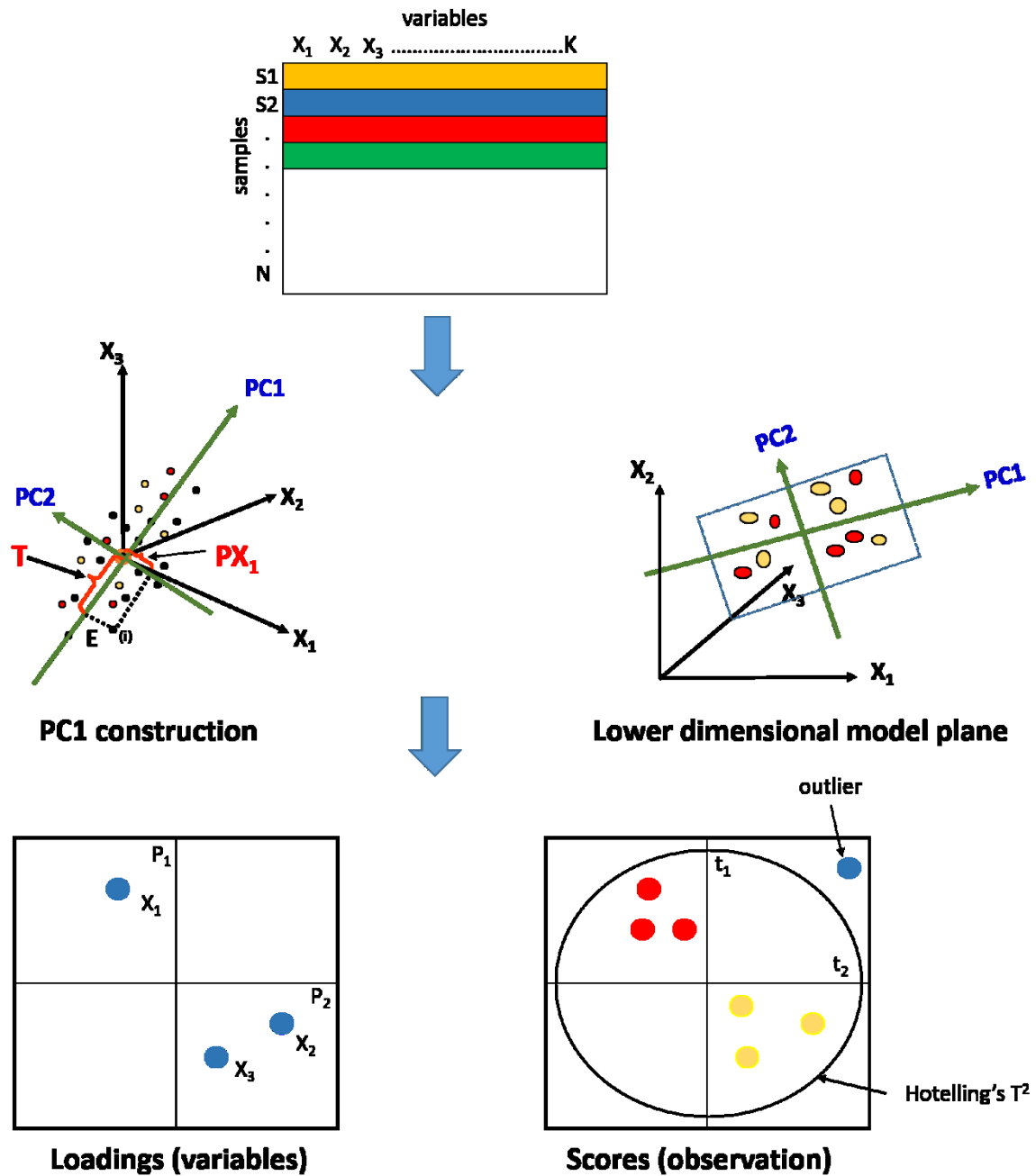


Figure 2.4: Diagrammatic representation of PCA. PCA is used to define the data in a lower dimensional space. The first principal component (PC1) describes the largest variations within the samples, followed by PC2 etc. The s samples are projected onto a hyperspace with x dimensions. Thus, a plane with dimensions k is built from the principal components. The score (T) characterises the position of every observation in the plane and the loading (P) shows the positions in space of s variation. Unexplained data is referred to as residual matrix (E).

2.3.2 Supervised methods

Unlike unsupervised methods, supervised methods rely on prior knowledge of classes. In metabonomics, most of the researchers are focusing on group classification such as between treated and untreated groups, therefore the use of supervised method is desirable (2006). One of the most commonly used supervised methods is partial least squares (PLS) (Nicholson *et al.*, 2007).

Supervised PLS regression is a method that relates a matrix that contains variables from samples (*e.g.* spectral data, the X matrix), to a second matrix (Y) containing quantitative values such as time or concentration of the treatments by linear regression (**Figure 2.5**). PLS aims to construct a model that maximises the covariance between X, *e.g.*, the spectral data, and the response variable (Y) (Bollard *et al.*, 2005). It can be used to investigate the influence of time or the dose responses on a data set, which is useful for NMR profiling of biofluids. PLS can also be used in a discriminant analysis, termed (PLS-DA), in which Y matrix contains dummy variables to maximise discriminant between the two classes.

However, X matrices often comprises a certain level of variation uncorrelated to the Y matrix which lowering the interpretability of the PLS model, typically when there is high within-group variance not directly associated with the between-group variance of interest. Therefore, orthogonal partial least square discriminant analysis (OPLS-DA) was developed as an extension of PLS-DA in which a built-in Orthogonal Signal Correlation (OSC) filter is added in the construction of the model (Cloarec *et al.*, 2005a; Fonville *et al.*, 2010; 2006). This OSC filter is used to model the within-class variation independently as orthogonal component (X_{ortho}) to the between-class variation (X_{pred}/Y_{pred}), thus improve the interpretation of the model (Trygg and Wold, 2002). Analysis of the score plot and the loadings plot of the orthogonal component can provide extra information on subgroup structure within the data (Cloarec *et al.*, 2005a; Trygg *et al.*, 2007). **Figure 2.6** illustrates comparison between PCA, PLS-DA, and OPLS-DA.

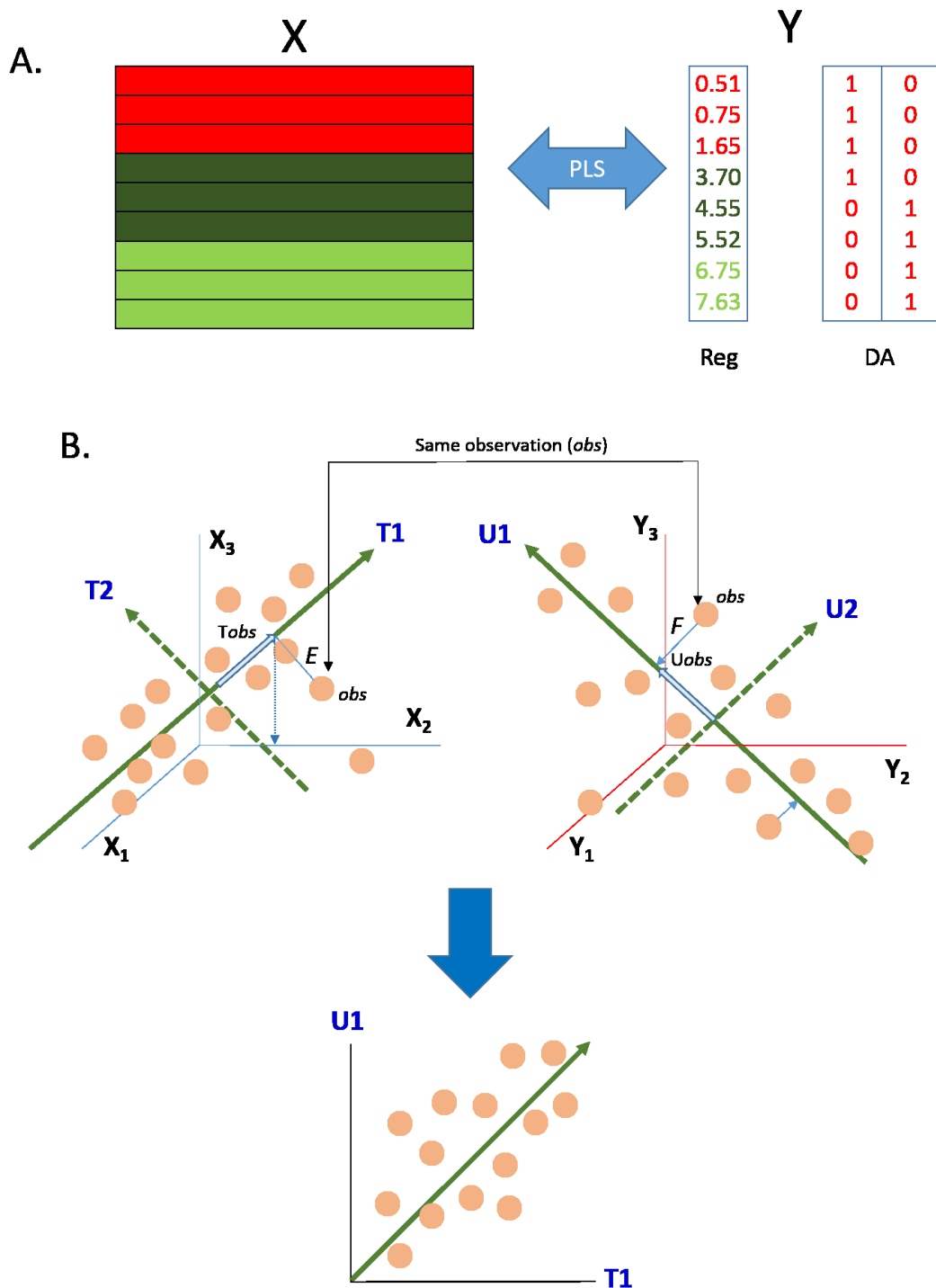


Figure 2.5: PLS schematic. (A) PLS regression tries to explain Y using X variables and PLS-DA models separation between classes. (B) Multidimensional X matrix (top left) represents the predictor and the multidimensional Y matrix (top right) represents the response to predict. In each multivariate space, the orientation of the first component must approximate as well as possible the shape of the point cloud and the scores T1 and U1 should be maximally correlated. The second component is orthogonal to the first component using the same principle.

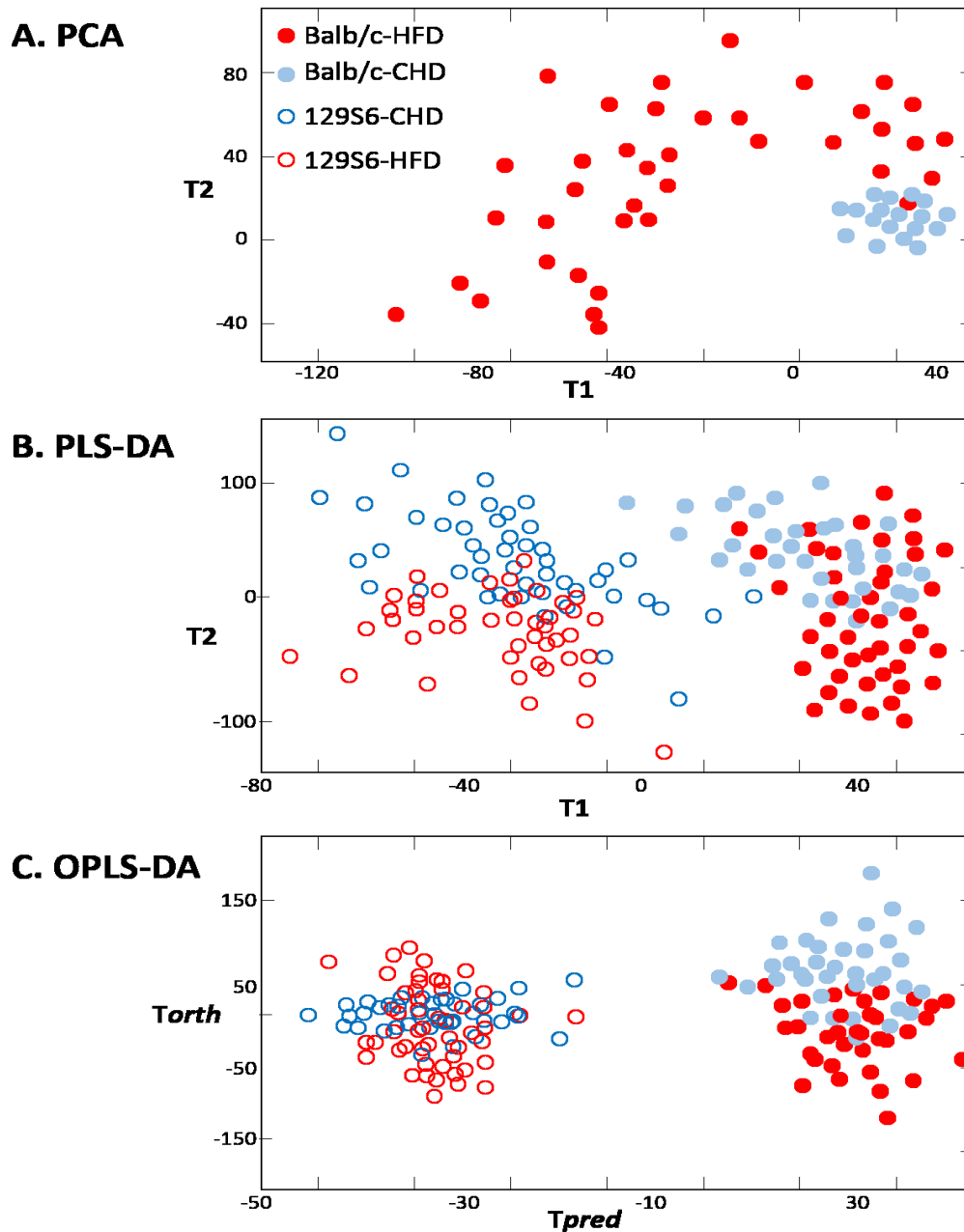


Figure 2.6: Comparison between PCA, PLS-DA, and O-PLS-DA. (A) Unsupervised PCA shows that the two diet groups have very different variance structure, which overwhelms the genetic background. (B) PLS-DA discriminates the two strains resulting in good separation of the genetic background, but because of the strong diet-related within-group variance (i.e. orthogonal noise), the scores plot shows a significant dietary effect on T2, but a weak genetic discrimination on T1. (C) OPLS-DA shows a clear discrimination on Tpred, while Torth provides a strong within-group variance based on the effect of diet. Adapted from Fonville *et al.*, (2010) with modification.

Additionally, in OPLS regression and OPLS-DA models, R^2_X and R^2_Y indicate the proportion of explained variance and so estimate the robustness of the model. However, in constructing multivariate models, it is easy to over-fit the models. Thus, in order to avoid over-fitting, a cross-validation (CV) step is applied to assess the real predictability of the model (**Figure 2.7**). In 7-fold cross-validation, 6/7th of the data are considered as training set, and 1/7th of the data as test set. A model is fitted on calibration set and then the test set is projected back into the models to test the performance of the model. This step is repeated until all data have been once kept out. This results in the determination of the cross-validation parameters (Q^2_Y), indicating the percentage of predicted variance from the Y vector in the tested model. Q^2 value above 0.5 is regarded as a good value, thus the model is strong enough to be used for data interpretation (Eriksson *et al.*, 2004). In addition, a permutation test can also be used for model validation which estimates the significance of the estimated predicted power (Q^2_Y). The significance of the model is determined by the p -value calculated from the permutation test (Eriksson *et al.*, 2004).

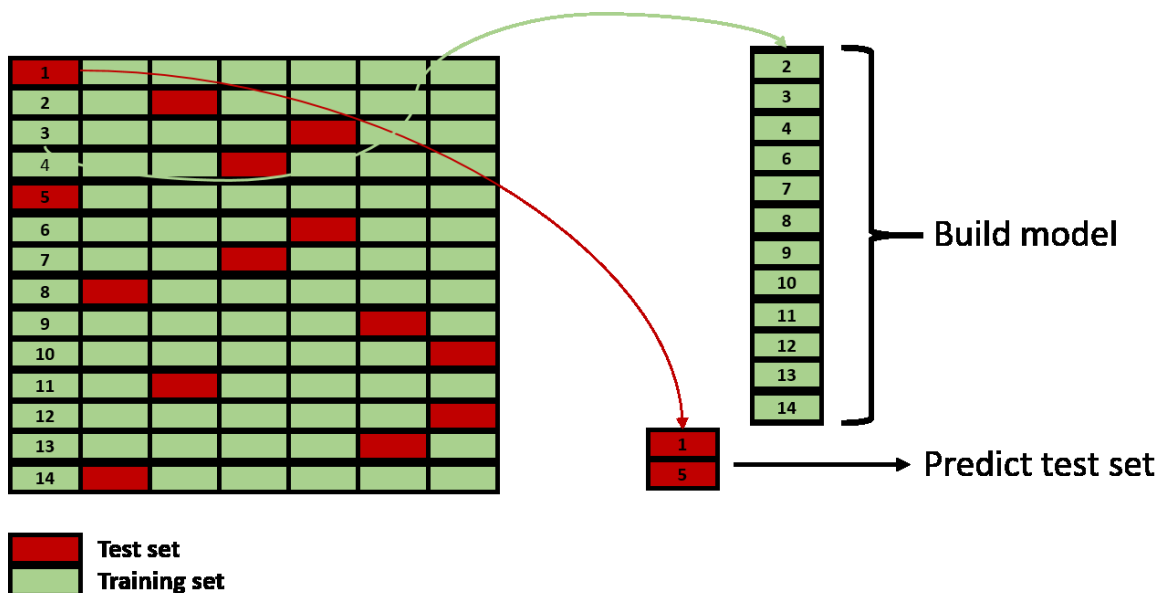


Figure 2.7: A 7-fold cross validation. Cross validation is a technique used to protect against over-fitting in a predictive model.

Using a back-scaling method, OPLS regression coefficients are displayed, producing a pseudo unit-variance scaled NMR spectrum, which is colour coded (from red to blue) according to correlation coefficient. This is represented by the squared regression coefficients (R^2) (Cloarec *et al.*, 2005a). While the hot colours are assigned to high correlated variables, the cold colours represent the non-significant correlation variables. This method has been shown to be a useful tool in helping the interpretation of the loadings plot by facilitating the identification of the most influential metabolites (Cloarec *et al.*, 2005b).

2.4 Cell culture

2.4.1 HepG2 cell line

HepG2 is an immortalised hepatocarcinoma cell line derived from liver tissue of patient with well-differentiated hepatocellular carcinoma. HepG2 cells are adherent, epithelial-like, and grow as monolayers. These cells synthesise and secrete a variety of major human plasma proteins including albumin and transferrin (Knowles *et al.*, 1980). HepG2 cells can be used as a model system for liver cancer metabolism study as well as for studying the toxicity of xenobiotics (Knowles *et al.*, 1980). The protocols used for maintaining and subculturing of this cell line are explained in chapter 3 (**section 3.2.1**).

2.4.2 HepaRG™ cell line

HepaRG™ are terminally differentiated hepatic cell line derived from a human hepatic progenitor cell. HepaRG cell line has been established from a liver tumour associated with chronic hepatitis C, and is capable to differentiate into two different cell phenotypes, which are biliary-like epithelial and hepatocyte-like cells when differentiation medium containing DMSO is introduced (Parent *et al.*, 2004). HepaRG™ cells exhibit many features and characteristics of primary human hepatocytes, and has been used to investigate drugs metabolism and toxicity studies (Marion *et al.*, 2010).

2.4.3 3T3-L1 cell line

3T3-L1 cell line is derived from clonal expansion from murine fibroblast 3T3 cells (Green and Meuth, 1974). This cell line has been used extensively as an *in vitro* model of adipocyte because of its ability to differentiate from fibroblasts to adipocytes under appropriate conditions (Poulos *et al.*, 2010). 3T3-L1 cells stop growing when they reach a confluent monolayer, and the addition of pro-differentiation agents such as insulin, dexamethasone, and 3-isobutyl-1-methylxanthine (IBMX), at concentrations of usually 1 µg/mL, 0.25 µM, and 0.5 mM, respectively, induced the differentiation into adipocytes-like cells (Green and Kehinde, 1975; Rubin *et al.*, 1978; Russell and Ho, 1976). After hormonal induction, the 3T3-L1 preadipocytes begin to accumulate lipid and undergo terminal differentiation into mature adipocytes. Mature adipocytes are characterised by having high expression of adipogenic genes and high cytoplasmic storage of triglyceride (Student *et al.*, 1980). The protocols for 3T3-L1 differentiation were elaborated in chapter 6 (**section 6.2.2**).

2.4.4 CHO-K1 cell line

In chapter 5, the assays used in this chapter for the screening of the ligands were provided by DiscoverRx, USA. CHO-K1 cells overexpress human receptors, FFAR2, FFAR3, and GPR109A were used as the cell model for these kits. CHO-K1 cell line is derived from the original Chinese hamster ovary (CHO) cell line (Lewis *et al.*, 2013). CHO-derived cell lines are the most preferred host expression system due to having manufacturing adaptability (Xu *et al.*, 2011). The genes of these cells also can easily be manipulated and can be grown as adherent or in suspension. Moreover, the methods for cell transfection, gene amplification in CHO cells also have been well optimised. In addition, CHO cells have fast growth rate and high protein productivity, as well as stable gene expression (Lim *et al.*, 2010).

2.4.5 Justification of the cell line used for chapter 3 and chapter 4

In chapter 3 and chapter 4, HepG2 cell line has been selected as the hepatocyte cell model to investigate the effect of SCFAs on the host's metabolism. This cell line is a hepatocarcinoma cell line and has been previously used to study drugs metabolism and toxicity. Hence the findings generated from this study will therefore explain the effect of SCFAs on hepatic cancer metabolism and not the metabolism of normal hepatocytes. Another cell line has also been tested and considered which was HepaRG™. However, a number of problems were encountered when dealing with this cell line, such as inconsistent growth rate, long differentiation time, and cost ineffective. Moreover, the cell line also is a terminally differentiated cell line and licence is needed in order to propagate the cell line. Due to these stated reasons, it is decided to not continue working with the HepaRG cell line and HepG2 is used as the hepatic cell model for the study carried out in chapter 3 and chapter 4.

2.5 Biological assays

2.5.1 Cell viability

Measuring cell viability is important in cell culture experiments. A cell viability assay is often used to determine if the test compounds have effects on cell proliferation at certain concentration. It is very important to know the number of viable cells at the end of the experiment. In this thesis, two types of cell viability assays were used: PrestoBlue, a resazurin-based reagent measuring mitochondrial activity and crystal violet dye which stain the nucleus.

2.5.1.1 PrestoBlue® (Invitrogen) reagent

PrestoBlue, a resazurin-based reagent, contains a cell-permeant compound that is blue in colour and almost non-fluorescent in solution. This reagent is rapidly taken up by the cells when added to the culture media. Inside viable cells, resazurin is reduced by the

reducing environment in mitochondria, thus indicating mitochondrial metabolic activity. In this condition, resazurin is converted into its reduced form of resorufin, resulting in a red-fluorescent dye which can be quantitatively measured to determine viability (**Figure 2.8**). This reagent can measure as low as 12 cells/well with a short incubation time (≥ 10 min) (Invitrogen, 2010). This method is used in chapter 3 and 4.

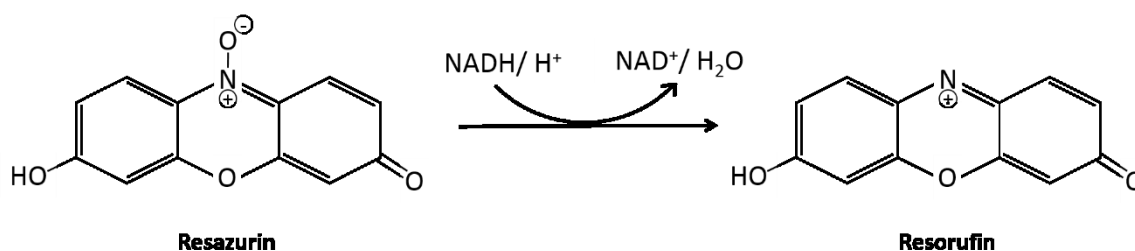


Figure 2.8: Reduction of resazurin to resorufin in living cells.

2.5.1.2 Crystal violet staining assay

The crystal violet staining (CVS) method was developed by Saotome *et al.*, (1989) for evaluating the cytotoxicity of the chemicals. It is a triarylmethane used as a histological staining and also can be used to stain adherent cells. It is in blue-violet colour and can be measured at the maximum of 590 nm (Adams and Rosenstein, 1914). This dye stains nuclei, thus enhancing their visualisation under the microscope, whilst providing a quantitative readout. This method is used in chapter 6.

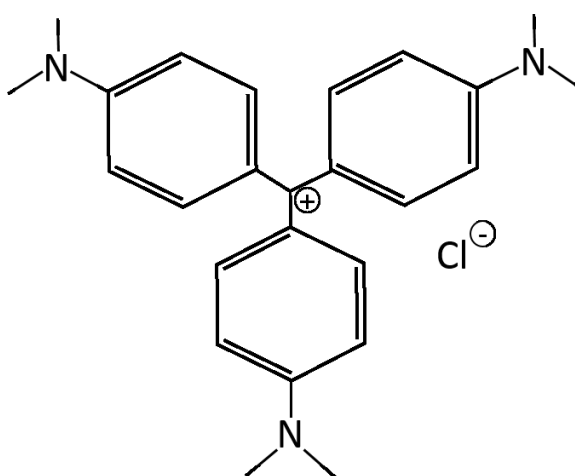


Figure 2.9: Chemical structure of crystal violet.

2.5.2 Lipid staining (Oil Red-O)

When 3T3-L1 cells undergo differentiation, they change their fibroblastic shape cells to rounded cells with an increasing number of intracytoplasmic lipid droplets (Green and Meuth, 1974). The accumulation of intracytoplasmic lipid has been shown to be directly proportional to the differentiation of the cells (Kuri-Harcuch and Green, 1978). Based on this relationship, staining of the intracytoplasmic lipid droplets using Oil Red-O (ORO) staining method has been used to qualitatively measure the differentiation of this cell line from 3T3 pre-adipocytes to 3T3 adipocytes (Kuri-Harcuch and Green, 1978). ORO ($C_{26}H_{24}N_4O$, **Figure 2.10**) is a fat soluble diazot dye that is suitable for the histochemical staining of neutral lipids and cholesteryl esters, but not biological membranes (Fowler and Greenspan, 1985). The principle of ORO staining is that this dye has a very low solubility in the solvent, and the solubility even lower when ORO is diluted in water prior to be used. Therefore, this dye will move from the solvent, and stain the lipid within the cytoplasm. ORO can be measured with a maximum absorption at 518 nm (Kuri-Harcuch, 1978; Kuri-Harcuch and Green, 1978). This method is used in chapter 6.

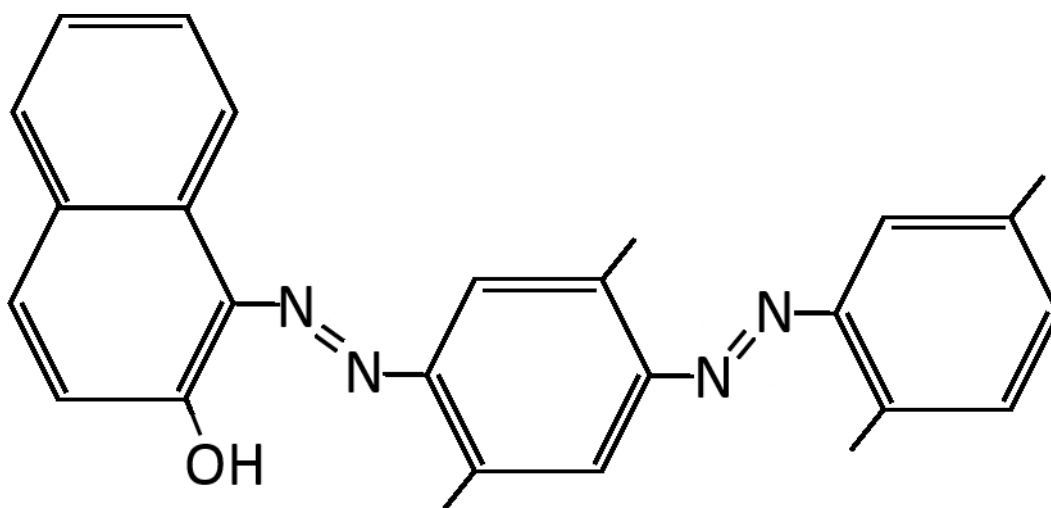


Figure 2.10: Chemical structure of Oil Red-O (1-(2,5-dimethyl-4-(2,5-dimethylphenyl)phenyldiazenyl) azonaphthalen-2-ol).

2.5.3 Lipolysis assay

In vitro, an increase in lipid accumulation can be observed in well-differentiated 3T3-L1 adipocytes. The stored TGs in lipid droplets undergo continuous synthesis and breakdown. The hydrolysis of TGs produces free fatty acids (FFAs) and glycerol, which are subsequently released into the surrounding environment. In cells, lipolysis is triggered by the activation of β -adrenergic receptors by its ligand. These receptors are coupled with Gs protein family which activation leads to the stimulation of cAMP-dependent pathway by adenylate cyclase. This resulted in the increase of intracellular cAMP level which in turn activates protein kinase A (PKA), resulting in increased activity of the enzyme, hormone sensitive lipase (Kim, 2005). Lipolytic activity in the cells can be assessed by measuring the glycerol release into the medium as a consequence of TGs hydrolysis. In this study, Free Glycerol Determination Kit (FG0100, Sigma) was used to measure the glycerol in the medium. The kit measures free glycerol using several steps of enzymatic reactions. Glycerol released to the medium is first phosphorylated by adenosine triphosphate (ATP) forming glycerol-1-phosphate (G-1-P) and adenosine-5'-diphosphate (ADP) in the reaction catalysed by glycerol kinase (GK). Then the G-1-P is oxidized by glycerol phosphate oxidase (GPO) to dihydroxyacetone phosphate (DAP) and hydrogen peroxide (H_2O_2). Peroxidase then catalyses the coupling of 4-aminoantipyrine (4-AAP) and sodium N-ethyl-N-(3-sulfopropyl) m-anisidine (ESPA) with H_2O_2 to produce a quinoneimine dye. This dye shows an absorbance maximum at 540 nm. The absorbance at 540 nm is directly proportional with the glycerol concentration in the sample (Sigma-Aldrich, 2014). This method is used in chapter 6.

CHAPTER 3

3. METHODOLOGICAL OPTIMISATION OF NEGATIVE CONTROL GROUPS: THE EFFECT OF SODIUM CHLORIDE (NaCl) TREATMENT ON HEPG2 CELLS GROWTH AND METABOLISM.

3.1 INTRODUCTION

Inorganic ions are one of the essential compounds for living systems to maintain the system homeostasis. Ions such as sodium (Na^+), potassium (K^+), and chloride (Cl^-), are not only involved in many enzymatic reactions, but they also contribute to other physiological role such as maintaining the osmotic pressure of body fluid and regulating the macromolecular behaviour (Northwestern University, 2011). Na^+ is the main electrolyte that functions in regulating extracellular fluid in the body (Pohl *et al.*, 2013). It is also essential in balancing the concentration gradient for the transmission of signal in nerve and muscle cells, as well as maintaining acid-base balance and plasma volume (Bouchard *et al.*, 1993).

Cell culture medium, also called growth medium, is a culture medium used to supply nutrients to support the growth of cells. Typically it is in the form of liquid or gel (Arora, 2013). Generally, culture media contain the complete nutrients for the growth of the cells such as amino acids, vitamins, glucose, and several other essential compounds. Culture media also contain a mixture of different concentration of inorganic salts, also called balanced salt solution. These inorganic salts are introduced to balance osmotic pressure and maintain optimum pH of the medium (Ham and McKeegan, 1979). Making

sure that the pH of the culture media is in an optimum range will ensure the survival of the cells in the culture. NaCl is the major inorganic salt in most of the culture media and the optimum growth for most of the cell line can be achieved at NaCl molarity between 100-130 mM (Stubblefield and Mueller, 1960). The importance of NaCl in mammalian cell culture experiment has been studied extensively over the years. High NaCl concentration has been shown to cause DNA damage in both cell culture and *in vivo* experiments (Dmitrieva, 2004). Kidney cells, however, have been shown to be exposed to high NaCl levels which can be in excess of 500 mM. Although these cells appear to be healthy, DNA damage could be detected (Dmitrieva and Burg, 2005). In addition to high NaCl concentrations, a previous study has also shown that reducing sodium chloride concentration to 90 mM below the normal levels affects proliferation of chicken fibroblasts (Balk and Polimeni, 1982).

This current chapter aimed to assess the effect of NaCl on the growth and metabolism of HepG2 hepatocarcinoma cell line using cell biology and ¹H NMR-based metabolomic approaches. This is particularly relevant as the ultimate aim is to assess the effect of short-chain fatty acids (propionate and butyrate) in regulating HepG2 cells metabolism, in the next chapter. SCFAs will be used in the form of sodium propionate and sodium butyrate, sodium being used as a counter-ion. So, the current chapter will serve as a preliminary methodological optimisation study deciphering the effect of sodium as a counter-ion from the effect of short-chain fatty acids (propionate and butyrate) and eliminate potential biases in later experiments.

3.2 MATERIALS AND METHODS

3.2.1 Cell culture

In this study, HepG2 cell line, which is a perpetual cell line originated from the 15-years-old Caucasian American male's liver tissue with a well-differentiated hepatocellular carcinoma, was used as a hepatocyte model to assess the effects of sodium salt have on liver metabolism and signalling. The HepG2 cell line were obtained from American Type

Culture Collection (ATCC) and were maintained in complete growth medium containing Eagle's Minimum Essential Media (MEM, Gibco®), 1% v/v of L-glutamine (Gibco®) and 10% v/v fetal bovine serum (FBS, Gibco®) as recommended by the manufacturer. The complete growth media was also supplemented with 1% v/v Penicillin-Streptomycin (100U/mL, 100µg/mL respectively) (Gibco®) to prevent any contamination caused by gram-positive and gram-negative bacteria that might occur.

Nutrients to support the cell growth are supplemented to the FBS. The FBS contains nutrients such as essential fatty acids, cholesterol, serum growth factors (insulin, insulin-like growth factor (IGF) and epidermal growth factor (EGF)), endocrine growth factors (androgen, triiodothyronine), as well as cell attachment proteins such as fetuin (Hedlund and Miller, 1994).

3.2.2 Cell thawing and seeding

To culture the cell line, a cell vial was removed from liquid nitrogen storage and was immediately placed on dry ice in a covered container prior to thawing. The cell vial was left in the container for at least one minute before opening the vial in order to allow any liquid nitrogen inside the vial to evaporate. The cell vial was then allowed to reach room temperature for 1-2 minutes, and was warmed in a water bath (37°C) until partially thawed. Approximately 0.5 mL of pre-warmed complete growth media was added to the vial and the mixture was then centrifuged at 300 x g for 5 minutes to pellet the cells. The cell freezing media containing DMSO was removed and the cell pellet was resuspended in 15 mL pre-warmed complete growth media. The cells were transferred to a T75 flask and were incubated for 24 hours at 37°C and 5% air in cell culture incubator. After 24 hours, the growth media was gently removed, and was replaced with 15 mL fresh complete growth media. Upon reaching confluency, the cells were transferred into T75 flasks for routine culturing.

3.2.3 Cell maintenance and passaging

HepG2 cells were routinely maintained in T75 plastic flasks (Falcon, Merck Eurolab, Strasbourg, France) with 15 mL complete growth media with sub-cultivation ratio of 1:4 to 1:6 and medium renewal twice a week. The cells were used between passage 4 and 30. After reaching ~80% confluency at day 4-5 in culture, the cell monolayer was first washed twice with sterile 1x Dulbecco's phosphate-buffered saline (DPBS, Gibco®) to remove all traces of serum. 1x dissociation reagent (Trypsin-EDTA (ethylenediaminetetraacetic acid), Gibco®), prepared by diluting the stock solution of 10x Trypsin-EDTA using sterile DPBS was used to detach the cells. Cells were gently pipetted up and down to minimise the trypsinisation time. Once the cells are detached, 1 volume of complete medium was added to the cells-trypsin mixture to deactivate the trypsin-EDTA. The mixture was then centrifuged at 1000 rpm for 5 minutes to pellet the cells. The supernatant was removed and the cell pellet was re-suspended in fresh complete growth medium and then seeded into new T75 flask.

3.2.4 Cell count

Cells were manually counted by using haemocytometer and Trypan Blue reagent was used to determine cell viability. Trypan Blue dye method of determining cell viability is based on the principle that live cells do not taken up certain dyes, but dead cells do, due to permeabilisation of their cell membrane, allowing differentiation between live and dead cells. Briefly, an aliquot of the cell suspension (10 µL) was added to an equal volume of 0.4% Trypan Blue (dilution factor of two). The mixture of cells and Trypan Blue were gently mixed by pipetting up and down and incubated at room temperature for 1-2 minutes. Approximately 8 µL of the mixture was then loaded onto each side of the haemocytometer. Live cells (non-blue) were counted in 10 squares, averaged, and the total number of live cells was determined by:

$$\text{Cell number} = \text{cell count (per square)} * 2(\text{dilution factor}) * 10^4$$

3.2.5 Cell freezing

To prepare stocks of cells, the early passage number of cells was frozen in liquid nitrogen. Cells were harvested, pelleted, and counted as described in previous section. The cell pellet was resuspended in freezing media containing 95% complete growth media and 5% of the cryoprotectant dimethylsulphoxide (DMSO) at final concentration of 1.0×10^6 cells/mL. The cells were frozen at -80°C in a foam cooler for 24 hours before finally transferred to liquid nitrogen dewar for long term storage.

3.2.6 Cell proliferation assay- PrestoBlue®

PrestoBlue® (Life Technologies) is a cell-permeable resazurin-based dye that use as cell viability indicator. This reagent uses the reducing power of living cells, and when added to cells, the reducing environment of the live cells modified the PrestoBlue® reagent and changes the colour to red, thus make it highly fluorescent. The fluorescent signal is directly proportional to the viable cells present in the sample and used to quantitatively measure the cell number.

In this experiment, HepG2 cells were incubated with complete growth medium with the addition of different doses of sodium chloride (NaCl). The cells were incubated at three different time points, which are 24, 48, and 72 hours. Briefly, at the start of the experiment, 60,000 cells/well were seeded in 96 well-plates and were culture in complete growth medium at 37°C . Twenty-four hours later, the growth media was changed and NaCl was added to the fresh complete growth media at final doses of 0.1 nM, 1.0 μM , and 1.0 mM. Complete growth medium without the addition of NaCl was used as control for this experiment. Upon reaching the time points described above, PrestoBlue® reagent was added directly to the cells in each well to obtain 1x final PrestoBlue® concentration in the well. The sample was then incubated at 37°C for 30 minutes and the plate was read on the FLUOStar microplate reader, at 535 nanometres (nm) excitation and 615 nm emission (ex/em) to measure cell viability. The reading of the well that contains only media and dye was used for background removal.

3.2.7 pH optimisation of the culture media

Culture media pH plays an important role in maintaining the optimum growth of the cells. In order to maintain its pH level, the growth media contains a mixture of inorganic salts known as a balanced salt solution. This allows the medium to maintain the pH and the osmotic pressure. In this part, in order to assess the effect of salt addition on the pH of the growth media, the complete growth media was prepared with the addition of different types of salts (sodium chloride (NaCl), sodium bicarbonate (NaHCO₃), sodium hydroxide (NaOH)) with varying final doses of 0.1 nM, 1.0 μM, and 1.0 mM. The sample was warmed in a water bath (37°C) and the pH of the media was then measured using bench top pH meter (Sigma).

3.2.8 Cell culture preparation for ¹H NMR study

HepG2 cells from ~80% confluent T75 culture flask were harvested and seeded at a density of 6.0×10^4 cells/well in 24 well-plates using complete growth medium prior to the experiment. The cells were left to grow in cell culture incubator for 24 hours for adhesion. After 24 hours, growth medium was removed and a fresh growth medium with the addition of NaCl at different final doses as describe in previous section (**section 3.2.7**) was added. Experiment was performed for 24, 48, and 72 hours with sample number of six for each conditions (n=6). At each designed time points (24-, 48-, and 72-hr exposure of NaCl), the cells were harvested and the culture medium samples were collected for ¹H-NMR analysis. **Figure 3.1** summarises the design for this experiment.

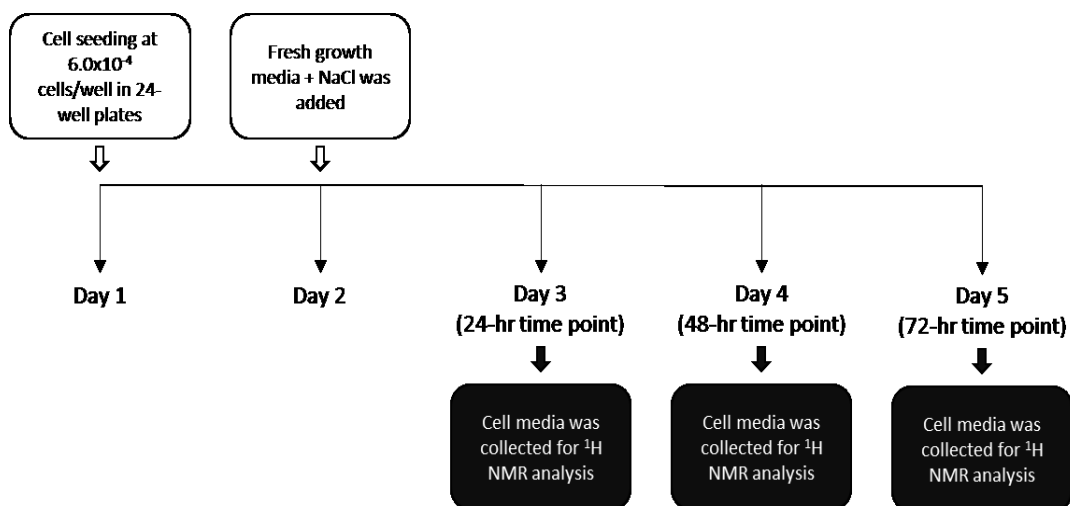


Figure 3.1: Experimental design for the exposure of HepG2 cell to the NaCl treatment.

3.2.9 Sample preparation for ¹H-NMR cell supernatant analysis

After reaching each incubation time point, cell media supernatant was collected and prepared for ¹H-NMR analysis according to Ellis *et al.*, (2011). Briefly, 1 mL of cell medium was transferred to Eppendorf tube and was centrifuged 5 minutes at 10 000 rpm to remove any remaining cell pellet. After centrifugation, 550 μ L of cell media supernatant was carefully transferred to a new clean tube. A volume of 50 μ L of D₂O (mix with 0.2% TSP (w/v)) was then added into the tube and the mixture was vortex to mix. 550 μ L of the mixture was transferred into 5 mm NMR tubes for analysis.

3.2.10 Metabolic profiling by ¹H-NMR spectroscopy

The metabolic profiling of the HepG2 cell culture media was carried out on a Bruker spectrometer operating at 600-MHz ¹H frequency. High-resolution, 1D, ¹H NMR spectra of culture media were acquired at 14.1 T (600.13 MHz ¹H frequency) using a Bruker AVANCE 600 spectrometer (Bruker Biospin, Rheinstetten, Germany) by performing 128 scans and 16 dummy transients. The temperature of NMR experiment was maintained at 300 K. The water signal was suppressed at δ 4.7 by a presaturation pulse during relaxation delay (RD, 3 s). For each sample, free induction decays (FID) were multiplied by an exponential function

corresponding to a line broadening of 0.3 Hz before Fourier transformation. Data NMR spectra were phased automatically, baseline corrected, and normalised to TSP signal at $\delta 0.00$. The metabolites identification and assignment were carried out from 1D NMR data using Chenomx NMR suite 7.0 software, published assignments and The Human metabolome database (HMDB)(<http://www.hmdb.ca/>) (Wishart *et al.*, 2007).

3.2.11 Data processing and multivariate data analysis

The spectral data were exported in Matlab software (R2012b version Mathwork Inc, Natwick MA) and signals were aligned using in-house software (Shintu *et al.*, 2012). The spectra were discarded at the region of $\delta 4.68$ -5.00 to remove the variation caused by the residual water resonance. The pre-processed spectra were then analysed by using multivariate data analysis such as Orthogonal Partial Least-Squares (OPLS) and Discriminant Analysis based on Orthogonal Partial Least-Squares (OPLS-DA). To identify relevant features in the metabolic profiles, OPLS regression coefficients were back-scaled using a back-scaling method which allows the estimation of the proportion of variance for each NMR variable.

3.2.12 Metabolite-Set Enrichment Analysis (MSEA)

In order to identify pattern of the significant metabolites (significant metabolic signature) in biologically meaningful context, Metabolite-Set Enrichment Analysis (MSEA) was carried out. The list of the significant metabolites obtained from OPLS-loadings plots was tested to see whether there is an enrichment of metabolites of a particular pathway within the significant metabolic signature. (<http://www.msea.ca/>) (Xia and Wishart, 2010).

3.3 RESULTS

3.3.1 Complete growth media is able to maintain its pH after the addition of different types of sodium salts.

In order to study the effect of the addition of different salts concentrations on the growth and metabolism of HepG2 cells, first the pH reading of the media after the addition of the salts were measured. This is to eliminate any effect that might be seen later on that caused by the extreme pH change of the media. Complete growth media was prepared as described in methodology section and was mixed individually with sodium chloride, sodium bicarbonate, and sodium hydroxide at different final doses of 0.1 nM, 1.0 μ M, and 1.0 mM. The pH of the complete growth media-sodium mixture was then measured to see if the addition of sodium at any doses were able to change the pH of the media out of the optimum range for cell growth. The addition sodium chloride (NaCl), sodium hydroxide (NaOH), and sodium bicarbonate (NaHCO_3) to the complete growth medium did not show any extreme variations on the pH of the growth media as shown in **Figure 3.2**. Under normal conditions, the pH of the complete growth media was measured at around pH 7.5. The addition of NaOH and NaHCO_3 at the molarity of 0.1 nM, 1.0 μ M, and 1.0 mM, but not for NaCl, slightly increased the pH of the growth media. However, these pH change are not extreme, and the net effect of the pH change compared to the control (complete growth media) is only a small reduction by about 0.02 and for the highest pH is by 0.03. The complete growth media was able to maintain its pH in optimum pH range due to the good buffering ability of the media. The initial molarity of NaCl and NaHCO_3 in the cell medium (MEM medium) are 117.24 mM and 26.20 mM, respectively. In this study, the highest molarity added was 1.0 mM which was approximately 1/100 the initial molarity of NaCl in the medium. This dose is respectively low to have any effect on the pH of the media as the buffering capacity of the media was able to maintain its pH. This result shows that the addition of all tested sodium doses in this study were not able to bring the pH of the media out of the optimum pH range. It also suggests that any effects shown by growing HepG2 cells with these doses are unlikely to be due to the modulation of the pH of the growth media.

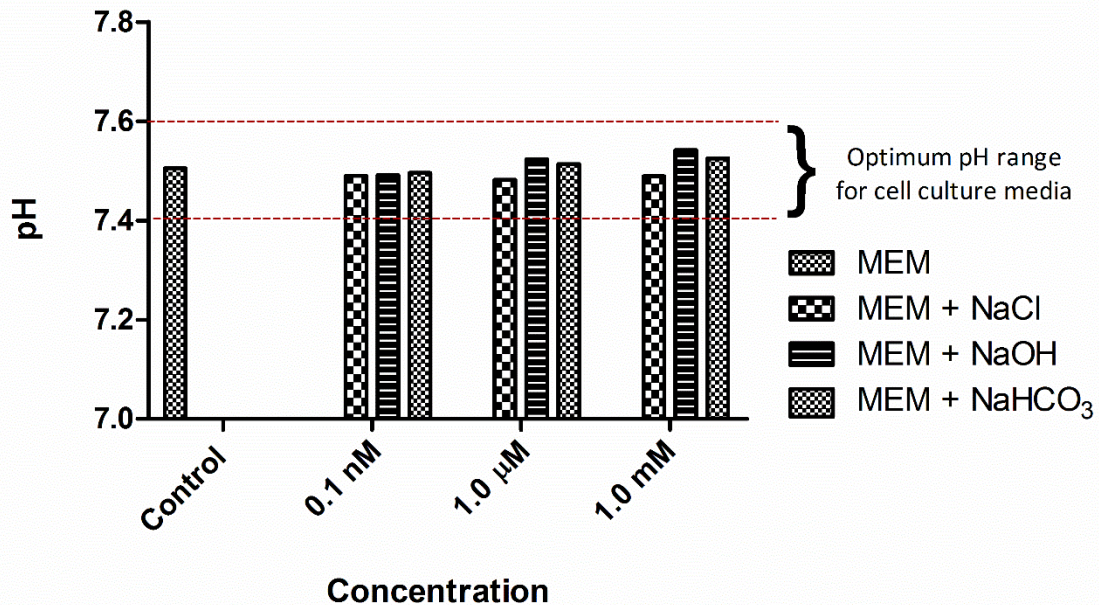


Figure 3.2: pH of growth media. NaCl, NaOH, and NaHCO₃ were individually added to the complete growth media at different final doses and the pH of the media was read using bench top pH reader to see any change in the pH.

3.3.2 The effect of different sodium chloride (NaCl) doses on the growth of HepG2 cells.

In the previous section, it has been shown that the growth media was able to maintain its pH even after the addition of the highest dose of sodium. In this study, NaCl was selected as sodium control due to the fact that it has been used widely in molecular biology applications and considered as an essential nutrient for living cell. The effect of NaCl on HepG2 cells viability was assessed by adding NaCl to the complete growth media to have the final NaCl doses of 0.1 nM, 1.0 μM, and 1.0 mM. **Figure 3.3** presents the results obtained when HepG2 cells were cultured in the growth media containing different doses of NaCl at three different time points which are 24, 48, and 72 hours. At 24 hours incubation, the addition of NaCl increases the cell viability when compared to the control in a dose-dependent manner. The highest cell viability reading was measured at 1.0 μM of NaCl with approximately 10% more viable cells when compared to the control. This however, was not statistically significant ($p > 0.05$) when compared to the control group.

The same trend was also observed for the samples at 48- and 72-hour time points with an increase in cell viability of ~3% and ~8% of the control's level respectively. Despite showing an increasing trend in cell viability except for the highest tested dose, none of the conditions were significantly different when compared to their respective control ($p>0.05$). These cell viability results suggest that the addition of sodium in the form of NaCl to the complete growth media was not able to cause any significant changes in HepG2 cells growth and viability even at the highest tested dose.

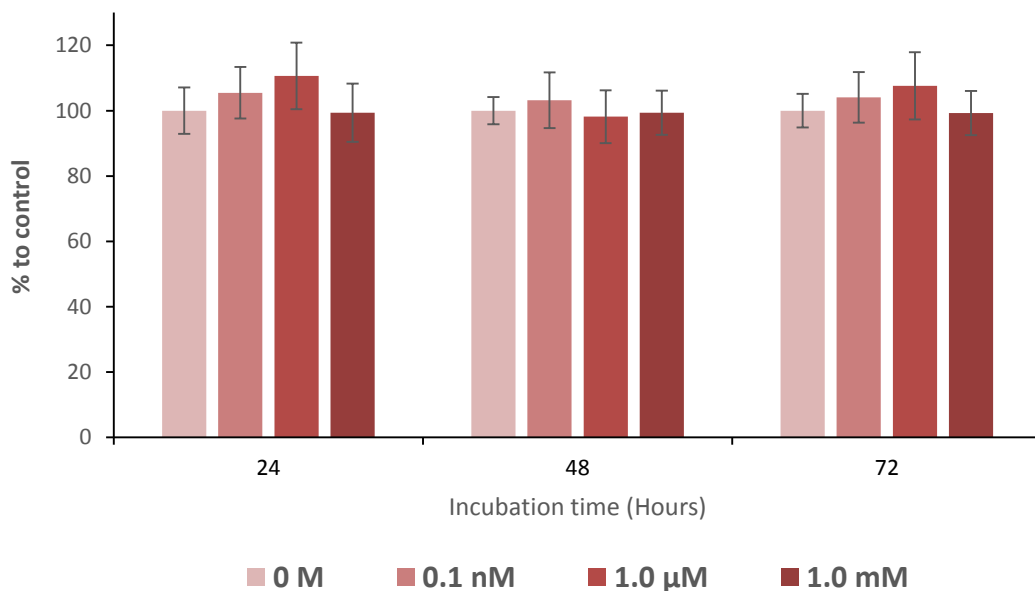


Figure 3.3: Proliferation of HepG2 cells in growth media containing various doses of NaCl. HepG2 cells were seeded in 96-well plates at approximately 60,000 cells/cm² using complete growth media and left to adhere to the surface of the well for 24 hours (37°C, 5% CO₂). After 24 hours (post-seeding), the growth media was changed to fresh complete growth media containing different doses of NaCl. Cell proliferation was assessed every 24 hours starting from this point using PrestoBlue®. Results are represented as percentage fluorescence of each conditions vs respective control for every time points with SEM errors bar (n=6). Mann-Whitney two-tailed test was performed. No significant difference across all the conditions were observed ($p>0.05$).

3.3.3 ^1H NMR cell media supernatant metabolic profiling of sodium chloride (NaCl) treatment on HepG2 cells.

To investigate if a specific metabolic signature associated with the treatment of NaCl on HepG2 cells, cell culture media metabolic profiles were acquired from growth media supernatant collected at 24-hr, 48-hr, and 72-hr time points using ^1H NMR spectroscopy. OPLS-DA models were constructed to compare the cell media metabolic profiles from four different experimental conditions at each time point. The OPLS-DA models were built by using three predictive components and several orthogonal components. The optimal number of the orthogonal component to be used for the models was determined by checking the good value of R^2Y (goodness of fit) and Q^2Y (goodness of prediction) (**Table 3.1**). OPLS-DA scores plots for all time points were able to separate control from treated group, as well as between doses within the treated groups (**Figure 3.4-A.i, B.i, C.i**). There was a good discrimination between the groups along the predictive components (Tpred1, Tpred2, Tpred3). However, the validation of the models using permutation testing with 10,000 iterations were only able to significantly validate the model for 72-hr time point ($p=0.0036$) but not the models of 24- and 48-hr time point with high p value of $p=0.0707$ and $p=0.1617$ respectively (**Figure 3.4-A.ii, B.ii, C.ii**).

To identify dose-dependent features in cell media metabolic profiles, an O-PLS regression analysis was then carried out for each time point. O-PLS regression is used to determine whether ^1H NMR cell medium spectra could show the dose-related response of NaCl treatment on HepG2 cells (**Figure 3.5**). For each model, OPLS scores plots showed a good discrimination between the groups and also showed that there is a linear effect of NaCl treatment on HepG2 cells along the predictive score 1 (Tpred 1) (**Figure 3.5-A.i, B.i, C.i**). The OPLS-loadings plots allowed to identify the metabolites that positively or negatively correlated with the treatment of NaCl for each time point (**Figure 3.6-A, B, C**). For all models, the optimal number of component was determined by R^2Y and Q^2Y values (**Table 3.2**). The models were then validated by using permutation test with 10,000 iterations, resulting in significant p values for the 48- and 72-hr models ($p= 0.0122$ and 0.0001) but not for 24-hr model ($p>0.05$) (**Figure 3.5-A.ii, B.ii, C.ii**). The Q^2Y value for the

24-hr model was also noticeably low ($Q^2Y=0.1884$) while higher value obtained for the rest of the models (48-hr and 72-hr) ($Q^2Y>0.3$).

Table 3.1: Value of Q^2Y , R^2Y , and validation of OPLS-DA models.

Time points	PC	OC	Q^2Y	R^2Y	Permutation p-value
24-hr	3	2	0.2896	0.9891	0.0707
48-hr	3	5	0.3243	0.9979	0.1617
72-hr	3	3	0.3569	0.9319	0.0036

Abbreviations; PC- Number of Predictive components, OC- Number of Orthogonal components.

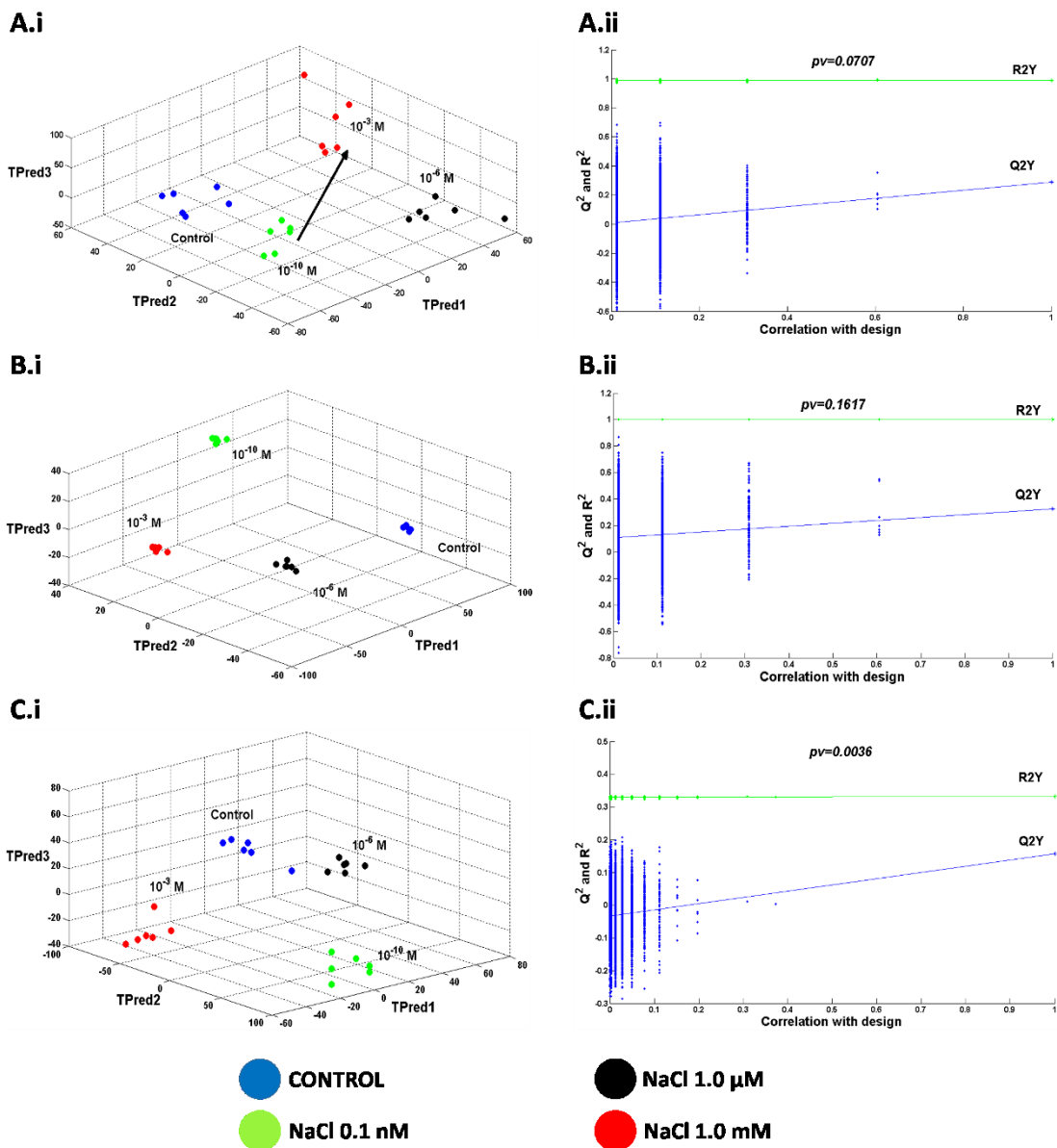


Figure 3.4: OPLS-DA score and validation plots separating the control group and the treatment groups (NaCl) as well as separating between the treatments groups themselves. Score plots of different doses of NaCl treatment on HepG2 cells at (A.i) 24-hr (B.i) 48-hr and (C.i) 72-hr. All the OPLS-DA models were validated with multiple permutations testing with 10,000 iterations and cross validations in figures A.ii, B.ii, and C.ii for the models of 24-hr, 48-hr, and 72-hr respectively. Only model for 72-hr time point shows significant p value when validated with permutation test ($p < 0.05$). **Please note, the dose-related trajectory visualised by black arrow is not a regression line.*

The loadings plot for 24-hr model could not be validated by permutation testing as revealed by high p value ($p>0.05$). As a result it did not show any strong correlation and no biomarker could be visualised. This might be due to the reason that the treatment of NaCl does not possess any detectable biological effect on HepG2 cells when compared to the control (**Figure 3.6-A**). The loadings plot for the model of 48-hr time point showed that leucine, isoleucine and valine were negatively correlated with the treatment, while lactate was positively correlated with the treatment of NaCl on HepG2 cells (**Figure 3.6-B**). Loadings plot for 72-hr time point showed that branched chain amino acids (BCAAs) valine, leucine, and isoleucine, as well as glutamine and phenylalanine, were negatively correlated with the treatment (**Figure 3.6-C**). The R values for all assigned metabolites were listed in **Table 3.3**. Moreover, a specific time-dependent markers in α -keto- β -methylvalerate and formate are observed, as these metabolites were strongly correlated with the treatment only at the 72-hr time point. Although the R values for some of the metabolites are high which makes them look highly correlated with the treatment of NaCl, they are however, not significantly difference when compared to the control group for all time points ($p>0.05$ **Table 3.3**). Although the exposure of NaCl on HepG2 cells caused slight modulation on cell metabolism, the effect however, was not significant based on statistical test using <http://vassarstats.net/> for Significance of a Correlation Coefficient. These results indicate that NaCl at all tested doses (0.1 nm, 1.0 μ M, and 1.0 mM) does not have significant effect on HepG2 cells.

Table 3.2: Goodness of fit (R^2Y), prediction (Q^2Y) and validation values for OPLS regression models of NaCl-treated vs control.

Time points	PC	OC	Q^2Y	R^2Y	p-value
24-hr	1	2	0.1884	0.9883	0.216
48-hr	1	2	0.3939	0.9594	0.0122
72-hr	1	3	0.6650	0.9953	0.0001

Abbreviations; PC- Number of Predictive components, OC- Number of Orthogonal components.

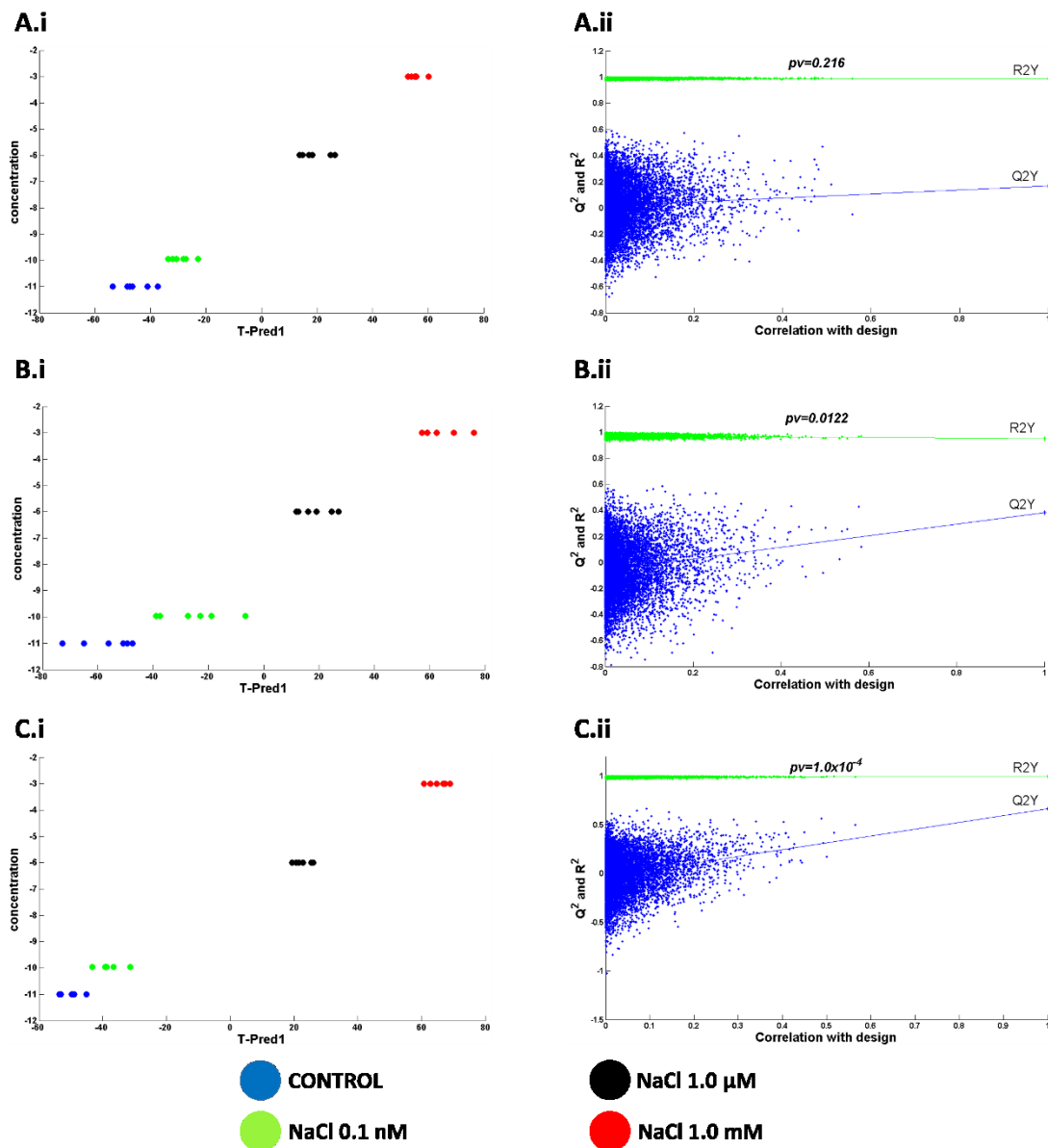


Figure 3.5: OPLS- regression models predicting the dose-related response of NaCl treatment on HepG2 cells. For each model, the scores plots indicate a linear effect of NaCl treatment on HepG2 cells at (A.i) 24-hr (B.i) 48-hr and (C.i) 72-hr exposure. Results of random permutation with 10,000 iterations for models validation in figures A.ii, B.ii, and C.ii showing a good validation of models for 48-hr and 72-hr time points ($p < 0.05$) but not for 24-hr ($p > 0.05$).

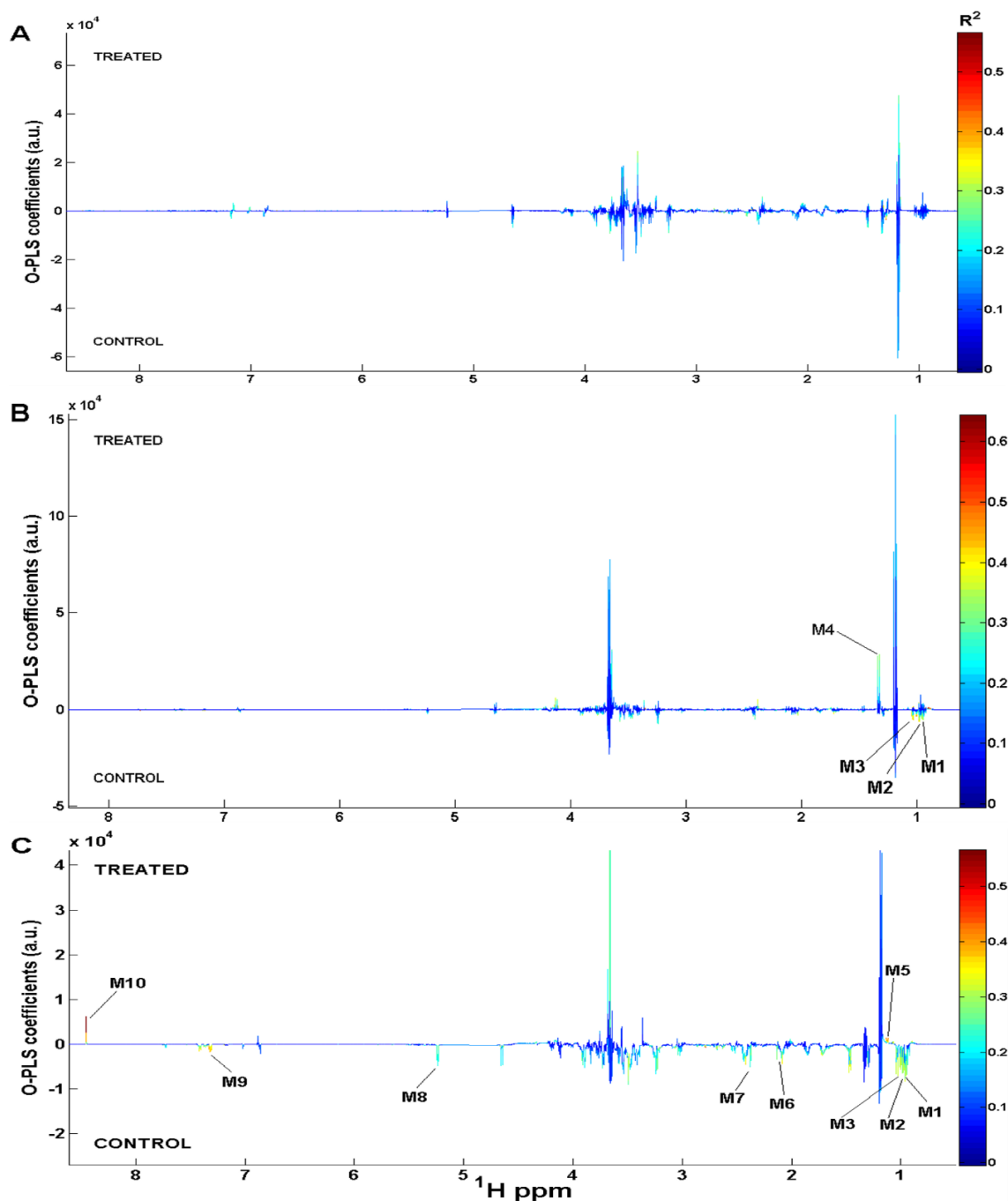


Figure 3.6: Loadings plots of OPLS-regression models showing the quantitative dose-response of NaCl on HepG2 cells culture media samples at (A) 24-hr, (B) 48-hr, and (C) 72-hr exposure. Horizontal axis corresponds to the NMR chemical shift scale; vertical axis corresponds to the O-PLS model coefficients (also referred to as loadings). The line variation corresponds to model covariance derived from the mean-centred model, whereas the colour map corresponds to model correlation derived from the unit-variance model. Metabolites that correlated significantly and associated with the NaCl dose response were assigned on the model coefficient plot. R^2 : square.

Table 3.3: List of metabolites assigned in the loadings plots of OPLS-regression models shown in **Figure 3.6**). The significant R values were identified by using <http://vassarstats.net/> for Significance of a Correlation Coefficient.

			Correlation with treatment (R values)		
Metabolite key	Metabolites	Chemical shift (¹ H ppm)	24-hr	48-hr	72-hr
M1	Leucine	0.93 (d), 0.94 (d), 1.71 (m)	-	-0.5011 (ns)	-0.6003 (<i>p</i> =0.039)
M2	Isoleucine	0.94 (t), 1.02 (t)	-	-0.5412 (ns)	-0.4910 (ns)
M3	Valine	0.98 (d), 1.04 (d), 3.62 (d)	-	-0.4841 (ns)	-0.5109 (ns)
M4	Lactate	1.32 (d), 4.11 (q)	-	0.4606 (ns)	-0.1268 (ns)
M5	α-keto-β-methylvalerate	1.10 (d)	-	-	0.5572 (ns)
M6	Glutamine	2.15 (m), 2.44 (m), 3.77 (t)	-	-0.2853 (ns)	-0.5612 (ns)
M7	Pyruvate	2.37 (s)	-	0.3662 (ns)	-0.4148 (ns)

M8	α -D-Glucose	5.24 (d)	-	-0.2920 (ns)	-0.4153 (ns)
M9	Phenylalanine	7.31 (m), 7.36 (m), 7.4 (m)	-	-0.2711 (ns)	-0.5716 (ns)
M10	Formate	8.45 (s)	-	0.1439 (ns)	0.7519 ($p=0.005$)

***Notes: (+) values correlate with NaCl doses, (-) values correlate with control. ns= non-significant R value.

3.3.4 Metabolite-Set Enrichment Analysis of the list of significant metabolites revealed a significant enrichment in the BCAA degradation pathway.

Metabolites that strongly correlated with both control and treatment groups were analysed using Over Representative Analysis in MSEA web server to identify the pathway involved (Xia and Wishart, 2010). MSEA analysis revealed a significant enrichment in “protein biosynthesis” and “BCAA degradation” pathways ($p < 0.01$) (**Table 3.4**). However, the fact that the list of the signature metabolites consists of an essential amino acid such as phenylalanine, valine, leucine, and isoleucine, no amino acids synthesis occurred. MSEA revealed that branched-chain amino acids in valine, leucine, and isoleucine belong to BCAA degradation pathway. As for the other metabolites such as lactate and formate, the analysis was not able to identify the enrichment of these metabolites in their respective pathways.

Table 3.4: Result from Over Representation Analysis (ORA) of MSEA based on the set of significant metabolites.

Metabolite set	Number of related metabolite (metabolite hits)	<i>p</i> value
Protein biosynthesis	5	7.54e-8
Valine, leucine and isoleucine degradation	3	0.00237
Phenylalanine and tyrosine metabolism	1	0.106
Pyruvate metabolism	1	0.158

3.4 DISCUSSION

This study assessed the effect of NaCl treatment on HepG2 cells growth and proliferation as well as using ^1H NMR based metabonomics approach to assess the effect of sodium as a SCFA counter ion on hepatocyte metabotypes.

3.4.1 The addition of sodium salt did not alter the pH of the growth media.

Eagle's Minimum Essential Media (MEM) was used as the growth medium in this study and it uses sodium bicarbonate as the buffering system (life technologies). (Supplementary data Table S1). The pH of the complete growth media (prepared as describe in **section 3.2.1**) should be kept in a range of pH 7.0-7.6 as this range is the optimum pH range for most of the mammalian cell culture works (Ceccarini and Eagle, 1971). The pH of the complete growth media after the addition of different types of sodium salt (NaCl, bicarbonate, and NaOH) at three different final doses; 0.1 nM, 1.0 μM , and 1.0 mM is determined in this experiment. The addition of the salt to the growth media was not able to alter the pH of the media outside the optimum range that serves best for cell culture purpose. The buffering system of the media functioned in maintaining the pH so that the pH of the media is well balanced when there is an exogenous compound added. The highest molarity of salt used in this study was 1.0 mM for all tested sodium types, and even at this dose the pH change was very small. MEM media already contains a mixture of inorganic salts such as NaCl and NaHCO_3 in its composition. The final molarity of these inorganic salts (before experiment) was 117.24 mM for NaCl and 26.20 mM for NaHCO_3 . As mentioned earlier, the highest dose used in the experiment was only 1.0 mM, which was approximately 1/100 of the initial NaCl concentration and 1/26 for NaHCO_3 . This concentration when compared to the initial concentration in the media was very small and it was unlikely to cause any modulation in pH.

3.4.2 Exposure to NaCl at different doses and time points did not affect HepG2 cell viability.

The previous section has demonstrated that the addition of salt even at the highest dose tested does not change to pH of the culture media. Based on this, the effect of different doses of sodium on HepG2 cell viability is then assessed. The doses used in this experiment are similar to the previous section. NaCl has been selected as the test compound in this chapter. This is due to the fact that NaCl has been used widely in molecular biology and cell biology applications and considered as an essential micronutrient for living cell and a classical negative control for osmolarity and pH (Pohl *et al.*, 2013). The effect of NaCl on cell viability was assessed at different doses; 0.1 nM, 1.0 μ M, and 1.0 mM after 24, 48, and 72 hours exposure. HepG2 cell viability, measured using Prestobluereagent, shows an increase of viable cells when NaCl dose increases from 0.1 nM to 1.0 μ M, and decreases when the highest dose was introduced. However, there was no significant difference across all the conditions that were observed. The highest dose used in this experiment was not enough to modulate the cell growth as revealed by previous studies that only at high \sim 220 mM of NaCl, cell growth was affected and DNA damage was observed (Dmitrieva *et al.*, 2003; Kultz and Chakravarty, 2001). High concentration of NaCl prevents DNA damage response from taking place by preventing the Mre11 exonuclease to localise on DNA damage sites, as well as inhibits the phosphorylation of histone H2AX protein (Dmitrieva, 2004).

More recently, study has shown that increasing the culture media NaCl concentration from 270 to 295-380 mosmol/kg (145-188 mmol/L) for HUVEC cells resulted in increase in the expression of genes that play role in the inflammation and pathophysiological of cardiovascular disease (CVD) (Dmitrieva and Burg, 2015). However, in the present study, the doses of NaCl used were not as high as those studies to cause any of these effects, thus no significant effect on cell viability was observed at all tested time points.

3.4.3 NaCl does not possess significant effect on HepG2 cells metabolism at.

To investigate the signature metabolites related to the exposure of HepG2 cells to NaCl, OPLS models were constructed, and loadings plots of OPLS-regression were assigned. In order to identify the metabolic marker related to the NaCl dose-response, the HepG2 cell media was analysed. The HepG2 cells response to NaCl doses lead to an increase in extracellular accumulation of lactate, α -keto- β -methylvalerate, and formate and a decrease in branched chain amino acids (BCAA) valine, leucine, and isoleucine, as well as glutamine and phenylalanine. Interestingly, all of the metabolites only found when the cells were incubated with NaCl for 48 and 72 hours, but not during early time point, which was 24-hr. One possible explanation for this is that, in the treated-group, more amino acids being consumed by the cells for energy production or higher rate of protein synthesis occurred. Based on this observation, these particular metabolites could be a markers of the dose- and time-response of NaCl exposure on HepG2 cells. However, further analysis testing the significant of the correlation coefficient of the signature metabolites was not able to observe any significant effect of the NaCl on HepG2 cells ($p>0.05$). Thus nullifies all the initial observation made by observing the degree of the correlation alone.

BCAA (valine, leucine, and isoleucine), glutamine, and phenylalanine that decreased or negatively correlated with the NaCl dose corresponding to the following KEGG pathways in the MSEA: "protein biosynthesis" and "valine, leucine and isoleucine degradation". In addition, from the analysis, α -keto- β -methylvalerate was detected and assigned. This metabolite is an intermediate product of isoleucine degradation, suggesting that the extracellular accumulation of this metabolite is caused by the higher rate of isoleucine degradation in the NaCl-treated group compare to the control group.

The other metabolites that positively correlated with NaCl treatment on HepG2 cells were lactate and formate. Lactate is involved in pyruvate metabolism. Lactate dehydrogenase (LDH) catalyses the interconversion of pyruvate and lactate with the interconversion of NADH and NAD⁺ (Gray *et al.*, 2014). Surprisingly, only at the 72-hr time point does formate shows a strong correlation with the NaCl treatment, but not at the other time points, 24- and 48-hr. The accumulation of formate can be explained by the

hepatic cells as well as cancer cells that can produce large amounts of formate by the folate cycle (Nijhout *et al.*, 2006; Tedeschi *et al.*, 2013).

In this study, a number of significant metabolites that can be considered as metabolic markers of NaCl treatment on HepG2 cell have been initially identified by observing the R values of the metabolites when compared to the control. However, when calculating the level of significance of these R values using the 'Significance of Correlation Coefficient' test, none of the identified metabolites are significantly different when compared to their respective control (time point). Thus, these findings show that NaCl at all tested doses does not able to significantly modulate HepG2 cell metabolism.

3.5 CONCLUSION

In conclusion, experiments carried out in this chapter demonstrated that the addition of sodium in the form of sodium chloride (NaCl) has no effect on pH nor does it affect the growth of HepG2 cells in all tested conditions. In addition to this result, metabolomic experiments were carried out to investigate if the exposure of HepG2 cells with NaCl can reveal a specific biomarker related to dose- and/or time-dependent response. It has been demonstrated in this chapter that NaCl treatment on HepG2 cells has no significant effect on the cell metabolism even at the highest tested dose (1.0 mM). These results highlighted that there are no dose-dependent and time-dependent effects of NaCl on HepG2 cells when incubating the cells with this compound for 24, 48, and 72 hours. Thus, any effects that might be observed in the next chapter when treating the HepG2 cell with sodium propionate and sodium butyrate will be solely caused by the SCFAs themselves but not their sodium counter ion.

CHAPTER 4

4. THE EFFECT OF SHORT-CHAIN FATTY ACIDS; PROPIONATE AND BUTYRATE ON HEPG2 CELL METABOLISM.

4.1 INTRODUCTION

The occurrence of obesity and the related disorders such as metabolic syndromes have increased drastically over the past decades. Data from World Health Organisation stated that there are more than 1 billion overweight adults, with 300 million classified as clinically obese (Hotamisligil, 2006). Obesity is associated with an array of additional health problems, including increased risk of insulin resistance, type 2 diabetes, fatty liver disease, atherosclerosis, and some cancers (Tilg and Kaser, 2011). It is a result of a long-term imbalance between energy intake and expenditure, which is regulated by a number of pathways involving metabolites and hormones (Greenwood *et al.*, 2011).

Recent research has suggested that the gut microbiota is involved in the development of obesity and metabolic disorders (Greiner and Bäckhed, 2011; Kau *et al.*, 2011). Enzyme cellulase which cannot be synthesised by human body is needed to break down cellulose, the main component of plant cell wall. Thus gut microbiota plays an important role in fermenting dietary fibres that cannot be fully hydrolysed by the host enzymes during digestion processes (Topping and Clifton, 2001). The main metabolites produced during this fermentation process are short-chain fatty acids (mainly acetate, propionate, and butyrate) and other intermediate metabolites such as lactate, succinate, formate, ethanol, and gases (CO₂, CH₄, and H₂) (Flint *et al.*, 2007). Short-chain fatty acids (SCFAs) formed were then absorbed into the colonocytes which act as substrate for energy production.

Many studies have been focusing on the role of SCFAs acetate (C₂), propionate (C₃), and butyrate (C₄) in the host. The majority of butyrate produced in the GI tract is in fact metabolised by colonocytes – as it is their preferred energy source, accounting for up to 80% of their CO₂ production (Roediger, 1982). Moreover, it is also involved in regulating differentiation and proliferation of cells (Scheppach *et al.*, 1992; Topping and Clifton, 2001). SCFA that is not consumed by the colonocytes gets transported across the basolateral membrane of the gut (Harig *et al.*, 1996; Tyagi *et al.*, 2002) and enters portal circulation towards the liver where they may be metabolised (e.g. propionate), or distributed to peripheral tissues (e.g. acetate) (Cummings and Macfarlane, 1997; Roediger, 1982). While acetate has been demonstrated as the primary substrate for cholesterol synthesis, and may interfere directly in lipid metabolism (Day and Fidge, 1964), propionate is metabolised primarily in liver. This metabolite is a recognised gluconeogenic substrate that enters the TCA cycle via the succinyl-coenzyme A (succinyl-CoA) entry point and is then converted into oxaloacetate (den Besten *et al.*, 2015; Jin *et al.*, 2015; Wolever *et al.*, 1991). Propionate also has been demonstrated to inhibit *de novo* biosynthesis of both cholesterol and fatty acids in rat hepatocytes and human models (Wolever *et al.*, 1991; Wright *et al.*, 1990).

SCFAs also act as ligands for G protein-coupled receptors (GPCRs), thus activating subsequent signalling pathways (Brown *et al.*, 2003). Free fatty acid receptor 2 and 3 (FFAR2 and FFAR3) are GPCRs, the activation of which results in the inhibition of cAMP production via interaction with G α i protein (Le Poul *et al.*, 2003; Stoddart *et al.*, 2008). Several studies have shown that SCFA receptors, FFAR2 and FFAR3 play roles in modulating host energy metabolism. Propionate directly regulates FFAR3-mediated sympathetic nervous system (SNS) activity, thus resulting in the increase of oxygen consumption in WT mice, but not in *Ffar3*-KO mice (Kimura *et al.*, 2011). Moreover, a study conducted by De Vadder *et al.*, suggests that propionate induces intestinal gluconeogenesis via gut-brain neural circuit involving the FFAR3 (De Vadder *et al.*, 2014). Similarly, another study reported that SCFAs including acetate, propionate, and butyrate regulate energy uptake in adipose tissue and also regulate energy expenditure in other tissues, including liver and muscle (Kimura *et al.*, 2013).

In this chapter, the effect of SCFAs; propionate and butyrate on hepatic cancer metabolic network was assessed and investigated. As the liver is a known metabolism hub in human body here, using HepG2 hepatocarcinoma cell line, the dose-dependent effects of

propionate and butyrate on hepatic metabolism was investigated. To approach this, a ^1H NMR-based metabolomics approach is used to profile the HepG2 cell culture medium in identifying the metabolic markers associated with SCFAs (propionate and butyrate) treatment on the cells.

4.2 MATERIALS AND METHODS

4.2.1 Preliminary cell viability test (toxicity test).

A cell toxicity assay was conducted to observe the effect of different SCFAs concentrations on HepG2 cell growth and to determine the non-toxic range for further experiments. This experiment was carried out at three different time points (24-hr, 48-hr, and 72-hr). Briefly, 60,000 cells/well were seeded in 96 well-plates and were grown in complete growth medium (as described previously) at 37°C in a humidified atmosphere comprised of 5% CO₂ and 95% air. The cells were left for 24 hour to form a monolayer. After 24 hours, the growth medium was changed and SCFAs (propionate or butyrate) were added to the final doses ranging from 0.01 nM to 100 mM. Upon reaching the time points described above, PrestoBlue® (Invitrogen) reagent, an oxidation-reduction indicator based on Resazurin dye was added to each well. The sample was then incubated at 37°C for 30 minutes before read with a plate reader for fluorescence measurement at 535 nm (excitation) and 615 nm (emission) observing the cell viability.

4.2.2 Detection of FFAR2 and FFAR3 expression in HepG2 cell line using Western blot analysis.

In order to decipher between the metabolism and the signalling properties of SCFA (propionate and butyrate), the expression of free fatty acid receptors (FFAR2 and FFAR3) in HepG2 cells was first investigated. These receptors have been shown previously to be activated by SCFA (mainly acetate, propionate, and butyrate) (Brown *et al.*, 2003; Nilsson *et al.*, 2003). Briefly, HepG2 cells from ~80% confluence flasks were washed twice with ice-cold

PBS, scraped off, and suspended in RIPA Buffer (Sigma) and incubated for 5 minutes on ice. The lysates were then centrifuged for 10 minutes at 8,000 *g* at 4°C to pellet the cell debris. The supernatant containing the soluble proteins was separated using sodium dodecyl sulphate-polyacrylamide gel electrophoresis (SDS-PAGE 10% gel). Proteins were then transferred from the gel to a polyvinylidene difluoride (PVDF) membrane (Bio-Rad Japan, Tokyo, Japan) by electroblotting. The membranes were blocked using 5% skim milk in Tris-buffered saline containing 0.1% Tween-20 (TBST) at room temperature for 1 hour after which the membranes were incubated with each primary antibody at 4°C overnight. On the next day, the membranes were washed 3 times with TBST and were incubated with the secondary antibody for 1 hour at room temperature. Finally, the membranes were washed before visualised using ECL on Kodak Image Station 2000MM or onto photographic film (Amersham GE) to reveal the proteins band. The antibodies used were Anti- GPR41 antibody (ab103718, abcam®), Anti-GPR43 antibody (ab131003, abcam®), and Goat anti-Rabbit (1721019, Biorad).

4.2.3 Cell culture preparation for ¹H NMR analysis.

For NMR metabolomics analysis, HepG2 cells were plated in six well-plates using complete medium prior to the experiment at the seeding density of 60,000 cells/well. After 24 hours, new medium was added with the additional of SCFAs (propionate or butyrate) according to the non-toxic concentration range selected based on results from the toxicity study. Propionate and butyrate were used in the form of sodium salt in this chapter. The selected doses were 0.1 nM, 1.0 μM, and 1.0 mM. Medium without propionate or butyrate supplementation serves as control for this experiment. The experiment was performed for 24, 48, and 72 hours. After reaching each incubation time point, cell media supernatant was collected for ¹H-NMR analysis and at the same time the cells were counted by using Moxi Z™ mini automated cell counter (ORFLO Technologies) for the normalisation of the rate of metabolite production and consumption later on. In order to assess sole effect of propionate and butyrate on HepG2 cells metabolism, the identified metabolic signatures in this chapter will be compared with the results obtained from the experiment on the effect of NaCl on HepG2 cells in previous chapter (Chapter 3), thus eliminating the effect of sodium.

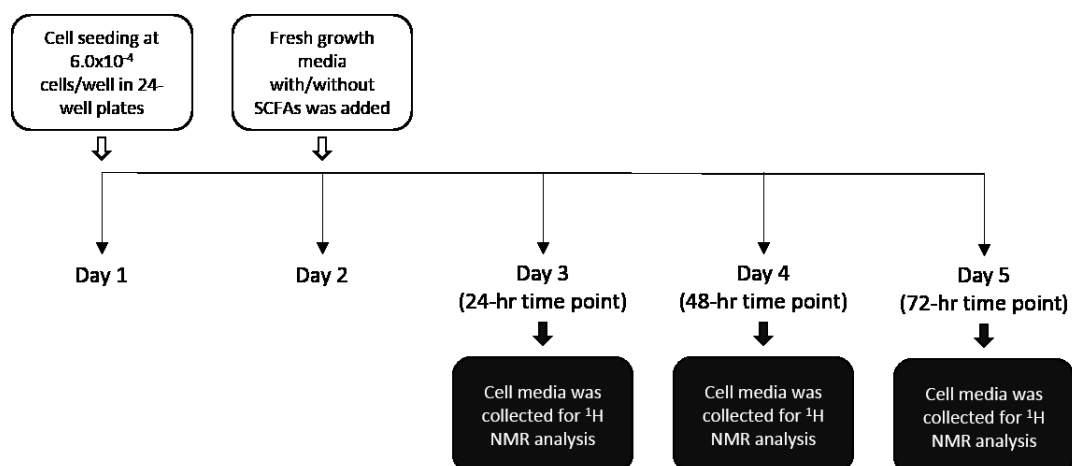


Figure 4.1: Experimental design for the exposure of HepG2 cells to the SCFAs treatment.

4.2.4 Sample preparation and ¹H NMR spectroscopy.

The method for this part is as described previously in Chapter 3, *section 3.2.9* (for sample preparation of cell media NMR analysis), and in Chapter 3, *section 3.2.10* (for ¹H NMR spectroscopy).

4.2.5 ¹H NMR spectra pre-processing, ¹H NMR data processing, and multivariate data analysis.

See Chapter 3, *section 3.2.10* for ¹H NMR spectra pre-processing and Chapter 3, *section 3.2.11* for ¹H NMR data processing and multivariate data analysis.

4.2.6 Pathways-specific analysis using univariate analysis.

The concentration of highly correlated metabolites related to TCA cycle, BCAA catabolism and gluconeogenesis detected in cell media ¹H NMR spectra were quantified using Chenomx NMR suite 7.0 software. In order to calculate the consumption or production rate

per-cell for each metabolite, the concentration of the respective metabolite at each final time point was normalised to the initial concentration of that particular metabolite in fresh medium from the day 0 sample. Finally, to get the consumption or production rate per-cell for each metabolite, the net metabolite concentration after being normalised was divided by the number of cell from its respective time point. The number of cell was obtained by using Moxi Z™ mini automated cell counter (ORFLO Technologies) according to the manufacturer protocol. The net consumption or production rate per-cell obtained was then compared between SCFA-treated and control group at each time point using non-parametric Mann-Whitney tests.

4.3 RESULTS

4.3.1 Optimisation of the pharmacological concentrations of SCFA; propionate and butyrate on HepG2 cell viability.

In order to assess the effects of propionate and butyrate on HepG2 hepatocarcinoma cell line, a toxicity study was carried out. This chapter aims at preliminary screening of the SCFA concentrations that could have an effect on the growth of HepG2 cell line. A wide range of SCFA concentrations were initially assessed ranging from 0.01 nM to 100 mM. **Figure 4.2-B** shows that there were no significant changes observed on cell viability when propionate is added to growth medium of HepG2 cells at final doses from 0.01 nM to 1.0 mM for all tested time points. Microscopic observation of cell morphology further indicates that the cells grew healthy by having normal morphology at this range of concentration without any apparent changes observed (**Figure 4.2-A**). However, as seen in **Figure 4.2-B**, propionate significantly ($p < 0.01$) decreased cell viability in dose-dependent and time-dependent manners when used at 0.1 mM and 1.0 mM doses. When compared with the control condition, 10 and 100 mM propionate reduce the HepG2 cell viability by ~50% and ~90%, respectively. Propionate seems to exert its toxic effect when using at high dose starting from 10 mM and above.

Incubation of HepG2 cells with 4-carbon SCFA butyrate with the same range of concentration did not affect the proliferation rate of HepG2 cells. There was no significant

difference observed in cell viability from 0.01 nM to 1.0 mM (**Figure 4.3-B**). The same pattern of toxicity also observed when increasing the dose of butyrate to 10 mM and above. HepG2 cell viability dropped drastically up to 70% off from the control after 24 hours exposure to butyrate at this concentration, and even worse at 48 and 72 hours incubation where almost none survived. Butyrate concentrations at 10 mM and higher appear to be extreme for the cells to grow and observation on the cells morphologies under light microscope revealed that almost all cells died at this conditions (**Figure 4.3-A**). The results of this chapter indicate that low dose of SCFA; propionate and butyrate does not have an effect on the cell growth and viability, while exert their toxic effect when using at higher doses.

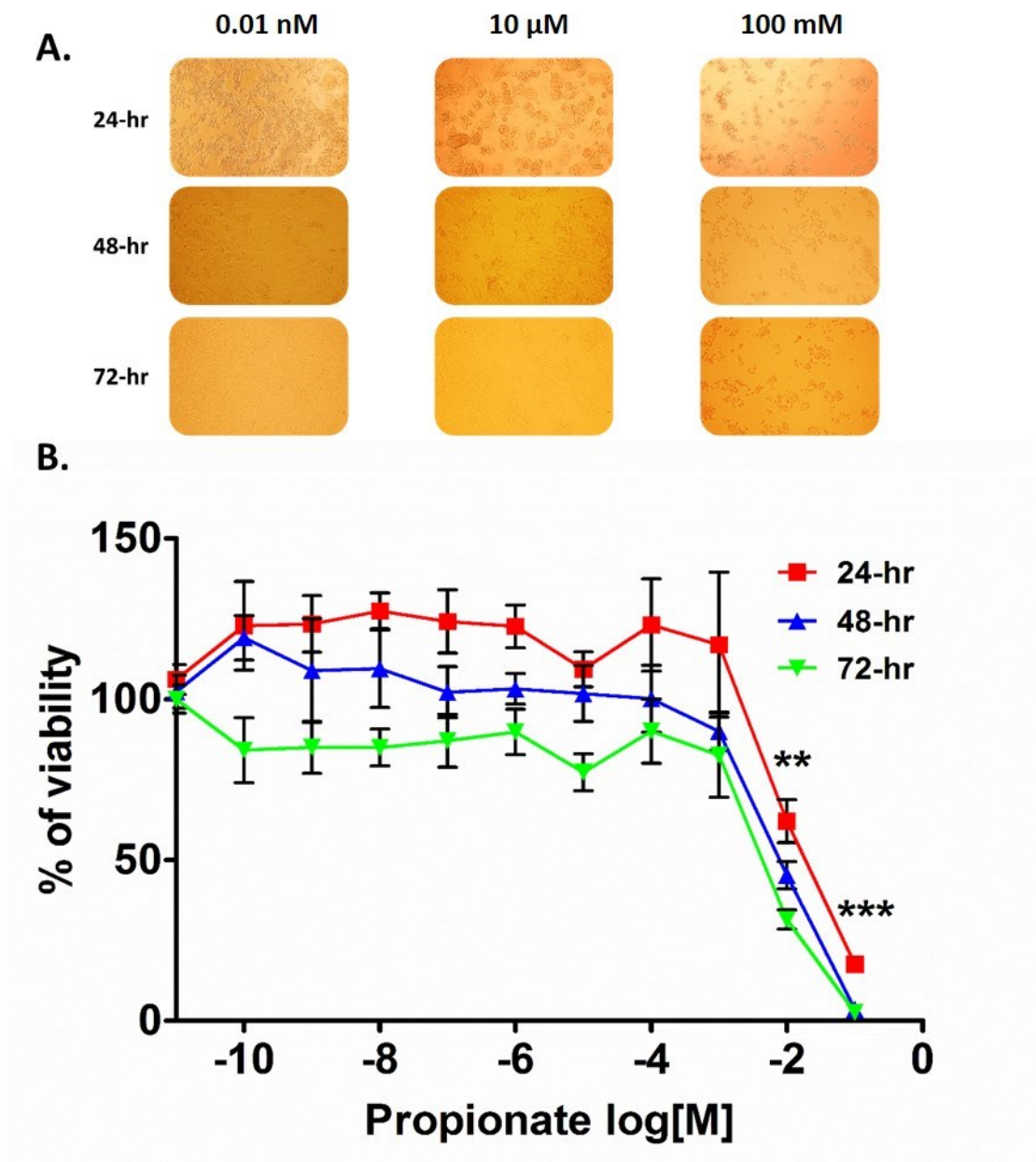


Figure 4.2: The effect of propionate on HepG2 cell viability. (A) Microscopic images (10x magnification) of HepG2 at different dose and time point were shown. (B) Viability was assessed by PrestoBlue® reagent (Invitrogen), and fluorescence measurement was measured at 535 nm (excitation) and 615 nm (emission). Results are represented as means \pm SEM of two independent experiments (n=6 replicates per condition, **p < 0.01). Mann-Whitney two-tail test was performed.

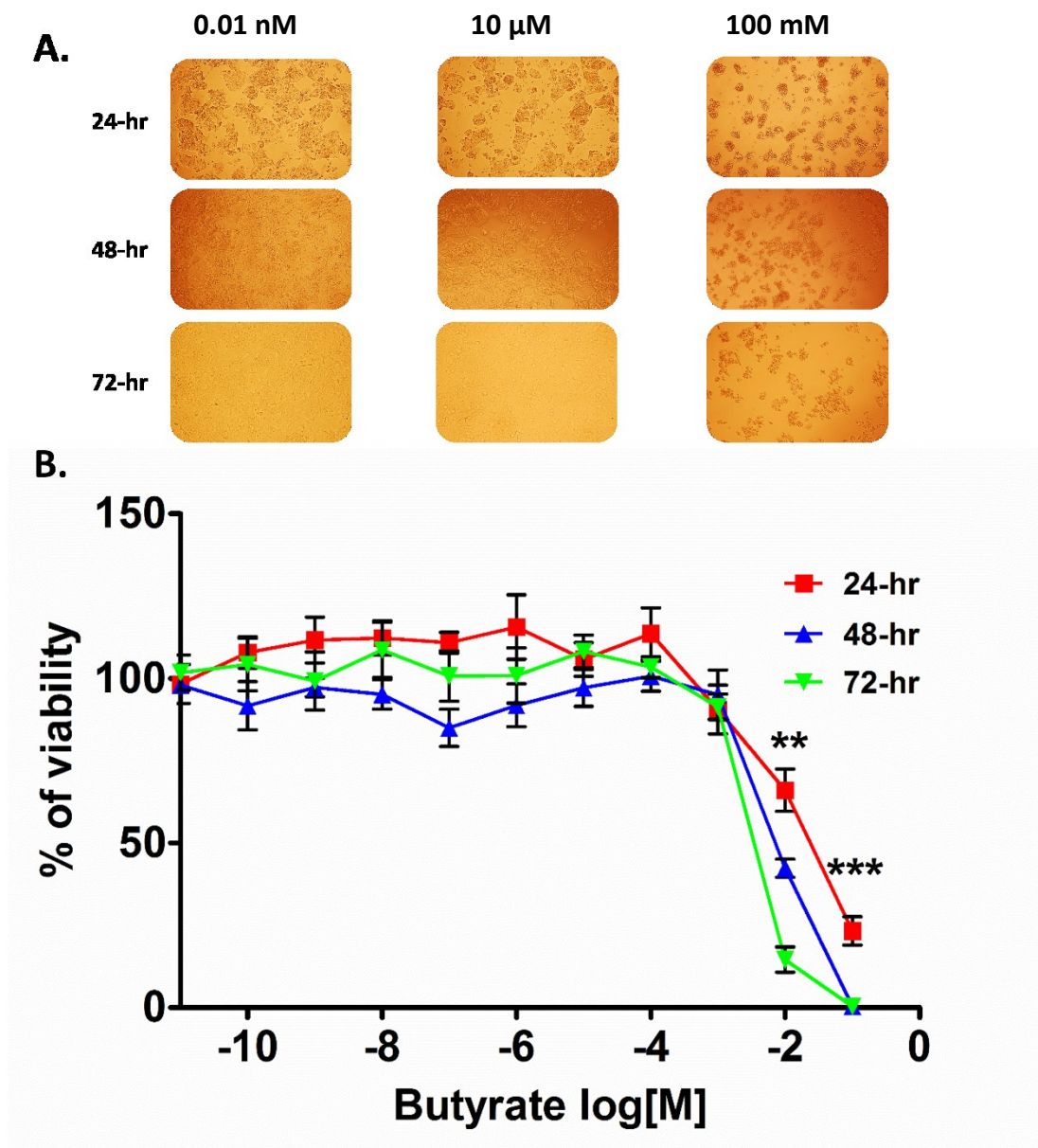


Figure 4.3: The effect of butyrate on HepG2 cell viability. (A) Microscopic images (10x magnification) of HepG2 at different dose and time point were shown. (B) Viability was assessed by PrestoBlue[®] reagent (Invitrogen), and fluorescence measurement was measured at 535 nm (excitation) and 615 nm (emission). Results are represented as means \pm SEM of two independent experiments (n=6 replicates per condition, **p < 0.01). Mann-Whitney two-tail test was performed.

4.3.2 Investigating the expression of free fatty acids receptor 2 (FFAR2) and free fatty acid receptor 3 (FFAR3) in HepG2 cells.

In this experiment, the protein expression of free fatty acid receptor 2 (FFAR2) and free fatty acid receptor 3 (FFAR3) in treated and non-treated HepG2 cells is first investigated. The Western blot analysis of HepG2 cell lysates was not able to detect protein expression of these two receptors, FFAR2 and FFAR3 in this cell line at all tested conditions (**Figure 4.4**). FFAR3 was found to be expressed in adipose tissue, gut, and the peripheral nervous system (Hong, 2005; Inoue *et al.*, 2014), while the expression of FFAR2 was reported in the adipose tissue, intestines, and immune tissues (Hong, 2005; Maslowski *et al.*, 2009). These results indicate that the effect that might be observed further in this chapter when dosing the HepG2 cells with propionate and butyrate might be mainly from the metabolism properties of SCFA and not via signalling through FFAR2 and FFAR3.

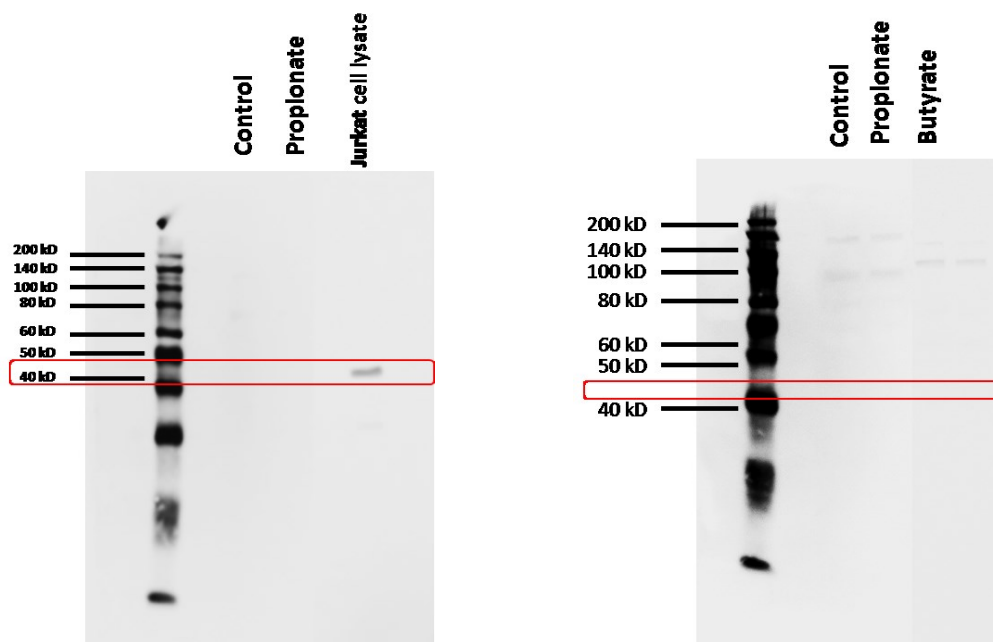


Figure 4.4: Examining the expression of free fatty acid receptor (FFAR2 and FFAR3) in HepG2 cell. In all conditions including the control (except for the positive control, using Jurkat cell lysate), the expression of both (A) FFAR3 and (B) FFAR2 in HepG2 cells were not detected. HepG2 cells were cultured with or without the addition SCFA until reaching ~80% confluence prior to harvest for western blotting analysis.

4.3.3 Characterisation of ^1H NMR metabolic profiles of HepG2 cell media.

To investigate the potential of metabolic profiling in characterizing the responses of HepG2 hepatocarcinoma cell line to SCFA, culture media obtained directly from 24, 48, and 72 hours incubation were profiled using 1D 600 MHz ^1H NMR spectroscopy. Based on the results from the preliminary study on pharmacological range of propionate and butyrate, certain SCFA concentrations that are not toxic to the HepG2 cell were selected for metabolic profiling of HepG2 cell medium. The chosen doses for the subsequent NMR study are therefore 0.1 nM, 1.0 μM , and 1.0 mM. Complete growth media without any addition of SCFA served as control for this experiment.

Mean ^1H NMR spectrum of HepG2 cell media was assigned with the help of appropriate database such “The Human metabolome database” (HMDB), published assignments, and Chenomx NMR suite 7.0 software. Representative ^1H NMR spectra of cell media samples metabolic profiles with metabolites assignment was shown in **Figure 4.5**. In total 30 metabolites were identified and assigned. Most of the identified metabolites, mainly amino acids are commonly found in Minimal Essential Media (MEM) culture media composition as this type of media being used in this experiment.

Numerous common signals from organic acids (acetate, butyrate, propionate, citrate, etc.), amino acids (leucine, isoleucine, valine, alanine, arginine, and many other) and sugar (D-glucose) were observed in HepG2 cell culture media. **Table 4.1** lists all the identified metabolites. Interestingly, large signals from a metabolite appears at ~ 1.17 and 3.65 ppm, which were identified as ethanol. This metabolite consistently produced high intensity resonance in all spectra from both propionate and butyrate study samples. This is suggestive of ethanol contamination during the experiment as the result of excessive use of ethanol spray as surface decontamination during routine cell culture work to prevent any biological contamination.

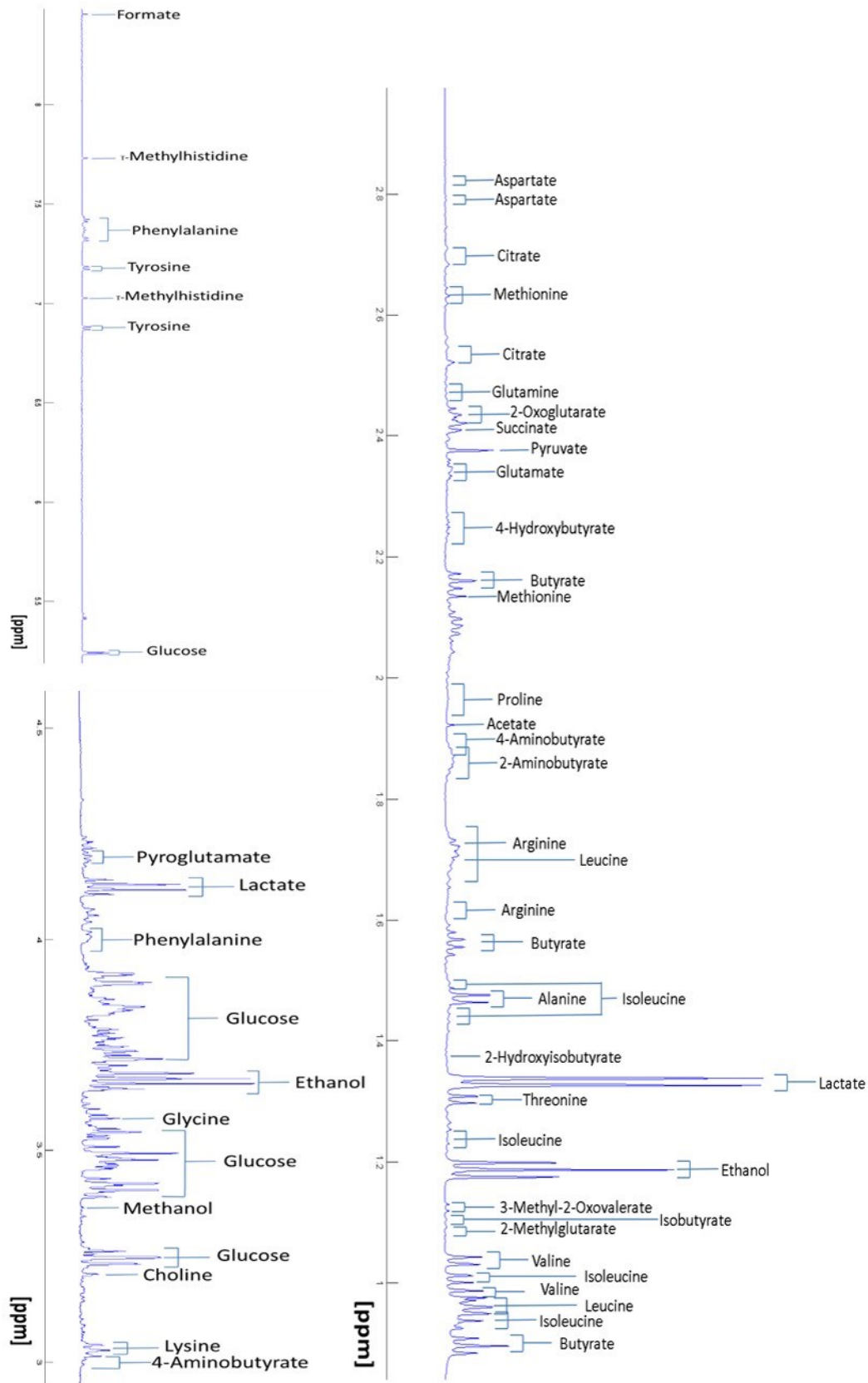


Figure 4.5: Mean of ^1H NMR spectra of cell media from SCFA-treated HepG2 cells at 24 hours exposure measured by 600-MHz ^1H NMR spectroscopy.

Table 4.1: ¹H NMR chemical shifts from metabolites assigned of cell media obtained from SCFA-treated HepG2 cells measured by 600-MHz ¹H NMR spectroscopy. The concentration of each metabolites was calculated based on the average of 6 samples from 2 separate experiments (n=6).

Metabolite	Chemical shift (¹ H ppm)	Status: Y (appear in media composition) N (not appear in media composition)	Concentration (mM)
2-Hydroxybutyrate	0.9 (t), 1.7 (m), 4.0 (dd)	N	0.2070
2-Hydroxyisobutyrate	1.36 (s)	N	0.0103
2-Oxoglutarate	2.44 (t), 3.01 (t)	N	1.0370
α-keto-β-methylvalerate	1.10 (d)	N	0.0550
4-Aminobutyrate	1.89 (m), 2.28 (t)	N	0.0794
Acetate	1.91 (s)	N	0.1726
Alanine	1.46 (d), 3.77 (q)	N	2.6011
Butyrate	0.88 (t), 1.55 (m), 2.15 (m)	N	1.1450
Choline	3.22 (s), 3.51 (dd), 4.06 (ddd)	Y	0.0171
Citrate	2.53 (d), 2.70 (d)	N	0.0505
Ethanol	1.17 (t), 3.65 (q)	N	2.6893
Formate	8.44 (s)	N	0.2531
α-D-Glucose	5.22 (d)	Y	5.1095
Glutamate	2.04 (m), 2.34 (m)	N	0.6751
Glutamine	2.12 (m), 2.44 (m), 3.76 (t)	Y	1.6429
Glycine	3.55 (s)	N	0.2054
Isoleucine	0.93 (t), 1.02 (d)	Y	0.3328
Lactate	1.32 (d), 4.11 (q)	N	5.1436
Leucine	9.94 (d), 9.95 (d), 1.70 (m)	Y	0.4084
Lysine	1.71 (m), 1.86 (m), 3.02 (t)	Y	0.4427
Methionine	2.12 (s), 2.13 (m), 3.01(t)	Y	0.1454
Phenylalanine	3.12 (dd), 3.26 (dd), 7.31 (m), 7.36 (m), 7.40 (m)	Y	0.1856
Propionate	1.06 (t), 2.18 (q)	N	1.1626
Pyruvate	2.36 (s)	Y	1.6698
Succinate	2.39 (s)	Y	0.1734
Threonine	1.31 (d), 3.60 (d), 4.24 (m)	Y	0.5102
Tryptophan	7.53 (d)	Y	0.0554
Tyrosine	6.89 (d), 7.10 (d)	Y	0.1750
Valine	0.98 (d), 1.03 (d), 2.26 (m), 3.59 (d)	Y	0.4348
3-methylhistidine	7.01 (s)	Y	0.2546

4.3.4 ¹H NMR cell media metabolic profiling of propionate-treated HepG2 cells identifies constant metabolic signature associated to isoleucine metabolism.

To investigate the specific metabolite signature associated with propionate treatment on HepG2 cell line, supervised multivariate statistics using orthogonal partial least-squares discriminant analysis (OPLS-DA) and orthogonal partial least-squares regression (OPLS-regression) were carried out. First, metabolic profiles from media of HepG2 cells treated with propionate were compared at each time point by using OPLS-DA models. Each OPLS-DA model was constructed by using three predictive components and several orthogonal components. To select the optimum number of orthogonal components, the value of R²Y (goodness of fit) and Q²Y (goodness-of-prediction) statistics were observed. OPLS-DA score plots present a clear discrimination between the control and the treated group as well as between doses within the treated groups with goodness-of-prediction parameters Q²Y equal to 0.3660, 0.5745, and 0.4950, for model of 24, 48, and 72-hr, respectively (**Table 4.2**). As shown in **Figure 4.6**, OPLS-DA score plots separate the doses within the treated group along predictive score-1 (Tpred 1), and between control and the treated group along predictive score-2 (Tpred2). The robustness of the models was then validated by multiple permutation tests with 10,000 iterations resulting in significant *p* value (*p*<0.05) for all three time points (**Figure 4.6-A.ii, B.ii, and C.ii**).

Table 4.2: Value of Q²Y, R²Y, and validation of OPLS-DA models for propionate experiment.

Time points	PC	OC	Q ² Y	R ² Y	p-value
24-hr	3	5	0.3660	0.9669	0.0107
48-hr	3	3	0.5745	0.9991	0.0021
72-hr	3	4	0.4950	0.9995	0.0106

Abbreviations; PC- Number of Predictive components, OC- Number of Orthogonal components.

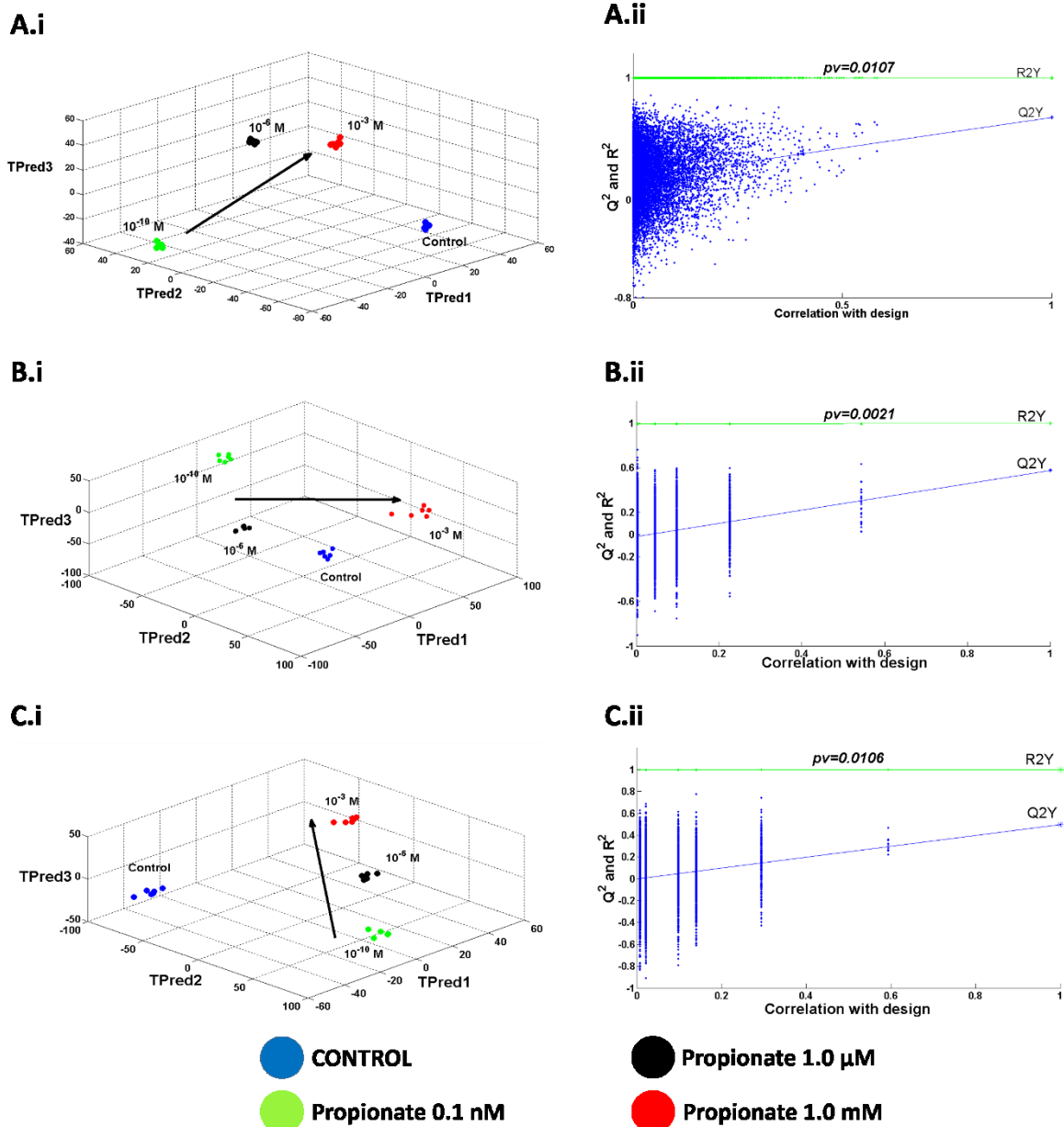


Figure 4.6: OPLS-DA score and validation plots separating the control group and the treatment groups (propionate) as well as separating between the treatment groups themselves. Score plots of different doses of propionate treatment on HepG2 cells at (Ai) 24-hr (Bi) 48-hr and (Ci) 72-hr. All the OPLS-DA models were validated with multiple permutations testing with 10,000 iterations and cross validations in figures A.ii, B.ii, and C.ii for the models of 24-, 48-, and 72-hr respectively. ($p < 0.05$). **Please note, the dose-related trajectory visualised by black arrow is not a regression line.*

In order to test whether there is a dose-response related to the treatment of propionate on HepG2 cells, supervised multivariate analysis was carried out using orthogonal partial least-squares regression (OPLS-regression). OPLS-regression was able to show the dose response of propionate (0.1 nM, 1.0 μ M, and 1.0 mM) in HepG2 cells (**Figure 4.7-A.i, B.i, and C.i**). The models were constructed with satisfactory values for goodness-of-fit and goodness-of-prediction parameters (**Table 4.3**). This is used as an indicator of how well the Y matrix is explained by the corresponding NMR X matrix (Fonville *et al.*, 2010). Permutation tests were carried out in order to validate the dose-response models for each time points (24, 48, and 72-hr).

Table 4.3: Goodness of fit (R^2Y), prediction (Q^2Y) and validation values for OPLS regression models of propionate -treated vs control.

Time points	PC	OC	Q^2Y	R^2Y	p-value
24-hr	1	3	0.4408	0.9977	0.0184
48-hr	1	4	0.4935	0.9997	0.0205
72-hr	1	3	0.4524	0.9981	0.0102

Abbreviations; PC- Number of Predictive components, OC- Number of Orthogonal components.

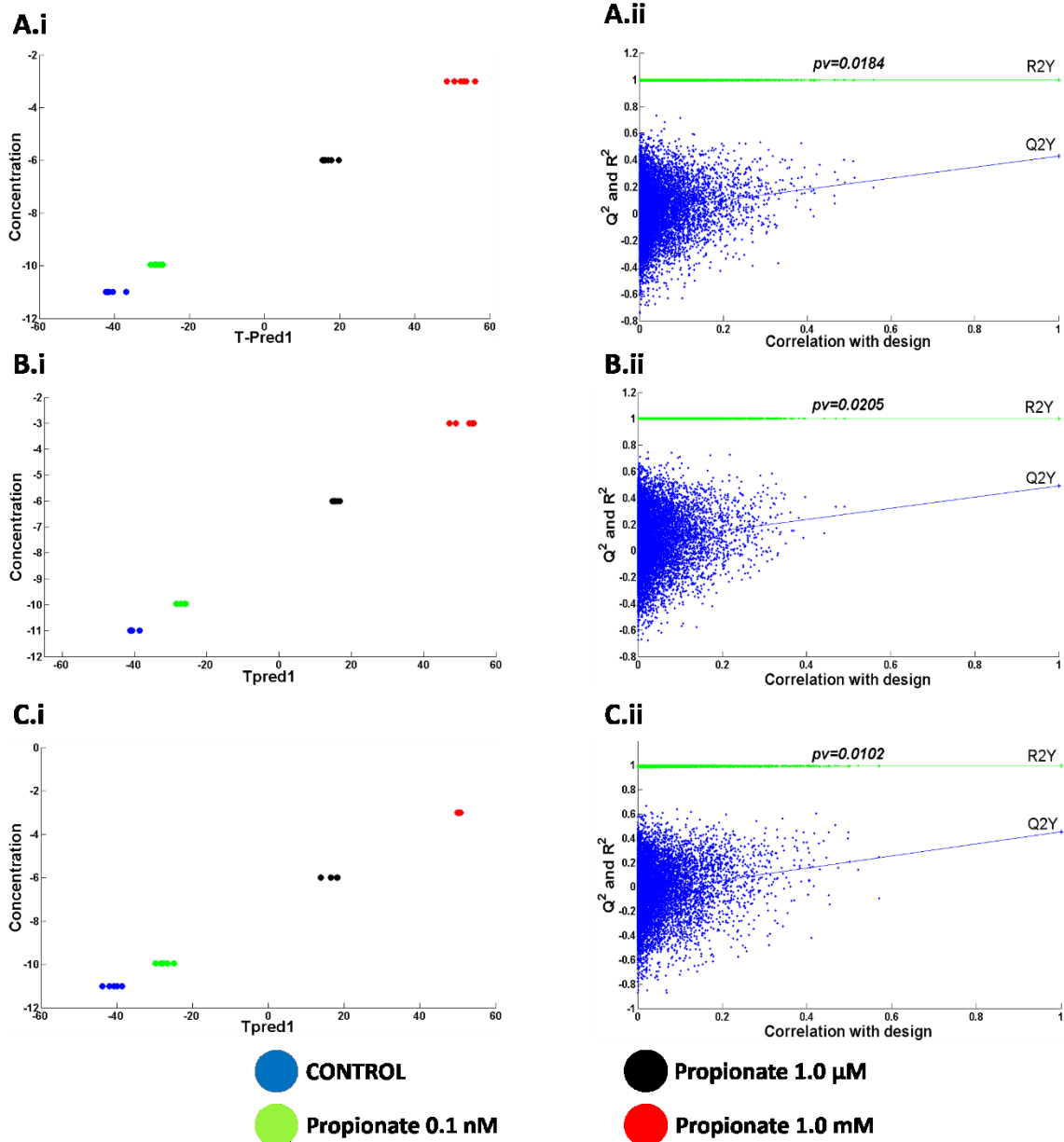


Figure 4.7: OPLS- regression models predicting the dose-related response of propionate treatment on HepG2 cells. For each model, the scores plots indicate a linear effect of propionate treatment on HepG2 cells at (A) 24, (B) 48, and (C) 72 hours of exposure. Results of random permutation with 10,000 iterations for models validation (A.ii), (B.ii), and (C.ii) showing a good validation of models ($p < 0.05$).

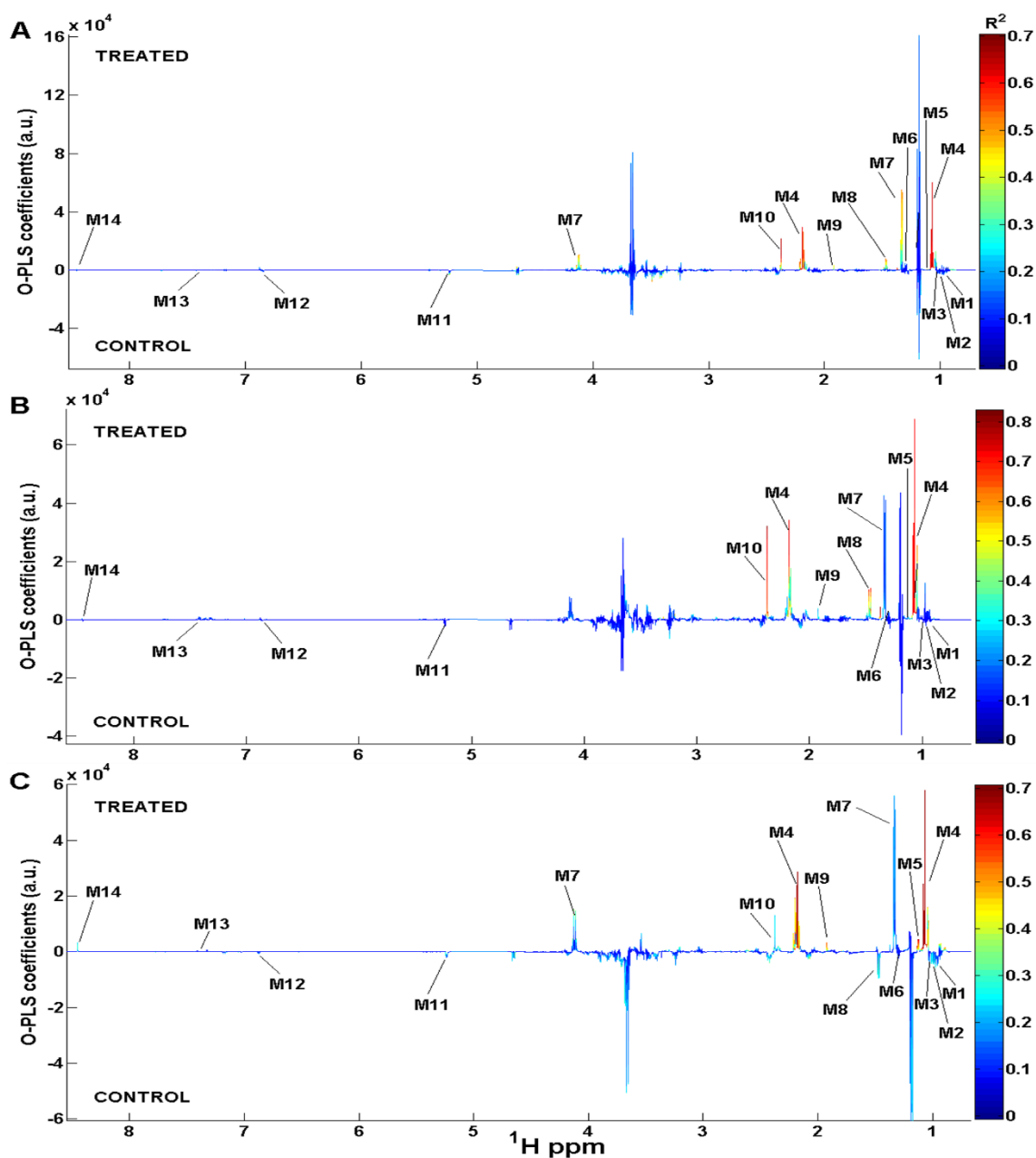


Figure 4.8: Loadings plots of OPLS-regression models showing the quantitative dose-response of propionate on HepG2 cells culture media samples at (A) 24, (B) 48, and (C) 72 hours of exposure. Horizontal axis corresponds to the NMR chemical shift scale; vertical axis corresponds to the O-PLS model coefficients (also referred to as loadings). The line variation corresponds to model covariance derived from the mean-centred model, whereas the colour map corresponds to model correlation derived from the unit-variance model. Metabolites that correlated significantly and associated with the propionate dose response were assigned on the model coefficient plot.

Table 4.4: List of metabolites assigned in the loadings plots of OPLS-regression models for propionate experiment (shown in **Figure 4.8**). R values and p-values were calculated by comparing the SCFA-treated group with control group for each time point. (n=12). The significant R values were identified by using <http://vassarstats.net/> for Significance of a Correlation Coefficient.

			Correlation with treatment values (R values) and the p-value for the significance metabolite		
Metabolite key	Metabolites	Chemical shift (¹ H ppm)	24-hr	48-hr	72-hr
M1	Leucine	0.93 (d), 0.94 (d), 1.71 (m)	-0.2354 (ns)	-0.1247 (ns)	-0.3427 (ns)
M2	Isoleucine	0.94 (t), 1.02 (t)	-0.3140 (ns)	-0.1887 (ns)	-0.4341 (ns)
M3	Valine	0.98 (d), 1.04 (d), 3.62 (d)	-0.2557 (ns)	-0.1733 (ns)	-0.4397 (ns)
M4	Propionate	1.06 (t), 2.183 (q)	0.7948 (p=0.004)	0.8511 (p=0.002)	0.8277 (p=0.0004)
M5	α-keto-β-methylvalerate	1.10 (d)	0.6660 (p=0.0180)	0.7058 (p=0.0104)	0.7944 (p=0.0020)
M6	Threonine	1.32 (d), 3.6 (d), 4.25 (m)	-0.1561 (ns)	-0.1680 (ns)	-0.1938 (ns)
M7	Lactate	1.32 (d), 4.11 (q)	0.6901 (p=0.0130)	0.3913 (ns)	0.4279 (ns)
M8	Alanine	1.46 (d)	0.6982 (p=0.0116)	0.8161 (p=0.0012)	-0.4608 (ns)

M9	Acetate	1.92 (s)	0.6281 (0.0287)	0.5040 (ns)	0.7214 (<i>p</i> =0.0081)
M10	Pyruvate	2.37 (s)	0.8113 (<i>p</i> =0.0014)	0.8661 (<i>p</i> =0.0003)	0.4411 (ns)
M11	α -D-Glucose	5.24 (d)	-0.6557 (<i>p</i> =0.0210)	-0.1317 (ns)	-0.2840 (ns)
M12	Tyrosine	6.89 (d), 7.18 (d)	-0.3362 (ns)	-0.2240 (ns)	-0.3907 (ns)
M13	Phenylalanine	7.31 (m), 7.36 (m), 7.4 (m)	-0.3252 (ns)	0.3316 (ns)	0.2960 (ns)
M14	Formate	8.45 (s)	0.2210 (ns)	0.0051 (ns)	0.4536 (ns)

Note: *** (-) values mean the metabolites negatively correlated with the treatment; ns, non-significance metabolite.

For OPLS-regression models, the metabolites with the highest correlation coefficients were identified and summarised in order to investigate the metabolic signature related to dose- and/or time-response of propionate on HepG2 cells. The OPLS-regression loadings plots of each model are presented in **Figure 4.8-A, B, and C**, while **Table 4.4** summarises the metabolite assignments with R values for each metabolites. The hot colours on the loadings plots show the high correlated variables whereas the cold colours represent the weak correlation. Specifically, α -keto- β -methylvalerate and acetate were the markers of the dose- and time-response as these two metabolites consistently positively correlated with the propionate treatment at all time points. When compared to the sodium control experiment, for α -keto- β -methylvalerate, 80% of the variance has been shown to be caused by the treatment of propionate, while 50% is caused by the sodium. Thus highlighting the major role of propionate in driving this effect. On the other hand, acetate is not a signature metabolite

in our sodium control experiment, therefore the effect that is observed here is solely caused by the propionate treatment on the cells. Moreover, lactate, alanine, and pyruvate were positively correlated, while glucose was negatively correlated in propionate-treated group at 24-hr time point.

In order to summarise the results, a synthetic metabolic pathways were constructed using a univariate analysis comparing the final concentration of these metabolites between the propionate and the control group at each time point. Based on the results from the univariate analysis however, only glucose and alanine were significantly modulated when the cells were treated with propionate at 24-hr time point with the p -values of $p=0.0021$ and $p=0.0474$, respectively (**Figure 4.9, Table S.1 in Appendix for detailed p values**). At 48-hr time point, only alanine was significantly modulated by the treatment of propionate ($p=0.0010$). The relative quantifications for 48-hr and 72-hr time points showed that all of the quantified metabolites, amino acids, lactate, pyruvate, as well as intermediate of BCAA catabolism α -keto- β -methylvalerate in particular were increased in the propionate treated group (**$p>0.05$, Figure 4.9, Table S.1 in Appendix for detailed p valuse**). However, univariate data analysis using Wilcoxon-Mann-Whitney tests was not able to show any significant difference in these metabolites when compared to the control group. Pyruvate is involved in many important pathways and reactions. Alanine transaminase is a transaminase enzyme that catalyses a reversible reaction between pyruvate and alanine. Moreover, pyruvate also can be generated from phosphoenolpyruvate (PEP) in glycolysis pathway, and in certain conditions, such as when oxygen supply is limited, it is reduced to generate lactate.

Interestingly, both the multivariate and univariate analysis showed that propionate was significantly and consistently difference in all time points (**Table 4.4, Figure 4.9**). Although the metabolites that is expected to be significantly modulated as the result of the consumption of propionate by the cells for energy metabolism (e.g., high level of glucose, amino acids, pyruvate, lactate, and succinyl-CoA) are not observed, based on the patterns of propionate consumption by the cell at all time point, it suggests the potential use of propionate by cells as substitute to glucose for energy production.

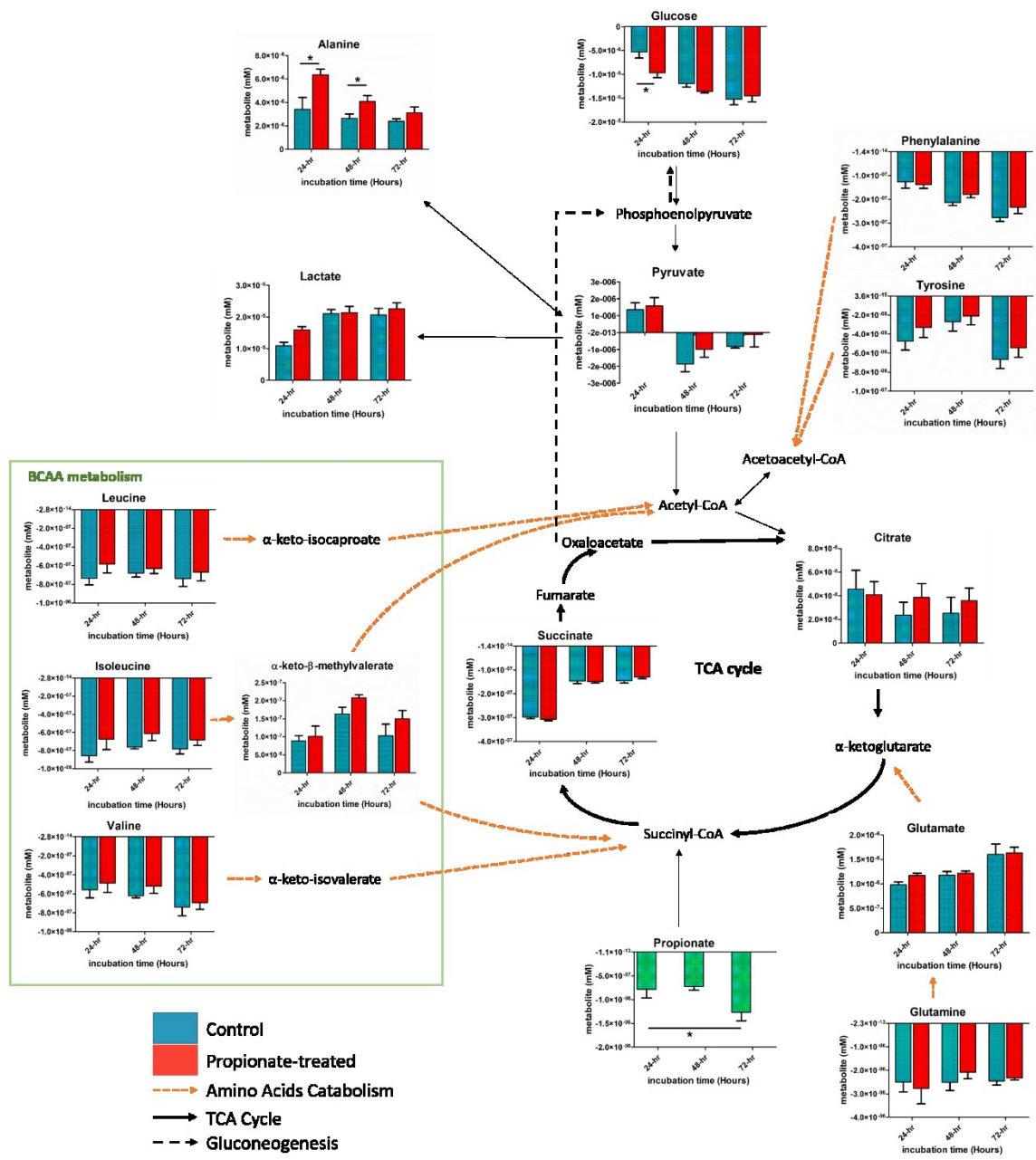


Figure 4.9: Mapping of HepG2 cells medium metabolites accumulation and consumption pattern involved in BCAAs metabolism, amino acids metabolism, TCA cycle, and gluconeogenesis for propionate experiment. The bar plots are expressed as the mean \pm SEM over control values ($n=6$). For each time point, metabolites concentration measured from cell medium were normalised by cell numbers. Significance difference between propionate-treated group and control group were calculated with non-parametric Wilcoxon-Mann Whitney test: * $p < 0.05$. (p values in **Table S.1** in Appendix).

Next, in order to identify patterns of these metabolic markers in a biologically perspective, Metabolite-Set Enrichment Analysis (MSEA) was carried out on the set of metabolites that have been identified as the markers of propionate treatment on HepG2 cells.

Table 4.5 shows the result of Over Representative Analysis in MSEA.

Table 4.5: Result from Over Representation Analysis (ORA) of MSEA based on the set of significant metabolites.

Metabolite set	Hit	<i>p-value</i>
Pyruvate metabolism	3	2.33E-4
Alanine metabolism	2	0.00155
Glucose-alanine cycle	2	0.0066
Propionate metabolism	2	0.0148
Gluconeogenesis	2	0.0332
BCAA degradation	2	0.0339

4.3.5 HepG2 cells treated with butyrate have an increase rate in nutrient consumption and nutrient uptake related to energy metabolism pathways.

Similar to previous section (*section 4.3.4*), supervised multivariate statistics were used in this chapter to investigate the specific metabolic signature associated with the treatment of butyrate (0.1 nM, 1.0 μ M, and 1.0 mM) on HepG2 cells. As a complementary analysis, the signature metabolites observed from the multivariate analysis were then quantified and compared between the butyrate-treated and the control group at each time point using non parametric Wilcoxon-Mann Whitney test. OPLS-DA models were constructed to compare cell media metabolic profiles at each time point. Three predictive components and several number of orthogonal components have been used to construct the OPLS-DA models. The optimal number of orthogonal components was determined by goodness-of-fit (R^2Y) and goodness-of-prediction (Q^2Y) statistics (*Table 4.6*). All OPLS-DA models (24, 48, and 72-hr time point), were able to separate between the control and the treated group. 3D OPLS-DA models also showed a good separation between the control and the treated group along the predictive component 1 (Tpred 1) and the Tpred 2 shows variations related to dose-response (*Figure 4.10-A.i, B.i, and C.i*). All models were validated by using permutation tests that show the significance of the models ($p < 0.05$) (*Figure 4.10-A.ii, B.ii, and C.ii*).

Table 4.6 : Value of Q^2Y , R^2Y , and validation of OPLS-DA models for butyrate experiment.

Time points	PC	OC	Q^2Y	R^2Y	p-value
24-hr	3	3	0.5072	0.9689	0.0001
48-hr	3	4	0.5028	0.9938	0.0036
72-hr	3	3	0.54529	0.9971	0.0001

Abbreviations; PC- Number of Predictive components, OC- Number of Orthogonal components.

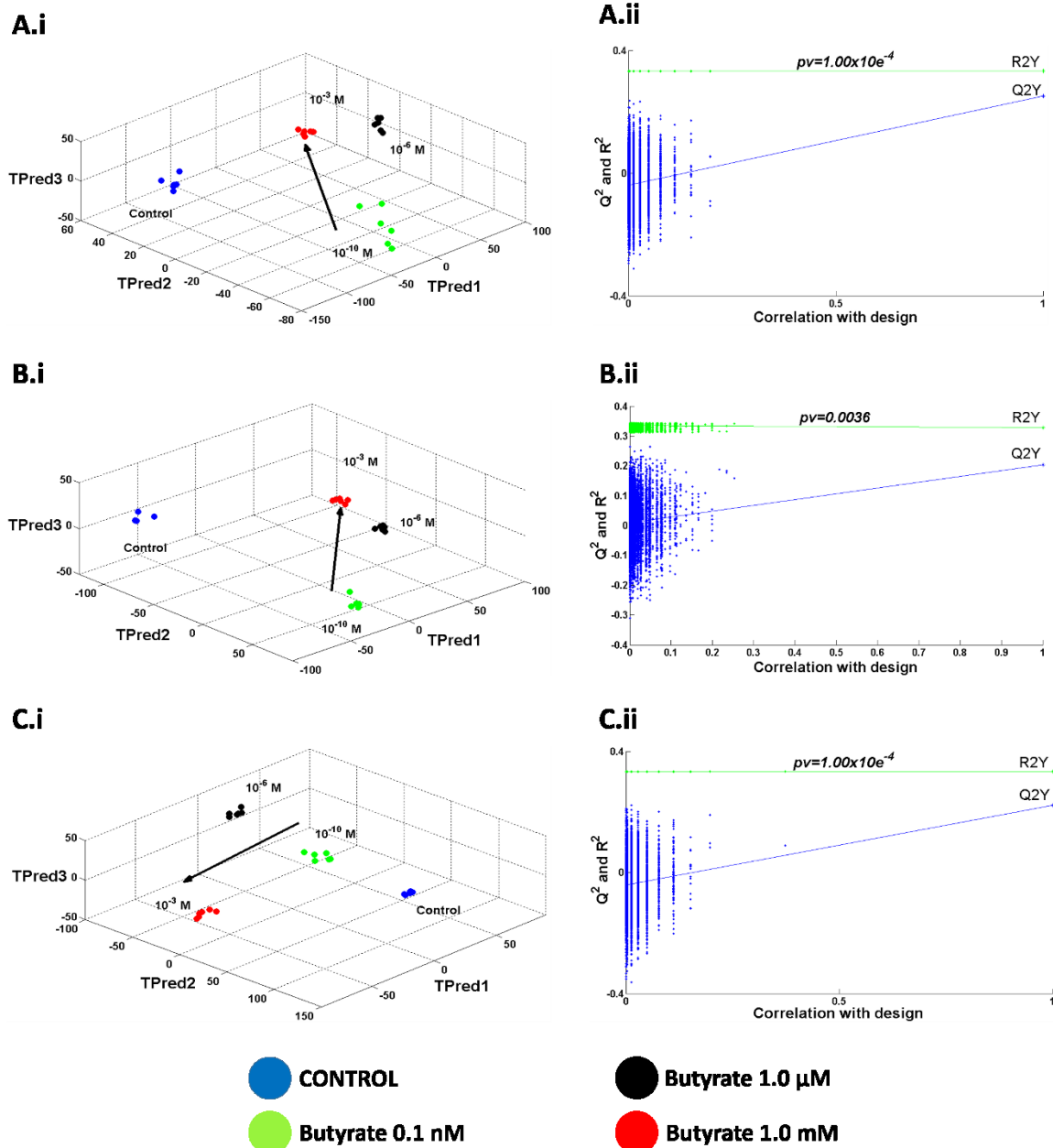


Figure 4.10: OPLS-DA score and validation plots separating the control group and the treatment groups (butyrate) as well as separating between the treatments groups themselves. Score plots of different doses of butyrate treatment on HepG2 cells at (Ai) 24 (Bi) 48 and (Ci) 72 hours exposure. All the OPLS-DA models were validated with multiple permutations testing with 10,000 iterations and cross validations in figures A.ii, B.ii, and C.ii for models of 24-hr, 48-hr, and 72-hr respectively. ($p < 0.05$).
**Please note the dose-related trajectory visualised by black arrow is not a regression line.*

In addition to discriminant analysis, OPLS-regression was able to significantly model the dose response of butyrate (0.1 nM, 1.0 μ M, and 1.0 mM) treatment on HepG2 cells at each time point. The numbers of predictive and orthogonal components for this analysis were listed in **Table 4.7**. OPLS-regression score plots showed a good linear dose response of butyrate treatment for all models (**Figure 4.11-A.i, B.i, and C.i**). Finally, model validations were performed which resulted in significant p value for all time points ($p < 0.05$).

Table 4.7: Goodness of fit (R^2Y), prediction (Q^2Y) and validation values for OPLS regression models of butyrate -treated vs control.

Time points	PC	OC	Q^2Y	R^2Y	p-value
24-hr	1	2	0.7585	0.9821	0.0001
48-hr	1	2	0.5360	0.9995	0.0392
72-hr	1	2	0.8121	0.9771	0.0001

Abbreviations; PC- Number of Predictive components, OC- Number of Orthogonal components.

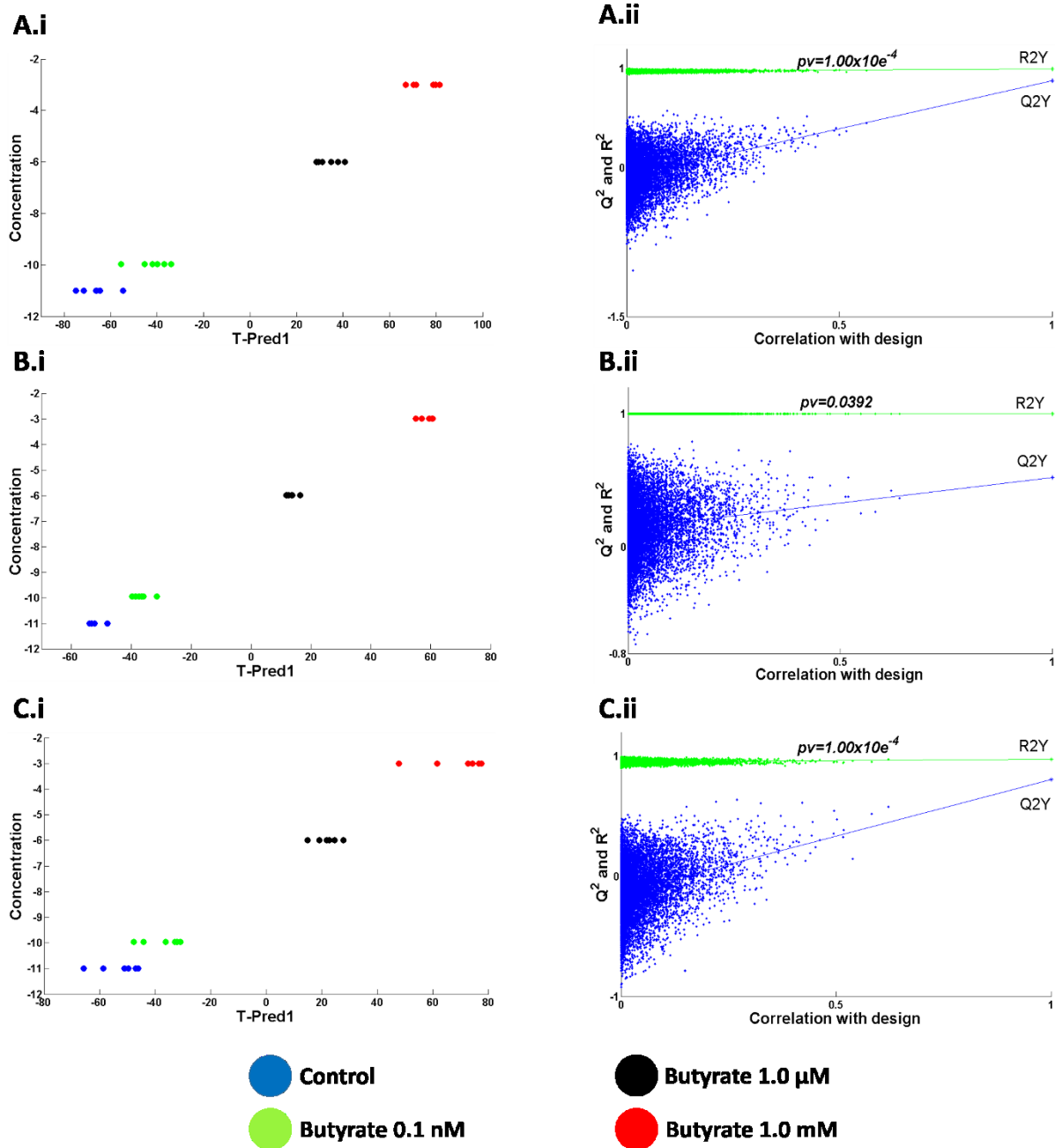


Figure 4.11: OPLS regression models predicting the dose-related response of butyrate treatment on HepG2 cells. For each model, the scores plots indicate a linear effect of butyrate treatment on HepG2 cells at (A) 24, (B) 48, and (C) 72 hours of exposure. Results of random permutation with 10,000 iterations for models validation (A.ii), (B.ii), and (C.ii) showing a good validation of models ($p < 0.05$).

In order to visualise the biomarkers that explain the variations in the models, metabolites with a strong degree of correlation were identified and assigned. OPLS-regression loadings plots of each models are presented in **Figure 4.12** and metabolite assignments along with their R values are summarised in **Table 4.8**.

At 24-hr time point, metabolites mainly amino acids were found negatively correlated with the treatment. In particular, a specific metabolic signature involving isoleucine degradation, pyruvate metabolism, and alanine metabolism has been found to be associated with butyrate treatment. Indeed, α -keto- β -methylvalerate, pyruvate, and alanine, as well as glucose were positively correlated with the treatment with high R values (0.7572, 0.7736, and 0.5985) (**Figure 4.12**) (**Table 4.8**). Univariate data analysis of the concentration of these metabolites at 24-hr time point confirms that these metabolites were significantly modulated in butyrate-treated group compared to control group (**Figure 4.13**, **Table S.2 in Appendix for detailed p values**).

Loadings plot for 48-hr model also show the same pattern of metabolites modulation as in 24-hr model (**Figure 4.12**). Amino acids, such as valine, leucine, isoleucine, threonine, and tyrosine were consistently high in control group compared to butyrate-treated group throughout the experiment, thus considered as markers of butyrate dose- response. Surprisingly, univariate data analysis using nonparametric Wilcoxon-Mann Whitney test on the final concentration of these signature metabolites at 48-hr time point, was not able to show any significant difference when comparing between the butyrate-treated and the control group ($p>0.05$) (**Figure 4.13**).

Interestingly, loadings plot of 72-hr model again revealed that α -keto- β -methylvalerate and alanine were positively correlated with the treatment of butyrate on HepG2 cell. As these metabolites were consistently up-regulated in the butyrate-treated group in all models, they constitute stable candidate markers of butyrate dose-response phenotype. However, despite showing strong correlation with the treatment of butyrate on HepG2 cells (**Table 4.8**), only alanine, glucose, and butyrate were significantly modulated in butyrate-treated group when compared to the control group at 72-hr time point, based on the nonparametric test using Mann Whitney test (**Figure 4.13**, **see Table S.2 for detailed p values**). While alanine can be generated from the transamination reaction with pyruvate that

catalyse by the alanine transaminase enzyme, α -keto- β -methylvalerate is produced during the BCAA isoleucine degradation by cytosolic branched chain aminotransferase 1 (EC: 2.6.1.42). The appearance of α -keto- β -methylvalerate in butyrate-treated group suggests that there is possibly less incorporation of this metabolite into TCA cycle in butyrate-treated condition as the cells might preferred butyrate as their energy source.

Combining multivariate data analysis and univariate data analysis using Wilcoxon-Mann-Whitney tests enabled us to better understand the link between β -oxidation, BCAA catabolism, and TCA cycle in the context of SCFA treatment on HepG2 cells. As butyrate has been established as the main energy substrate for colonocytes, the results of this study point out that there is a possibility that butyrate might also be the preferred source of energy as substitute to glucose in this hepatic cell model if this SCFA is available.

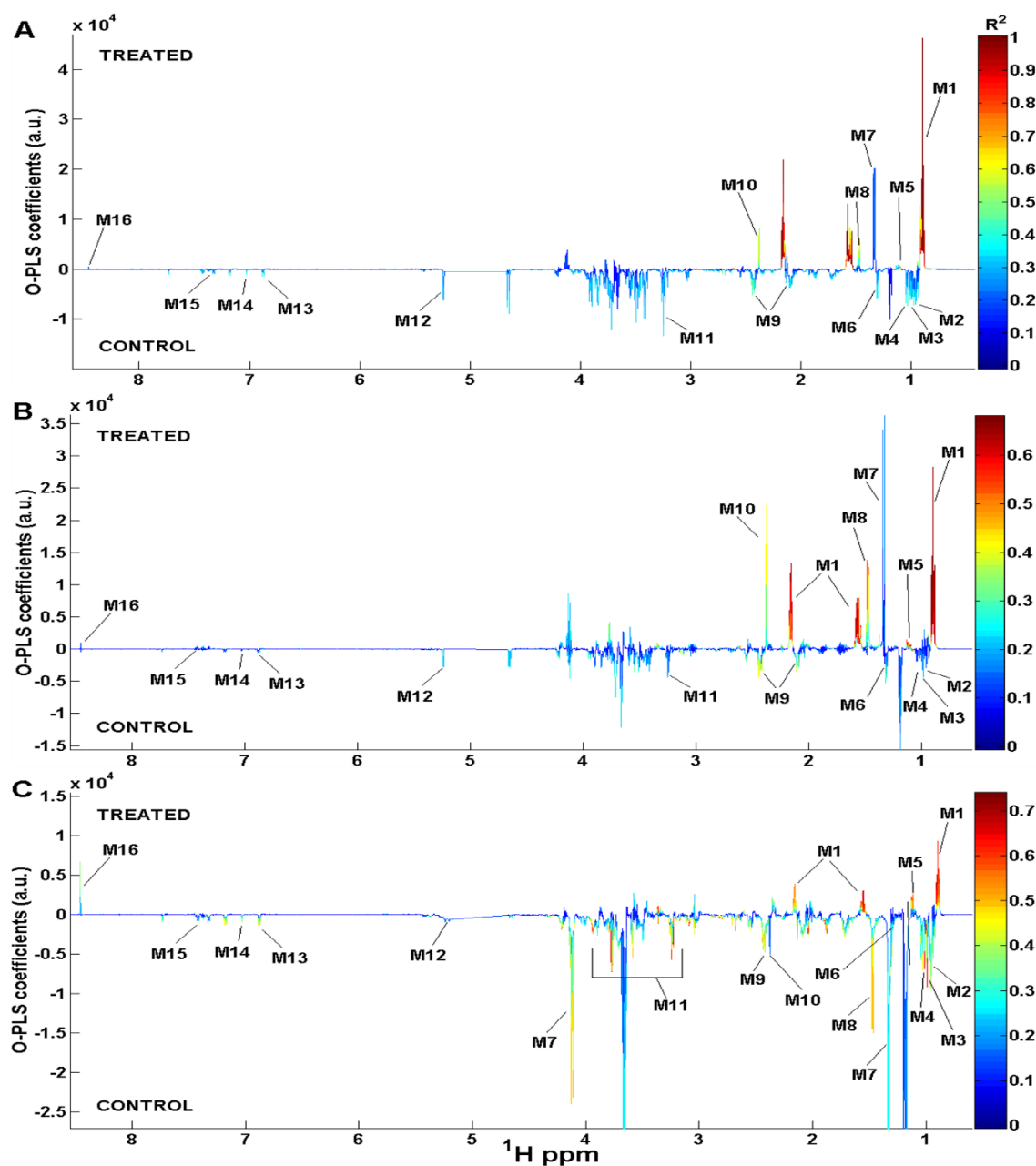


Figure 4.12: Loadings plots of OPLS-regression models showing the quantitative dose-response of butyrate on HepG2 cells culture media samples at (A) 24, (B) 48, and (C) 72 hours exposure. Horizontal axis corresponds to the NMR chemical shift scale; vertical axis corresponds to the O-PLS model coefficients (also referred to as loadings). The line variation corresponds to model covariance derived from the mean-centred model, whereas the colour map corresponds to model correlation derived from the unit-variance model. Metabolites that correlated significantly and associated with the butyrate dose response were assigned on the model coefficient plot.

Table 4.8: List of metabolites assigned in the loadings plots of OPLS-regression models for butyrate experiment (shown in **Figure 4.11**). R values and p-values were calculated by comparing the SCFA-treated group with control group for each time point. (n=12). The significant R values were identified by using <http://vassarstats.net/> for Significance of a Correlation Coefficient.

			Correlation with treatment values (R values) and the p-value for the significance metabolite		
Metabolite key	Metabolites	Chemical shift (¹ H ppm)	24-hr	48-hr	72-hr
M1	Butyrate	0.88 (s), 1.55 (m), 2.14 (m)	0.8816 (0.0015)	0.8030 (0.0016)	0.8001 (0.0017)
M2	Leucine	0.93 (d), 0.94 (d), 1.71 (m)	-0.5020 (ns)	-0.2687 (ns)	-0.5516 (ns)
M3	Isoleucine	0.94 (t), 1.02 (t)	-0.4245 (ns)	-0.3359 (ns)	-0.5340 (ns)
M4	Valine	0.98 (d), 1.04 (d), 3.62 (d)	-0.4544 (ns)	-0.4859 (ns)	-0.4970 (ns)
M5	α-keto-β-methylvalerate	1.10 (d)	0.7392 (p=0.0060)	0.7869 (p=0.0027)	0.7572 (p=0.0043)
M6	Threonine	1.32 (d), 3.6 (d), 4.25 (m)	-0.5259 (ns)	-0.4446 (ns)	-0.5125 (ns)
M7	Lactate	1.32 (d), 4.11 (q)	0.3952 (ns)	0.4340 (ns)	-0.5117 (ns)
M8	Alanine	1.46 (d)	0.7736 (p=0.0032)	0.7129 (p=0.0092)	0.6901 (p=0.0130)
M9	Glutamine	2.15 (m), 2.44 (m), 3.77 (t)	-0.4828 (ns)	-0.6281 (p=0.0290)	-0.6788 (p=0.0154)

M10	Pyruvate	2.37 (s)	0.57455 (ns)	0.6557 (<i>p</i> =0.0207)	-0.2073 (ns)
M11	α-D-Glucose	5.24 (d)	-0.5421 (ns)	-0.5107 (ns)	-0.4011 (ns)
M12	β-D-Glucose	3.25 (m), 3.49 (m), 3.49 (m), 3.5 (m), 3.91 (d), 4.66 (d)	-0.4202 (ns)	-0.3008 (ns)	-0.7709 (<i>p</i> =0.0034)
M13	Tyrosine	6.89 (d), 7.18 (d)	-0.5062 (ns)	-0.4413 (ns)	-0.5506 (ns)
M14	3-methylhistidine	7.05 (s), 7.70 (s)	-0.5355 (ns)	-0.3896 (ns)	-0.3004 (ns)
M15	Phenylalanine	7.31 (m), 7.36 (m), 7.4 (m)	-0.4849 (ns)	-0.2637 (ns)	-0.4666 (ns)
M16	Formate	8.45 (s)	0.2591 (ns)	0.3204 (ns)	0.6127 (<i>p</i> =0.034)

Note: *** (-) values mean the metabolites negatively correlated with the treatment; ns, non-significance metabolite.

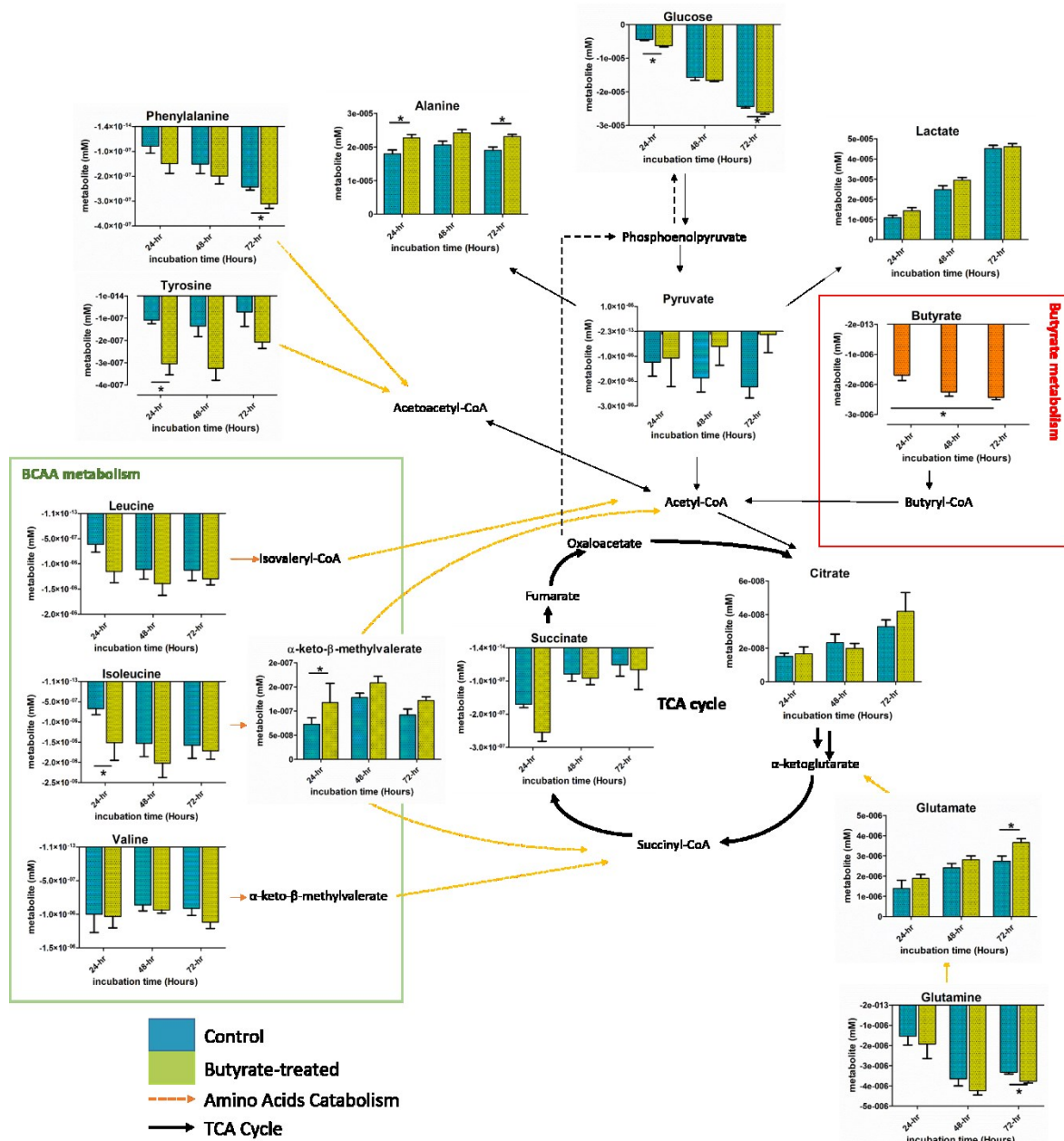


Figure 4.13: Mapping of HepG2 cells medium metabolites accumulation and consumption pattern involved in BCAAs metabolism, amino acids metabolism, TCA cycle, and gluconeogenesis for propionate experiment. The bar plots are expressed as the mean \pm SEM over control values ($n=6$). For each time point, metabolites concentration measured from cell medium were normalised by cell numbers. Significance difference between butyrate-treated group and control group were calculated with non-parametric Wilcoxon-Mann Whitney test: * $p < 0.05$. (p values in **Table S.2** in Appendix).

In order to put these results into biological perspective, the metabolites that show strong correlation were analysed using MSEA analysis. Over Representative Analysis in MSEA further revealed an enrichment of metabolites in a number of KEGG pathways within the signature metabolites. **Table 4.9** lists the results of the MSEA analysis.

Table 4.9: Metabolic pathway enrichment analysis of the set of metabolites that positively correlate with the treatment of butyrate in HepG2 cells. Enriched pathways were identified using Metabolite-Set Enrichment Analysis.

Description	Metabolites hit	p-value
BCAAs degradation	4	3.31E-4
Pyruvate metabolism	2	0.0182
Alanine metabolism	2	0.00155
Glucose-alanine cycle	2	0.0066

4.5 DISCUSSION

A growing body of evidence suggests microbiota-derived metabolites; SCFAs play a vital role in regulating host energy metabolism (den Besten *et al.*, 2015; Gao *et al.*, 2009; Lin *et al.*, 2012). In this chapter, HepG2 hepatocarcinoma cell line was used to investigate the effect of SCFAs: propionate and butyrate on hepatic cancer metabolism by using a cell metabonomics approach. Cell media obtained from different time of incubation was assessed and profiled by using ^1H NMR spectroscopy.

It has been demonstrated that there is a dose-response relationship of propionate and butyrate treatment on HepG2 cells. Dosing the cells with increasing doses of propionate and butyrate at each time point increased the accumulation of α -keto- β -methylvalerate, pyruvate, and alanine. These suggest that there was a modulation in a number of metabolic pathways including BCAA metabolism, pyruvate metabolism, as well as alanine metabolism, which link to host energy metabolism.

4.5.1 SCFA: propionate and butyrate demonstrate growth inhibition in HepG2 cells at dose above 10 mM.

In this chapter, a wide range of SCFA concentrations was first screened to assess their pharmacological range. This is a preliminary optimisation step to determine the concentration that is toxic to the cells. This is to make sure that this concentration is avoided in subsequent metabonomics analyses and keeping them in the pharmacological range. The screening experiment was based on the HepG2 cell viability after the exposure with SCFA: propionate and butyrate. Based on the results for both propionate and butyrate experiments, it has been demonstrated that 0.01 nM to 1.0 mM of these two compounds did not affect cell viability at all tested time points (24-, 48-, and 72-hr). This range of concentration further considered as the pharmacological concentration. A previous study has shown that butyrate and other SCFAs decreased cell proliferation in intestinal HT29-MTX cells when use at concentration higher than 0.5 mM (Giromini *et al.*, 2015). Based on our results, both propionate and butyrate at 10 mM and higher have been shown to drastically decreased cell viability.

Propionate has been reported to inhibit the growth of rat basophilic leukaemia cell lines, RBL-2H3, as well as demonstrated the inhibitory role in rat and human lymphocytes at the dose of 2 mM and higher (Curi *et al.*, 1993; Vecchia *et al.*, 1997). In human neutrophil model, 4 mM butyrate and propionate were able to induce the apoptosis and growth arrest via histone deacetylase inhibitor (HDAC) activities that lead to caspase-dependent apoptotic pathways and not GPR41/GPR43-dependent pathways (Aoyama *et al.*, 2010).

The effect of butyrate in inhibiting proliferation and stimulating differentiation of a number of colorectal cancer cell lines has been well studied (Gamet *et al.*, 1992; Siavoshian *et al.*, 1997, 2000; Whitehead *et al.*, 1986). A previous study by Hinnebusch *et al.*, indicated that slightly higher concentrations of butyrate and propionate at 5 mM but not at 1 mM caused growth arrest and differentiation of HT-29 cell line (Hinnebusch *et al.*, 2002). The effect of butyrate and propionate on growth arrest was said to be associated with the increase of p21, cell cycle regulator gene expression and down-regulation of cyclin B1 (CB1) (Hinnebusch *et al.*, 2002). Our results highlight that high doses used in our study, which were 10 mM and 100 mM might also inhibit HepG2 cells proliferation and viability via pathways discussed above, thus signifies the role of propionate and butyrate in regulating cell growth.

To summarise, based on our experiment, HepG2 cells undergo normal proliferation when exposed to different doses of propionate and butyrate ranging from 0.01 nM to 1.0 mM for 72 hours. This range of concentration is considered as a safe pharmacological range for both SCFAs. Both propionate and butyrate exert their toxic effect when using at 10 mM and higher.

4.5.2 Accumulation of α -keto- β -methylvalerate associated to modulation of BCAA isoleucine metabolism in propionate-treated HepG2 cells.

In this chapter, HepG2 cells treated with propionate showed an increase in extracellular lactate, α -keto- β -methylvalerate, acetate, pyruvate, and alanine metabolite. Propionate is a substrate for hepatic gluconeogenesis (Anderson and Bridges, 1984). Propionate is one of the major SCFAs produced during the fermentation of dietary fibres in gut. This metabolite is metabolised primarily in liver where it enters the TCA cycle via the

succinyl-CoA entry point. Besides being used as fuel, propionate also has been reported to play significant role in maintaining metabolic homeostasis. Recently, a study has shown that this metabolite increased the rate of intestinal gluconeogenesis by acting as free fatty acid receptor 3 (FFAR3) agonist to induce intestinal gluconeogenesis gene expression via a gut-brain neural circuit (De Vadder *et al.*, 2014). Den Besten *et al.*, demonstrated that propionate and other SCFAs were able to protect against diet-induced obesity *via* a PPAR γ -dependent pathway in *in vivo* and *in vitro* models with HepG2 as one of their cellular model. In addition, a study conducted by Lin *et al.*, using *Ffar3* knockout mice showed that the ability of propionate and butyrate in stimulating gut hormone release, suppressing food intake, and protect against diet-induced obesity is via FFAR3-independent pathway (Lin *et al.*, 2012).

To summarise the results, a synthetic metabolic pathways consisting of all the signature metabolites identified in this analysis is constructed (**Figure 4.9**). Higher production of lactate by the HepG2 cells was observed in the propionate-treated condition as compared to the control. The possible explanation for this is that, in the presence of propionate, this metabolite might involve in the gluconeogenesis producing glucose. More glucose will then be available to be metabolised to produce pyruvate in glycolysis. As pyruvate can be reduced to lactate by lactate dehydrogenase (LDH) in cytosol, more lactate can be generated in this condition. Under certain conditions, such as when there is a limited oxygen supply, mammalian cells undergo anaerobic glycolysis, producing large amount of lactate (Mulukutla *et al.*, 2010). However, in cancer cells or fast proliferating cells, the consumption of glucose is high even under normal oxygen condition, resulting in the end product lactate. Lactate produced is then excreted to the extracellular environment (Mulukutla *et al.*, 2010; Vazquez *et al.*, 2010; Warburg, 1956). This phenomenon is known as Warburg effect or also called an aerobic glycolysis (Warburg, 1956). In cells, the levels of lactate and pyruvate are always kept in balance by a reversible reaction catalysed by lactate dehydrogenase enzyme as it converts NADH to NAD⁺ and back (Latham *et al.*, 2012). A previous study demonstrated that the level of lactate was found to increase significantly in muscle during intense exercise as glycolysis exceeded the ability of mitochondria to metabolised the pyruvate produced (Putman *et al.*, 1995). In this chapter, the excreted level of lactate and pyruvate were observed when assessing the extracellular environment (cell media). Moreover, both lactate and pyruvate were found to be positively correlated with the treatment of propionate on HepG2 cells.

Alanine is another metabolite that can be produced from pyruvate. Like lactate, alanine is the other signature metabolite in this study, as revealed by the strong correlation of this metabolite in propionate-treated group. Alanine, a non-essential amino acid can be produced from pyruvate by the glucose-alanine cycle. This primarily happens in skeletal muscle to eliminate nitrogen and at the same time replenishing the energy supply. Pyruvate produced from glucose oxidation is then converted to alanine by alanine transaminase enzyme. The synthetic metabolic pathway illustrates that the accumulation of alanine is concurrently with the accumulation of lactate in HepG2 cells media for propionate-treated group (**Figure 4.9**).

α -keto- β -methylvalerate is one of the dose- and time-response metabolic markers of propionate treatment on HepG2 cells. This metabolite is produced during the degradation of amino acid isoleucine by cytosolic branched chain aminotransferase 1 (BCAT). This keto-acid is then further degraded by branched chain keto acid dehydrogenase E1 (BCKHD) to 2-Methyl-1-hydroxybutyl-ThPP and eventually to acetyl-CoA which enters TCA cycle for ATP production (Rennie *et al.*, 2006). In addition, higher accumulation of α -keto- β -methylvalerate in propionate-treated group compared to the control group suggests that propionate preferentially enters TCA cycle at the level of succinyl-CoA, thus caused an accumulation of α -keto- β -methylvalerate in the growth media (**Figure 4.9**). However, α -ketoisocaproate and α -ketoisovalerate, the intermediate metabolites from the degradation of BCAAs leucine and valine, respectively were not able to be detected. BCAAs catabolism, occurs in most tissues such as kidney, liver, heart, and brain, but was found to be at the highest rates in skeletal muscle (Harris *et al.*, 2005; Rennie *et al.*, 2006).

4.5.3 Butyrate changes HepG2 cells energy metabolism by modulating BCAA metabolism.

Butyrate, alongside with acetate and propionate is the major product of intestinal fermentation (Roediger, 1982). It has been well documented that colonocytes metabolised majority of the butyrate produced as substrate for fuel, however, some portion can reach the liver via portal vein (Beauvieux *et al.*, 2001). In this chapter, the cell specific-markers of

butyrate dose responses were investigated when HepG2 cells were treated with sodium butyrate. Butyrate, unlike propionate does not enter the TCA cycle via succinyl-CoA but undergoes β -oxidation in mitochondria to produce acetyl-CoA, which then enters the TCA cycle (Donohoe *et al.*, 2011). Based on the metabonomics analysis, a number of amino acids, including phenylalanine, tyrosine, and BCAAs (valine, leucine, and isoleucine) have been found to be consistently down-regulated in butyrate-treated group. Moreover, when analysing the rate of metabolites consumed by the cells, it is confirmed that there were higher consumptions rate per cell for these amino acids in butyrate-treated groups when compared to the control group (**Figure 4.13**). These results suggest that more amino acids consumption occurred to generate intermediates for TCA cycle for energy production when HepG2 cell were treated with butyrate. It has been shown that there was an increase levels of amino acids including BCAAs in germ-free mice colonocytes compared to conventionally-raised mice, where autophagy is used to generate amino acids for energy production (Donohoe *et al.*, 2011). Autophagy is a mechanism that involves the breakdown of cellular components to maintain cellular energy levels during starvation. However, in our study it is not possible that the cells were in substrate-starved condition as glucose and other essential growth components were supplied at a normal level in the growth media during the experiment.

As butyrate is the preferred energy substrate for colonocytes, most of the studies carried out in this area focusing on the role of butyrate in colonocytes. As mentioned earlier, butyrate has to be converted into acetyl-CoA before it can enter the TCA cycle. It is then converted to citrate in the first step of TCA cycle before being transported out of mitochondria. In present study, HepG2 cells have been found to produce more citrate in butyrate-treated group compared to control. The mode of transportation for citrate to be transported across mitochondrial membrane into the cytoplasm is *via* the citrate channel (Donohoe *et al.*, 2012; Sun *et al.*, 2015). However, the mechanism of its release outside of the cell is still not well understood and it was suggested via K⁺ ion transporter based on previous study carried out on prostatic epithelial cells (Mycielska and Djamgoz, 2004).

In this study, the treatment of butyrate has been shown to consistently increase the levels of extracellular lactate. As previously discussed (**section 4.5.2**), production of lactate came from the reversible reaction between lactate and pyruvate by the action of enzyme lactate dehydrogenase. As the cell might switch to use butyrate as substitute to glucose,

acetyl-CoA is synthesised and incorporating into the TCA cycle for energy production. When there is enough acetyl-CoA generated from the oxidation of butyrate, pyruvate may not be used, thus reversible reaction between pyruvate and lactate might occur resulting in the increase level of lactate. Moreover, cancer cells as in HepG2 cells produce high amount of lactate from pyruvate even in the presence of oxygen, described as “Warburg effect” (Cairns *et al.*, 2011; Feron, 2009). Lactate transport across plasma membrane is of fundamental importance in mammalian cells. In order to maintain the high rate of glycolysis, glycolytic cells must transport lactate out of the cell and this is mediated by a family of monocarboxylate transporters (MCTs) (Juel and Halestrap, 1999; Ullah *et al.*, 2006). In contrast, other tissues that require lactate to fuel respiration (red muscle and heart) or gluconeogenesis (liver and kidney) needed to transport lactate into the cell (Halestrap and Meredith, 2004; Halestrap and Price, 1999).

Additionally, there was also a marked increase of alanine in butyrate-treated group. Univariate analysis of the individual metabolite per cells also revealed that HepG2 cells accumulated more alanine in the butyrate-treated group compared to the control (**Figure 4.13**). Alanine can be produced and excreted during the catabolism of glutamine to lactate. In cells, glutamine is used to replenish TCA cycle intermediates, and the secretion of nitrogen as ammonia and alanine accompanies this process. Glutamine was converted to glutamate, producing α -ketoglutarate by transamination reaction. Alanine aminotransferase removes an α -amino group from glutamate and transfers it to non-essential amino acids. The decrease in glutamine levels and at the same time an increase in glutamate production was also observed in this experiment. The accumulation of alanine in the cell medium was significantly higher in butyrate-treated group when compared to the control ($p < 0.05$). This suggests that less alanine is being taken up and converted into pyruvate by the cells, as the cells may possibly prefer to utilise butyrate for their energy source instead.

Catabolism of BCAA valine, leucine, and isoleucine produced α -keto-isovalerate, α -keto-isocaproate, and α -keto- β -methylvalerate, respectively, as intermediate metabolites by transamination reactions. These metabolites either can serve as a source of acetyl-CoA for the TCA cycle, or enter via the succinyl-CoA entry point. However, only α -keto- β -methylvalerate was able to be detected and measured in this study. The increase in α -keto- β -methylvalerate suggests that the activity of branched chain aminotransferase (BCAT) and

branched-chain keto acid dehydrogenase (BCKDH) during early steps of BCAA catabolism outstrips the capacity of the downstream enzymes in metabolising α -keto- β -methylvalerate and incorporating acetyl-CoA in TCA cycle. In this study, higher level of α -keto- β -methylvalerate was observed in HepG2 cells treated with butyrate compared to the control group. This may suggest that the treatment of butyrate may up-regulate the expression of enzymes that play role in regulating the BCAA catabolism. It has been shown previously that fatty acids oxidation and the activation of peroxisome proliferator-activated receptor- α (PPAR α) activate rat hepatic BCKDH complex by decreasing BCKDH kinase, thus promote BCAA catabolism (Shimomura *et al.*, 2004). To summarise, in the presence of butyrate, instead of using glucose, HepG2 cells might possibly use butyrate to generate acetyl-CoA for TCA cycle. The influx of acetyl-CoA appears to exceed the capacity for incorporating in TCA cycle, thus potentially cause an accumulation of β -oxidation and BCAA intermediates (*i.e.*, α -keto- β -methylvalerate) which can be exported out of the mitochondria.

4.6 CONCLUSION

This study provides an explanation on the mechanisms related to the treatment of propionate and butyrate on hepatic cancer cell line (HepG2) as well as highlighting the signature metabolites related to the dose-response of these SCFAs. Firstly, SCFAs; propionate and butyrate from 0.01 nM to 1.0 mM have been demonstrated to not able to alter the HepG2 cell viability, while the concentrations of 10 mM and above are toxic to the cells. Subsequent experiments using several doses selected from pharmacological range of propionate and butyrate further demonstrate an up-regulation of a number of metabolites related to several pathways including BCAAs metabolism, pyruvate metabolism, alanine metabolism, and gluconeogenesis. Dosing HepG2 cells with propionate and butyrate also displayed an increase in isoleucine catabolism product, α -keto- β -methylvalerate as revealed by the accumulation of this metabolite in the cell media. To summarise, in response to SCFA (propionate and butyrate) treatment, HepG2 cells might switch from glucose to SCFA as substrate for acetyl-CoA synthesis and incorporation into TCA cycle for energy production. Thus, this *in vitro* study further highlights the role of SCFA in regulating host's energy metabolism in a view of hepatic cancer metabolism in HepG2 cell line.

CHAPTER 5

5. PHARMACOLOGICAL EFFECT OF SHORT-CHAIN FATTY ACIDS IN RECEPTOR ACTIVATION: GPR109A (HYDROXYCARBOXYLIC ACID RECEPTOR 2 OR HCAR2), FREE FATTY ACID RECEPTOR 2 (FFAR2/GPR43), AND FREE FATTY ACID RECEPTOR 3 (FFAR3/GPR41).

5.1 INTRODUCTION

Short-chain fatty acids (SCFAs), mainly acetate, propionate, butyrate, and valerate are produced by gut microbiota through the fermentation of complex carbohydrates such as dietary fibres (Cummings, 1981). SCFA concentrations can reach up to 100 mM in the lumen of the colon and provide 6-9% of our daily energy requirement (Stevens and Hume, 1998). However, SCFAs not only serve as energy source, but also act as signalling molecules by activating G-protein coupled receptors, therefore activating subsequent signalling pathways.

G-protein coupled receptors (GPCRs), also known as 7TM receptors, are the largest protein family of receptors in mammals (Trzaskowski *et al.*, 2012). This receptor family is involved in the regulation of almost all physiological processes in the body. G-protein coupled receptors sense molecules outside the cell and activates intracellular signal transduction pathways thus regulating cellular responses. GPCRs have been shown to be activated by a number of endogenous ligands, such as hormones, neurotransmitters, peptides, proteins, and fatty acids(Howard *et al.*, 2001; Kirkham *et al.*, 1992). Upon ligand binding, GPCRs can

activate four different families of heterotrimeric G proteins (G_s , $G_{i/o}$, $G_{q/11}$, and $G_{12/13}$) inside the cell, which in turn activate cellular responses through a variety of second messenger cascades (Lefkowitz, 2007; Oldham and Hamm, 2007; Wettschureck and Offermanns, 2005). Recently, several groups identified that fatty acids act as ligands for GPCRs and play a significant role in the body's function. Three independent groups simultaneously deorphanised G-protein coupled receptor 41 (GPR41) and 43 (GPR43), and that short-chain fatty acids as a ligand for these receptors, hence the name of FFAR3 and FFAR2 for GPR41 and GPR43, respectively (Brown *et al.*, 2003; Le Poul *et al.*, 2003; Nilsson *et al.*, 2003). FFAR2 belongs to the same family as FFAR3 which shares 42% amino acid identity (Brown *et al.*, 2003). These receptors are activated by SCFAs, particularly acetate, propionate, and butyrate at high micromolar or millimolar concentrations.

Recently, another type of GPCR, GPR109A (also known as hydroxycarboxylic acid receptor 2 or HCA2) was identified to be activated by nicotinic acid or niacin. Niacin, also known as nicotinamide or nicotinic acid, is one of the essential human nutrients and must be obtained either from the diet or the gut microbiota (Rucker, 2007). Humans are able to synthesise niacin in the liver from the essential amino acid tryptophan and distribute it to non-hepatic tissues (Fukuwatari and Shibata, 2013). The pathway in which tryptophan is converted to niacin is called tryptophan-nicotinamide pathway and requires 9 steps of reaction. Although niacin can be produced from tryptophan, it is considered as the byproduct of the kynurenine pathway; the first part of the tryptophan-nicotinamide pathway (Fukuwatari and Shibata, 2013). **Figure 5.1** summarises the tryptophan-nicotinamide pathway.

Recently, genomic assessment of 256 common human gut microbiota revealed that niacin is one of the most commonly synthesised vitamins of the human gut microbiota genomes with 162 predicted producers. This study revealed that the phyla Actinobacteria, Firmicutes, Fusobacteria, Bacilli, and Proteobacteria are the main niacin producers (Magnúsdóttir *et al.*, 2015).

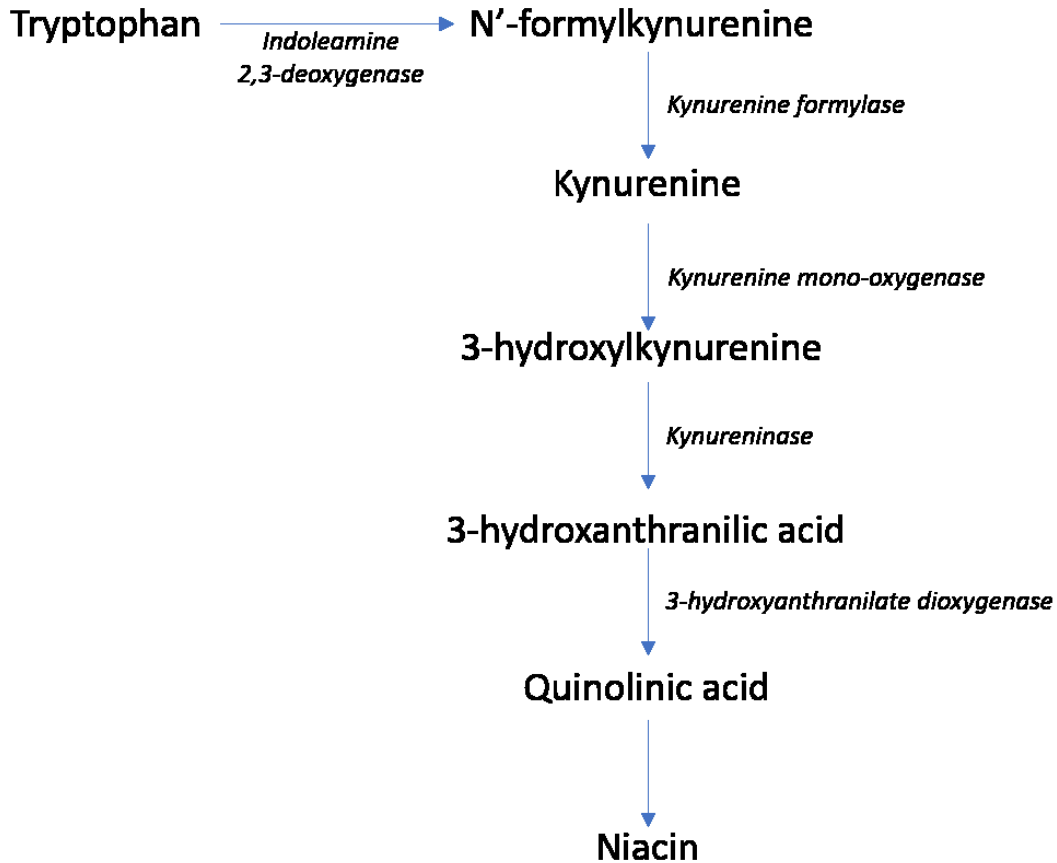


Figure 5.1: Biosynthesis of niacin from essential amino acid tryptophan. Information taken from Fukuwatari and Shibata, (2013).

Niacin has been used for treating dyslipidaemia for years (Knopp, 1999). It has been shown that niacin significantly reduces cardiovascular events and atherosclerosis based on meta-analysis of seven trials of secondary prevention (Duggal *et al.*, 2010). In addition, study conducted on statin-treated and statin-intolerant patients has shown that niacin increases HDL-C plasma concentration by 20% while decreases plasma concentrations of LDL cholesterol and lipoprotein-(a) (Bruckert *et al.*, 2010). Using mice lacking the gene coding for this receptor, the lipid-lowering effects of niacin was demonstrated to be via receptor activation (Tunaru *et al.*, 2003; Wise *et al.*, 2003). GPR109A in humans corresponds to PUMA-G in rodents. This receptor also can be activated by butyrate as demonstrated by Blad *et al.*, (2012) and Taggart *et al.*, (2005), and has been shown to suppress colonic inflammation and carcinogenesis in GPR109A-dependent manner (Singh *et al.*, 2014b).

Due to the fact that butyrate activates GPR109A and exhibits the same effect as niacin, it is hypothesised that the other SCFAs may also have the same properties in activating this receptor. To test this hypothesis, the role of SCFAs (1 to 5 carbons) in GPR109A activation is investigated by using a cAMP accumulation assay. In addition to this, a harmonised pharmacological assessment of a comprehensive SCFA panel, as well as niacin on FFAR2 and FFAR3 are also implemented.

5.2 MATERIALS AND METHODS

5.2.1 GPR109A activation assay.

The pharmacological effect of short-chain fatty acids in GPR109A activation was carried out using cAMP Hunter™ eXpress GPCR Assays kit (DiscoverX, USA) according to the manufacturer's protocol. The functional status of GPR109A activation is monitored by measuring the accumulation of cellular cAMP using a homogeneous, gain-of-signal competitive immunoassay based on Enzyme Fragment Complementation (EFC). The cAMP Hunter eXpress cells expressing stably GPR109A (DiscoverX, USA), and stimulated with forskolin were used in this experiment. The experiment was carried out in two days. Briefly, on day 1, the frozen cAMP Hunter eXpress CHO-K1 cells expressing GPR109A were thawed and plated on a 96-well microplate at the seeding density of 30,000 cells/well. The microplate was then placed in a humidified incubator with an atmosphere of 5% CO₂ at 37°C for 18-24 hours prior to testing. On day 2, the media was carefully aspirated and 45 µL of diluted cAMP Antibody was added. Then, the test compounds (formate, acetate, propionate, butyrate, valerate, isobutyrate, isovalerate, and niacin) were prepared in 8-point dose curve serial dilution in Cell Assay Buffer containing 15 µM forskolin. The agonist-forskolin mixture was added to the well and then was incubated for 30 minutes at 37°C. Following agonist incubation, 60 µL of working cAMP detection reagents/cAMP Solution D mixture was added to the wells, and the microplate was incubated for 1 hour at room temperature, protected from light. Then 60 µL of cAMP solution A was gently added to the wells and the plate was incubated for another 3 hours at room temperature, protected from light. Finally, the microplate was read for luminescence using spectrophotometer plate reader.

5.2.2 Free fatty acid receptor 3 (FFAR3) activation assay.

The effect of short-chain fatty acids and related compounds on free fatty acid receptor 3 (FFAR3) was carried out using cAMP Hunter™ eXpress GPCR Assays kit (DiscoverX, USA). This assay was carried out according to the manufacturer's protocol with slight modifications to suit the experimental design. This kit is highly sensitive to measure G-protein coupled receptor (GPCR) activation based on 3'-5'-cyclic adenosine monophosphate (cAMP) production in cells. This kit was used in line with cAMP Hunter™ eXpress FFAR3 CHO-K1 cell line (DiscoverX, USA).

In brief, CHO-K1 cells expressing FFAR3 were mixed with cell plating reagent and plated in 96-well plate at the seeding density of 30,000 cells/well. Cells were incubated at 5% CO₂ at 37°C overnight prior to the assay. The next day, designed as day 2, the cell-plating reagent was gently removed, and the cells were treated with several concentrations of agonist with 15 μM forskolin. The cells were then incubated for 30 minutes at 37°C. Following agonist incubation, 15 μL of cAMP antibody reagent and 60 μL of cAMP detection solution were added to the wells and the plate was incubated for another 1 hour at room temperature in the dark to allow the immunocompetition reaction to occur. Then, 60 μL of cAMP Solution A was added and the plate was incubated at room temperature in the dark for another 3 hours. Finally the samples were read on a standard luminescence plate reader.

5.2.3 Free fatty acid receptor 2 (FFAR2) activation assay.

In this experiment, the pharmacological effect of short-chain fatty acids and niacin in activating FFAR2 are investigated. Similar with FFAR3 activation experiment, activation of the FFAR2 by the agonist was carried out by measuring the accumulation of cAMP in the cells. cAMP accumulation was measured by HitHunter® cAMP XS+ Assay kit (DiscoverX, USA). CHO-K1 cells expressing stably FFAR2, and stimulated with forskolin was used as a reporter cells. The same protocol as FFAR3 activation assay was applied for this assay with slight modification on the volume of the reagents to suit the experimental design (*section 5.2.2*).

5.3 RESULTS

5.3.1 SCFAs: C₄ and C₅ SCFAs as well as niacin, induced activation of GPR109A.

The pharmacology of GPR109A was investigated by assaying several short-chain carboxylic acids and related molecules using cAMP Hunter™ eXpress GPCR Assays kit (DiscoverRx, USA). The compounds tested in this experiment were carboxylic acids with 1 to 6 carbons, either linear or branched, with niacin as a positive control. **Table 5.1** lists the compounds tested together with their EC₅₀ value.

Being the classical agonist for GPR109A, niacin shows the highest affinity for the receptor with EC₅₀ of 0.02 μM (**Figure 5.2**). This indicates that our assay worked and allowed us to progress with analysis of the test compounds which were short-chain fatty acids. Based on the analysis, butyrate, valerate, isobutyrate, and isovalerate were found to display an agonist activity on GPR109A (**Figure 5.2**). These compounds were characterized by similar micromolar potency in activating the receptor, except for butyrate where we were not able to calculate the EC₅₀ for this metabolite (**Figure 5.2**). Butyrate is an agonist of this receptor based on the study carried out by Taggart *et al.*, (2005) with EC₅₀ of 1590 μM. Out of the other three agonists metabolites, only valerate displayed a full cAMP inhibition curve and showed the highest affinity for GPR109A with calculated EC₅₀ of ~280 μM. Isobutyrate and isovalerate (C₄ and C₅), only displayed a partial agonist for this receptor with low affinity for GPR109A for both compounds (EC₅₀= ~ 0.1 mM) (**Figure 5.2**). Shorter carbon chain of carboxylic acids, in formate (C₁), acetate, (C₂), and propionate (C₃) however, are found to be a non-agonist for this receptor (**Figure 5.2**) (**Table 5.1**).

These screening results indicate that *i*) GPR109A is activated by longer chain length SCFAs with valerate being the strongest agonist for the receptor, *ii*) SCFAs being partial agonists and finally *iii*) shorter chain length SCFAs below 3 carbons (formate, acetate, and propionate) could not activate GPR109A.

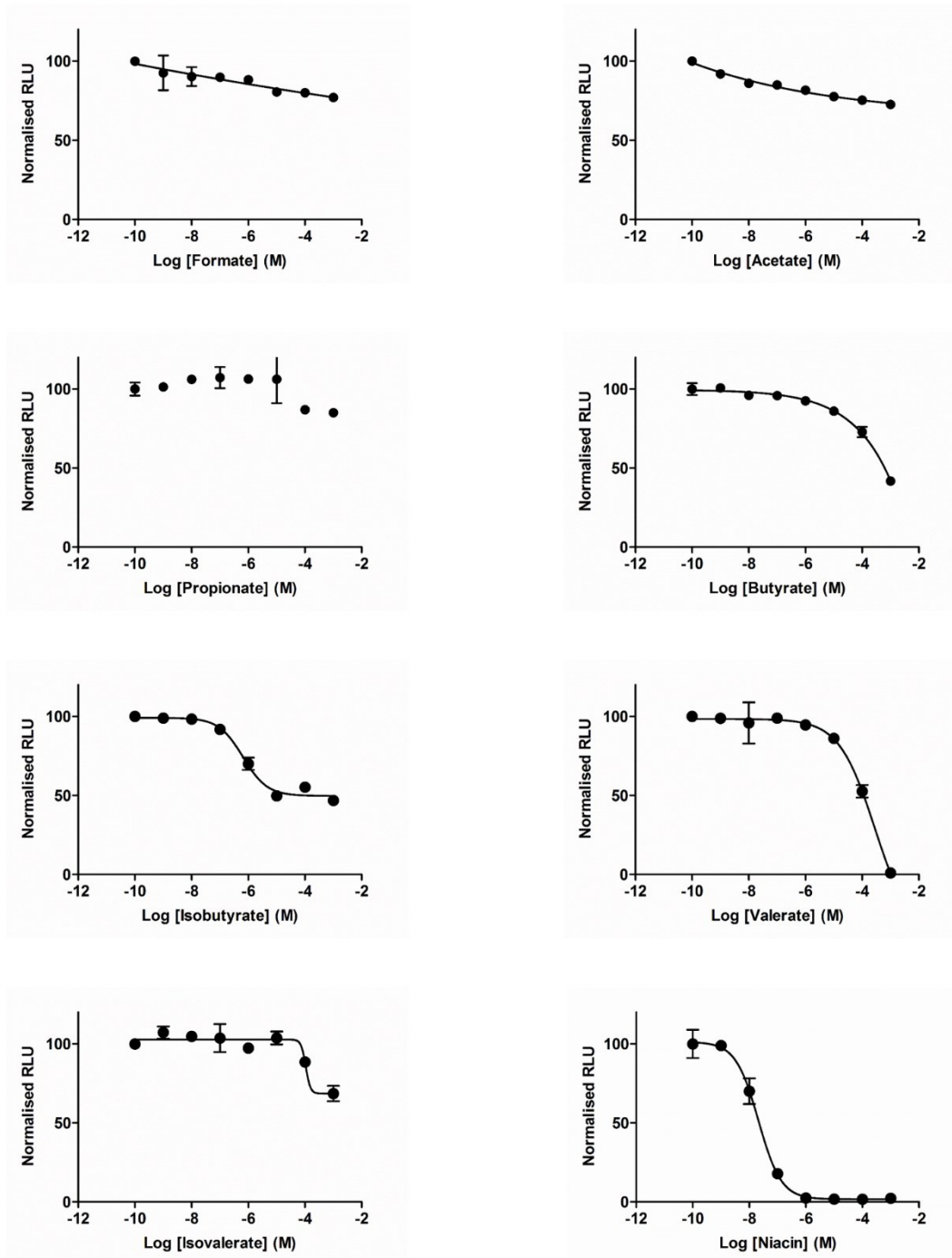


Figure 5.2: Pharmacology of GPR109A in a cAMP accumulation assay. cAMP Hunter eXpress cells expressing GPR109A (DiscoverX, USA) were incubated with various concentrations of SCFA and niacin, together with 15 μ M forskolin. The data represent the mean \pm S.E. for triplicate data points ($n=3$).

5.3.2 SCFAs and niacin –induced activation of FFAR3.

Next, the pharmacology of free fatty acid receptor 3 (FFAR3), or also called G-protein coupled receptor 41 (GPR41), was extended by assaying the same compounds as previous section (5.2.1) in a cAMP accumulation assay using cAMP Hunter™ eXpress CHO-K1 cells (DiscoverRx, USA), expressing stably FFAR3, and stimulated with forskolin. As expected, FFAR3 was found to be activated by all tested compounds with different affinity for each compounds (Figure 5.3). Propionate, a known ligand for FFAR3 was used as control in this assay and was found to be the strongest agonist for this receptor. The order of potency for FFAR3 was propionate > valerate > isobutyrate > butyrate > isovalerate > acetate > niacin > formate. The shortest carbon chain fatty acid tested which was carbon 1, formate shows the lowest affinity for FFAR3 with EC₅₀ value of 7017 μM. Surprisingly, niacin, a classical agonist for GPR109A, also was found to activate FFAR3 (EC₅₀=1465 μM), which has not been reported before. However, the potency of niacin in activating FFAR3 is relatively low and only considered as partial agonist based on the result generated using this cell model (Figure 5.3). Table 5.2 lists the complete EC₅₀ values for each of the tested compound.

The results of this screening experiment was in agreement with previous studies that demonstrated FFAR3 has affinity for slightly longer chain length SCFAs with formate and acetate as the weakest agonist for this receptor compared to longer chain SCFAs with 3-5 carbons.

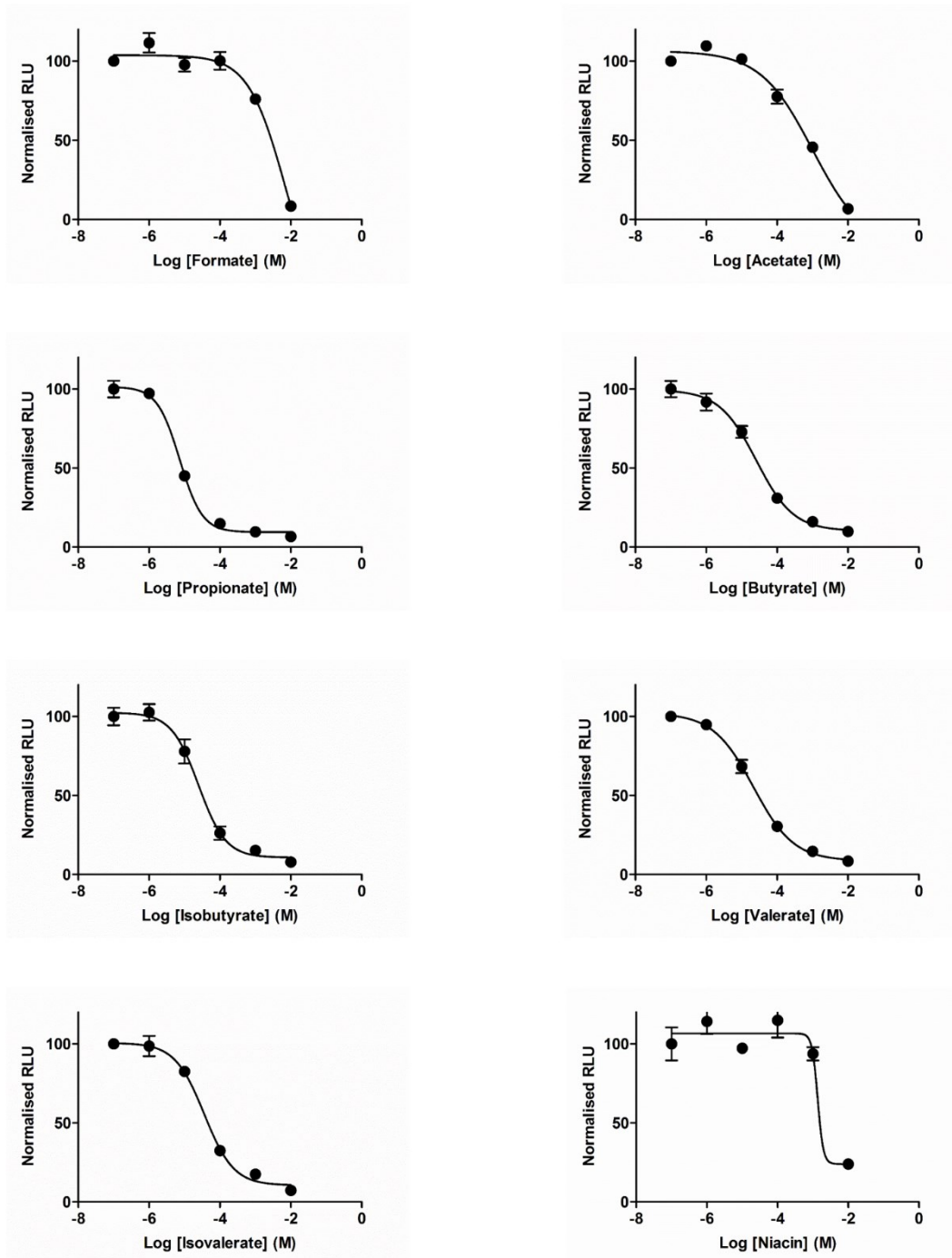


Figure 5.3: Pharmacology of FFAR3 in a cAMP accumulation assay. CHO-K1 cell lines expressing FFAR3 (DiscoverRx, USA) were incubated with various concentrations of SCFA and niacin, together with 15 μ M forskolin. The data represent the mean \pm S.E. for triplicate data points (n=3).

5.3.3 SCFAs and niacin –induced activation of FFAR2.

In this study, the ability of SCFA and niacin have been screened in activating free fatty acid receptor 2 (FFAR2), another member of the GPR40-43 receptor subfamily. This receptor is also known as GPR43.

The results of this experiment show that all tested compounds were able to activate the receptor with different potency. Propionate served as the positive control for this assay as it was the most potent agonist for FFAR2 with EC_{50} of 0.443 μ M. Among the compounds displaying an agonist activity on this receptor, acetate, propionate, and butyrate activated FFAR2 with similar micromolar potency (**Figure 5.4**). Isobutyrate also showed an agonist activity but was slightly less potent compared to acetate, propionate, and butyrate. The linear and the branched chain of carbon 5, valerate and isovalerate, were also able to activate the receptor and decreased the level of forskolin-induced cAMP levels in the cells. However, these compounds were lower efficacy agonists of FFAR2 relative to propionate with millimolar range of potency. Carbon 1 short-chain fatty acid, formate, and the other test compound, niacin were also able to activate the receptor but to a lesser extent. Although these compounds were able to activate FFAR2, the EC_{50} values were relatively high when compared to propionate. Using the reporter cells, approximate EC_{50} value of formate was determined to be 1920 μ M. The agonist activity of SCFAs and niacin on FFAR2 can be ranked as follows: propionate > butyrate > acetate > isobutyrate > isovalerate > valerate > formate > niacin.

Table 5.3 lists the complete EC_{50} value for all tested compounds. Based on the results of this experiment, the same pattern of receptor activation by SCFAs as previously shown by Le Poul *et al.*, (2003) were generated. Interestingly, this study is the first study to report on the activation of FFAR2 by niacin (EC_{50} >10 mM), which is a known GPR109A classical ligand.

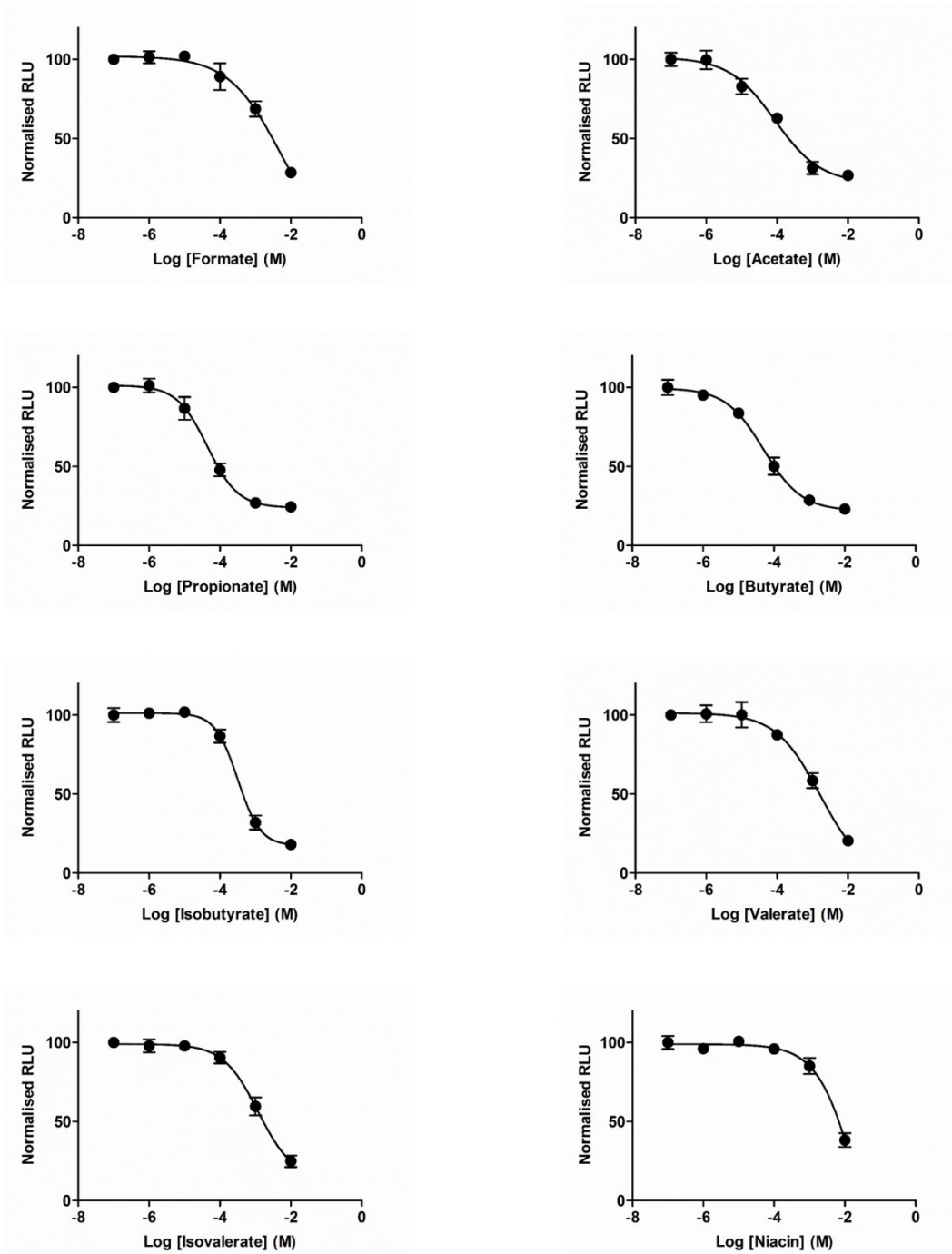


Figure 5.4: Short-chain fatty acids (SCFA) activate FFAR2. SCFA, from 1 to 5 carbons, and niacin were screened on FFAR2 activation using cAMP accumulation assay. CHO-K1 cell lines expressing FFAR2 (DiscoverRx, USA) were incubated with various concentrations of SCFA and niacin, together with 15 μ M forskolin. The data represent the mean \pm S.E. for triplicate data points (n=3).

Table 5.1: EC₅₀ values of SCFAs and related molecule for GPR109A. The functional parameter of GPR109A activation by SCFAs and related molecule were determined using a cAMP accumulation assay (in the presence of forskolin).

Compounds	Carbon	EC ₅₀ (μ M)
Formate	1	NA
Acetate	2	NA
Propionate	3	NA
Butyrate	4	> 1000*
Isobutyrate	4	Partial agonist \approx 100
Valerate	5	279.9
Isovalerate	5	Partial agonist \approx 100
Niacin	6	0.02

*Butyrate has an EC₅₀ of 1590 μ M based on previous study (Taggart *et al.*, 2005). *NA-non agonist

Table 5.2: EC₅₀ values of SCFAs and related molecule for FFAR3. The functional parameter of FFAR3 activation by SCFAs and related molecule were determined using a cAMP accumulation assay (in the presence of forskolin).

Compounds	Carbon	EC ₅₀ (μ M)
Formate	1	7017
Acetate	2	1007
Propionate	3	7.41
Butyrate	4	26.63
Isobutyrate	4	24.90
Valerate	5	9.45
Isovalerate	5	36.08
Niacin	6	1465

Table 5.3: EC₅₀ values of SCFAs and related molecule for FFAR2. The functional parameter of FFAR2 activation by SCFAs and related molecule were determined using a cAMP accumulation assay (in the presence of forskolin).

Compounds	Carbon	EC₅₀ (μM)
Formate	1	1920
Acetate	2	0.866
Propionate	3	0.443
Butyrate	4	0.523
Isobutyrate	4	31.8
Valerate	5	1624
Isovalerate	5	1195
Niacin	6	>10 mM

5.4 DISCUSSION

SCFAs have been shown to activate several GPCRs (FFAR2, FFAR3, and GPR109A), thus activating intracellular cascades that regulate many intracellular processes. The development of new agonist for these receptors is important as it could potentially be used in treating disorders. In this chapter, the agonist activity of SCFAs and niacin in activating FFAR2, FFAR3, and GPR109A were investigated. This was carried out by measuring the accumulation of intracellular cAMP in CHO-K1 cells overexpressing these receptors. Interestingly, this study is the first to demonstrate the agonist activity of niacin on FFAR2 and FFAR3. Moreover, it has also been demonstrated that isobutyrate and isovalerate as the partial agonists for GPR109A, which is to our knowledge is a novel finding.

5.4.1 Butyrate and valerate are full agonists of G-protein coupled receptor 109A (GPR109A) whereas isobutyrate and isovalerate are partial agonists.

SCFAs have been identified as endogenous ligands for the GPCRs; FFAR3 (GPR41) and FFAR2 (GPR43) (Brown *et al.*, 2003; Le Poul *et al.*, 2003). These receptors have been shown to be expressed in adipocytes, which also happen to express another G-protein-coupled receptor, GPR109A (Tunaru *et al.*, 2003; Xiong *et al.*, 2004). Given their similarity in butyrate-induced activation of these receptors, this study investigated whether other short-chain fatty acids are able to activate GPR109A. The activation of GPR109A by SCFAs was investigated by measuring the levels of cellular cAMP after agonist incubation. Stronger agonist activity by longer chain length SCFAs has been observed, with valerate as the strongest agonist for GPR109A. This result is in agreement with previous studies that demonstrated valeric acid (C₅) and caproic acid (C₆) were the most active on this receptor, in both human and mouse models (Taggart *et al.*, 2005). Though, the latter compound was not screened in our work. The reason for us to not incorporate caproate in our study is because this metabolite is produced in low amounts in the colon compared to others (Cummings, 1981). GPR109A has affinity for slightly longer chain length SCFAs with the

minimum of 4 carbons needed to activate this receptor. Butyrate is an agonist for this receptor with EC_{50} of 1590 μ M. It has been shown in this screening experiment that butyrate was also able to activate GPR109A.

The concentration of SCFAs was found to be around 0.1 to 1.5 μ M in blood based on the data from Human Metabolome Database (HMDB). The physiological levels of SCFAs in blood are not sufficient to activate GPR109A, suggesting that, even though some of these SCFA able to activate this receptor, these are not physiological ligands of the receptor. In addition, the concentrations of butyrate in both portal and hepatic venous are around 30.1 and 12 μ mol/L respectively, which are not enough to act as endogenous ligand for GPR109A in this tissues (Bloemen *et al.*, 2009). The first endogenous ligand of this receptor is ketone body 3-hydroxybutyrate, with an EC_{50} of 767 μ M (Taggart *et al.*, 2005).

GPR109A is expressed in various tissues including white and brown adipose tissue (Soga *et al.*, 2003; Tunaru *et al.*, 2003; Wise *et al.*, 2003), as well as in many immune cells including monocytes, neutrophils, and macrophages (Benyó *et al.*, 2005; Kostylina *et al.*, 2008; Schaub *et al.*, 2001). Recently GPR109A also has been shown to be expressed in colon (Thangaraju *et al.*, 2009b). Since butyrate is an agonist of this receptor and present in high millimolar concentrations in colon, this metabolite is a biologically-relevant agonist for GPR109A in this tissue (Thangaraju *et al.*, 2009b). The presence of butyrate and niacin induces death of colon cancer cells, suggesting the involvement of GPR109A (Ganapathy *et al.*, 2013).

It has been demonstrated in this study that branched chain fatty acids of isobutyrate and isovalerate are partial agonists (EC_{50} around 0.1 mM) for GPR109A. The concentration of these compounds in blood is around 0.7-4.4 μ M for isobutyrate and 0.3-2.7 μ M for isovalerate. It is therefore unlikely that these compounds reach appropriate concentrations in plasma to activate this receptor. So, their low affinity for GPR109A is not physiologically relevant. The shorter carbon chain length of SCFA tested in this study, which were formate (C_1), acetate (C_2), and propionate (C_3), were not agonists of GPR109A. This present study is the first to identify isobutyrate and isovalerate as partial agonists for GPR109A and also further confirmed the previously reported activation of GPR109A by SCFAs butyrate and valerate.

5.4.2 SCFAs 3 to 5 carbons are stronger FFAR3 agonists.

Free fatty acid receptor 3 (FFAR3) is a G-protein coupled receptor which is also known as GPR41, belonging to a group of four GPCRs together with GPR43 (FFAR2), GPR40, and GPR42 (Le Poul *et al.*, 2003). In this chapter, several SCFAs have been screened in activating FFAR3 using cAMP accumulation assay. Short-chain carboxylic acids, including acetate, propionate, butyrate, isobutyrate, valerate, and isovalerate have been shown to have agonist activity on FFAR3 with different potency. Propionate (C₃), being the positive control for this experiment, is the most potent and effective ligand for FFAR3. This receptor has been previously orphanised by several groups, and has been identified to be activated by SCFA. In the present chapter, a similar activation pattern of FFAR3 by SCFAs as demonstrated by others was obtained. In general, it has also been shown that the ranked agonists and dose-dependent responses to SCFAs were consistent between research groups, and assay formats, with propionate being the most potent agonist while acetate (C₂) and formate (C₁) displaying lower potencies. Based on this study, valerate (C₅) has been found to be more potent than butyrate (C₄) in activating FFAR3, which was different with what has been reported by others. When comparing the EC₅₀ of both compounds however, the EC₅₀ values between valerate and butyrate is very close. The values are 9.45 μM and 26.6 μM, respectively.

FFAR3 has been shown to couple exclusively to G_{i/o} proteins family (Covington *et al.*, 2006). FFAR3 activation following ligand binding triggers a series of second messenger cascades that result in an intracellular response. G_{αi} activation inhibits cAMP-dependent pathway by inhibiting adenylate cyclase, thus decreasing the production of intracellular cAMP from ATP (Birnbaumer, 2007; Le Poul *et al.*, 2003). In this study, it has been demonstrated that the optimal length of carbon atoms for FFAR3 activation is from three to five carbons. Interestingly, it has also been demonstrated in this study that niacin, a known GPR109A agonist are able to activate FFAR3, but in much lower potency compared to propionate, butyrate, isobutyrate, and valerate, but higher when compared to formate. The EC₅₀ of niacin for FFAR3 is determined to be around 1500 μM. Straight chain of 5 carbons SCFA in valerate is more potent agonist than the branched-chain isovalerate which contains methyl group chain.

FFAR3 appears to be expressed in kidney, colon, spleen, lymph node, and bone marrow (Brown *et al.*, 2003; Hong, 2005; Le Poul *et al.*, 2003). However the expression of FFAR3 in adipose tissue is rather controversial where some investigators were able to detect the expression of the receptor in human and mouse adipose tissue (Brown *et al.*, 2003; Le Poul *et al.*, 2003; Nilsson *et al.*, 2003; Xiong *et al.*, 2004), other groups were not (Frost *et al.*, 2014a; Hong, 2005; Kimura *et al.*, 2011; Zaibi *et al.*, 2010). Despite the fact that SCFAs are able to activate FFAR3, the concentration of these metabolites in blood is low and very unlikely to reach the desired concentration to activate the receptor. The concentration of these metabolites in portal blood is around 258 μM for acetate, $\sim 88 \mu\text{M}$ for propionate, and $\sim 29 \mu\text{M}$ for butyrate (Cummings *et al.*, 1987). Moreover, acetate concentration in plasma can increase up to 10-fold in the event of alcohol administration, resulting in the conversion of around 75% of alcohol to acetate (Siler *et al.*, 1999). Accumulation of propionate, butyrate, and isobutyrate are characteristic features in some inherited diseases (Thompson *et al.*, 1990; Trauner *et al.*, 1975). The accumulation of propionate in the blood can be caused by the disease called propionic acidemia (PA). This rare inherited disorder is caused by the inability of the body to convert propionyl-CoA to methylmalonyl-CoA. Propionyl-CoA, the product of the catabolism of essential amino acids and odd numbers fatty acids cannot be metabolised due to the deficiency of the enzyme propionyl-CoA carboxylase (Brown *et al.*, 2003).

The physiologically relevant site of FFAR3 activation is in the gut where the concentrations of SCFAs in this tissue are known to be much higher than in the blood. SCFAs levels in this tissue can be found up to 500 mM through the gut microbiota fermentation of dietary fibres (Cummings, 1981).

5.4.3 SCFAs with 2 to 4 carbons are stronger FFAR2 agonists.

In this part of the chapter, SCFA, ranging from 1 to 5 carbons, linear and branched, as well as niacin were used to screen on the activation of free fatty acid receptor 2 (FFAR2), or GPR43. Free fatty acid receptor 2 (FFAR2) is structurally related to FFAR3, where FFAR3 shares 42% amino acid identity with FFAR2 (Brown *et al.*, 2003; Le Poul *et al.*, 2003). As

expected, FFAR2 was activated by the same carboxylate ligands as FFAR3, whereas all SCFAs tested in this study displaying an agonist activity on FFAR2. For this receptor however, the rank order of potency was found to be slightly different when compared to FFAR3. For the instance, acetate was demonstrated to be less potent on FFAR3 compared to valerate, but was more potent in activating FFAR2. In fact, acetate activates FFAR2 with similar potency as propionate and butyrate. This observation was in line with what has been reported by previous studies conducted by Brown *et al.*, (2003) and Le Poul *et al.*, (2003), the first two groups to demonstrate that SCFA as ligands for FFAR2 and FFAR3.

In the present study, another compound has also been screened, which was niacin. As mentioned earlier in previous section **(5.3.1)**, niacin is a known agonist of other type of G-protein coupled receptor, GPR109A. moreover, butyrate, a ligand for FFAR2 and FFAR3 also has been shown to activate GPR109A (Taggart *et al.*, 2005). To standardise these three assays, therefore it has been decided for this experiment to test whether niacin could also activate FFAR2 and FFAR3. Interestingly, niacin was found to decrease the intracellular cAMP level in a dose-dependent manner and displayed an agonist activity on this receptor at least based on the screening assay used in this study. However, the EC₅₀ value was relatively higher (EC₅₀ >10 mM) when compared to acetate, propionate, and butyrate. The concentration of niacin in plasma is around 0.1–0.4 μM (Gille *et al.*, 2008), and is unlikely to be the endogenous ligand of FFAR2.

FFAR2 has been shown to be coupled through G_q and G_{i/o} proteins family. Activation of this receptor results in the activation of intracellular pathways including inositol 1,4,5-triphosphate production, intracellular Ca²⁺ release, activation of ERK1/2, and inhibition of cAMP production (Le Poul *et al.*, 2003). This receptor is highly expressed in adipose tissue (Hong, 2005), and in various immune cells (Karaki *et al.*, 2006; Le Poul *et al.*, 2003; Maslowski *et al.*, 2009; Nilsson *et al.*, 2003). As discussed in the previous section **(5.4.2)**, the average concentrations of propionate and butyrate in blood are very low and not likely to trigger an activation of FFAR2. The relevant SCFAs *in vivo* are acetate, propionate, and butyrate, as these metabolites are produced in significant amounts from the fermentation of dietary fibres by gut microbiota in the hindgut. Moreover, SCFAs also can be produced as metabolic by-products of pathogenic bacteria metabolism at sites of anaerobic infection in periodontal disease (Niederman *et al.*, 1997). More recently, a study has shown that

SCFAs have an anti-inflammatory properties and that SCFA-FFAR2 interactions greatly affect inflammatory responses (Maslowski *et al.*, 2009).

In addition to the previous studies, this present study further confirms SCFA as a ligand for free fatty acid receptor 2 (FFAR2). FFAR2 activation by SCFAs inhibits intracellular cAMP production by inhibiting adenylate cyclase activity through G_i protein pathway. The optimal length is from two to four carbon atoms of SCFA for FFAR2 activation.

5.5 CONCLUSION

In this chapter, the pharmacological effects of a comprehensive SCFA panel on their GPCRs, *i.e.*, GPR109A, FFAR3, and FFAR3 have successfully been characterised using a cAMP accumulation assay. This study further confirms previously reported studies on the receptors' activation by SCFAs and extended the knowledge on niacin activation of FFAR3 and FFAR2. Although niacin is not a strong agonist for these receptors, to our knowledge, this is the first study to report on the activation of the receptors by this compound at least based on the cAMP accumulation assay used in this study. The overlapping pattern of expression for FFAR2 and FFAR3, and their somewhat common ligand suggests that both receptors might function similarly. Since many studies have demonstrated that these three receptors play an important role in various body functions, it became clear that these receptors are important targets for the development of high affinity agonist and antagonist. Thus, this study provides a new knowledge on the novel agonists for these receptors that could potentially be used for treating disorders such as cardiovascular and metabolic diseases as well as inflammatory diseases and some cancers.

CHAPTER 6

6. EFFECTS OF SHORT-CHAIN FATTY ACIDS ON 3T3-L1 DIFFERENTIATION AND 3T3-L1 ADIPOCYTE LIPOLYSIS.

6.1 INTRODUCTION

Mature adipocytes are spherical cells with the majority of its cellular component being a lipid droplet. These cells are metabolically active and dynamic in response to different hormones stimulation. Adipocytes plays a vital role in maintaining lipid and energy homeostasis in vertebrate organisms (Klaus, 1997). In the event of food intake, which causes nutritional abundance, the ratio of insulin/glucagon is increased, causing a net influx of free fatty acids and glucose into adipocytes by up-regulating lipoprotein lipase and GLUT4. Acetyl-CoA generated from glycolytic pathway then serves as a precursor for *de novo* fatty acid synthesis which is then subsequently esterified with glycerol and stored in forms of triacylglycerol (TG). This process occurs mainly in adipose tissue and liver (Pearce, 1983). During fasting, TG is mobilised and then hydrolysed by desnutrin, hormone-sensitive lipase and monoacylglycerol lipase to generate free fatty acids, which are subsequently exported from adipose tissue into the blood stream to undergo mitochondrial β -oxidation in energy-demanding tissues such as muscle and liver (Duncan *et al.*, 2007a).

Excess adipose tissue and its dysregulation have a major role in the development of obesity and type 2 diabetes. During adipose tissue expansion, there is an accumulation of fat mass attributed to both hypertrophy and hyperplasia. In general, hypertrophy without hyperplasia generates adipocytes that are metabolically unhealthy (Stephens,

2012). Moreover, during the development of obesity, there is an increase in angiogenesis and macrophage infiltration into adipose tissue, as well as alterations in its secretory profile (Bourlier *et al.*, 2008). For years, we thought that less fat mass is healthy. However, it has been shown that this is not necessarily true as revealed by studies conducted in human and mouse (Stephens, 2012). Ectopic lipid, a condition in which lipid accumulates in other tissues due to not being stored in adipocytes, has been linked with insulin resistance and the development of type 2 diabetes (Gastaldelli, 2011). In addition, obesity is also associated with an increase in basal lipolysis (Reynisdottir *et al.*, 1995). Due to its vital role in regulating lipid and whole body energy homeostasis, the dysregulation of adipocyte function can contribute to metabolic disorders. Hence, a great understanding of these processes is important for maintaining metabolic health.

High dietary fibres cannot be hydrolysed in the small intestine and are fermented in the colon, producing short-chain fatty acids (SCFAs). These gut microbial fermentation products have previously been shown to decrease obesity (Pawlak *et al.*, 2004; So *et al.*, 2007). The increase in plasma SCFAs concentration has been demonstrated to affect adipocyte size and function (Frost *et al.*, 1998; Pawlak *et al.*, 2004). Furthermore, Hong *et al.*, showed that SCFAs increase 3T3-L1 differentiation, and this effect is mediated via its receptor, FFAR2 (Hong, 2005). In another study, adipocytes treated with SCFAs show a reduction in lipolytic activity, and further revealed the involvement of FFAR2 activation as this effect is abolished in adipocytes isolated from FFAR2 knockout mice (Ge *et al.*, 2008).

In this chapter, the role of a comprehensive SCFA panel on adipocytes differentiation and lipolysis was investigated using 3T3-L1 cell line as adipocyte cell model. In order to address their role, a combination of cell-based assays and molecular approaches was used.

6.2 MATERIALS AND METHODS

6.2.1 Cell culture

3T3-L1 mouse embryo fibroblast was obtained from Sigma Aldrich. In brief, preadipocytes were cultured in Dulbecco's Minimal Eagle Medium (DMEM, Gibco®) containing high glucose (4500 mg/L), supplemented with 10% of fetal bovine serum (FBS), 1% of penicillin-streptomycin and 1% of glutamine, in an atmosphere of 5% CO₂ at 37°C. When reaching 70-80% confluent, cells were sub-cultured at the ratio of 1:2 to 1:6, equal to seeding density of 2-5x10⁴ cells/cm² twice a week in order to prevent the culture to become fully confluent. Cells were maintained in T75 flask during routine subculturing. Cells with passage number between 3 and 10 were used for experiment.

6.2.2 Differentiation to adipocytes.

3T3-L1 preadipocytes were plated in 24-well plates, at a density of 2000 cells/cm². Two days after confluence (designated as day 0), differentiation into adipocytes was induced by adding 0.25 µM dexamethasone, 500 µM isobutylmethylxanthine (IBMX), and 0.4 µM insulin into basic culture medium (DMEM, 10% FBS, 1% penicillin-streptomycin, 1% glutamine) with or without the addition of SCFAs for 2 days. This medium is called induction medium. On day 2, the medium was replaced with differentiation medium (DMEM containing 10% FBS, 1% penicillin-streptomycin, 1% glutamine, 0.4 µM insulin) with or without the addition of SCFAs for another 2 days and maintained in basic culture medium thereafter. This medium was replenished every two days until end of experiment. Preadipocyte and adipocyte were treated with vehicle or several concentrations of test compounds from the induction of differentiation until end of differentiation (day 0 until day 10). The short-chain fatty acids used were formate, acetate, propionate, butyrate, and valerate, while for the branched short-chain fatty acids were isobutyrate, and isovalerate. These compounds were tested at different final doses of 1.0 µM, 10 µM, and 100 µM. Cells were considered fully differentiated 10 days after the induction of differentiation (noted as day 10).

6.2.3 Cell viability assay

At day 10 post differentiation (differentiation process described above - see **section 6.2.2**), 3T3-L1 adipocytes were fixed with 3.7% of paraformaldehyde for 20 min, stained during 30 minutes with 0.05% (w/v) Crystal Violet, and washed twice with tap water. A third of the total volume of methanol was then added to solubilise the dye. Cell viability was measured by reading the absorbance in a spectrophotometer plate reader at 540 nm.

6.2.4 Adipogenesis assay

At day 10 post-differentiation, adipogenesis was assessed in 3T3-L1 adipocyte by lipid staining with freshly made Oil Red-O (Sigma Aldrich Co, LCC). Cell monolayers were gently rinsed with phosphate-buffered saline (PBS) and fixed with 3.7% paraformaldehyde for 20 min. The cells were then stained with filtered Oil Red-O solution (0.5% (w/v) in isopropanol) and incubated for 1 hour at room temperature. After washing four times with water, the stained lipids were observed under microscope and picture was taken. Oil Red-O dye retained in the cell was quantified by elution into isopropanol (100%) and the absorbance was measured at 500 nm using spectrophotometer plate reader.

6.2.5 Lipolysis assay

On day 10 of differentiation, mature 3T3-L1 adipocytes were washed twice with PBS and starved with minimal volume of serum-free medium (DMEM with 1% P/S, 1% L-Glutamine and 0.1% free fatty acids-BSA (Sigma)) for 2 hours at 37°C prior to treatment. Cells were then treated with minimal volume of serum-free medium containing either vehicle (0.1% Dimethyl sulfoxide, (DMSO)) or selected doses (1.0 µM, 10 µM, and 100 µM) of test compounds (see **section 6.2.2**). After 3 hours of incubation, samples of the media were collected, transferred into clean Eppendorf tubes, and centrifuged at 8000 rpm for 5 minutes to remove cell debris. Supernatant was transferred to fresh Eppendorf tubes for glycerol release assay.

Glycerol release from lipolysis during treatment of 3T3 adipocyte with test compounds was measured by Free Glycerol Reagent kit (Sigma F6248) according to the manufacturer's protocol with slight modification to suit the design of the experiment. Briefly, the glycerol reagent was added with 40 mL of distilled water and was left at room temperature prior to the assay. Cell medium was mixed with the glycerol reagent in a 1:1 volume ratio and the cell medium-reagent mixture was then incubated at room temperature for 30 minutes. Absorbance was measured with spectrophotometer plate reader at 540 nm.

6.2.6 RNA extraction and quantification.

RNA extraction was performed using RNA extraction kit according to the manufacturer's instruction. Adhered cells in the 24-well plates were directly lysed with lysis buffer provided by the extraction kit supplemented with 1% 2-mecapethanol. Lysates were transferred to Eppendorf tubes, reduced viscosity and homogenised manually by repeated pipetting, vortex, and centrifuging. Homogenised lysate was mixed with 70% ethanol in a 1:1 volume ratio to adjust column binding condition. The mixtures were then transferred to the RNA binding column and centrifuged at 11000 rpm for 30s. After one wash with RW1 buffer and two washes with RW2 buffer provided by the extraction kit, the RNA binding column was dry spun at 11000 rpm for 1 minutes followed by RNA elution with 40uL RNase-free water. RNA concentration in each sample was quantified using nanodrop and stored at -80°C until used.

6.2.7 Reverse transcription.

300ng RNA was reversed transcribed into cDNA using a SuperScript® II Reverse Transcriptase kit and random hexamers. A calculated volume of RNA was topped up to a total volume of 13 uL with RNase-free water then mixed with random primers and heated at 65°C for 5 minutes (calculation is stated in *Table 6.1*). The master-mix consisting of transcriptase, DTT and first strand buffer were then added to the mixture. The volume of

each component in the master-mix is stated in **Table 6.2**. Samples were then run on Peltier Thermal Cycler PTC-200 (MJ Research) with following program: 10 minutes at 25°C, 90 minutes at 42°C and 15 minutes at 70°C.

Table 6.1: Calculation of sample preparation for reverse transcription. [RNA]=RNA concentration in each sample (ng/μL).

	Volume (μL)
RNA	300/[RNA]
RNase-free water	13- (300/[RNA])
Random Hexamer	3
Total volume	16

Table 6.2: Preparation of MasterMix. (#samples=number of samples)

	Volume per sample (μL)	Volume in MasterMix
dNTP (10 mM)	1.5	X #samples + 10% excess
5X First Strand Buffer	5	
DTT (0.1 mM)	2	
Superscript II enzyme	0.5	

6.2.8 Quantitative polymerase chain reaction (q-PCR).

Expression of *Pparg*, *Fasn*, *Adipoq*, *Hcar2*, *Ffar2*, and *Ffar3* were determined by qPCR with StepOne Plus Instrument (Applied Biosystems) using TaqMan® Array 96-Well Fast Plates (Applied Biosystem, USA) according to the manufacturer protocols. Briefly, 10uL of cDNA in a total volume of 20uL reaction mix per well in a 96-well PCR plate was used to carry out the reaction. The reaction mix containing the enzymes and pre-designed Taqman Gene Expression primers for the targeted genes was customised from Thermo Fisher Scientific webpage. Quantification was carried out with the comparative Ct method.

$$\delta Ct = Ct_{(\text{target gene})} - Ct_{(\text{reference gene})}$$

$$\delta\delta Ct = \delta Ct_{(\text{condition2})} - \delta Ct_{(\text{condition1})}$$

$$\text{Fold change} = 2^{(-\delta\delta Ct)}$$

6.2.9 Statistical analysis.

Comparisons between groups (compounds-treated vs vehicle-treated) were performed using two-tailed, Mann-Whitney test for all experiments. All data are presented as mean \pm SEM from 2 separate experiment with the total of 6 samples (n=6) and the critical *p* value for statistical significance was <0.05.

6.3 RESULTS

6.3.1 Validation of GPR41/*Ffar3*, GPR43/*Ffar2*, and GPR109A/*Hcar2* expression in 3T3-L1.

In order to investigate the role of SCFA and niacin on 3T3-L1 cells differentiation, the expression of the genes encoding the receptors for free fatty acids and niacin, which are *Ffar3*, *Ffar2*, and *Hcar2* in this cell model was first investigated. The expression of the genes encoding for the receptors were determined by analysing their mRNA levels using RT-qPCR analysis. The mRNA was extracted on day 2, 5, 7 and 10 post differentiation induction.

To investigate the involvement of GPR109A, FFAR2, and FFAR3 in adipocyte differentiation *in vitro*, the mRNA levels of *Ffar2*, *Ffar3*, and *Hcar2* were analysed during several differentiation stages of 3T3-L1 cells. The levels of *Hcar2* and *Ffar2* mRNAs in our 3T3-L1 cells increased significantly as the cells differentiated ($p < 0.01$). We also found that the mRNA expression level of these genes were significantly increased when compared among the differentiation days ($p < 0.01$) (**Figure 6.1-A, B**). However, *Ffar3* mRNA was not detected during any stage of adipocyte differentiation as shown by the high Ct value obtained for all samples (Ct value ≥ 35).

The expression levels of *Pparg* mRNA during 3T3-L1 differentiation to adipocyte were also investigated. *Pparg* is an adipocyte differentiation marker, and has been used widely as marker of preadipocyte differentiation. Indeed, the expression of this gene was significantly increased as the 3T3-L1 preadipocytes differentiated into adipocytes ($p < 0.01$) (**Figure 6.1-C**). This indicates that our 3T3-L1 differentiation protocol worked and can be used for subsequent experiments.

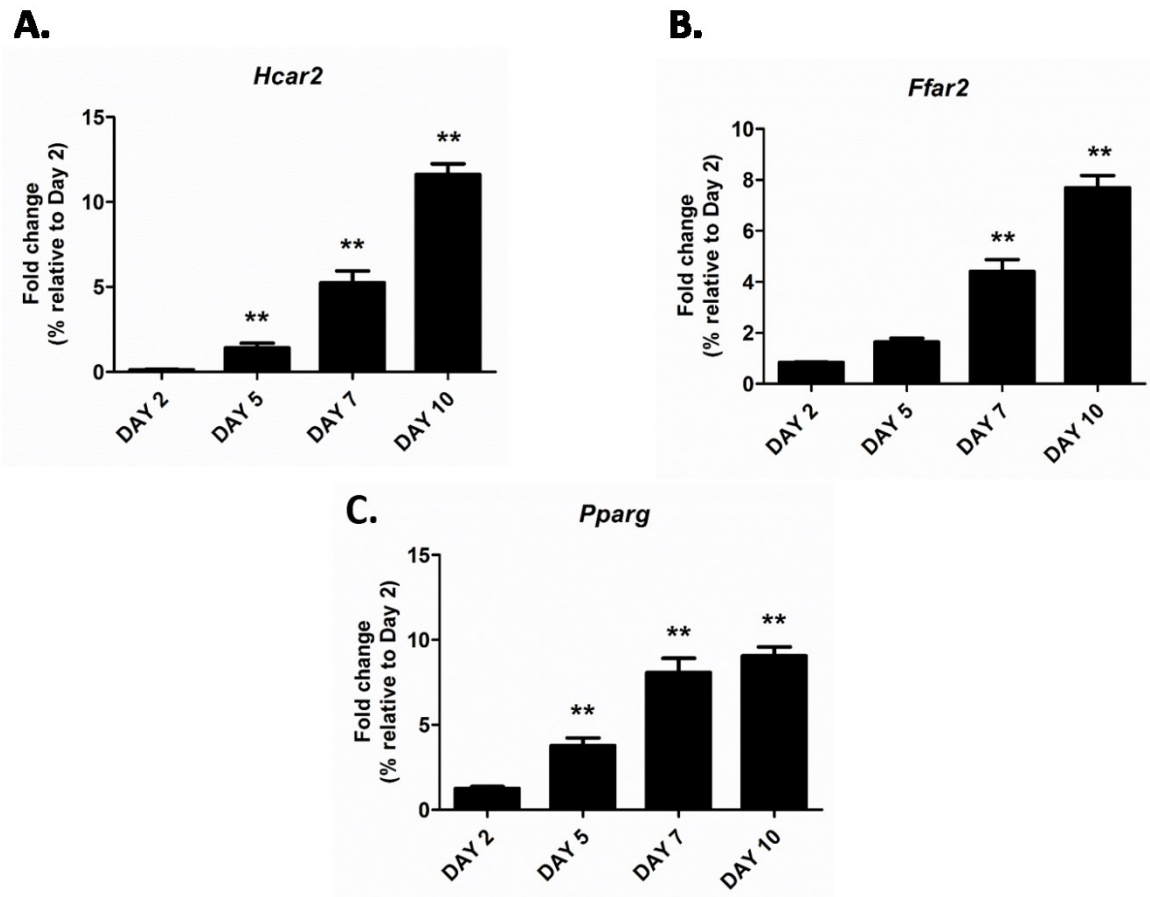


Figure 6.1: The levels of *Hcar2*, *Ffar2*, and *Pparg* mRNA during differentiation of 3T3-L1 adipocytes. RT-qPCR analysis was performed on post confluent preadipocytes (Day 0) and adipocytes that had differentiated for 2, 5, 7, and 10 days. (A) *Hcar2*, (B) *Ffar2*, and (C) *Pparg* genes expression. Data were normalized using the *Nono* gene (Arsenijevic *et al.*, 2012) and expressed as fold change relative to day 2. Results are expressed as mean \pm SEM of two separate experiments with the same protocol (n=6). A Mann-Whitney two-tailed test was performed; * $p < 0.05$, ** $p < 0.01$, *** $p < 0.001$.

6.3.2 The effect of SCFA on 3T3-L1 differentiation and functions.

6.3.2.1 The effect of SCFA on 3T3-L1 adipocytes cell viability.

To provide initial evidence of the effect SCFA has on the differentiation of 3T3-L1 cells, first the effect of these compounds on cell viability was studied. The 3T3-L1 cells were allowed to proliferate to confluence and then to differentiate to adipocytes in induction and differentiation medium with or without SCFA (1 to 5 carbons) (1.0 μM , 10 μM , 100 μM) for up to 10 days. On day 10 post induction of differentiation, cells were fixed and nuclei stained with crystal violet. Among compounds tested, only isobutyrate has been shown to increase the cell viability when used at the highest concentration when compared to control (**Figure 6.2**). In this condition, 3T3-L1 adipocyte cell viability was significantly increased by approximately 10% ($p < 0.05$). However, no significant difference was observed when comparing among the treated conditions themselves. Moreover, no increasing or decreasing trend from this cell viability assay was observed for all tested compounds. This suggests that the selected concentrations were still within the pharmacological range that allows the cells to undergo normal proliferation.

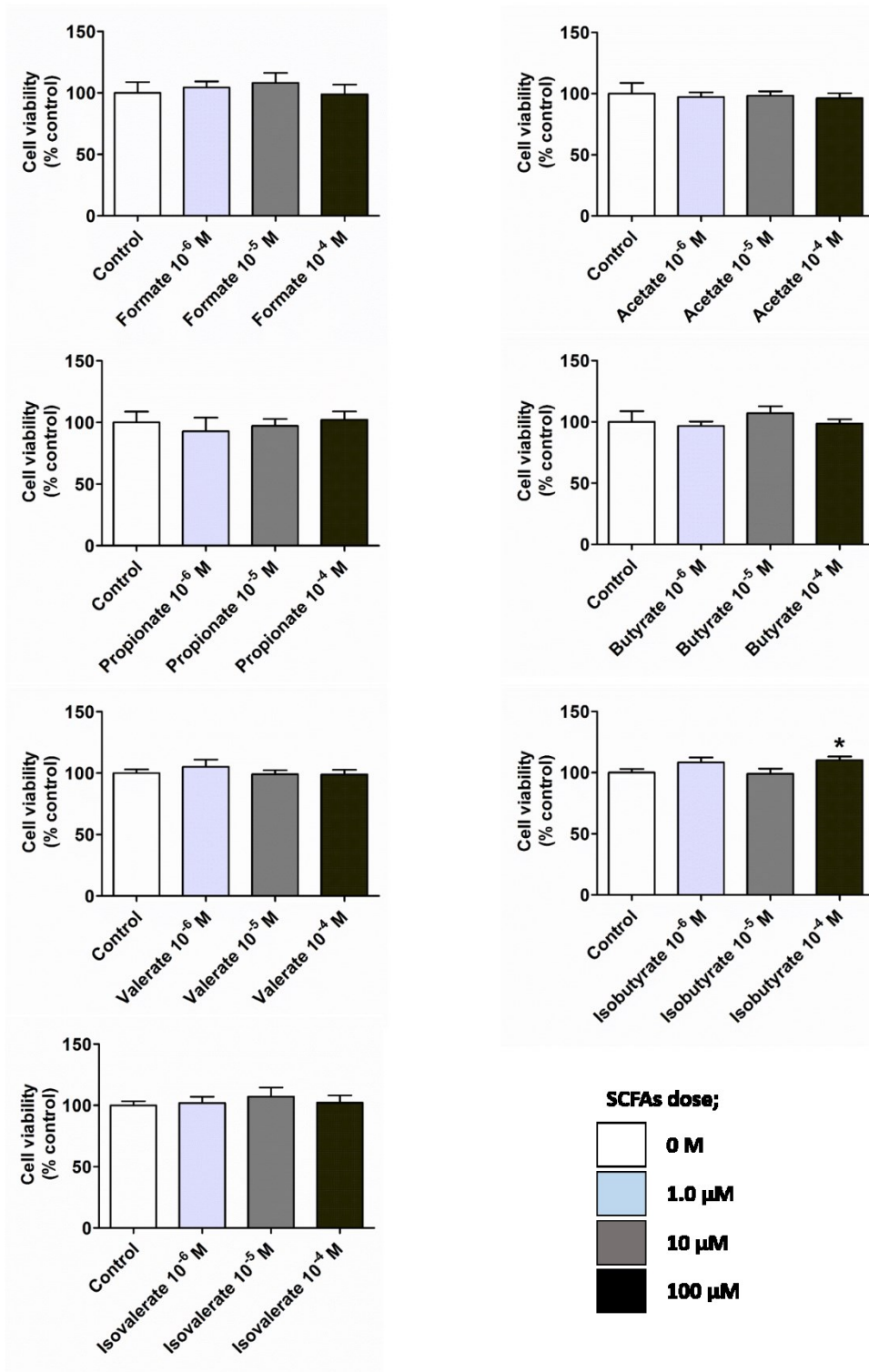


Figure 6.2: Isobutyrate, but not other tested SCFAs, increases 3T3-L1 adipocytes cell viability at 100 μM dose. After 10 days incubation with different types of SCFA (1.0 μM, 10 μM, 100 μM), cells were fixed and nuclei stained with crystal violet and O.D. 540 nm was measured on a microplate reader. Results are expressed as mean ± SEM of two separate experiments with the same protocol (n=6). A Mann-Whitney two-tailed test was performed; * $p < 0.05$, ** $p < 0.01$, *** $p < 0.001$.

6.3.2.2 SCFA; valerate, isobutyrate, and isovalerate promote *de novo* lipogenesis in 3T3-L1 adipocytes.

In order to assess the effect of SCFAs on 3T3-L1 cells adipogenesis, Oil Red-O staining was performed and cellular morphology was assessed. The Oil Red-O staining allows us to assess the intracellular triglyceride content and provides a qualitative analysis of cellular morphology. Oil Red-O staining of cellular lipid in **Figure 6.3** displays that 3T3-L1 was able to differentiate to adipocytes at all tested conditions. In order to determine the rate of lipogenesis for each condition, the triglyceride contents were extracted and were normalised to the cell viability. The treatment of 3T3-L1 cells with 100 μ M dose of valerate, isobutyrate, and isovalerate during differentiation, promotes a significant increase ($p=0.047$, $p=0.037$, and $p=0.029$, respectively) in the rate of lipogenesis (normalised to cell viability) of respectively, 16%, 16.6%, and 15% when compared to vehicle-treated cells (**Figure 6.4-E, F, G**). Treatment of shorter chain-length of SCFA of formate, acetate, propionate, and butyrate, however did not have any significant effect on the rate of lipid production per cells in 3T3-L1 adipocyte ($p>0.05$) (**Figure 6.4**).

Based on this results, there was a carbon length preference effect on lipogenesis of 3T3-L1. Higher rate of lipogenesis was found in C₄ and C₅ branched-chain fatty acids, i.e. isobutyrate and isovalerate, as well as in straight-chain C₄ and C₅ SCFAs. In addition to this, there was also a dose-response effect of the treatment as the rate of lipogenesis is significantly higher when the cells were treated with 100 μ M dose compared to the control. However, no significant effect was observed among the treated conditions themselves ($p>0.05$).

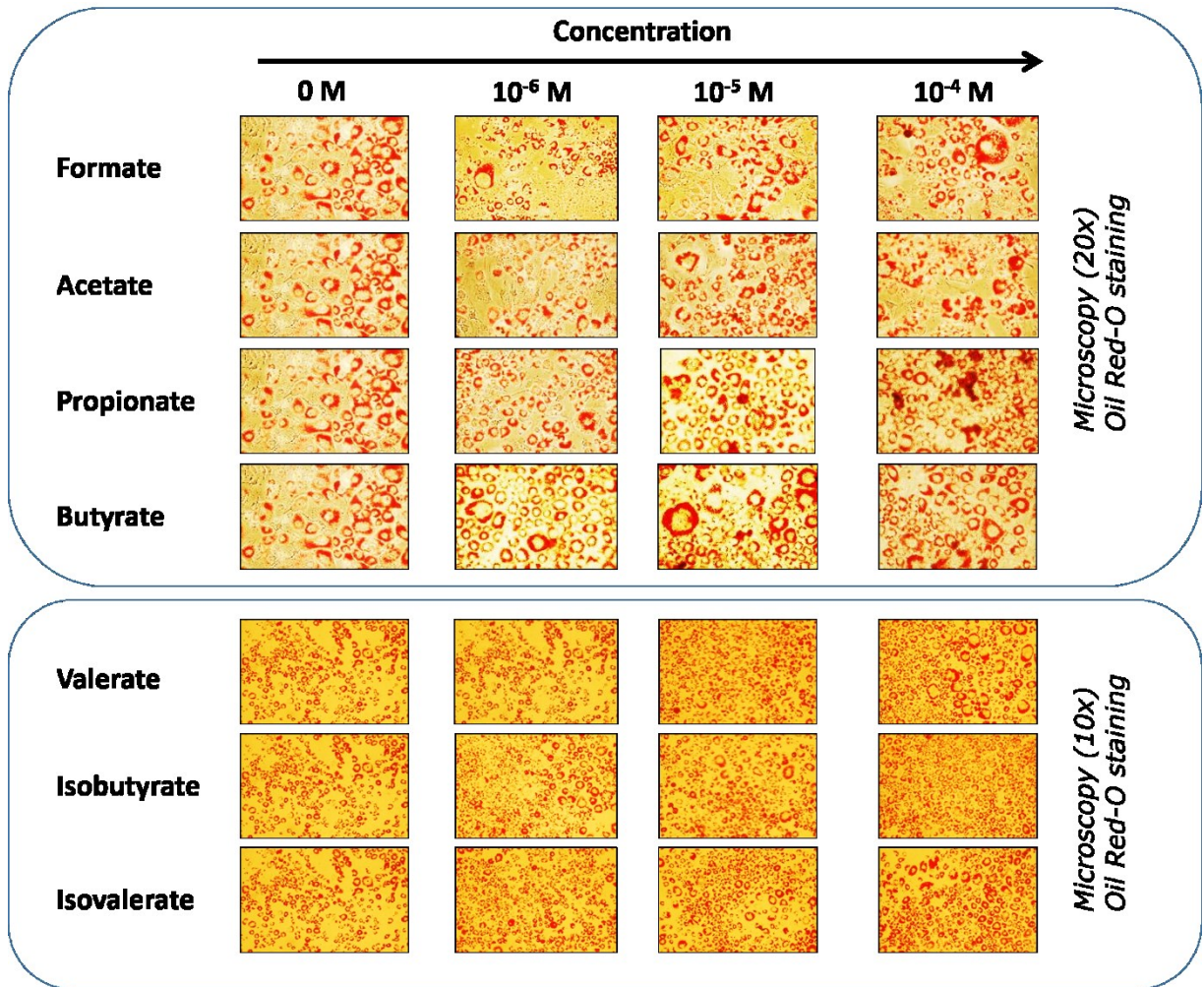


Figure 6.3: Functional role of selected compounds on differentiation of 3T3-L1 cells. The 3T3-L1 preadipocytes were allowed to grow to confluence and then to differentiate to adipocytes in differentiation medium with SCFAs (1.0 μ M, 10 μ M, 100 μ M) for 10 days. Oil Red-O staining was carried out on day 10. Results are from two different experiments (n=6).

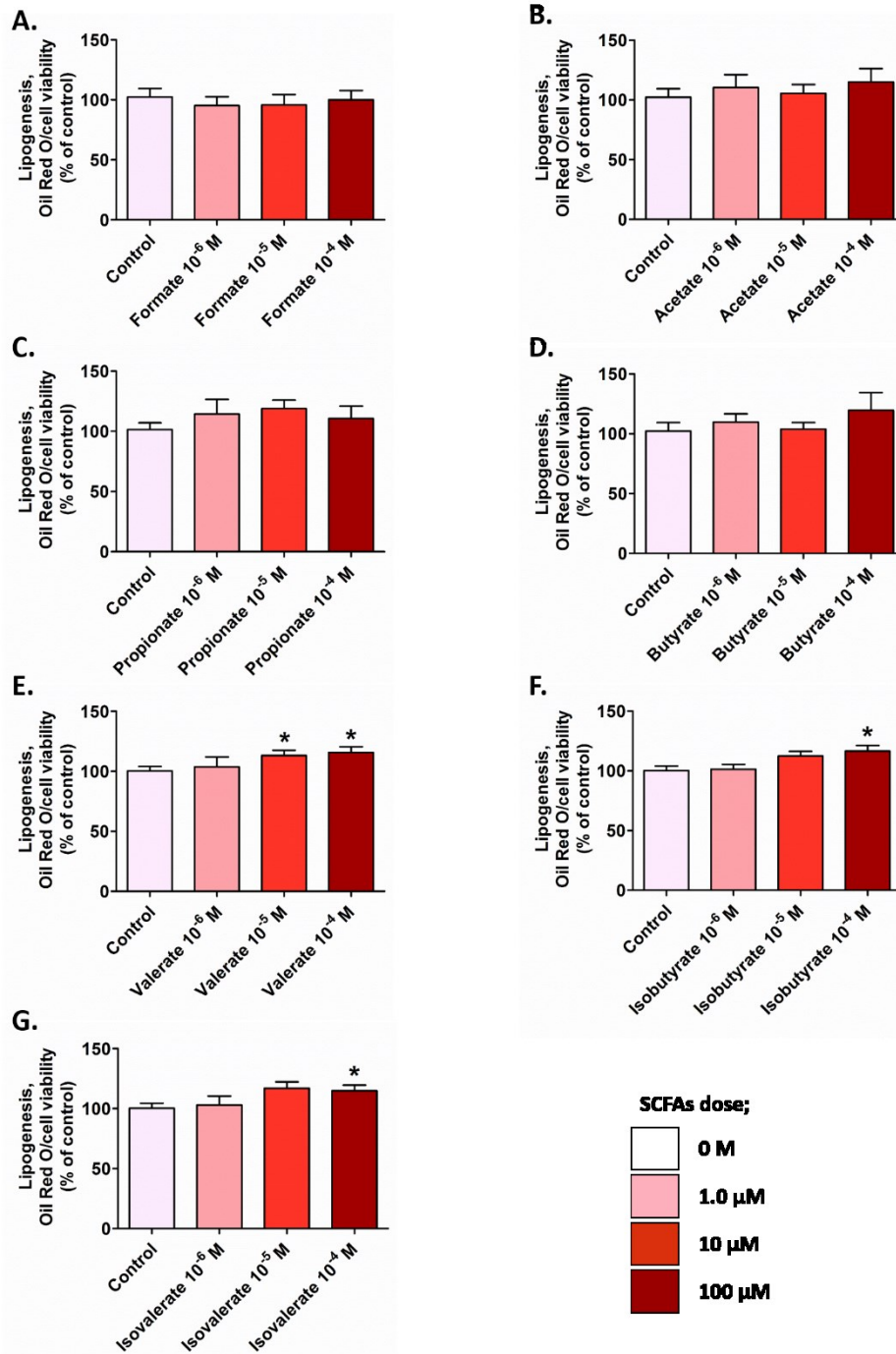


Figure 6.4: Isobutyrate, valerate, and isovalerate stimulate *de novo* lipogenesis in 3T3-L1 adipocytes. 3T3-L1 adipocytes were treated with different doses of SCFAs (1.0 μM, 10 μM, 100 μM) or vehicle (DMSO) during differentiation. At day 10, triglycerides contents stained with Oil Red-O was extracted and was measured at 520 nm and then was normalised to cell viability to get the rate of lipogenesis. Results are expressed as mean ± SEM of two different experiments (n=6). A Mann-Whitney two-tailed test was performed; * $p < 0.05$, ** $p < 0.01$, *** $p < 0.001$.

6.3.2.3 Adipogenic genes expression in 3T3-L1 cells during differentiation into adipocytes.

Based on the results from previous section, 100 μ M dose of valerate, isobutyrate, and isovalerate significantly increase the 3T3-L1 cells lipogenesis. Here in this experiment, the involvement of single dose (100 μ M) of SCFAs on the expression of genes that are correlated with adiposity and represent markers of adipogenesis and lipid formation was investigated. This is a complement method to check the adipogenesis and to relate with our lipogenesis results. Cells were treated with single dose of SCFAs throughout the differentiation process and mRNA was extracted on day 2, 5, 7, and 10 to determine the level of adipogenesis markers with RT-qPCR. The qPCR results are expressed as fold change relative to control-treated group from day 2 samples, and slope analysis was then used to compare the nonlinear fit of the curve between SCFAs-treated and control group, which results in p values (**Figure 6.5-Aii**) (**Table S.1 in Appendix**). These p values were then used in constructing a heatmap to simplify the observations (**Figure 6.5-Ai**). The expression levels of all tested genes are increased during 3T3-L1 differentiation, and peaked at day 10 in both SCFAs-treated and control group (**Figure S.2 in appendix**). Slope analysis for the induction of the gene expression however, was not able to show any significant different when comparing the level of marker genes for adipocytes differentiation, *Pparg*, *Adipoq*, and *Fasn*, between SCFAs-treated and control group.

SCFAs have been shown earlier to activate both FFAR2 and GPR109A. Indeed, a significant increase ($p < 0.05$) in the expression level of *Ffar2* was observed when the cells were treated with acetate, propionate, butyrate, isobutyrate, and valerate (**Figure 6.5**). These SCFAs are known strong agonist of this receptor. Butyrate, a known agonist of GPR109A also significantly increases the expression of this gene during 3T3-L1 differentiation when compared to control group (**Figure 6.5**). However, none of these observations correlates with the adipogenesis result measured by using Oil Red-O staining method. In this study, due to the time constraint, the qPCR experiment was only able to be carried out once with only three samples from one biological replicate ($n=3$). Thus, our qPCR data lacked power of test which did not yield any significant conclusion. As for *Ffar3* expression, high CT values were obtained from our RT-qPCR analysis. This might suggest

the low expression level of this gene or possibly it is not express in this adipocyte cell model.

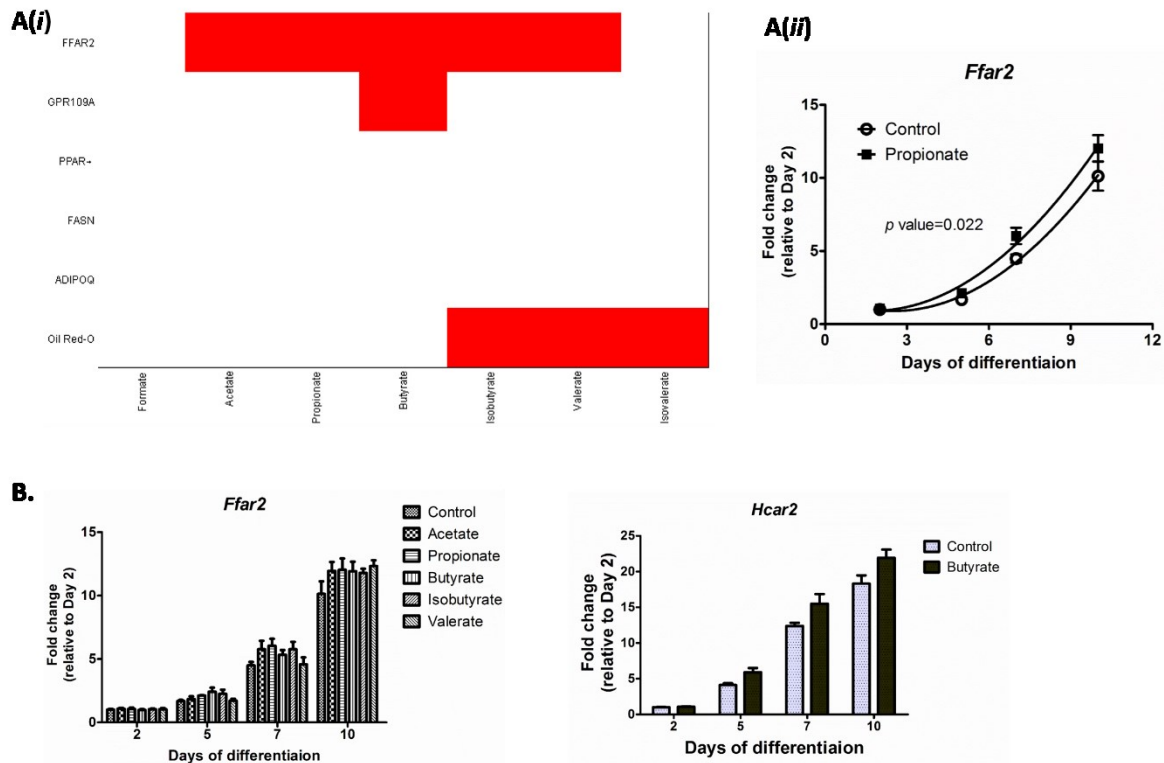


Figure 6.5: RT-qPCR analysis of the gene expression during 3T3-L1 cell differentiation. **(Ai)** The RT-qPCR results are expressed as fold change relative to control-treated group from day 2 samples, and slope analysis was then used to compare the nonlinear fit of the curve between SCFAs-treated and control-treated group, which results in p values. These p values were then used to construct a heatmap to summarise the results. Red colour represents the significant up-regulation of the gene ($p < 0.05$), while the non-significant ($p > 0.05$) is represented by the no colour. **(Aii)** Slope analysis comparing the effect between propionate-treated with control group on Ffar2 expression. **(B)** The non-linear fit curve of the genes that significantly ($p < 0.05$) up-regulated by the treatment of SCFAs.

6.3.2.4 The anti-lipolysis activity of SCFAs in 3T3-L1 adipocytes.

Finally, the effect of SCFAs on 3T3-L1 adipocytes lipolysis rate was investigated. In this experiment, fully differentiated 3T3-L1 adipocytes were treated with different SCFAs from 1 to 5 carbons at 100 μ M dose for 3 hours. Niacin was used as positive control in this experiment since it has been shown to inhibit adipocytes triglyceride lipolysis previously (Carlson, 1963). The rate of lipolysis was assessed by measuring the release of glycerol in the culture media. As shown in **Figure 6.6**, propionate, butyrate, and valerate show an anti-lipolytic effect by significantly reducing ($p < 0.05$) the basal rates of lipolysis of respectively, 9.63% ($p = 0.0274$), 9.55% ($p = 0.0161$), and 11.5% ($p = 0.0171$) when compared to the vehicle-treated condition. As for the niacin-treated cells, the lipolysis was significantly reduced ($p < 0.01$) by 23.5% ($p = 0.0011$) relative to control. However, no significant effect ($p > 0.05$) on 3T3-L1 adipocytes lipolysis was observed when the cells were treated with formate, acetate, isobutyrate, and isovalerate. The rank for anti-lipolytic activity of SCFA is valerate > butyrate = propionate. These results suggest that longer chain of SCFAs with minimal of carbon 3 inhibits basal adipocytes lipolysis. Strikingly, the anti-lipolytic activity of C₄ and C₅ SCFAs, *i.e.*, butyrate and isovalerate, disappear when the compounds have another branched chain methyl group chain (*i.e.*, isobutyrate and isovalerate).

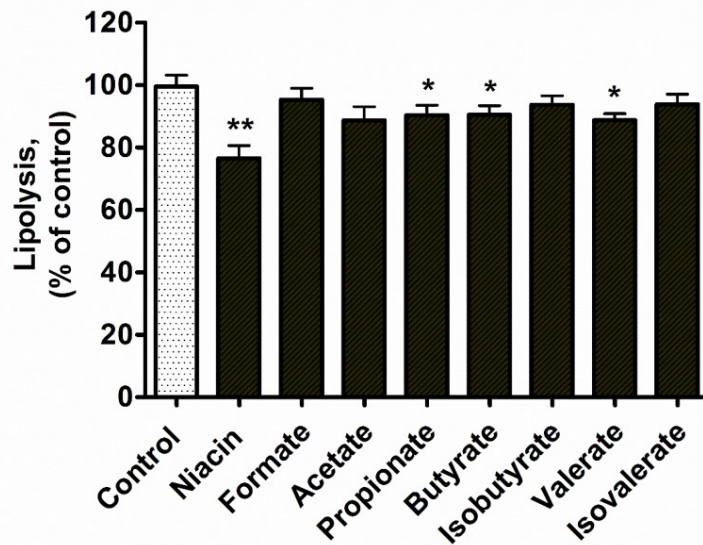


Figure 6.6: Propionate, butyrate, and valerate inhibit lipolysis in 3T3-L1 adipocytes. Differentiated 3T3-L1 cells were treated with a numbers of SCFAs from carbon 1 to carbon 5 at 100 μ M dose for 3 hours. Lipolysis was assessed by measuring the release of glycerol in the culture medium. Results are expressed as percentages of the basal rate of 100% in the control group without SCFAs. The data represent the mean \pm SEM of two different experiments (n=6). A Mann-Whitney two-tailed test was performed; * $p < 0.05$, ** $p < 0.01$, *** $p < 0.001$.

6.4 DISCUSSION

Adipocytes are highly specialised cells which are important in regulating lipid and energy homeostasis in mammals (Klaus, 1997). In the event of excess in nutrition, these cells store energy in the form of TG, and release it in the form of free fatty acids in response to energy needs. A dysregulation in adipocytes is associated with many metabolic abnormalities (Frayn *et al.*, 2007). Previous studies have demonstrated the role of acetate and propionate in adipogenesis and lipolysis (Ge *et al.*, 2008; Hong, 2005). In this study, the role of a comprehensive SCFA panel on 3T3-L1 adipocytes differentiation and mature adipocytes function *i.e.*, adipogenesis and lipolysis was assessed.

In this chapter SCFAs in valerate, isobutyrate, and isovalerate have been shown to promote 3T3-L1 cells lipogenesis by having an increase in total lipid accumulation after 10 days of differentiation process. Furthermore, valerate, along with propionate and butyrate

at 100 μM dose exhibit anti-lipolytic effect in 3T3-L1 adipocytes by reducing the glycerol release into the culture medium after 3 hours exposure. These results suggest that SCFAs, valerate in particular could play an important role in regulating adipocytes development differentiation and function.

6.4.1 Valerate, isobutyrate, and isovalerate (100 μM) stimulate 3T3-L1 differentiation.

In this chapter, the effect of several doses of SCFAs on 3T3-L1 cells differentiation was first investigated. Since the maximum concentration of these compounds in blood can be found in a range of 1-5 μM , it is decided to test a number of doses which were 1.0 μM , 10 μM , and 100 μM to increase chance of observing any effects. First, viability test was carried out. Only the highest dose of isobutyrate shows an increase in cell viability. The increase in the 3T3-L1 adipocytes viability is slightly but statistically significant when compared to the vehicle-treated group ($p < 0.05$). No effect for other tested SCFAs was observed. In order to investigate the effect of SCFAs on 3T3-L1 differentiation, cells were differentiated in the presence of SCFAs (1.0 μM , 10 μM , and 100 μM). At day 10 after the induction of differentiation, cellular lipid accumulation was qualitatively and quantitatively measured by Oil Red-O staining. Indeed, 3T3-L1 cells were able to differentiate into adipocytes at the end of the experiment (Day 10). However, no significant changes in Oil Red-O staining or gross cellular morphology between SCFAs-treated and vehicle-treated group were able to detect.

Recently, study has revealed that acetate and propionate were able to reduce the free fatty acids release from adipocyte via the stimulation of FFAR2 activation, and this effect was abolished in adipose tissue from *Ffar2* knockout mouse (Ge *et al.*, 2008). Moreover, previous *in vitro* study using 3T3-L1 cell model has demonstrated that low dose of acetate and propionate (0.1 μM) increases the 3T3-L1 differentiation as revealed by the increase in intracellular lipid content based on Oil Red-O staining. In present study, the rate of lipogenesis was calculated by normalising the Oil Red-O value with its respective viability value. Only valerate, isobutyrate, and isovalerate were demonstrated to significantly

increase *de novo* lipogenesis in 3T3-L1 cells when these compounds were used at the highest tested dose which was 100 μM . Treatment of acetate and propionate, as well as other SCFAs, even at the highest dose during the 3T3-L1 differentiation were unable to significantly effecting the rate of lipogenesis even though the doses that is used were higher than what has been reported previously. In addition, Frost *et al.*, also unable to observe any changes in 3T3-L1 lipogenesis when treating the cells with 0.1-10 μM of acetate and propionate throughout the differentiation process (Frost *et al.*, 2014a). In general, SCFAs levels in blood can be found in micromolar concentration.

In present study, the low doses (1.0 and 10 μM) of all tested SCFAs except for valerate did not have significant effect in term of modulating cell viability and differentiation of the cells. Valerate has been shown previously to increase insulin-stimulated glucose uptake in 3T3-L1 adipocytes (Han *et al.*, 2014). Our finding that valerate increases lipogenesis might be linked with the reason that it increases the glucose uptake by the cells via the action of insulin. The most common tissue where insulin-stimulated glucose uptake occurred is in skeletal muscle, where it stores glucose as glycogen (Kraegen *et al.*, 1985). However, an approximately 10% of this process also occurs in adipose tissue, where glucose is stored as TG (Leto and Saltiel, 2012).

6.4.2 Adipogenic genes expression was not affected by the treatment of SCFAs on 3T3-L1 cells.

Adipocyte differentiation is regulated by a set of gene-expression events (Rosen and MacDougald, 2006). In order to test whether SCFAs influence the expression of related genes during the differentiation of 3T3-L1 cells, the expression level of adipocyte differentiation marker, *Pparg*, *Fasn*, and *Adipoq* were measured. *Pparg* belongs to the nuclear receptor superfamily of ligand-activated transcription factors and is essential for both white and brown adipocytes differentiation (Kajimura *et al.*, 2008). It has been shown previously that the expression level of *Pparg* is high in adipose tissue and adipocyte cell line, while low expression level or even absent in other tissues and cell lines (Braissant *et al.*, 1996; Forman *et al.*, 1995; Schoonjans *et al.*, 1996). The expression level of this gene is

low in *in vitro* model of 3T3-L1 preadipocytes, but dramatically induced during the differentiation into adipocytes in the presence of differentiation medium (Chawla *et al.*, 1994). In agreement with this study, our qPCR analysis demonstrates that *Pparg* expression is greatly increased during the differentiation of 3T3-L1 into adipocytes and was peaked at day 10 (end of differentiation).

The mRNA levels of one of the *Pparg* target genes, fatty acid synthase (*Fasn*) were then investigated. Fatty acid synthase is one of the markers of the final stage of adipocyte differentiation and the key enzyme in the *de novo* lipogenesis (Liu *et al.*, 2004). During adipogenesis, *de novo* fatty acid synthesis is an important step as it provides precursor to be incorporated into triglyceride. In 3T3-L1 adipocytes culture model, the major component in its growth medium is glucose, therefore the degree of adipogenesis may be highly dependent on expression and activity of enzymes involved in glucose metabolism, fatty acid synthesis, and esterification (Sul *et al.*, 2000). Previously, it has been demonstrated that *Pparg* expression was highly up-regulated when the cells differentiated into adipocytes. Based on this, it is speculated that the expression of *Pparg* target gene, *Fasn* might also be up-regulated. Indeed, *Fasn* expression was significantly ($p < 0.001$) up-regulated when the cells differentiated into adipocytes at day 10 as compared to its expression at day 2 after induction of differentiation. Consistent with our finding, a previous study reported that both increase in *Fasn* gene transcription and the stabilisation of *Fasn* mRNA caused a dramatic increase in *Fasn* mRNA levels during 3T3-L1 cells differentiation (Moustaid and Sul, 1991). However, no SCFAs treatment was found to significantly up-regulate the expression of this gene when compared to the control during the differentiation of 3T3-L1 to adipocytes.

Adipose tissue secretes hormones and cytokines that regulate many biological processes such as food intake, energy expenditure, and carbohydrate and lipid metabolism (Havel, 2002). Adiponectin, one of the adipocyte-specific genes, plays an important role in modulating differentiation of preadipocytes into mature adipocyte by acting as endocrine factor, regulating many biological processes by effecting target organs (Lara-Castro *et al.*, 2007). The expression of adiponectin gene, *Adipoq* has been shown to increase during adipocyte differentiation in both 3T3-L1 and 3T3-F442A cells, and that the expression was first observe at day 4 after induction of differentiation (Hu *et al.*, 1996). This result is

consistent with what have been demonstrated in this study that the expression of this gene is significantly increased at day 5 after induction of differentiation and reaching the highest level at day 10. When a single dose of SCFAs (100 μ M) was introduced in the culture medium throughout the differentiation process, no significant increase in *Adipoq* gene expression between SCFAs-treated and control group was observed. Low circulating level of adiponectin was suggested to have a role in the pathogenesis of diseases linked to obesity and metabolic syndrome (Funahashi *et al.*, 1999; Matsuzawa *et al.*, 1999). A previous study has demonstrated that overexpression of adiponectin protected ob/ob mice from diabetes and ApoE-deficient mice from atherosclerosis (Yamauchi *et al.*, 2003). Moreover, in adipose tissues, insulin sensitivity was improved when adiponectin circulating levels are increased as a result of overexpression of this gene (Combs *et al.*, 2004).

In a previous chapter (Chapter 5), it has been demonstrated that some of the SCFAs used in this study showed an agonist activity for free fatty acid receptors, FFAR2, and FFAR3 as well as for GPR109A. In order to assess if any of these SCFAs able to affect the expression of the genes encoding for these receptors, the expression levels of *Hcar2*, *Ffar2*, and *Ffar3* genes during the differentiation of 3T3-L1 cells were measured. The expression levels of *Ffar2* and *Hcar2* genes increase dramatically when 3T3-L1 cells differentiated into adipocytes and peaked at day 10 after induction of differentiation. These result is in line with study conducted by Hong, (2005), that showed an increase of *Ffar2* mRNA level in 3T3-L1 cells during differentiation from pre-adipocytes to adipocytes. As for GPR109A, previous study has shown that low expression level of this receptor in their native 3T3-L1 adipocytes when compared to primary adipocytes (Plaisance *et al.*, 2008). In this study, using RT-qPCR analysis, an increase on the expression of *Hcar2* during 3T3-L1 differentiation was observed. This study however, was not measuring the expression of the receptor, GPR109A itself. Despite showing that there was a significant ($p < 0.05$) effect of time on expression of GPR109A, only butyrate but not other SCFAs has been found to significantly up-regulate this gene. A previous study has demonstrated that acetate and propionate (0.1 μ M) stimulate *Ffar2* expression in 3T3-L1 adipocytes, with an increase in the accumulation of fat as revealed by Oil Red-O staining (Hong, 2005). Despite showing an up-regulation in the *Ffar2* gene expression, no effect on Oil Red-O staining was observed when the cells were treated with acetate, propionate, and butyrate during the

differentiation process. On the other hand, consistent with previously published data, a very low expression level of *Ffar3* was found with high cycle threshold value (Ct), thus can be considered as not express (Frost *et al.*, 2014a; Hong, 2005).

6.4.3 Single dose (100 μ M) of propionate, butyrate, and valerate decrease basal level of lipolysis in 3T3-L1 adipocytes.

Fat accumulation within the cell in the form of triacylglycerol (TG) is determined by the equilibrium between lipogenesis (fat synthesis) and lipolysis (fat breakdown/fatty acid oxidation) (Kersten, 2001). In the event of food intake, the excess of non-esterified fatty acids (NEFA) in the diet are esterified to TG, which are then stored in the form of lipid droplets in the cytosol (Lass *et al.*, 2011). During times of energy deprivation, adipose tissue undergoes higher rate of lipolysis to generate fatty acids and glycerol, which are subsequently used as energy substrates. Lipolysis is as great importance as lipogenesis in regulating lipid and energy homeostasis.

In the present study, effort has been made to investigate the effects of SCFAs in the rate of adipocyte lipolysis using a fully differentiated 3T3-L1 adipocytes. A single dose (100 μ M) of propionate, butyrate, and valerate has been shown to significantly ($p < 0.05$) inhibit basal lipolysis rate in differentiated 3T3-L1 adipocytes by measuring the release of glycerol in the medium. The inhibition of lipolysis in 3T3-L1 adipocytes has been shown previously by other group when the cells were incubated with acetate and propionate for 4 hours (Ge *et al.*, 2008). More recently, a study has demonstrated that butyrate reduces lipolysis and inflammatory signalling generated by interaction of macrophages and adipocytes (Ohira *et al.*, 2013). Lipolysis process begins with the hydrolysis of TG to form diacylglycerol (DAG), which is then followed by monoacylglycerol (MAG) formation, with the release of fatty acids at each step. Final step of this process is when MAG is hydrolysed to release fatty acids and glycerol (Duncan *et al.*, 2007a). In this study, niacin is used as a positive control due to its well-documented anti-lipolytic effect in both *in vivo* and *in vitro* (Plaisance *et al.*, 2008). Indeed, an inhibition in the basal lipolysis rate is observed, with significant ($p < 0.001$) reduction (15%) of glycerol release in the medium. Niacin has been used for over fifty years

for treating dyslipidaemia, the risk factor for atherosclerosis, by altering plasma lipid profile (Carlson, 2005). Furthermore, niacin reduces the levels of atherogenic VLDL and LDL-lipoprotein, as well as Lp(a). In addition, it also raises the level of HDL lipoprotein which is known as good lipid (Carlson, 2005).

Even though the inhibition of basal lipolysis by propionate, butyrate and valerate is less potent than niacin, the reduction of glycerol release in the medium is significant ($p < 0.05$) when compared to the vehicle-treated cells. Out of the SCFAs that significantly inhibit basal lipolysis in mature 3T3-L1 adipocyte, valerate shows the most interesting findings. Earlier in this chapter (**section 6.3.2.2**), it has been demonstrated that 100 μ M valerate promotes *de novo* 3T3-L1 lipogenesis. As the adipogenesis rate is controlled by the balance of TG formation and TG hydrolysis, it is possible that the effect of valerate in promoting lipogenesis in 3T3-L1 adipocyte is based on its ability in inhibiting lipolysis, thus allowing more fat accumulation in the cells. In striking contrast, isobutyrate and isovalerate did not show a significant effect on lipolysis. Thus, these results suggest the anti-lipolytic effect of short-chain fatty acids (propionate, butyrate and valerate) is lost when another methyl group is added (*i.e.*, isobutyrate and isovalerate).

6.5 CONCLUSION

This chapter aimed at investigating the role of a comprehensive SCFA panel on adipocytes differentiation and function. It has been shown that the selected SCFAs doses were not able to reduce or inhibit the 3T3-L1 cell viability. Thus, the selected SCFAs doses were not toxic to this cell line. Moreover, Oil Red-O lipid staining revealed that 100 μ M of valerate, isobutyrate, and isovalerate increased adipogenesis in 3T3-L1 cells. Despite showing a significant role in promoting adipogenesis for isobutyrate, valerate, and isovalerate, no significant difference ($p > 0.05$) was observed in adipogenic genes expression in *Pparg*, *Fasn*, and *Adipoq* between SCFAs-treated and control group. While it has been suggested that SCFAs promote adipogenesis in 3T3-L1 cell via GPCR-mediated pathways, however as mentioned previously, with low sample number for the qPCR analysis, no significant conclusion on the relationship between the effect of SCFAs treatment on 3T3-

L1 adipogenesis and gene expression was able to yield. Furthermore, this present study also demonstrated that propionate, butyrate, and valerate significantly decrease basal lipolysis in this cell model but with less potent than niacin. Valerate in particular, has been shown to promote 3T3-L1 adipogenesis by inhibiting basal lipolysis rate in 3T3-L1 adipocyte. Taken together, for the first time, using 3T3-L1 cell model, valerate has been shown to stimulate adipogenesis and exert its anti-lipolytic property in adipocyte. These findings suggest the potential role of valerate in regulating lipid metabolism and adipocyte differentiation, thus highlight its potential to be used in the treatment of dyslipidaemia.

CHAPTER 7

7. GENERAL DISCUSSION

Although SCFAs have been heavily studied, there are still gaps in the knowledge of their biological effects. The aim of this PhD is to characterise the subtle metabolic and pharmacological effects of SCFAs on important metabolic tissues which are liver and adipose tissue. To address this, a set of hypothesis has been set up; 1) SCFAs may act as substrates for energy metabolism of the cell, 2) SCFAs may act as ligands in activating GPCRs (i.e., FFAR2, FFAR3, GPR109A), 3) SCFAs may play important role in regulating adipocytes differentiation and mature adipocyte function. Based on the results of the first study (Chapter 3), the effect of SCFAs (propionate and butyrate) on HepG2 cells is then investigated by identifying the metabolic signature of the exposure (Chapter 4). As SCFAs have been shown to act as agonist for GPCRs, the pharmacological assessment of a comprehensive SCFAs panel on their GPCRs, *i.e.*, FFAR2, FFAR3, GPR109A is then implemented (Chapter 5). Finally, the cellular response of a comprehensive panel of SCFAs in regulating adipocyte differentiation and function by using 3T3-L1 cell model is assessed (Chapter 6).

7.1 Key findings

The gut microbiota influences human health through a number of mechanisms. One of the highlight of its benefits is from the microbial metabolites that have been shown to have major influence on host physiology. Here in this PhD thesis, the effect of several SCFAs on two important metabolic tissues were investigated. Two cell culture models were used which are HepG2 hepatocarcinoma cell line (hepatocyte) and 3T3-L1 cell line (adipocyte).

Sodium is one of the most important electrolytes in human body as it regulates extracellular fluid as well as essential in balancing the concentration gradient for the signal

transmission in nerve and muscle (Bouchard *et al.*, 1993). Sodium chloride (NaCl) is the most commonly used salt in the molecular biology and cell biology, and is the essential micronutrient for living cell (Pohl *et al.*, 2013). As SCFAs (propionate and butyrate) were used in the form of sodium salt (chapter 4), the effect of NaCl on HepG2 cell was first investigated (chapter 3). High concentration of NaCl can be genotoxic as evidenced by the increase in DNA damage in cell culture study (Kultz and Chakravarty, 2001). Consistent with the previous observation made by Dmitrieva *et al.*, (2003) that only at ~200 mM of NaCl cell growth was affected and DNA damage was observed, here in this study the highest dose of NaCl tested (1.0 mM) shows no effect on HepG2 cell viability. Multivariate data analysis on the data generated from ¹H NMR metabolic profiling of HepG2 cell media further confirmed that no significant modulation of HepG2 cell metabolism occurs when the cells were treated with NaCl at all tested doses when compared to the control.

Out of the SCFAs produced in the colon, butyrate has caught most attention and has been studied widely. It has been demonstrated previously that butyrate at certain concentrations plays a role in protecting against colon cancer and colitis by suppressing colonic inflammation, which then causes cell cycle arrest and induces apoptosis (Ganapathy *et al.*, 2013; Roediger, 1990). SCFAs (C₃, C₄, and C₅) at 5 mM dose have been shown to inhibit colorectal adenocarcinoma cell line, HT-29. The anti-proliferative effects of SCFAs, propionate and butyrate in particular, have been suggested due to their histone deacetylase inhibitor (HDAC) properties (Aoyama *et al.*, 2010; Hinnebusch *et al.*, 2002). In this study, using HepG2 hepatocarcinoma cell line, dosing the cell with 10 mM and 100 mM of sodium propionate and sodium butyrate decreases cell viability and proliferation (Chapter 4). Although no attempt has been made to measure histone hyperacetylation, the results of this study suggest that the anti-proliferative effect of propionate and butyrate appears to be dependent upon their histone hyperacetylation effects as evidenced by Hinnebusch *et al.*, (2002). HDAC inhibitors provide a great potential for the development of anti-cancer drugs (Jung, 2001).

It has been known for some time that SCFAs are used as a source of energy which accounts for ~10% of the daily caloric requirement in humans (Bergman, 1990b). Based on the relatively high affinity of colonocytes for butyrate, these cells prefer butyrate as their main energy source. Approximately 60-70% of the colonocytes' energy supply comes from

butyrate oxidation (Roediger, 1982), whilst others (propionate and butyrate) will be transported by hepatic vein to the liver to get metabolised (den Besten *et al.*, 2013). In order to investigate the effect of SCFAs on hepatic cancer metabolism and to identify dose-response metabolic signature associated with the exposure of HepG2 cells to sodium propionate and sodium butyrate, ¹H-NMR metabolic profiling approach was carried out. Decrease in the cell media concentration of propionate and butyrate after 72 hours treatment of HepG2 cell when compared to the control, and at the same time increase in alanine, lactate, and α -keto- β -methylvalerate suggest the possibility of the HepG2 cell in metabolising these SCFAs as substitute to glucose for their energy source (Chapter 4).

Butyrate enters the mitochondria, and undergoes β -oxidation to acetyl-CoA, which then enters the TCA cycle generating NADH. NADH enters electron transport chain producing ATP as the main product and CO₂ as a by-product (Roediger, 1980b). As a glucogenic compound, propionate might undergo gluconeogenesis in the event of high glucose demand. It has been shown recently that propionate increased the rate of intestinal gluconeogenesis (IGN) which has beneficial effects on glucose and energy homeostasis (De Vadder *et al.*, 2014). Glucose released by IGN is detected by portal glucose sensor, sodium glucose co-transporter (SGLT), which sends signal to the brain thus inducing satiety and regulating glucose homeostasis (Delaere *et al.*, 2013). Cytosolic pyruvate produced by glycolysis has a number of fates. Primarily, pyruvate can be transported/diffused from the cell. In low oxygen conditions (hypoxia) and in high proliferating cell such as in cancer cell, pyruvate is reduced to lactate to recover NAD⁺. It also can undergo oxidation via TCA cycle in mitochondria or is converted to alanine via transamination with glutamate. In addition to pyruvate, we also observed extracellular accumulation of lactate and alanine. As HepG2 cell is a hepatic cancer cell line, the accumulation of lactate is expected due to the 'Warburg effects' (Cairns *et al.*, 2011).

A number of studies have demonstrated that the increase in protein turn over produces gluconeogenic amino acids, which in turn increases the gluconeogenesis rate in T2D patients (Gastaldelli *et al.*, 2000). α -keto- β -methylvalerate is an intermediate metabolite of isoleucine catabolism. The accumulation of this metabolite suggests that the activity of BCAT enzyme in the early step of BCAA catabolism exceed the downstream enzymes responsible in incorporating this keto-acid into TCA cycle. BCAA have been shown

to play role in the development of obesity-associated insulin resistance. Accumulation of BCAA catabolism intermediates cause incomplete oxidation of glucose and fatty acids, leading to an increase in mitochondrial stress, impaired glucose homeostasis, and insulin resistance (Newgard, 2012; Newgard *et al.*, 2009). The metabolomics analysis also highlighted α -keto- β -methylvalerate, a BCAA isoleucine catabolism intermediate as a candidate marker of both propionate and butyrate dose-response, though the significant modulation of this metabolite only observed at 24-hr time point. The increase in accumulation of this metabolite throughout the study suggests that HepG2 cells might prefer SCFAs for their energy source, and less incorporation of isoleucine catabolism intermediate into the TCA cycle. Although the highest tested dose for propionate and butyrate used in this study are not physiologically observed in this tissue (hepatic), these data provide insight into the potential role of propionate and butyrate in modulating hepatic cancer cell metabolism that relate to the energy production, thus adding new knowledge on the biological effects of SCFAs.

Apart from their role as fuel substrates, SCFAs also act as signalling molecules at the cell-surface level. FFAR3 (GPR41) and FFAR2 (GPR43) along with GPR40, are a small family of GPCRs that are able to respond to fatty acids (Covington *et al.*, 2006). While GPR40 responds to medium and long chain fatty acids (Briscoe *et al.*, 2003), FFAR2 (GPR43) and FFAR3 (GPR41) are activated by short-chain fatty acids (Brown *et al.*, 2003; Le Poul *et al.*, 2003). Using short-chain carboxylic acids to reduce the intracellular cAMP by activating FFAR2 and FFAR3 allowed the pharmacology of a variety of SCFAs to be determined (Chapter 5). Consistent with the observations made by other groups, data from this study demonstrate the agonist activity of SCFAs were in agreement with potencies measured in different assay systems (Brown *et al.*, 2003; Le Poul *et al.*, 2003; Nilsson *et al.*, 2003). FFAR2 has a preference for acetate and propionate (2 and 3 carbons), whereas longer SCFAs (≥ 3 carbons) are preferred by FFAR3. Furthermore, niacin or nicotinic acid has been found to act as partial agonist for FFAR3 with relatively low EC_{50} value ($EC_{50}=1465 \mu M$) and much lower for FFAR2. Although niacin is a weak agonist for these receptors, interestingly, this is the first study to report on the activation of FFAR2 by niacin, at least based on the experiments conducted in this study.

The highest expression of FFAR2 is in immune cells, especially in neutrophils (Brown *et al.*, 2003), where its activation by SCFAs plays a crucial role in regulating immune responses (Maslowski *et al.*, 2009). FFAR3 expression is more widespread than FFAR2, with the highest expression found in adipose tissue (Brown *et al.*, 2003). FFAR3 activation by SCFAs has been shown to increase leptin secretion, thus increases satiety, and suppresses food intake (Cohen *et al.*, 2001a). Moreover, it has also been shown that both FFAR2 and FFAR3 activation by SCFAs in L cells promotes the release of a potent anorectic hormone, GLP-1, which then regulates insulin secretion from pancreatic β -cells, and increases insulin sensitivity in target tissues (Tolhurst *et al.*, 2012). The metabolic function of FFAR2 and FFAR3 makes them an attractive target for drug development. Thus, the new agonists for these receptor as revealed in this study could potentially be used in the treatment of obesity.

Previous study demonstrated that butyrate is a ligand for GPR109A in the colon (Thangaraju *et al.*, 2009a), and that the activation of this receptor by butyrate suppresses inflammation and carcinogenesis in colon (Singh *et al.*, 2014a). Based on these findings, I hypothesised that other SCFAs might also activate GPR109A the same way as butyrate and niacin. Indeed, consistent with the data reported by Taggart *et al.*, (2005), I found that niacin, butyrate, and valerate are able to activate GPR109A receptor. Interestingly, in this study, isobutyrate and isovalerate have been identified as the partial agonist for GPR109A, which is a novel findings. These branched chain fatty acids are produced in small amount by gut microbiota that are capable in breaking down protein and fermenting amino acid (Macfarlane *et al.*, 1986). However, due to its low physiological concentrations, BCFA are not likely to reach the desired concentration to activate the receptor. In contrast, butyrate concentration, but not valerate, can reach up to ~ 20 mmol/L in colon (Thangaraju *et al.*, 2009b). GPR109A has been shown to express in abundance on the luminal membrane of colonic epithelial cells in human and mouse, where its activation by butyrate induces tumour suppression (Thangaraju *et al.*, 2009a). In addition, GPR109A activation also has been shown to mediate the anti-lipolytic effect of niacin in adipocyte, thus revealing the underlying mechanism of its lipid-lowering effect (Tunaru *et al.*, 2003; Wise *et al.*, 2003). Together, data obtained from this study (Chapter 5) on the novel agonists (isobutyrate and isovalerate) of GPR109A expand the knowledge on the pharmacological effects of SCFAs

and new therapies specifically targeting this receptor could be used for the treatment of metabolic syndrome related diseases, as well as for the protection against inflammation and carcinogenesis.

Adipose tissue is one of the important metabolic tissues in human body. In normal condition, excess energy is stored in adipocytes in the form of TGs and only low amount of TGs are found in non-adipocytes. The dysregulation of adipocytes has been shown to play a major role in the development of T2D and many metabolic abnormalities (Frayn *et al.*, 2007). Ectopic lipid deposition in non-adipocytes such as liver, pancreas, and muscle as a result of the limited number of adipocytes decrease insulin sensitivity (Unger *et al.*, 2010). This condition may be caused by the limited number of hypertrophic adipocytes that unable to store lipid efficiently in a high caloric environment (Unger *et al.*, 2010). A good understanding of adipocytes differentiation and development is therefore important in maintaining metabolic health. In this study (Chapter 6), the effect of SCFAs on adipocyte differentiation in murine 3T3-L1 cell was investigated. Out of the tested SCFAs, only isobutyrate, valerate, and isovalerate have been found to significantly enhance the formation of Oil Red O-stained cells. These results indicate that these SCFAs promote adipocyte differentiation in 3T3-L1 adipocyte cell model. The findings of this study however, are not consistent with what have been reported previously on the positive role of acetate and propionate in promoting adipogenesis in 3T3-L1 cell (Hong, 2005). This study failed to observe any significant changes in intracellular TG content as revealed by the Oil Red-O staining as well as in gross cellular morphology when the 3T3-L1 cells were incubated with acetate, butyrate, and propionate during the differentiation to adipocyte.

While it has been demonstrated that SCFAs (isobutyrate, valerate, and isovalerate) stimulate adipocyte differentiation in 3T3-L1 cell, SCFAs has no effect on adipocyte differentiation in human stromal vascular fraction (SVF) (Dewulf *et al.*, 2013). In addition, the differentiation of human bone marrow-derived mesenchymal stem cells into adipocytes has been shown to be inhibited by butyrate (Chen *et al.*, 2003). The inconsistent findings on the effect of SCFAs on adipocyte differentiation may be related to the use of different cell line and different cell culture condition among the research groups.

SCFA is a ligand for FFAR2 and FFAR3. The stimulatory effect of acetate and propionate on adipocyte differentiation in 3T3-L1 cells has been suggested to be mediated by FFAR2 and not via FFAR3 as the *Ffar3* mRNA was not expressed in this cell culture model (Hong, 2005). In this study however, the adipogenic effect of SCFAs (isobutyrate, valerate, and isovalerate) on 3T3-L1 cell has been shown to be FFAR2-independent. Exposing 3T3-L1 preadipocytes to SCFAs throughout the differentiation process made no difference to the *Ffar2* mRNA expression pattern as the control group also displayed similar pattern of expression of this gene over the time course studied. The observation of the mRNA expression pattern however, was obtained from only one single experiment. Thus, more data needed before any conclusions can be made on the role of FFAR2 in mediating SCFAs effect on 3T3-L1 adipogenesis.

As the accumulation of TG in the cells is determined by the balance between fat synthesis and fat breakdown (lipolysis), next, the role of SCFAs in inhibiting basal adipocytes lipolysis is assessed. Propionate, butyrate, and valerate have been found to significantly inhibit lipolysis in 3T3-L1 adipocyte as evidenced by the reduction of glycerol release to the cell culture media. It is interesting to note that there have been reports on the anti-lipolytic activity of both propionate and butyrate (Ge *et al.*, 2008; Ohira *et al.*, 2013), but as far as our knowledge is concerned, the anti-lipolytic activity shown by valerate is a novel finding. As mentioned previously, valerate has been shown to promote 3T3-L1 differentiation. Due to its pronounced anti-lipolytic activity, it is possible that the stimulatory effect of SCFA in adipocyte differentiation is based on its ability in inhibiting lipolysis, thus allowing more fat storage in the cell. These properties could present a great potential for the treatment of dyslipidaemia. As niacin also inhibits lipolysis and has been shown to raise the level of HDL and at the same time reducing VLDL and LDL, it is of interest to see if SCFAs could also have the same properties as niacin in reducing the risk factor of atherosclerosis. Given the fact that adipocytes development plays an important role in maintaining energy homeostasis, SCFAs could potentially serve as a good regulator in regulating energy storage and expenditure in adipose tissue.

Future research

To take this thesis further, the role of GPCRs in mediating the effect of SCFAs on hepatic metabolism could be explored by carrying out receptor knockdown experiment. By doing this, it is interesting to see if we can decipher between metabolic response and signalling response via GPCRs in hepatic tissue, and assessing this effect on the metabolic signature. Selection for the most suitable hepatic model that expressing the interested GPCRs and has a close properties as primary hepatocytes also important. It is also interesting to compare the metabolic signatures that we have identified in our study with signatures obtained in livers from mice treated with butyrate or propionate. In addition, the assessment of the pharmacological role of a comprehensive SCFAs panel in activating GPCRs also can be improved by repeating this study using different assay to confirm the agonist activity for the novel agonists. Due to the time constrain, we were only managed to generate a small number of sample with only one biological replicate in assessing adipogenic and GPCRs gene expression profiles using qPCR array. This lack of power of test has resulted in non-conclusive observation, as we were not able to draw a link between the role of GPCRs and adipogenesis (no significant effect of SCFAs on gene expression). With more time, we would generate a follow-up 3T3-L1 experiment including more biological replicates to assess the adipogenic gene expression profiles related to SCFA treatment during adipocytes differentiation. It is also interesting to measure the level of cAMP as a complement method to confirm the activation of the GPCRs during the adipogenesis. In order to confirm the clinical significance of the observations made in this study, these effects need to be tested using other *in vitro* adipocytes model such as human primary hepatocytes.

Conclusion

As a conclusion, in this PhD, considerable effort has been made in assessing the biological effects of SCFAs on important metabolic target tissues, which are hepatic and adipose tissue. We have successfully applied a novel approach, using ^1H NMR metabonomics to investigate hepatocyte-specific metabolic signature related to SCFA exposure and demonstrated that the effect of SCFAs in this cell model are mainly metabolic. Furthermore, the pharmacological assessment of a comprehensive SCFA panel on related GPCRs revealed a new agonists for GPR109A. Our cell-based assays of a comprehensive SCFA panel reveal the role of SCFAs in promoting adipogenesis and inhibiting adipocytes lipolysis. In general, the results reported in this thesis provide a new knowledge on the biological effects of SCFAs, and signify the gut-microbial metabolites-host interaction.

REFERENCES

Adams, E.Q., and Rosenstein, L. (1914). The Color and Ionization of Crystal-Violet. *J. Am. Chem. Soc.* *36*, 1452–1473.

Adler, A. (2002). Obesity and target organ damage: diabetes. *Int. J. Obes. Relat. Metab. Disord. J. Int. Assoc. Study Obes.* *26 Suppl 4*, S11–S14.

Alberti, K.G.M.M., Zimmet, P., Shaw, J., and IDF Epidemiology Task Force Consensus Group (2005). The metabolic syndrome--a new worldwide definition. *Lancet Lond. Engl.* *366*, 1059–1062.

Allan, E.S., Winter, S., Light, A.M., and Allan, A. (1996). Mucosal enzyme activity for butyrate oxidation; no defect in patients with ulcerative colitis. *Gut* *38*, 886–893.

Anderson, J.W., and Bridges, S.R. (1984). Short-Chain Fatty Acid Fermentation Products of Plant Fiber Affect Glucose Metabolism of Isolated Rat Hepatocytes. *Exp. Biol. Med.* *177*, 372–376.

Aoyama, M., Kotani, J., and Usami, M. (2010). Butyrate and propionate induced activated or non-activated neutrophil apoptosis via HDAC inhibitor activity but without activating GPR-41/GPR-43 pathways. *Nutr. Burbank Los Angel. Cty. Calif* *26*, 653–661.

Aronoff, S.L., Berkowitz, K., Shreiner, B., and Want, L. (2004). Glucose Metabolism and Regulation: Beyond Insulin and Glucagon. *Diabetes Spectr.* *17*, 183–190.

Arora, M. (2013). Cell Culture Media: A Review. *Mater. Methods* *3*, 175.

Arsenijevic, T., Grégoire, F., Delforge, V., Delporte, C., and Perret, J. (2012). Murine 3T3-L1 Adipocyte Cell Differentiation Model: Validated Reference Genes for qPCR Gene Expression Analysis. *PLoS ONE* *7*, e37517.

Bäckhed, F., Ding, H., Wang, T., Hooper, L.V., Koh, G.Y., Nagy, A., Semenkovich, C.F., and Gordon, J.I. (2004). The gut microbiota as an environmental factor that regulates fat storage. *Proc. Natl. Acad. Sci. U. S. A.* *101*, 15718–15723.

Bäckhed, F., Ley, R.E., Sonnenburg, J.L., Peterson, D.A., and Gordon, J.I. (2005). Host-bacterial mutualism in the human intestine. *Science* *307*, 1915–1920.

Bales, J.R., Higham, D.P., Howe, I., Nicholson, J.K., and Sadler, P.J. (1984). Use of high-resolution proton nuclear magnetic resonance spectroscopy for rapid multi-component analysis of urine. *Clin. Chem.* *30*, 426–432.

Balk, S.D., and Polimeni, P.I. (1982). Effect of reduction of culture medium sodium, using different sodium chloride substitutes, on the proliferation of normal and Rous sarcoma virus-infected chicken fibroblasts. *J. Cell. Physiol.* *112*, 251–256.

- Barsh, G.S., Farooqi, I.S., and O'Rahilly, S. (2000). Genetics of body-weight regulation. *Nature* 404, 644–651.
- Bauer, H., Horowitz, R.E., Levenson, S.M., and Popper, H. (1963). The response of the lymphatic tissue to the microbial flora. Studies on germfree mice. *Am. J. Pathol.* 42, 471–483.
- Beauvieux, M.C., Tissier, P., Gin, H., Canioni, P., and Gallis, J.L. (2001). Butyrate impairs energy metabolism in isolated perfused liver of fed rats. *J. Nutr.* 131, 1986–1992.
- Beckonert, O., Keun, H.C., Ebbels, T.M.D., Bundy, J., Holmes, E., Lindon, J.C., and Nicholson, J.K. (2007). Metabolic profiling, metabolomic and metabonomic procedures for NMR spectroscopy of urine, plasma, serum and tissue extracts. *Nat. Protoc.* 2, 2692–2703.
- Belenguier, A., Duncan, S.H., Holtrop, G., Anderson, S.E., Lobley, G.E., and Flint, H.J. (2007). Impact of pH on lactate formation and utilization by human fecal microbial communities. *Appl. Environ. Microbiol.* 73, 6526–6533.
- Belfort, R., Mandarino, L., Kashyap, S., Wirfel, K., Pratipanawat, T., Berria, R., Defronzo, R.A., and Cusi, K. (2005). Dose-response effect of elevated plasma free fatty acid on insulin signaling. *Diabetes* 54, 1640–1648.
- Benveniste, J., Lespinats, G., Adam, C., and Salomon, J.C. (1971). Immunoglobulins in intact, immunized, and contaminated axenic mice: study of serum IgA. *J. Immunol. Baltim. Md* 1950 107, 1647–1655.
- Benyó, Z., Gille, A., Kero, J., Csiky, M., Suchánková, M.C., Nüsing, R.M., Moers, A., Pfeffer, K., and Offermanns, S. (2005). GPR109A (PUMA-G/HM74A) mediates nicotinic acid-induced flushing. *J. Clin. Invest.* 115, 3634–3640.
- Berg, R.D. (1996). The indigenous gastrointestinal microflora. *Trends Microbiol.* 4, 430–435.
- Bergman, E.N. (1990a). Energy contributions of volatile fatty acids from the gastrointestinal tract in various species. *Physiol. Rev.* 70, 567–590.
- Bergman, E.N. (1990b). Energy contributions of volatile fatty acids from the gastrointestinal tract in various species. *Physiol. Rev.* 70, 567–590.
- Bernalier, A., Willems, A., Leclerc, M., Rochet, V., and Collins, M.D. (1996). *Ruminococcus hydrogenotrophicus* sp. nov., a new H₂/CO₂-utilizing acetogenic bacterium isolated from human feces. *Arch. Microbiol.* 166, 176–183.
- den Besten, G., Lange, K., Havinga, R., van Dijk, T.H., Gerding, A., van Eunen, K., Müller, M., Groen, A.K., Hooiveld, G.J., Bakker, B.M., *et al.* (2013). Gut-derived short-chain fatty acids are vividly assimilated into host carbohydrates and lipids. *Am. J. Physiol. Gastrointest. Liver Physiol.* 305, G900–G910.
- den Besten, G., Havinga, R., Bleeker, A., Rao, S., Gerding, A., van Eunen, K., Groen, A.K., Reijngoud, D.-J., and Bakker, B.M. (2014). The short-chain fatty acid uptake fluxes by mice on a guar gum supplemented diet associate with amelioration of major biomarkers of the metabolic syndrome. *PLoS One* 9, e107392.

den Besten, G., Bleeker, A., Gerding, A., van Eunen, K., Havinga, R., van Dijk, T.H., Oosterveer, M.H., Jonker, J.W., Groen, A.K., Reijngoud, D.-J., *et al.* (2015). Short-Chain Fatty Acids Protect Against High-Fat Diet-Induced Obesity via a PPAR γ -Dependent Switch From Lipogenesis to Fat Oxidation. *Diabetes* 64, 2398–2408.

Birnbaumer, L. (2007). Expansion of signal transduction by G proteins. *Biochim. Biophys. Acta BBA - Biomembr.* 1768, 772–793.

Blad, C.C., Tang, C., and Offermanns, S. (2012). G protein-coupled receptors for energy metabolites as new therapeutic targets. *Nat. Rev. Drug Discov.* 11, 603–619.

Bleich, S., Cutler, D., Murray, C., and Adams, A. (2008). Why is the developed world obese? *Annu. Rev. Public Health* 29, 273–295.

Bloemen, J.G., Venema, K., van de Poll, M.C., Olde Damink, S.W., Buurman, W.A., and Dejong, C.H. (2009). Short chain fatty acids exchange across the gut and liver in humans measured at surgery. *Clin. Nutr. Edinb. Scotl.* 28, 657–661.

Bloemen, J.G., Olde Damink, S.W.M., Venema, K., Buurman, W.A., Jalan, R., and Dejong, C.H.C. (2010). Short chain fatty acids exchange: Is the cirrhotic, dysfunctional liver still able to clear them? *Clin. Nutr.* 29, 365–369.

Bokoch, G.M., Katada, T., Northup, J.K., Ui, M., and Gilman, A.G. (1984). Purification and properties of the inhibitory guanine nucleotide-binding regulatory component of adenylate cyclase. *J. Biol. Chem.* 259, 3560–3567.

Bollard, M.E., Stanley, E.G., Lindon, J.C., Nicholson, J.K., and Holmes, E. (2005). NMR-based metabolomic approaches for evaluating physiological influences on biofluid composition. *NMR Biomed.* 18, 143–162.

Bouchard, R.A., Clark, R.B., and Giles, W.R. (1993). Role of sodium-calcium exchange in activation of contraction in rat ventricle. *J. Physiol.* 472, 391–413.

Bourlier, V., Zakaroff-Girard, A., Miranville, A., De Barros, S., Maumus, M., Sengenès, C., Galitzky, J., Lafontan, M., Karpe, F., Frayn, K.N., *et al.* (2008). Remodeling phenotype of human subcutaneous adipose tissue macrophages. *Circulation* 117, 806–815.

Braissant, O., Foufelle, F., Scotto, C., Dauça, M., and Wahli, W. (1996). Differential expression of peroxisome proliferator-activated receptors (PPARs): tissue distribution of PPAR-alpha, -beta, and -gamma in the adult rat. *Endocrinology* 137, 354–366.

Briscoe, C.P., Tadayyon, M., Andrews, J.L., Benson, W.G., Chambers, J.K., Eilert, M.M., Ellis, C., Elshourbagy, N.A., Goetz, A.S., Minnick, D.T., *et al.* (2003). The orphan G protein-coupled receptor GPR40 is activated by medium and long chain fatty acids. *J. Biol. Chem.* 278, 11303–11311.

Brown, A.J., Goldsworthy, S.M., Barnes, A.A., Eilert, M.M., Tcheang, L., Daniels, D., Muir, A.I., Wigglesworth, M.J., Kinghorn, I., Fraser, N.J., *et al.* (2003). The Orphan G protein-coupled receptors GPR41 and GPR43 are activated by propionate and other short chain carboxylic acids. *J. Biol. Chem.* 278, 11312–11319.

- Bruckert, E., Labreuche, J., and Amarenco, P. (2010). Meta-analysis of the effect of nicotinic acid alone or in combination on cardiovascular events and atherosclerosis. *Atherosclerosis* *210*, 353–361.
- Cairns, R.A., Harris, I.S., and Mak, T.W. (2011). Regulation of cancer cell metabolism. *Nat. Rev. Cancer* *11*, 85–95.
- Camp, J.G., Kanther, M., Semova, I., and Rawls, J.F. (2009). Patterns and scales in gastrointestinal microbial ecology. *Gastroenterology* *136*, 1989–2002.
- Candido, E. (1978). Sodium butyrate inhibits histone deacetylation in cultured cells. *Cell* *14*, 105–113.
- Carlson, L.A. (1963). Studies on the effect of nicotinic acid on catecholamine stimulated lipolysis in adipose tissue in vitro. *Acta Med. Scand.* *173*, 719–722.
- Carlson, L.A. (2005). Nicotinic acid: the broad-spectrum lipid drug. A 50th anniversary review. *J. Intern. Med.* *258*, 94–114.
- Ceccarini, C., and Eagle, H. (1971). pH as a determinant of cellular growth and contact inhibition. *Proc. Natl. Acad. Sci. U. S. A.* *68*, 229–233.
- Chavez, A.O., Kamath, S., Jani, R., Sharma, L.K., Monroy, A., Abdul-Ghani, M.A., Centonze, V.E., Sathyanarayana, P., Coletta, D.K., Jenkinson, C.P., *et al.* (2010). Effect of short-term free Fatty acids elevation on mitochondrial function in skeletal muscle of healthy individuals. *J. Clin. Endocrinol. Metab.* *95*, 422–429.
- Chawla, A., Schwarz, E.J., Dimaculangan, D.D., and Lazar, M.A. (1994). Peroxisome proliferator-activated receptor (PPAR) gamma: adipose-predominant expression and induction early in adipocyte differentiation. *Endocrinology* *135*, 798–800.
- Chen, J.S., Faller, D.V., and Spanjaard, R.A. (2003). Short-chain fatty acid inhibitors of histone deacetylases: promising anticancer therapeutics? *Curr. Cancer Drug Targets* *3*, 219–236.
- Cloarec, O., Dumas, M.E., Trygg, J., Craig, A., Barton, R.H., Lindon, J.C., Nicholson, J.K., and Holmes, E. (2005a). Evaluation of the Orthogonal Projection on Latent Structure Model Limitations Caused by Chemical Shift Variability and Improved Visualization of Biomarker Changes in ¹ H NMR Spectroscopic Metabonomic Studies. *Anal. Chem.* *77*, 517–526.
- Cloarec, O., Dumas, M.-E., Craig, A., Barton, R.H., Trygg, J., Hudson, J., Blancher, C., Gauguier, D., Lindon, J.C., Holmes, E., *et al.* (2005b). Statistical Total Correlation Spectroscopy: An Exploratory Approach for Latent Biomarker Identification from Metabolic ¹ H NMR Data Sets. *Anal. Chem.* *77*, 1282–1289.
- Coen, M., Holmes, E., Lindon, J.C., and Nicholson, J.K. (2008). NMR-Based Metabolic Profiling and Metabonomic Approaches to Problems in Molecular Toxicology. *Chem. Res. Toxicol.* *21*, 9–27.
- Cohen, P., Zhao, C., Cai, X., Montez, J.M., Rohani, S.C., Feinstein, P., Mombaerts, P., and Friedman, J.M. (2001a). Selective deletion of leptin receptor in neurons leads to obesity. *J. Clin. Invest.* *108*, 1113–1121.

- Cohen, P., Zhao, C., Cai, X., Montez, J.M., Rohani, S.C., Feinstein, P., Mombaerts, P., and Friedman, J.M. (2001b). Selective deletion of leptin receptor in neurons leads to obesity. *J. Clin. Invest.* *108*, 1113–1121.
- Combs, T.P., Pajvani, U.B., Berg, A.H., Lin, Y., Jelicks, L.A., Laplante, M., Nawrocki, A.R., Rajala, M.W., Parlow, A.F., Cheeseboro, L., *et al.* (2004). A transgenic mouse with a deletion in the collagenous domain of adiponectin displays elevated circulating adiponectin and improved insulin sensitivity. *Endocrinology* *145*, 367–383.
- Counotte, G.H., Prins, R.A., Janssen, R.H., and Debie, M.J. (1981). Role of *Megasphaera elsdenii* in the Fermentation of dl-[2-C]lactate in the Rumen of Dairy Cattle. *Appl. Environ. Microbiol.* *42*, 649–655.
- Covington, D.K., Briscoe, C.A., Brown, A.J., and Jayawickreme, C.K. (2006). The G-protein-coupled receptor 40 family (GPR40-GPR43) and its role in nutrient sensing. *Biochem. Soc. Trans.* *34*, 770–773.
- Cummings, J.H. (1981). Short chain fatty acids in the human colon. *Gut* *22*, 763–779.
- Cummings, J.H., and Macfarlane, G.T. (1997). Role of intestinal bacteria in nutrient metabolism. *JPEN J. Parenter. Enteral Nutr.* *21*, 357–365.
- Cummings, J.H., Pomare, E.W., Branch, W.J., Naylor, C.P., and Macfarlane, G.T. (1987). Short chain fatty acids in human large intestine, portal, hepatic, and venous blood. *Gut* *28*, 1221–1227.
- Cummings, J.H., Macfarlane, G.T., and Englyst, H.N. (2001). Prebiotic digestion and fermentation. *Am. J. Clin. Nutr.* *73*, 415S – 420S.
- Curi, R., Bond, J.A., Calder, P.C., and Newsholme, E.A. (1993). Propionate regulates lymphocyte proliferation and metabolism. *Gen. Pharmacol. Vasc. Syst.* *24*, 591–597.
- Day, A.J., and Fidge, N.H. (1964). Incorporation of C14-Labeled Acetate into Lipids by Macrophages in Vitro. *J. Lipid Res.* *5*, 163–168.
- Delaere, F., Duchampt, A., Mounien, L., Seyer, P., Duraffourd, C., Zitoun, C., Thorens, B., and Mithieux, G. (2013). The role of sodium-coupled glucose co-transporter 3 in the satiety effect of portal glucose sensing. *Mol. Metab.* *2*, 47–53.
- Delarue, J., and Magnan, C. (2007). Free fatty acids and insulin resistance. *Curr. Opin. Clin. Nutr. Metab. Care* *10*, 142–148.
- Demigné, C., Morand, C., Levrat, M.A., Besson, C., Moundras, C., and Rémésy, C. (1995). Effect of propionate on fatty acid and cholesterol synthesis and on acetate metabolism in isolated rat hepatocytes. *Br. J. Nutr.* *74*, 209–219.
- Després, J.-P., and Lemieux, I. (2006). Abdominal obesity and metabolic syndrome. *Nature* *444*, 881–887.
- De Vadder, F., Kovatcheva-Datchary, P., Goncalves, D., Vinera, J., Zitoun, C., Duchampt, A., Bäckhed, F., and Mithieux, G. (2014). Microbiota-generated metabolites promote metabolic benefits via gut-brain neural circuits. *Cell* *156*, 84–96.

- Dewulf, E.M., Ge, Q., Bindels, L.B., Sohet, F.M., Cani, P.D., Brichard, S.M., and Delzenne, N.M. (2013). Evaluation of the relationship between GPR43 and adiposity in human. *Nutr. Metab.* *10*, 11.
- DiBaise, J.K., Zhang, H., Crowell, M.D., Krajmalnik-Brown, R., Decker, G.A., and Rittmann, B.E. (2008). Gut Microbiota and Its Possible Relationship with Obesity. *Mayo Clin. Proc.* *83*, 460–469.
- Dmitrieva, N.I. (2004). Cells adapted to high NaCl have many DNA breaks and impaired DNA repair both in cell culture and in vivo. *Proc. Natl. Acad. Sci.* *101*, 2317–2322.
- Dmitrieva, N.I., and Burg, M.B. (2005). Hypertonic stress response. *Mutat. Res. Mol. Mech. Mutagen.* *569*, 65–74.
- Dmitrieva, N.I., and Burg, M.B. (2015). Elevated Sodium and Dehydration Stimulate Inflammatory Signalling in Endothelial Cells and Promote Atherosclerosis. *PLOS ONE* *10*, e0128870.
- Dmitrieva, N.I., Bulavin, D.V., and Burg, M.B. (2003). High NaCl causes Mre11 to leave the nucleus, disrupting DNA damage signalling and repair. *Am. J. Physiol. - Ren. Physiol.* *285*, F266–F274.
- Dobbs, R., and Manyika, J. (2015). The obesity crisis.
- Donohoe, D.R., Garge, N., Zhang, X., Sun, W., O’Connell, T.M., Bunger, M.K., and Bultman, S.J. (2011). The microbiome and butyrate regulate energy metabolism and autophagy in the mammalian colon. *Cell Metab.* *13*, 517–526.
- Donohoe, D.R., Collins, L.B., Wali, A., Bigler, R., Sun, W., and Bultman, S.J. (2012). The Warburg Effect Dictates the Mechanism of Butyrate-Mediated Histone Acetylation and Cell Proliferation. *Mol. Cell* *48*, 612–626.
- Duggal, J.K., Singh, M., Attri, N., Singh, P.P., Ahmed, N., Pahwa, S., Molnar, J., Singh, S., Khosla, S., and Arora, R. (2010). Effect of Niacin Therapy on Cardiovascular Outcomes in Patients with Coronary Artery Disease. *J. Cardiovasc. Pharmacol. Ther.* *15*, 158–166.
- Dumas, M.-E., and Davidovic, L. (2013). Metabolic phenotyping and systems biology approaches to understanding neurological disorders. *F1000Prime Rep.* *5*.
- Dumas, M.-E., Barton, R.H., Toye, A., Cloarec, O., Blancher, C., Rothwell, A., Fearnside, J., Tatoud, R., Blanc, V., Lindon, J.C., *et al.* (2006). Metabolic profiling reveals a contribution of gut microbiota to fatty liver phenotype in insulin-resistant mice. *Proc. Natl. Acad. Sci.* *103*, 12511–12516.
- Duncan, R.E., Ahmadian, M., Jaworski, K., Sarkadi-Nagy, E., and Sul, H.S. (2007a). Regulation of Lipolysis in Adipocytes. *Annu. Rev. Nutr.* *27*, 79–101.
- Duncan, S.H., Barcenilla, A., Stewart, C.S., Pryde, S.E., and Flint, H.J. (2002). Acetate utilization and butyryl coenzyme A (CoA): acetate-CoA transferase in butyrate-producing bacteria from the human large intestine. *Appl. Environ. Microbiol.* *68*, 5186–5190.
- Duncan, S.H., Holtrop, G., Lobley, G.E., Calder, A.G., Stewart, C.S., and Flint, H.J. (2004a). Contribution of acetate to butyrate formation by human faecal bacteria. *Br. J. Nutr.* *91*, 915–923.
- Duncan, S.H., Louis, P., and Flint, H.J. (2004b). Lactate-utilizing bacteria, isolated from human feces that produce butyrate as a major fermentation product. *Appl. Environ. Microbiol.* *70*, 5810–5817.

Duncan, S.H., Aminov, R.I., Scott, K.P., Louis, P., Stanton, T.B., and Flint, H.J. (2006). Proposal of *Roseburia faecis* sp. nov., *Roseburia hominis* sp. nov. and *Roseburia inulinivorans* sp. nov., based on isolates from human faeces. *Int. J. Syst. Evol. Microbiol.* 56, 2437–2441.

Duncan, S.H., Belenguer, A., Holtrop, G., Johnstone, A.M., Flint, H.J., and Lobley, G.E. (2007b). Reduced Dietary Intake of Carbohydrates by Obese Subjects Results in Decreased Concentrations of Butyrate and Butyrate-Producing Bacteria in Feces. *Appl. Environ. Microbiol.* 73, 1073–1078.

Eckburg, P.B., Bik, E.M., Bernstein, C.N., Purdom, E., Dethlefsen, L., Sargent, M., Gill, S.R., Nelson, K.E., and Relman, D.A. (2005). Diversity of the human intestinal microbial flora. *Science* 308, 1635–1638.

Ellis, J.K., Athersuch, T.J., Cavill, R., Radford, R., Slattery, C., Jennings, P., McMorrow, T., Ryan, M.P., Ebbels, T.M.D., and Keun, H.C. (2011). Metabolic response to low-level toxicant exposure in a novel renal tubule epithelial cell system. *Mol. Biosyst.* 7, 247–257.

Eriksson, L., Antti, H., Gottfries, J., Holmes, E., Johansson, E., Lindgren, F., Long, I., Lundstedt, T., Trygg, J., and Wold, S. (2004). Using chemometrics for navigating in the large data sets of genomics, proteomics, and metabonomics (gpm). *Anal. Bioanal. Chem.* 380, 419–429.

Falony, G., Vlachou, A., Verbrugghe, K., and De Vuyst, L. (2006). Cross-feeding between *Bifidobacterium longum* BB536 and acetate-converting, butyrate-producing colon bacteria during growth on oligofructose. *Appl. Environ. Microbiol.* 72, 7835–7841.

Feron, O. (2009). Pyruvate into lactate and back: from the Warburg effect to symbiotic energy fuel exchange in cancer cells. *Radiother. Oncol. J. Eur. Soc. Ther. Radiol. Oncol.* 92, 329–333.

Flint, H.J. (2006). The significance of prokaryote diversity in the human gastrointestinal tract. In *Prokaryotic Diversity*, N.A. Logan, H.M. Lappin-Scott, and P.C.F. Oyston, eds. (Cambridge: Cambridge University Press), pp. 65–90.

Flint, H.J., Duncan, S.H., Scott, K.P., and Louis, P. (2007). Interactions and competition within the microbial community of the human colon: links between diet and health. *Environ. Microbiol.* 9, 1101–1111.

Fonville, J.M., Richards, S.E., Barton, R.H., Boulange, C.L., Ebbels, T.M.D., Nicholson, J.K., Holmes, E., and Dumas, M.-E. (2010). The evolution of partial least squares models and related chemometric approaches in metabonomics and metabolic phenotyping. *J. Chemom.* 24, 636–649.

Forman, B.M., Tontonoz, P., Chen, J., Brun, R.P., Spiegelman, B.M., and Evans, R.M. (1995). 15-Deoxy- $\Delta^{12,14}$ -Prostaglandin J2 is a ligand for the adipocyte determination factor PPAR γ . *Cell* 83, 803–812.

Fowler, S.D., and Greenspan, P. (1985). Application of Nile red, a fluorescent hydrophobic probe, for the detection of neutral lipid deposits in tissue sections: comparison with oil red O. *J. Histochem. Cytochem. Off. J. Histochem. Soc.* 33, 833–836.

Frayn, K., Tan, G., and Karpe, F. (2007). Adipose Tissue: A Key Target for Diabetes Pathophysiology and Treatment? *Horm. Metab. Res.* 39, 739–742.

Fredstrom, S.B., Lampe, J.W., Jung, H.-J.G., and Slavin, J.L. (1994). Apparent Fiber Digestibility and Fecal Short-Chain Fatty Acid Concentrations with Ingestion of Two Types of Dietary Fiber. *J. Parenter. Enter. Nutr.* *18*, 14–19.

Frost, G., Leeds, A., Trew, G., Margara, R., and Dornhorst, A. (1998). Insulin sensitivity in women at risk of coronary heart disease and the effect of a low glycemic diet. *Metabolism.* *47*, 1245–1251.

Frost, G., Cai, Z., Raven, M., Otway, D.T., Mushtaq, R., and Johnston, J.D. (2014a). Effect of short chain fatty acids on the expression of free fatty acid receptor 2 (Ffar2), Ffar3 and early-stage adipogenesis. *Nutr. Diabetes* *4*, e128.

Frost, G., Sleeth, M.L., Sahuri-Arisoylu, M., Lizarbe, B., Cerdan, S., Brody, L., Anastasovska, J., Ghourab, S., Hankir, M., Zhang, S., *et al.* (2014b). The short-chain fatty acid acetate reduces appetite via a central homeostatic mechanism. *Nat. Commun.* *5*.

Fukuwatari, T., and Shibata, K. (2013). Nutritional Aspect of Tryptophan Metabolism. *Int. J. Tryptophan Res.* *3*.

Funahashi, T., Nakamura, T., Shimomura, I., Maeda, K., Kuriyama, H., Takahashi, M., Arita, Y., Kihara, S., and Matsuzawa, Y. (1999). Role of adipocytokines on the pathogenesis of atherosclerosis in visceral obesity. *Intern. Med. Tokyo Jpn.* *38*, 202–206.

Fürst, P., and Stehle, P. (2004). What are the essential elements needed for the determination of amino acid requirements in humans? *J. Nutr.* *134*, 1558S – 1565S.

Gamet, L., Daviaud, D., Denis-Pouxviel, C., Remesy, C., and Murat, J.C. (1992). Effects of short-chain fatty acids on growth and differentiation of the human colon-cancer cell line HT29. *Int. J. Cancer J.* *Int. Cancer* *52*, 286–289.

Ganapathy, V., Gopal, E., Miyauchi, S., and Prasad, P.D. (2005). Biological functions of SLC5A8, a candidate tumour suppressor. *Biochem. Soc. Trans.* *33*, 237–240.

Ganapathy, V., Thangaraju, M., Prasad, P.D., Martin, P.M., and Singh, N. (2013). Transporters and receptors for short-chain fatty acids as the molecular link between colonic bacteria and the host. *Curr. Opin. Pharmacol.* *13*, 869–874.

Gao, Z., Yin, J., Zhang, J., Ward, R.E., Martin, R.J., Lefevre, M., Cefalu, W.T., and Ye, J. (2009). Butyrate improves insulin sensitivity and increases energy expenditure in mice. *Diabetes* *58*, 1509–1517.

Gastaldelli, A. (2011). Role of beta-cell dysfunction, ectopic fat accumulation and insulin resistance in the pathogenesis of type 2 diabetes mellitus. *Diabetes Res. Clin. Pract.* *93 Suppl 1*, S60–S65.

Gastaldelli, A., Baldi, S., Pettiti, M., Toschi, E., Camastra, S., Natali, A., Landau, B.R., and Ferrannini, E. (2000). Influence of obesity and type 2 diabetes on gluconeogenesis and glucose output in humans: a quantitative study. *Diabetes* *49*, 1367–1373.

Ge, H., Li, X., Weizmann, J., Wang, P., Baribault, H., Chen, J.-L., Tian, H., and Li, Y. (2008). Activation of G protein-coupled receptor 43 in adipocytes leads to inhibition of lipolysis and suppression of plasma free fatty acids. *Endocrinology* *149*, 4519–4526.

- Gerich, J.E., Meyer, C., Woerle, H.J., and Stumvoll, M. (2001). Renal gluconeogenesis: its importance in human glucose homeostasis. *Diabetes Care* 24, 382–391.
- Gille, A., Bodor, E.T., Ahmed, K., and Offermanns, S. (2008). Nicotinic acid: pharmacological effects and mechanisms of action. *Annu. Rev. Pharmacol. Toxicol.* 48, 79–106.
- Giromini, C., Baldi, A., Fusi, E., Rebucci, R., and Purup, S. (2015). Effect of growth factors, estradiol 17- β , and short chain fatty acids on the intestinal HT29-MTX cells: Growth factors and SCFAs effects on intestinal E12 cells. *Cell Biol. Toxicol.*
- Giugliano, D., Ceriello, A., and Esposito, K. (2008). Glucose metabolism and hyperglycemia. *Am. J. Clin. Nutr.* 87, 217S – 222S.
- Gray, L.R., Tompkins, S.C., and Taylor, E.B. (2014). Regulation of pyruvate metabolism and human disease. *Cell. Mol. Life Sci.* 71, 2577–2604.
- Green, H., and Kehinde, O. (1975). An established preadipose cell line and its differentiation in culture II. Factors affecting the adipose conversion. *Cell* 5, 19–27.
- Green, H., and Meuth, M. (1974). An established pre-adipose cell line and its differentiation in culture. *Cell* 3, 127–133.
- Greenwood, H.C., Bloom, S.R., and Murphy, K.G. (2011). Peptides and their potential role in the treatment of diabetes and obesity. *Rev. Diabet. Stud. RDS* 8, 355–368.
- van Greevenbroek, M.M.J., Schalkwijk, C.G., and Stehouwer, C.D.A. (2013). Obesity-associated low-grade inflammation in type 2 diabetes mellitus: causes and consequences. *Neth. J. Med.* 71, 174–187.
- Greiner, T., and Bäckhed, F. (2011). Effects of the gut microbiota on obesity and glucose homeostasis. *Trends Endocrinol. Metab. TEM* 22, 117–123.
- Gupta, N., Martin, P.M., Prasad, P.D., and Ganapathy, V. (2006). SLC5A8 (SMCT1)-mediated transport of butyrate forms the basis for the tumor suppressive function of the transporter. *Life Sci.* 78, 2419–2425.
- Hadjiagapiou, C., Schmidt, L., Dudeja, P.K., Layden, T.J., and Ramaswamy, K. (2000). Mechanism(s) of butyrate transport in Caco-2 cells: role of monocarboxylate transporter 1. *Am. J. Physiol. Gastrointest. Liver Physiol.* 279, G775–G780.
- Halestrap, A.P., and Meredith, D. (2004). The SLC16 gene family—from monocarboxylate transporters (MCTs) to aromatic amino acid transporters and beyond. *Pflüg. Arch. Eur. J. Physiol.* 447, 619–628.
- Halestrap, A.P., and Price, N.T. (1999). The proton-linked monocarboxylate transporter (MCT) family: structure, function and regulation. *Biochem. J.* 343 Pt 2, 281–299.
- Ham, R.G., and McKeehan, W.L. (1979). Media and growth requirements. *Methods Enzymol.* 58, 44–93.

- Hamer, H.M., Jonkers, D., Venema, K., Vanhoutvin, S., Troost, F.J., and Brummer, R.-J. (2008). Review article: the role of butyrate on colonic function. *Aliment. Pharmacol. Ther.* *27*, 104–119.
- Han, J.-H., Kim, I.-S., Jung, S.-H., Lee, S.-G., Son, H.-Y., and Myung, C.-S. (2014). The Effects of Propionate and Valerate on Insulin Responsiveness for Glucose Uptake in 3T3-L1 Adipocytes and C2C12 Myotubes via G Protein-Coupled Receptor 41. *PLoS ONE* *9*, e95268.
- Hanson, J., Gille, A., Zwykiel, S., Lukasova, M., Clausen, B.E., Ahmed, K., Tunaru, S., Wirth, A., and Offermanns, S. (2010). Nicotinic acid- and monomethyl fumarate-induced flushing involves GPR109A expressed by keratinocytes and COX-2-dependent prostanoid formation in mice. *J. Clin. Invest.* *120*, 2910–2919.
- Harig, J.M., Ng, E.K., Dudeja, P.K., Brasitus, T.A., and Ramaswamy, K. (1996). Transport of n-butyrate into human colonic luminal membrane vesicles. *Am. J. Physiol.* *271*, G415–G422.
- Harris, R.A., Joshi, M., Jeoung, N.H., and Obayashi, M. (2005). Overview of the molecular and biochemical basis of branched-chain amino acid catabolism. *J. Nutr.* *135*, 1527S – 30S.
- Hauner, H. (2005). Secretory factors from human adipose tissue and their functional role. *Proc. Nutr. Soc.* *64*, 163–169.
- Havel, P.J. (2002). Control of energy homeostasis and insulin action by adipocyte hormones: leptin, acylation stimulating protein, and adiponectin. *Curr. Opin. Lipidol.* *13*, 51–59.
- Hedlund, T.E., and Miller, G.J. (1994). A serum-free defined medium capable of supporting growth of four established human prostatic carcinoma cell lines. *The Prostate* *24*, 221–228.
- Hinnebusch, B.F., Meng, S., Wu, J.T., Archer, S.Y., and Hodin, R.A. (2002). The effects of short-chain fatty acids on human colon cancer cell phenotype are associated with histone hyperacetylation. *J. Nutr.* *132*, 1012–1017.
- Holmes, E., Foxall, P.J., Spraul, M., Duncan Farrant, R., Nicholson, J.K., and Lindon, J.C. (1997). 750 MHz ¹H NMR spectroscopy characterisation of the complex metabolic pattern of urine from patients with inborn errors of metabolism: 2-hydroxyglutaric aciduria and maple syrup urine disease. *J. Pharm. Biomed. Anal.* *15*, 1647–1659.
- Holmes, E., Li, J.V., Athanasiou, T., Ashrafian, H., and Nicholson, J.K. (2011). Understanding the role of gut microbiome-host metabolic signal disruption in health and disease. *Trends Microbiol.* *19*, 349–359.
- Hong, Y.-H. (2005). Acetate and Propionate Short Chain Fatty Acids Stimulate Adipogenesis via GPCR43. *Endocrinology* *146*, 5092–5099.
- Hong, Y.-H., Nishimura, Y., Hishikawa, D., Tsuzuki, H., Miyahara, H., Gotoh, C., Choi, K.-C., Feng, D.D., Chen, C., Lee, H.-G., *et al.* (2005). Acetate and Propionate Short Chain Fatty Acids Stimulate Adipogenesis via GPCR43. *Endocrinology* *146*, 5092–5099.
- Hooper, L.V. (2001). Molecular Analysis of Commensal Host-Microbial Relationships in the Intestine. *Science* *291*, 881–884.
- Hotamisligil, G.S. (2006). Inflammation and metabolic disorders. *Nature* *444*, 860–867.

Howard, A.D., McAllister, G., Feighner, S.D., Liu, Q., Nargund, R.P., Van der Ploeg, L.H., and Patchett, A.A. (2001). Orphan G-protein-coupled receptors and natural ligand discovery. *Trends Pharmacol. Sci.* 22, 132–140.

Hu, E., Liang, P., and Spiegelman, B.M. (1996). AdipoQ is a novel adipose-specific gene dysregulated in obesity. *J. Biol. Chem.* 271, 10697–10703.

Hurowitz, E.H., Melnyk, J.M., Chen, Y.J., Kouros-Mehr, H., Simon, M.I., and Shizuya, H. (2000). Genomic characterization of the human heterotrimeric G protein alpha, beta, and gamma subunit genes. *DNA Res. Int. J. Rapid Publ. Rep. Genes Genomes* 7, 111–120.

Inoue, D., Tsujimoto, G., and Kimura, I. (2014). Regulation of Energy Homeostasis by GPR41. *Front. Endocrinol.* 5.

Invitrogen (2010). PrestoBlue® Cell Viability Reagent.

IOM (Institute of Medicine) (2002). IOM (Institute of Medicine) (2002) Dietary Reference Intakes for Energy, Carbohydrate, Fiber, Fat, Fatty Acids, Cholesterol, Protein, and Amino Acids 2002.

Jankovic, A., Korac, A., Buzadzic, B., Otasevic, V., Stancic, A., Daiber, A., and Korac, B. (2015). Redox implications in adipose tissue (dys)function—A new look at old acquaintances. *Redox Biol.* 6, 19–32.

Jardetzky, O., and Roberts, G.C.K. (1981). *NMR in molecular biology* (New York: Academic Press).

Jenkins, D.J., Wolever, T.M., Jenkins, A., Brighenti, F., Vuksan, V., Rao, A.V., Cunnane, S.C., Ocana, A., Corey, P., and Vezina, C. (1991). Specific types of colonic fermentation may raise low-density-lipoprotein-cholesterol concentrations. *Am. J. Clin. Nutr.* 54, 141–147.

Jin, E.S., Szuszkiewicz-Garcia, M., Browning, J.D., Baxter, J.D., Abate, N., and Malloy, C.R. (2015). Influence of Liver Triglycerides on Suppression of Glucose Production by Insulin in Men. *J. Clin. Endocrinol. Metab.* 100, 235–243.

Jobgen, W.S., Fried, S.K., Fu, W.J., Meininger, C.J., and Wu, G. (2006). Regulatory role for the arginine-nitric oxide pathway in metabolism of energy substrates. *J. Nutr. Biochem.* 17, 571–588.

Juel, C., and Halestrap, A.P. (1999). Lactate transport in skeletal muscle - role and regulation of the monocarboxylate transporter. *J. Physiol.* 517 (Pt 3), 633–642.

Jung, M. (2001). Inhibitors of histone deacetylase as new anticancer agents. *Curr. Med. Chem.* 8, 1505–1511.

Kajimura, S., Seale, P., Tomaru, T., Erdjument-Bromage, H., Cooper, M.P., Ruas, J.L., Chin, S., Tempst, P., Lazar, M.A., and Spiegelman, B.M. (2008). Regulation of the brown and white fat gene programs through a PRDM16/CtBP transcriptional complex. *Genes Dev.* 22, 1397–1409.

Karaki, S., Mitsui, R., Hayashi, H., Kato, I., Sugiya, H., Iwanaga, T., Furness, J.B., and Kuwahara, A. (2006). Short-chain fatty acid receptor, GPR43, is expressed by enteroendocrine cells and mucosal mast cells in rat intestine. *Cell Tissue Res.* 324, 353–360.

Kashyap, S., Belfort, R., Gastaldelli, A., Pratipanawatr, T., Berria, R., Pratipanawatr, W., Bajaj, M., Mandarino, L., DeFronzo, R., and Cusi, K. (2003). A sustained increase in plasma free fatty acids impairs insulin secretion in nondiabetic subjects genetically predisposed to develop type 2 diabetes. *Diabetes* 52, 2461–2474.

Kashyap, S.R., Belfort, R., Berria, R., Suraamornkul, S., Pratipanawatr, T., Finlayson, J., Barrentine, A., Bajaj, M., Mandarino, L., DeFronzo, R., *et al.* (2004). Discordant effects of a chronic physiological increase in plasma FFA on insulin signaling in healthy subjects with or without a family history of type 2 diabetes. *Am. J. Physiol. Endocrinol. Metab.* 287, E537–E546.

Kau, A.L., Ahern, P.P., Griffin, N.W., Goodman, A.L., and Gordon, J.I. (2011). Human nutrition, the gut microbiome and the immune system. *Nature* 474, 327–336.

Keeler, J. (2002). *Understanding NMR spectroscopy* (University of Cambridge).

Kersten, S. (2001). Mechanisms of nutritional and hormonal regulation of lipogenesis. *EMBO Rep.* 2, 282–286.

Kim, C. (2005). Crystal Structure of a Complex Between the Catalytic and Regulatory (RI) Subunits of PKA. *Science* 307, 690–696.

Kim, S.H., and Reaven, G.M. (2004). The metabolic syndrome: one step forward, two steps back. *Diab. Vasc. Dis. Res.* 1, 68–75.

Kim, M.H., Kang, S.G., Park, J.H., Yanagisawa, M., and Kim, C.H. (2013). Short-chain fatty acids activate GPR41 and GPR43 on intestinal epithelial cells to promote inflammatory responses in mice. *Gastroenterology* 145, 396–406.e1–e10.

Kimura, I., Inoue, D., Maeda, T., Hara, T., Ichimura, A., Miyauchi, S., Kobayashi, M., Hirasawa, A., and Tsujimoto, G. (2011). Short-chain fatty acids and ketones directly regulate sympathetic nervous system via G protein-coupled receptor 41 (GPR41). *Proc. Natl. Acad. Sci. U. S. A.* 108, 8030–8035.

Kimura, I., Ozawa, K., Inoue, D., Imamura, T., Kimura, K., Maeda, T., Terasawa, K., Kashihara, D., Hirano, K., Tani, T., *et al.* (2013). The gut microbiota suppresses insulin-mediated fat accumulation via the short-chain fatty acid receptor GPR43. *Nat. Commun.* 4, 1829.

Kirkham, D.M., Murphy, G.J., and Young, P. (1992). Demonstration of inhibitory guanine nucleotide regulatory protein (Gi) function in liver and hepatocyte membranes from streptozotocin-treated rats. *Biochem. J.* 284 (Pt 2), 301–304.

Klaus, S. (1997). Functional differentiation of white and brown adipocytes. *BioEssays News Rev. Mol. Cell. Dev. Biol.* 19, 215–223.

Knopp, R.H. (1999). Drug treatment of lipid disorders. *N. Engl. J. Med.* 341, 498–511.

Knowles, B.B., Howe, C.C., and Aden, D.P. (1980). Human hepatocellular carcinoma cell lines secrete the major plasma proteins and hepatitis B surface antigen. *Science* 209, 497–499.

Kostylina, G., Simon, D., Fey, M.F., Yousefi, S., and Simon, H.U. (2008). Neutrophil apoptosis mediated by nicotinic acid receptors (GPR109A). *Cell Death Differ.* 15, 134–142.

- Kraegen, E.W., James, D.E., Jenkins, A.B., and Chisholm, D.J. (1985). Dose-response curves for *in vivo* insulin sensitivity in individual tissues in rats. *Am. J. Physiol.* *248*, E353–E362.
- Kultz, D., and Chakravarty, D. (2001). Hyperosmolality in the form of elevated NaCl but not urea causes DNA damage in murine kidney cells. *Proc. Natl. Acad. Sci.* *98*, 1999–2004.
- Kuri-Harcuch, W. (1978). Interruption of the adipose conversion of 3T3 cells by biotin deficiency: differentiation without triglyceride accumulation. *Cell* *14*, 53–59.
- Kuri-Harcuch, W., and Green, H. (1978). Adipose Conversion of 3T3 Cells Depends on a Serum Factor. *Proc. Natl. Acad. Sci. U. S. A.* *75*, 6107–6109.
- Kurokawa, K., Itoh, T., Kuwahara, T., Oshima, K., Toh, H., Toyoda, A., Takami, H., Morita, H., Sharma, V.K., Srivastava, T.P., *et al.* (2007). Comparative metagenomics revealed commonly enriched gene sets in human gut microbiomes. *DNA Res. Int. J. Rapid Publ. Rep. Genes Genomes* *14*, 169–181.
- Lambert, D.W., Wood, I.S., Ellis, A., and Shirazi-Beechey, S.P. (2002). Molecular changes in the expression of human colonic nutrient transporters during the transition from normality to malignancy. *Br. J. Cancer* *86*, 1262–1269.
- Laparra, J.M., and Sanz, Y. (2010). Interactions of gut microbiota with functional food components and nutraceuticals. *Pharmacol. Res. Off. J. Ital. Pharmacol. Soc.* *61*, 219–225.
- Lara-Castro, C., Fu, Y., Chung, B.H., and Garvey, W.T. (2007). Adiponectin and the metabolic syndrome: mechanisms mediating risk for metabolic and cardiovascular disease. *Curr. Opin. Lipidol.* *18*, 263–270.
- Lass, A., Zimmermann, R., Oberer, M., and Zechner, R. (2011). Lipolysis – A highly regulated multi-enzyme complex mediates the catabolism of cellular fat stores. *Prog. Lipid Res.* *50*, 14–27.
- Latham, T., Mackay, L., Sproul, D., Karim, M., Culley, J., Harrison, D.J., Hayward, L., Langridge-Smith, P., Gilbert, N., and Ramsahoye, B.H. (2012). Lactate, a product of glycolytic metabolism, inhibits histone deacetylase activity and promotes changes in gene expression. *Nucleic Acids Res.* *40*, 4794–4803.
- Laurencikiene, J., Skurk, T., Kulyté, A., Hedén, P., Aström, G., Sjölin, E., Rydén, M., Hauner, H., and Arner, P. (2011). Regulation of lipolysis in small and large fat cells of the same subject. *J. Clin. Endocrinol. Metab.* *96*, E2045–E2049.
- Laurent, C., Simoneau, C., Marks, L., Braschi, S., Champ, M., Charbonnel, B., and Krempf, M. (1995). Effect of acetate and propionate on fasting hepatic glucose production in humans. *Eur. J. Clin. Nutr.* *49*, 484–491.
- Lebovitz, H.E. (2001). Insulin resistance: definition and consequences. *Exp. Clin. Endocrinol. Amp Diabetes* *109*, S135–S148.
- Lefkowitz, R.J. (2007). Seven transmembrane receptors: something old, something new. *Acta Physiol. Oxf. Engl.* *190*, 9–19.
- Le Poul, E., Loison, C., Struyf, S., Springael, J.-Y., Lannoy, V., Decobecq, M.-E., Brezillon, S., Dupriez, V., Vassart, G., Van Damme, J., *et al.* (2003). Functional characterization of human receptors for

short chain fatty acids and their role in polymorphonuclear cell activation. *J. Biol. Chem.* 278, 25481–25489.

Leto, D., and Saltiel, A.R. (2012). Regulation of glucose transport by insulin: traffic control of GLUT4. *Nat. Rev. Mol. Cell Biol.* 13, 383–396.

Lewis, N.E., Liu, X., Li, Y., Nagarajan, H., Yerganian, G., O'Brien, E., Bordbar, A., Roth, A.M., Rosenbloom, J., Bian, C., *et al.* (2013). Genomic landscapes of Chinese hamster ovary cell lines as revealed by the *Cricetulus griseus* draft genome. *Nat. Biotechnol.* 31, 759–765.

Lim, Y., Wong, N.S.C., Lee, Y.Y., Ku, S.C.Y., Wong, D.C.F., and Yap, M.G.S. (2010). Engineering mammalian cells in bioprocessing – current achievements and future perspectives. *Biotechnol. Appl. Biochem.* 55, 175–189.

Lin, H.V., Frassetto, A., Kowalik Jr, E.J., Nawrocki, A.R., Lu, M.M., Kosinski, J.R., Hubert, J.A., Szeto, D., Yao, X., Forrest, G., *et al.* (2012). Butyrate and Propionate Protect against Diet-Induced Obesity and Regulate Gut Hormones via Free Fatty Acid Receptor 3-Independent Mechanisms. *PLoS ONE* 7, e35240.

Liu, L.-H., Wang, X.-K., Hu, Y.-D., Kang, J.-L., Wang, L.-L., and Li, S. (2004). Effects of a fatty acid synthase inhibitor on adipocyte differentiation of mouse 3T3-L1 cells. *Acta Pharmacol. Sin.* 25, 1052–1057.

Liu, Q., Bengmark, S., and Qu, S. (2010). The role of hepatic fat accumulation in pathogenesis of non-alcoholic fatty liver disease (NAFLD). *Lipids Health Dis.* 9, 42.

Livesey, G. (1990). Energy values of unavailable carbohydrate and diets: an inquiry and analysis. *Am. J. Clin. Nutr.* 51, 617–637.

Louis, P., Duncan, S.H., McCrae, S.I., Millar, J., Jackson, M.S., and Flint, H.J. (2004). Restricted Distribution of the Butyrate Kinase Pathway among Butyrate-Producing Bacteria from the Human Colon. *J. Bacteriol.* 186, 2099–2106.

Macfarlane, G.T., and Gibson, G.R. (1995). Macfarlane, G. T., and G. R. Gibson. Microbiological aspects of the production of short-chain fatty acids in the large bowel. Vol. 87. Cambridge University Press, Cambridge, UK, 1995. In *Physiological and Clinical Aspects of Short-Chain Fatty Acids*, (Cambridge, UK: Cambridge University Press),.

Macfarlane, G.T., and Gibson, G.R. (1997). Carbohydrate Fermentation, Energy Transduction and Gas Metabolism in the Human Large Intestine. In *Gastrointestinal Microbiology*, R.I. Mackie, and B.A. White, eds. (Boston, MA: Springer US), pp. 269–318.

Macfarlane, S., and Macfarlane, G.T. (2003). Regulation of short-chain fatty acid production. *Proc. Nutr. Soc.* 62, 67–72.

Macfarlane, G.T., Cummings, J.H., and Allison, C. (1986). Protein Degradation by Human Intestinal Bacteria. *Microbiology* 132, 1647–1656.

Macia, L., Tan, J., Vieira, A.T., Leach, K., Stanley, D., Luong, S., Maruya, M., Ian McKenzie, C., Hijikata, A., Wong, C., *et al.* (2015). Metabolite-sensing receptors GPR43 and GPR109A facilitate dietary fibre-induced gut homeostasis through regulation of the inflammasome. *Nat. Commun.* 6, 6734.

Macpherson, A.J., and Harris, N.L. (2004). Opinion: Interactions between commensal intestinal bacteria and the immune system. *Nat. Rev. Immunol.* *4*, 478–485.

Magnúsdóttir, S., Ravcheev, D., de Crécy-Lagard, V., and Thiele, I. (2015). Systematic genome assessment of B-vitamin biosynthesis suggests co-operation among gut microbes. *Front. Genet.* *6*.

Marc Rhoads, J., and Wu, G. (2009). Glutamine, arginine, and leucine signaling in the intestine. *Amino Acids* *37*, 111–122.

Marion, M.-J., Hantz, O., and Durantel, D. (2010). The HepaRG cell line: biological properties and relevance as a tool for cell biology, drug metabolism, and virology studies. *Methods Mol. Biol. Clifton NJ* *640*, 261–272.

Maslowski, K.M., Vieira, A.T., Ng, A., Kranich, J., Sierro, F., Yu, D., Schilter, H.C., Rolph, M.S., Mackay, F., Artis, D., *et al.* (2009). Regulation of inflammatory responses by gut microbiota and chemoattractant receptor GPR43. *Nature* *461*, 1282–1286.

Matsuzawa, Y., Funahashi, T., and Nakamura, T. (1999). Molecular mechanism of metabolic syndrome X: contribution of adipocytokines adipocyte-derived bioactive substances. *Ann. N. Y. Acad. Sci.* *892*, 146–154.

Miller, T.L., and Wolin, M.J. (1996). Pathways of acetate, propionate, and butyrate formation by the human fecal microbial flora. *Appl. Environ. Microbiol.* *62*, 1589–1592.

Moustaïd, N., and Sul, H.S. (1991). Regulation of expression of the fatty acid synthase gene in 3T3-L1 cells by differentiation and triiodothyronine. *J. Biol. Chem.* *266*, 18550–18554.

Mulukutla, B.C., Khan, S., Lange, A., and Hu, W.-S. (2010). Glucose metabolism in mammalian cell culture: new insights for tweaking vintage pathways. *Trends Biotechnol.* *28*, 476–484.

Musri, M.M., and Párrizas, M. (2012). Epigenetic regulation of adipogenesis. *Curr. Opin. Clin. Nutr. Metab. Care* *15*, 342–349.

Mycielska, M.E., and Djamgoz, M.B.A. (2004). Citrate transport in the human prostate epithelial PNT2-C2 cell line: electrophysiological analyses. *J. Physiol.* *559*, 821–833.

Nazli, A., Yang, P.-C., Jury, J., Howe, K., Watson, J.L., Söderholm, J.D., Sherman, P.M., Perdue, M.H., and McKay, D.M. (2004). Epithelia Under Metabolic Stress Perceive Commensal Bacteria as a Threat. *Am. J. Pathol.* *164*, 947–957.

Neves, A.L., Chilloux, J., Sarafian, M.H., Rahim, M.B.A., Boulangé, C.L., and Dumas, M.-E. (2015). The microbiome and its pharmacological targets: therapeutic avenues in cardiometabolic diseases. *Curr. Opin. Pharmacol.* *25*, 36–44.

Newgard, C.B. (2012). Interplay between Lipids and Branched-Chain Amino Acids in Development of Insulin Resistance. *Cell Metab.* *15*, 606–614.

Newgard, C.B., An, J., Bain, J.R., Muehlbauer, M.J., Stevens, R.D., Lien, L.F., Haqq, A.M., Shah, S.H., Arlotto, M., Slentz, C.A., *et al.* (2009). A Branched-Chain Amino Acid-Related Metabolic Signature that Differentiates Obese and Lean Humans and Contributes to Insulin Resistance. *Cell Metab.* *9*, 311–326.

Nicholson, J.K., Buckingham, M.J., and Sadler, P.J. (1983). High resolution ^1H n.m.r. studies of vertebrate blood and plasma. *Biochem. J.* *211*, 605–615.

Nicholson, J.K., Lindon, J.C., and Holmes, E. (1999). “Metabonomics”: understanding the metabolic responses of living systems to pathophysiological stimuli via multivariate statistical analysis of biological NMR spectroscopic data. *Xenobiotica Fate Foreign Compd. Biol. Syst.* *29*, 1181–1189.

Nicholson, J.K., Connelly, J., Lindon, J.C., and Holmes, E. (2002). Metabonomics: a platform for studying drug toxicity and gene function. *Nat. Rev. Drug Discov.* *1*, 153–161.

Nicholson, J.K., Holmes, E., and Wilson, I.D. (2005). Opinion: Gut microorganisms, mammalian metabolism and personalized health care. *Nat. Rev. Microbiol.* *3*, 431–438.

Nicholson, J.K., Holmes, E., and Lindon, J.C. (2007). Metabonomics and Metabolomics Techniques and Their Applications in Mammalian Systems. In *The Handbook of Metabonomics and Metabolomics*, (Elsevier), pp. 1–33.

Niederman, R., Buyle-Bodin, Y., Lu, B.Y., Robinson, P., and Naleway, C. (1997). Short-chain carboxylic acid concentration in human gingival crevicular fluid. *J. Dent. Res.* *76*, 575–579.

Nijhout, H.F., Reed, M.C., Lam, S.-L., Shane, B., Gregory, J.F., 3rd, and Ulrich, C.M. (2006). In silico experimentation with a model of hepatic mitochondrial folate metabolism. *Theor. Biol. Med. Model.* *3*, 40.

Nilsson, N.E., Kotarsky, K., Owman, C., and Olde, B. (2003). Identification of a free fatty acid receptor, FFA2R, expressed on leukocytes and activated by short-chain fatty acids. *Biochem. Biophys. Res. Commun.* *303*, 1047–1052.

Nishina, P.M., and Freedland, R.A. (1990). Effects of propionate on lipid biosynthesis in isolated rat hepatocytes. *J. Nutr.* *120*, 668–673.

Northwestern University (2011). Sodium.

van Nuenen, M.H.M.C., Venema, K., van der Woude, J.C.J., and Kuipers, E.J. (2004). The metabolic activity of fecal microbiota from healthy individuals and patients with inflammatory bowel disease. *Dig. Dis. Sci.* *49*, 485–491.

Ohashi, Y., Igarashi, T., Kumazawa, F., and Fujisawa, T. (2007). Analysis of Acetogenic Bacteria in Human Feces with Formyltetrahydrofolate Synthetase Sequences. *Biosci. Microflora* *26*, 37–40.

Ohira, H., Fujioka, Y., Katagiri, C., Mamoto, R., Aoyama-Ishikawa, M., Amako, K., Izumi, Y., Nishiumi, S., Yoshida, M., Usami, M., *et al.* (2013). Butyrate attenuates inflammation and lipolysis generated by the interaction of adipocytes and macrophages. *J. Atheroscler. Thromb.* *20*, 425–442.

Oldham, W.M., and Hamm, H.E. (2007). How do receptors activate G proteins? *Adv. Protein Chem.* *74*, 67–93.

Palczewski, K., Kumasaka, T., Hori, T., Behnke, C.A., Motoshima, H., Fox, B.A., Le Trong, I., Teller, D.C., Okada, T., Stenkamp, R.E., *et al.* (2000). Crystal structure of rhodopsin: A G protein-coupled receptor. *Science* *289*, 739–745.

- Parent, R., Marion, M.-J., Furio, L., Trépo, C., and Petit, M.-A. (2004). Origin and characterization of a human bipotent liver progenitor cell line. *Gastroenterology* *126*, 1147–1156.
- Pawlak, D.B., Kushner, J.A., and Ludwig, D.S. (2004). Effects of dietary glycaemic index on adiposity, glucose homeostasis, and plasma lipids in animals. *Lancet* *364*, 778–785.
- Pearce, J. (1983). Fatty acid synthesis in liver and adipose tissue. *Proc. Nutr. Soc.* *42*, 263–271.
- Pedersen, B.K., and Febbraio, M.A. (2008). Muscle as an endocrine organ: focus on muscle-derived interleukin-6. *Physiol. Rev.* *88*, 1379–1406.
- Pi-Sunyer, F.X., Laferrère, B., Aronne, L.J., and Bray, G.A. (1999). Therapeutic controversy: Obesity—a modern-day epidemic. *J. Clin. Endocrinol. Metab.* *84*, 3–12.
- Pjetri, E., Schmidt, U., Kas, M.J., and Campbell, I.C. (2012). Epigenetics and eating disorders. *Curr. Opin. Clin. Nutr. Metab. Care* *15*, 330–335.
- Plaisance, E.P., Lukasova, M., Offermanns, S., Zhang, Y., Cao, G., and Judd, R.L. (2008). Niacin stimulates adiponectin secretion through the GPR109A receptor. *AJP Endocrinol. Metab.* *296*, E549–E558.
- Pohl, H.R., Wheeler, J.S., and Murray, H.E. (2013). Sodium and Potassium in Health and Disease. In *Interrelations between Essential Metal Ions and Human Diseases*, A. Sigel, H. Sigel, and R.K.O. Sigel, eds. (Dordrecht: Springer Netherlands), pp. 29–47.
- Poulos, S.P., Dodson, M.V., and Hausman, G.J. (2010). Cell line models for differentiation: preadipocytes and adipocytes. *Exp. Biol. Med.* Maywood NJ *235*, 1185–1193.
- Pouteau, E., Nguyen, P., Ballèvre, O., and Krempf, M. (2003). Production rates and metabolism of short-chain fatty acids in the colon and whole body using stable isotopes. *Proc. Nutr. Soc.* *62*, 87–93.
- Putman, C.T., Jones, N.L., Lands, L.C., Bragg, T.M., Hollidge-Horvat, M.G., and Heigenhauser, G.J. (1995). Skeletal muscle pyruvate dehydrogenase activity during maximal exercise in humans. *Am. J. Physiol.* *269*, E458–E468.
- Ramsey Bronk (1999). *Human metabolism* (addison-wesley longman, Harlow, England, 1999). (addison-wesley longman).
- Rawlings, N.D., and Barrett, A.J. (1994). Families of serine peptidases. *Methods Enzymol.* *244*, 19–61.
- Reeds, P.J. (2000). Dispensable and indispensable amino acids for humans. *J. Nutr.* *130*, 1835S – 40S.
- Reilly, K.J., and Rombeau, J.L. (1993). Metabolism and potential clinical applications of short-chain fatty acids. *Clin. Nutr.* *12*, S97–S105.
- Rennie, M.J., Bohé, J., Smith, K., Wackerhage, H., and Greenhaff, P. (2006). Branched-chain amino acids as fuels and anabolic signals in human muscle. *J. Nutr.* *136*, 264S – 8S.

Reynisdottir, S., Langin, D., Carlström, K., Holm, C., Rössner, S., and Arner, P. (1995). Effects of weight reduction on the regulation of lipolysis in adipocytes of women with upper-body obesity. *Clin. Sci. Lond. Engl.* 1979 *89*, 421–429.

Roberfroid, M., Gibson, G.R., and Delzenne, N. (1993). The biochemistry of oligofructose, a nondigestible fiber: an approach to calculate its caloric value. *Nutr. Rev.* *51*, 137–146.

Rodríguez, J.M., Murphy, K., Stanton, C., Ross, R.P., Kober, O.I., Juge, N., Avershina, E., Rudi, K., Narbad, A., Jenmalm, M.C., *et al.* (2015). The composition of the gut microbiota throughout life, with an emphasis on early life. *Microb. Ecol. Health Dis.* *26*.

Roediger, W.E. (1980a). Role of anaerobic bacteria in the metabolic welfare of the colonic mucosa in man. *Gut* *21*, 793–798.

Roediger, W.E. (1980b). Role of anaerobic bacteria in the metabolic welfare of the colonic mucosa in man. *Gut* *21*, 793–798.

Roediger, W.E. (1982). Utilization of nutrients by isolated epithelial cells of the rat colon. *Gastroenterology* *83*, 424–429.

Roediger, W.E. (1990). The starved colon--diminished mucosal nutrition, diminished absorption, and colitis. *Dis. Colon Rectum* *33*, 858–862.

Rosen, E.D., and MacDougald, O.A. (2006). Adipocyte differentiation from the inside out. *Nat. Rev. Mol. Cell Biol.* *7*, 885–896.

Roy, C.C., Kien, C.L., Bouthillier, L., and Levy, E. (2006). Short-chain fatty acids: ready for prime time? *Nutr. Clin. Pract. Off. Publ. Am. Soc. Parenter. Enter. Nutr.* *21*, 351–366.

Rubin, C.S., Hirsch, A., Fung, C., and Rosen, O.M. (1978). Development of hormone receptors and hormonal responsiveness in vitro. Insulin receptors and insulin sensitivity in the preadipocyte and adipocyte forms of 3T3-L1 cells. *J. Biol. Chem.* *253*, 7570–7578.

Rucker, R.B. (2007). *Handbook of vitamins* (Boca Raton: Taylor & Francis).

Russell, T.R., and Ho, R. (1976). Conversion of 3T3 fibroblasts into adipose cells: triggering of differentiation by prostaglandin F₂α and 1-methyl-3-isobutyl xanthine. *Proc. Natl. Acad. Sci. U. S. A.* *73*, 4516–4520.

Salminen, S., Bouley, C., Boutron-Ruault, M.C., Cummings, J.H., Franck, A., Gibson, G.R., Isolauri, E., Moreau, M.C., Roberfroid, M., and Rowland, I. (1998). Functional food science and gastrointestinal physiology and function. *Br. J. Nutr.* *80 Suppl 1*, S147–S171.

Saltiel, A.R., and Kahn, C.R. (2001). Insulin signalling and the regulation of glucose and lipid metabolism. *Nature* *414*, 799–806.

Saotome, K., Morita, H., and Umeda, M. (1989). Cytotoxicity test with simplified crystal violet staining method using microtitre plates and its application to injection drugs. *Toxicol. In Vitro* *3*, 317–321.

- Sartor, R.B. (2008). Microbial Influences in Inflammatory Bowel Diseases. *Gastroenterology* 134, 577–594.
- Schaub, A., Fütterer, A., and Pfeffer, K. (2001). PUMA-G, an IFN-gamma-inducible gene in macrophages is a novel member of the seven transmembrane spanning receptor superfamily. *Eur. J. Immunol.* 31, 3714–3725.
- Scheppach, W., Bartram, P., Richter, A., Richter, F., Liepold, H., Dusel, G., Hofstetter, G., Rütthlein, J., and Kasper, H. (1992). Effect of short-chain fatty acids on the human colonic mucosa in vitro. *JPEN J. Parenter. Enteral Nutr.* 16, 43–48.
- Schoonjans, K., Staels, B., and Auwerx, J. (1996). The peroxisome proliferator activated receptors (PPARs) and their effects on lipid metabolism and adipocyte differentiation. *Biochim. Biophys. Acta BBA - Lipids Lipid Metab.* 1302, 93–109.
- Seidell, J.C., and Flegal, K.M. (1997). Assessing obesity: classification and epidemiology. *Br. Med. Bull.* 53, 238–252.
- Sekirov, I., Russell, S.L., Antunes, L.C.M., and Finlay, B.B. (2010). Gut Microbiota in Health and Disease. *Physiol. Rev.* 90, 859–904.
- Sharma, M., Garber, A., and Farmer, J. (2008). Role of Insulin Signaling in Maintaining Energy Homeostasis. *Endocr. Pract.* 14, 373–380.
- Shimomura, Y., Murakami, T., Nakai, N., Nagasaki, M., and Harris, R.A. (2004). Exercise promotes BCAA catabolism: effects of BCAA supplementation on skeletal muscle during exercise. *J. Nutr.* 134, 1583S – 1587S.
- Shintu, L., Baudoin, R., Navratil, V., Prot, J.-M., Pontoizeau, C., Defernez, M., Blaise, B.J., Domange, C., Péry, A.R., Toulhoat, P., *et al.* (2012). Metabolomics-on-a-chip and predictive systems toxicology in microfluidic bioartificial organs. *Anal. Chem.* 84, 1840–1848.
- Siavoshian, S., Blottière, H.M., Le Foll, E., Kaeffer, B., Cherbut, C., and Galniche, J.P. (1997). Comparison of the effect of different short chain fatty acids on the growth and differentiation of human colonic carcinoma cell lines in vitro. *Cell Biol. Int.* 21, 281–287.
- Siavoshian, S., Segain, J.P., Kornprobst, M., Bonnet, C., Cherbut, C., Galniche, J.P., and Blottière, H.M. (2000). Butyrate and trichostatin A effects on the proliferation/differentiation of human intestinal epithelial cells: induction of cyclin D3 and p21 expression. *Gut* 46, 507–514.
- Sigma-Aldrich (2014). Free Glycerol Determination Kit.
- Siler, S.Q., Neese, R.A., and Hellerstein, M.K. (1999). De novo lipogenesis, lipid kinetics, and whole-body lipid balances in humans after acute alcohol consumption. *Am. J. Clin. Nutr.* 70, 928–936.
- Singh, N., Gurav, A., Sivaprakasam, S., Brady, E., Padia, R., Shi, H., Thangaraju, M., Prasad, P.D., Manicassamy, S., Munn, D.H., *et al.* (2014a). Activation of Gpr109a, Receptor for Niacin and the Commensal Metabolite Butyrate, Suppresses Colonic Inflammation and Carcinogenesis. *Immunity* 40, 128–139.

Singh, N., Gurav, A., Sivaprakasam, S., Brady, E., Padia, R., Shi, H., Thangaraju, M., Prasad, P.D., Manicassamy, S., Munn, D.H., *et al.* (2014b). Activation of Gpr109a, Receptor for Niacin and the Commensal Metabolite Butyrate, Suppresses Colonic Inflammation and Carcinogenesis. *Immunity* 40, 128–139.

Skurk, T., Alberti-Huber, C., Herder, C., and Hauner, H. (2007). Relationship between adipocyte size and adipokine expression and secretion. *J. Clin. Endocrinol. Metab.* 92, 1023–1033.

Sleeth, M.L., Thompson, E.L., Ford, H.E., Zac-Varghese, S.E.K., and Frost, G. (2010). Free fatty acid receptor 2 and nutrient sensing: a proposed role for fibre, fermentable carbohydrates and short-chain fatty acids in appetite regulation. *Nutr. Res. Rev.* 23, 135–145.

Smolinska, A., Blanchet, L., Buydens, L.M.C., and Wijmenga, S.S. (2012). NMR and pattern recognition methods in metabolomics: from data acquisition to biomarker discovery: a review. *Anal. Chim. Acta* 750, 82–97.

Snel, M., Jonker, J.T., Schoones, J., Lamb, H., de Roos, A., Pijl, H., Smit, J.W.A., Meinders, A.E., and Jazet, I.M. (2012). Ectopic Fat and Insulin Resistance: Pathophysiology and Effect of Diet and Lifestyle Interventions. *Int. J. Endocrinol.* 2012, 1–18.

So, P.-W., Yu, W.-S., Kuo, Y.-T., Wasserfall, C., Goldstone, A.P., Bell, J.D., and Frost, G. (2007). Impact of Resistant Starch on Body Fat Patterning and Central Appetite Regulation. *PLoS ONE* 2, e1309.

Soga, T., Kamohara, M., Takasaki, J., Matsumoto, S., Saito, T., Ohishi, T., Hiyama, H., Matsuo, A., Matsushime, H., and Furuichi, K. (2003). Molecular identification of nicotinic acid receptor. *Biochem. Biophys. Res. Commun.* 303, 364–369.

Stephens, J.M. (2012). The Fat Controller: Adipocyte Development. *PLoS Biol.* 10, e1001436.

Stevens, C.E., and Hume, I.D. (1998). Contributions of microbes in vertebrate gastrointestinal tract to production and conservation of nutrients. *Physiol. Rev.* 78, 393–427.

Stoddart, L.A., Smith, N.J., Jenkins, L., Brown, A.J., and Milligan, G. (2008). Conserved Polar Residues in Transmembrane Domains V, VI, and VII of Free Fatty Acid Receptor 2 and Free Fatty Acid Receptor 3 Are Required for the Binding and Function of Short Chain Fatty Acids. *J. Biol. Chem.* 283, 32913–32924.

Stubblefield, E., and Mueller, G.C. (1960). Effects of Sodium Chloride Concentration on Growth, Biochemical Composition, and Metabolism of HeLa Cells. *Cancer Res.* 20, 1646–1655.

Student, A.K., Hsu, R.Y., and Lane, M.D. (1980). Induction of fatty acid synthetase synthesis in differentiating 3T3-L1 preadipocytes. *J. Biol. Chem.* 255, 4745–4750.

Sul, H.S., Latasa, M.J., Moon, Y., and Kim, K.H. (2000). Regulation of the fatty acid synthase promoter by insulin. *J. Nutr.* 130, 315S – 320S.

Sun, Y., Luo, J., Zhu, J., Shi, H., Li, J., Qiu, S., Wang, P., and Loo, J.J. (2015). Effect of short-chain fatty acids on triacylglycerol accumulation, lipid droplet formation and lipogenic gene expression in goat mammary epithelial cells. *Anim. Sci. J. Nihon Chikusan Gakkaiho.*

- Suzuki, T., Yoshida, S., and Hara, H. (2008). Physiological concentrations of short-chain fatty acids immediately suppress colonic epithelial permeability. *Br. J. Nutr.* *100*, 297–305.
- Taggart, A.K.P., Kero, J., Gan, X., Cai, T.-Q., Cheng, K., Ippolito, M., Ren, N., Kaplan, R., Wu, K., Wu, T.-J., *et al.* (2005). (D)-Hydroxybutyrate Inhibits Adipocyte Lipolysis via the Nicotinic Acid Receptor PUMA-G. *J. Biol. Chem.* *280*, 26649–26652.
- Takebe, K., Nio, J., Morimatsu, M., Karaki, S.-I., Kuwahara, A., Kato, I., and Iwanaga, T. (2005). Histochemical demonstration of a Na (+)-coupled transporter for short-chain fatty acids (slc5a8) in the intestine and kidney of the mouse. *Biomed. Res. Tokyo Jpn.* *26*, 213–221.
- Tang, Y., Chen, Y., Jiang, H., Robbins, G.T., and Nie, D. (2011). G-protein-coupled receptor for short-chain fatty acids suppresses colon cancer. *Int. J. Cancer* *128*, 847–856.
- Tazoe, H., Otomo, Y., Kaji, I., Tanaka, R., Karaki, S.-I., and Kuwahara, A. (2008). Roles of short-chain fatty acids receptors, GPR41 and GPR43 on colonic functions. *J. Physiol. Pharmacol. Off. J. Pol. Physiol. Soc.* *59 Suppl 2*, 251–262.
- Tedeschi, P.M., Markert, E.K., Gounder, M., Lin, H., Dvorzhinski, D., Dolfi, S.C., Chan, L.L.-Y., Qiu, J., DiPaola, R.S., Hirshfield, K.M., *et al.* (2013). Contribution of serine, folate and glycine metabolism to the ATP, NADPH and purine requirements of cancer cells. *Cell Death Dis.* *4*, e877.
- Teramae, H., Yoshikawa, T., Inoue, R., Ushida, K., Takebe, K., Nio-Kobayashi, J., and Iwanaga, T. (2010). The cellular expression of SMCT2 and its comparison with other transporters for monocarboxylates in the mouse digestive tract. *Biomed. Res. Tokyo Jpn.* *31*, 239–249.
- Thangaraju, M., Cresci, G.A., Liu, K., Ananth, S., Gnanaprakasam, J.P., Browning, D.D., Mellinger, J.D., Smith, S.B., Digby, G.J., Lambert, N.A., *et al.* (2009a). GPR109A is a G-protein-coupled receptor for the bacterial fermentation product butyrate and functions as a tumor suppressor in colon. *Cancer Res.* *69*, 2826–2832.
- Thangaraju, M., Cresci, G.A., Liu, K., Ananth, S., Gnanaprakasam, J.P., Browning, D.D., Mellinger, J.D., Smith, S.B., Digby, G.J., Lambert, N.A., *et al.* (2009b). GPR109A Is a G-protein-Coupled Receptor for the Bacterial Fermentation Product Butyrate and Functions as a Tumor Suppressor in Colon. *Cancer Res.* *69*, 2826–2832.
- Thibault, R., De Coppet, P., Daly, K., Bourreille, A., Cuff, M., Bonnet, C., Mosnier, J.-F., Galmiche, J.-P., Shirazi-Beechey, S., and Segain, J.-P. (2007). Down-regulation of the monocarboxylate transporter 1 is involved in butyrate deficiency during intestinal inflammation. *Gastroenterology* *133*, 1916–1927.
- Thompson, G.N., Walter, J.H., Bresson, J.L., Ford, G.C., Lyonnet, S.L., Chalmers, R.A., Saudubray, J.M., Leonard, J.V., and Halliday, D. (1990). Sources of propionate in inborn errors of propionate metabolism. *Metabolism.* *39*, 1133–1137.
- Tilg, H., and Kaser, A. (2011). Gut microbiome, obesity, and metabolic dysfunction. *J. Clin. Invest.* *121*, 2126–2132.
- Todesco, T., Rao, A.V., Bosello, O., and Jenkins, D.J. (1991). Propionate lowers blood glucose and alters lipid metabolism in healthy subjects. *Am. J. Clin. Nutr.* *54*, 860–865.

- Tolhurst, G., Heffron, H., Lam, Y.S., Parker, H.E., Habib, A.M., Diakogiannaki, E., Cameron, J., Grosse, J., Reimann, F., and Gribble, F.M. (2012). Short-Chain Fatty Acids Stimulate Glucagon-Like Peptide-1 Secretion via the G-Protein-Coupled Receptor FFAR2. *Diabetes* *61*, 364–371.
- Topping, D.L., and Clifton, P.M. (2001). Short-chain fatty acids and human colonic function: roles of resistant starch and nonstarch polysaccharides. *Physiol. Rev.* *81*, 1031–1064.
- Trauner, D.A., Nyhan, W.L., and Sweetman, L. (1975). Short-chain organic acidemia and Reye's syndrome. *Neurology* *25*, 296–298.
- Trygg, J., and Wold, svante (2002). Orthogonal projections to latent structures (O-PLS). *J. Chemom.* *119–128*.
- Trygg, J., Holmes, E., and Lundstedt, T. (2007). Chemometrics in metabonomics. *J. Proteome Res.* *6*, 469–479.
- Trzaskowski, B., Latek, D., Yuan, S., Ghoshdastider, U., Debinski, A., and Filipek, S. (2012). Action of Molecular Switches in GPCRs - Theoretical and Experimental Studies. *Curr. Med. Chem.* *19*, 1090–1109.
- Tunaru, S., Kero, J., Schaub, A., Wufka, C., Blaukat, A., Pfeffer, K., and Offermanns, S. (2003). PUMA-G and HM74 are receptors for nicotinic acid and mediate its anti-lipolytic effect. *Nat. Med.* *9*, 352–355.
- Turnbaugh, P.J., Ley, R.E., Mahowald, M.A., Magrini, V., Mardis, E.R., and Gordon, J.I. (2006). An obesity-associated gut microbiome with increased capacity for energy harvest. *Nature* *444*, 1027–1031.
- Tyagi, S., Venugopalakrishnan, J., Ramaswamy, K., and Dudeja, P.K. (2002). Mechanism of n-butyrate uptake in the human proximal colonic basolateral membranes. *Am. J. Physiol. Gastrointest. Liver Physiol.* *282*, G676–G682.
- Ullah, M.S., Davies, A.J., and Halestrap, A.P. (2006). The plasma membrane lactate transporter MCT4, but not MCT1, is up-regulated by hypoxia through a HIF-1alpha-dependent mechanism. *J. Biol. Chem.* *281*, 9030–9037.
- Unger, R.H., Clark, G.O., Scherer, P.E., and Orci, L. (2010). Lipid homeostasis, lipotoxicity and the metabolic syndrome. *Biochim. Biophys. Acta* *1801*, 209–214.
- Vazquez, A., Liu, J., Zhou, Y., and Oltvai, Z.N. (2010). Catabolic efficiency of aerobic glycolysis: The Warburg effect revisited. *BMC Syst. Biol.* *4*, 58.
- Vecchia, M.G., Filho, M.C., Fellipe, C.R.C., Curi, R., and Newsholme, E.A. (1997). Acetate and propionate potentiate the antiproliferative effect of butyrate on RBL-2H3 growth. *Gen. Pharmacol. Vasc. Syst.* *29*, 725–728.
- Venter, C.S., Vorster, H.H., and Cummings, J.H. (1990). Effects of dietary propionate on carbohydrate and lipid metabolism in healthy volunteers. *Am. J. Gastroenterol.* *85*, 549–553.
- Vidyasagar, S. (2005). Role of short-chain fatty acids in colonic HCO₃ secretion. *AJP Gastrointest. Liver Physiol.* *288*, G1217–G1226.

- Vinolo, M.A.R., Rodrigues, H.G., Nachbar, R.T., and Curi, R. (2011). Regulation of inflammation by short chain fatty acids. *Nutrients* 3, 858–876.
- Walker, A.W., Duncan, S.H., McWilliam Leitch, E.C., Child, M.W., and Flint, H.J. (2005). pH and peptide supply can radically alter bacterial populations and short-chain fatty acid ratios within microbial communities from the human colon. *Appl. Environ. Microbiol.* 71, 3692–3700.
- Wang, J., Chen, L., Li, P., Li, X., Zhou, H., Wang, F., Li, D., Yin, Y., and Wu, G. (2008). Gene expression is altered in piglet small intestine by weaning and dietary glutamine supplementation. *J. Nutr.* 138, 1025–1032.
- Warburg, O. (1956). On the origin of cancer cells. *Science* 123, 309–314.
- Wettschureck, N., and Offermanns, S. (2005). Mammalian G proteins and their cell type specific functions. *Physiol. Rev.* 85, 1159–1204.
- Whitehead, R.H., Young, G.P., and Bhathal, P.S. (1986). Effects of short chain fatty acids on a new human colon carcinoma cell line (LIM1215). *Gut* 27, 1457–1463.
- WHO (2015). Obesity and overweight.
- Wilcox, P.E. (1970). Chymotrypsinogens—chymotrypsins. In *Methods in Enzymology*, (Elsevier), pp. 64–108.
- Wildman, R.P., Janssen, I., Khan, U.I., Thurston, R., Barinas-Mitchell, E., El Khoudary, S.R., Everson-Rose, S.A., Kazlauskaitė, R., Matthews, K.A., and Sutton-Tyrrell, K. (2011). Subcutaneous adipose tissue in relation to subclinical atherosclerosis and cardiometabolic risk factors in midlife women. *Am. J. Clin. Nutr.* 93, 719–726.
- Williams, E.A., Coxhead, J.M., and Mathers, J.C. (2003). Anti-cancer effects of butyrate: use of micro-array technology to investigate mechanisms. *Proc. Nutr. Soc.* 62, 107–115.
- Wise, A., Foord, S.M., Fraser, N.J., Barnes, A.A., Elshourbagy, N., Eilert, M., Ignar, D.M., Murdock, P.R., Steplewski, K., Green, A., *et al.* (2003). Molecular identification of high and low affinity receptors for nicotinic acid. *J. Biol. Chem.* 278, 9869–9874.
- Wishart, D.S., Tzur, D., Knox, C., Eisner, R., Guo, A.C., Young, N., Cheng, D., Jewell, K., Arndt, D., Sawhney, S., *et al.* (2007). HMDB: the Human Metabolome Database. *Nucleic Acids Res.* 35, D521–D526.
- Wolever, T.M., Spadafora, P., and Eshuis, H. (1991). Interaction between colonic acetate and propionate in humans. *Am. J. Clin. Nutr.* 53, 681–687.
- Wright, R.S., Anderson, J.W., and Bridges, S.R. (1990). Propionate inhibits hepatocyte lipid synthesis. *Proc. Soc. Exp. Biol. Med. Soc. Exp. Biol. Med. N. Y. N* 195, 26–29.
- Wu, G. (2009). Amino acids: metabolism, functions, and nutrition. *Amino Acids* 37, 1–17.
- Wu, G., Fang, Y.-Z., Yang, S., Lupton, J.R., and Turner, N.D. (2004). Glutathione metabolism and its implications for health. *J. Nutr.* 134, 489–492.

Xia, J., and Wishart, D.S. (2010). MSEA: a web-based tool to identify biologically meaningful patterns in quantitative metabolomic data. *Nucleic Acids Res.* 38, W71–W77.

Xiong, Y., Miyamoto, N., Shibata, K., Valasek, M.A., Motoike, T., Kedzierski, R.M., and Yanagisawa, M. (2004). Short-chain fatty acids stimulate leptin production in adipocytes through the G protein-coupled receptor GPR41. *Proc. Natl. Acad. Sci. U. S. A.* 101, 1045–1050.

Xu, S., and Xue, Y. (2015). Pediatric obesity: Causes, symptoms, prevention and treatment (Review). *Exp. Ther. Med.*

Xu, J., Mahowald, M.A., Ley, R.E., Lozupone, C.A., Hamady, M., Martens, E.C., Henrissat, B., Coutinho, P.M., Minx, P., Latreille, P., *et al.* (2007). Evolution of Symbiotic Bacteria in the Distal Human Intestine. *PLoS Biol.* 5, e156.

Xu, X., Nagarajan, H., Lewis, N.E., Pan, S., Cai, Z., Liu, X., Chen, W., Xie, M., Wang, W., Hammond, S., *et al.* (2011). The genomic sequence of the Chinese hamster ovary (CHO)-K1 cell line. *Nat. Biotechnol.* 29, 735–741.

Yamauchi, T., Kamon, J., Waki, H., Imai, Y., Shimosawa, N., Hioki, K., Uchida, S., Ito, Y., Takakuwa, K., Matsui, J., *et al.* (2003). Globular adiponectin protected ob/ob mice from diabetes and ApoE-deficient mice from atherosclerosis. *J. Biol. Chem.* 278, 2461–2468.

Zaibi, M.S., Stocker, C.J., O’Dowd, J., Davies, A., Bellahcene, M., Cawthorne, M.A., Brown, A.J.H., Smith, D.M., and Arch, J.R.S. (2010). Roles of GPR41 and GPR43 in leptin secretory responses of murine adipocytes to short chain fatty acids. *FEBS Lett.* 584, 2381–2386.

Zhang, Y., Proenca, R., Maffei, M., Barone, M., Leopold, L., and Friedman, J.M. (1994). Positional cloning of the mouse obese gene and its human homologue. *Nature* 372, 425–432.

Multi- and megavariable data analysis (Umeå: Umetrics) (2006).

APPENDIX:

Table S.1: List of *p value* obtained from pair-wise comparison between propionate-treated and control group at 24-, 48-, and 72-hr time points using non parametric Wilcoxon-Mann-Whitney test.

Metabolites	Chemical shift (¹ H ppm)	p-value		
		24-hr	48-hr	72-hr
Leucine	0.93 (d), 0.94 (d), 1.71 (m)	0.2438	0.3021	0.5857
Isoleucine	0.94 (t), 1.02 (t)	0.1707	0.1156	0.2622
Valine	0.98 (d), 1.04 (d), 3.62 (d)	0.6123	0.2468	0.6918
Propionate	1.06 (t), 2.183 (q)	0.0033	0.0022	0.0051
α-keto-β-methylvalerate	1.10 (d)	0.0671	0.0620	0.0529
Threonine	1.32 (d), 3.6 (d), 4.25 (m)	0.8549	0.7368	0.6824
Lactate	1.32 (d), 4.11 (q)	0.0156	0.8914	0.5160
Alanine	1.46 (d)	0.0474	0.0010	0.0910
Acetate	1.92 (s)	0.0063	0.0182	0.0022
Pyruvate	2.37 (s)	0.0610	0.0581	0.0993
α-D-Glucose	5.24 (d)	0.0021	0.0877	0.1571
Tyrosine	6.89 (d), 7.18 (d)	0.4721	0.4484	0.7406
Phenylalanine	7.31 (m), 7.36 (m), 7.4 (m)	0.1015	0.1194	0.0650
Formate	8.45 (s)	0.2172	0.2595	0.8806

Table S.2: List of *p* value obtained from pair-wise comparison between butyrate-treated and control group at 24-, 48-, and 72-hr time points using non parametric Wilcoxon-Mann-Whitney test.

Metabolites	Chemical shift (¹ H ppm)	p-value		
		24-hr	48-hr	72-hr
Butyrate	0.88 (s), 1.55 (m), 2.14 (m)	0.0083	0.0046	0.0031
Leucine	0.93 (d), 0.94 (d), 1.71 (m)	0.0962	0.3895	0.4931
Isoleucine	0.94 (t), 1.02 (t)	0.1161	0.3431	0.7337
Valine	0.98 (d), 1.04 (d), 3.62 (d)	0.9133	0.4909	0.1893
α-keto-β-methylvalerate	1.10 (d)	0.0248	0.1100	0.1740
Lactate	1.32 (d), 4.11 (q)	0.1052	0.0920	0.6074
Alanine	1.46 (d)	0.0206	0.0539	0.0131
Glutamine	2.15 (m), 2.44 (m), 3.77 (t)	0.6560	0.2029	0.0106
Glutamate	2.04 (m), 2.34 (m)	0.3191	0.2084	0.0292
Pyruvate	2.37 (s)	0.9040	0.2318	0.0651
α-D-Glucose	5.24 (d)	0.0055	0.5715	0.0281
Tyrosine	6.89 (d), 7.18 (d)	0.0088	0.6052	0.0588
Phenylalanine	7.31 (m), 7.36 (m), 7.4 (m)	0.2040	0.3651	0.0205
Formate	8.45 (s)	0.0574	0.1215	0.5125

Un-normalised Oil Red-O data.

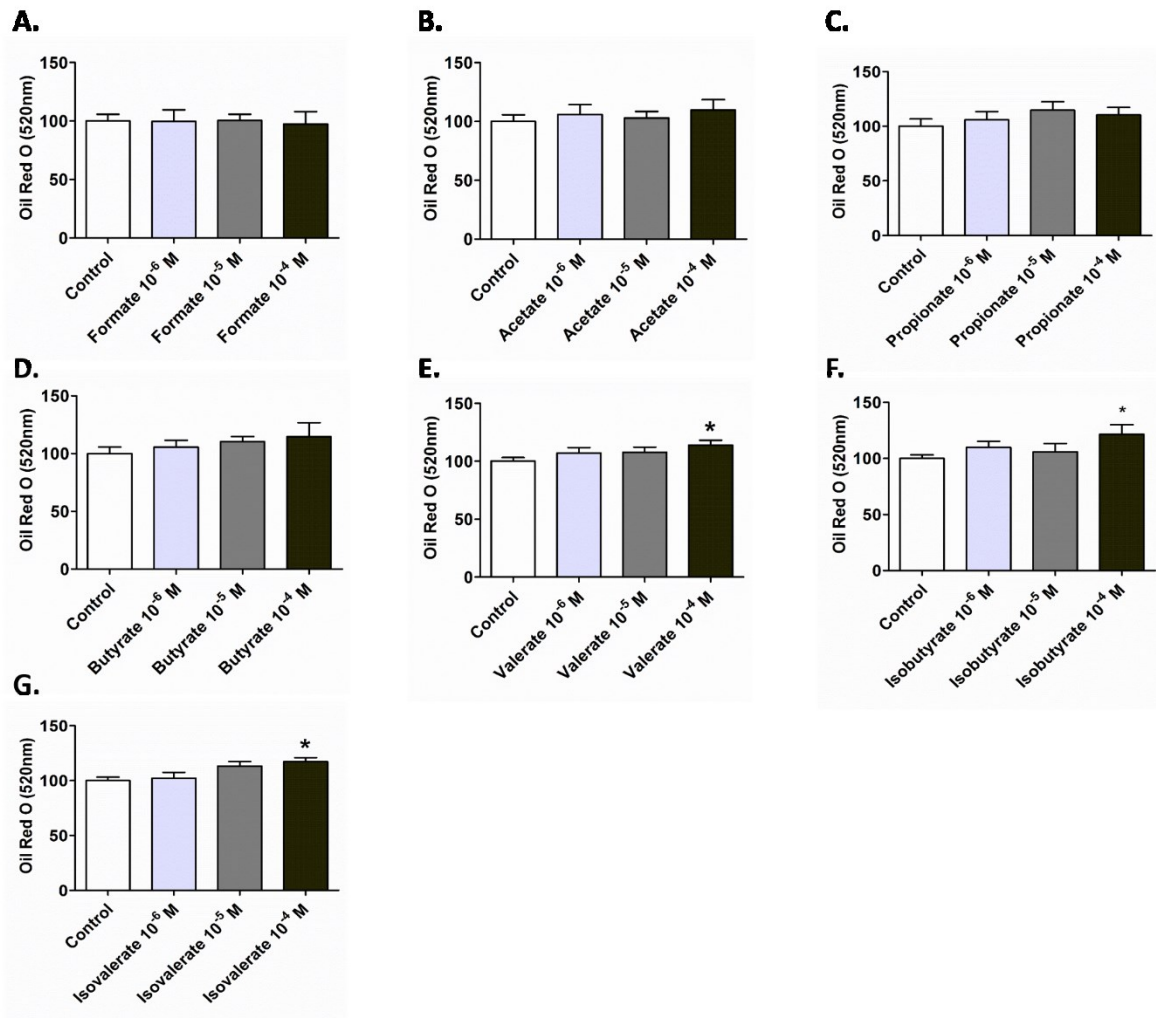


Figure S.1: Valerate, isobutyrate, and isovalerate at 100 μ M dose increase lipogenesis in 3T3-L1 cells. After 10 days incubation, cells were fixed and stained with Oil Red-O and O.D.520 nm was measured. Results are expressed as mean \pm SEM and a Mann-Whitney two-tailed test was performed; * $p < 0.05$, ** $p < 0.01$, *** $p < 0.001$.

Expression of the GPCRs and markers for adipogenesis genes during 3T3-L1 differentiation.

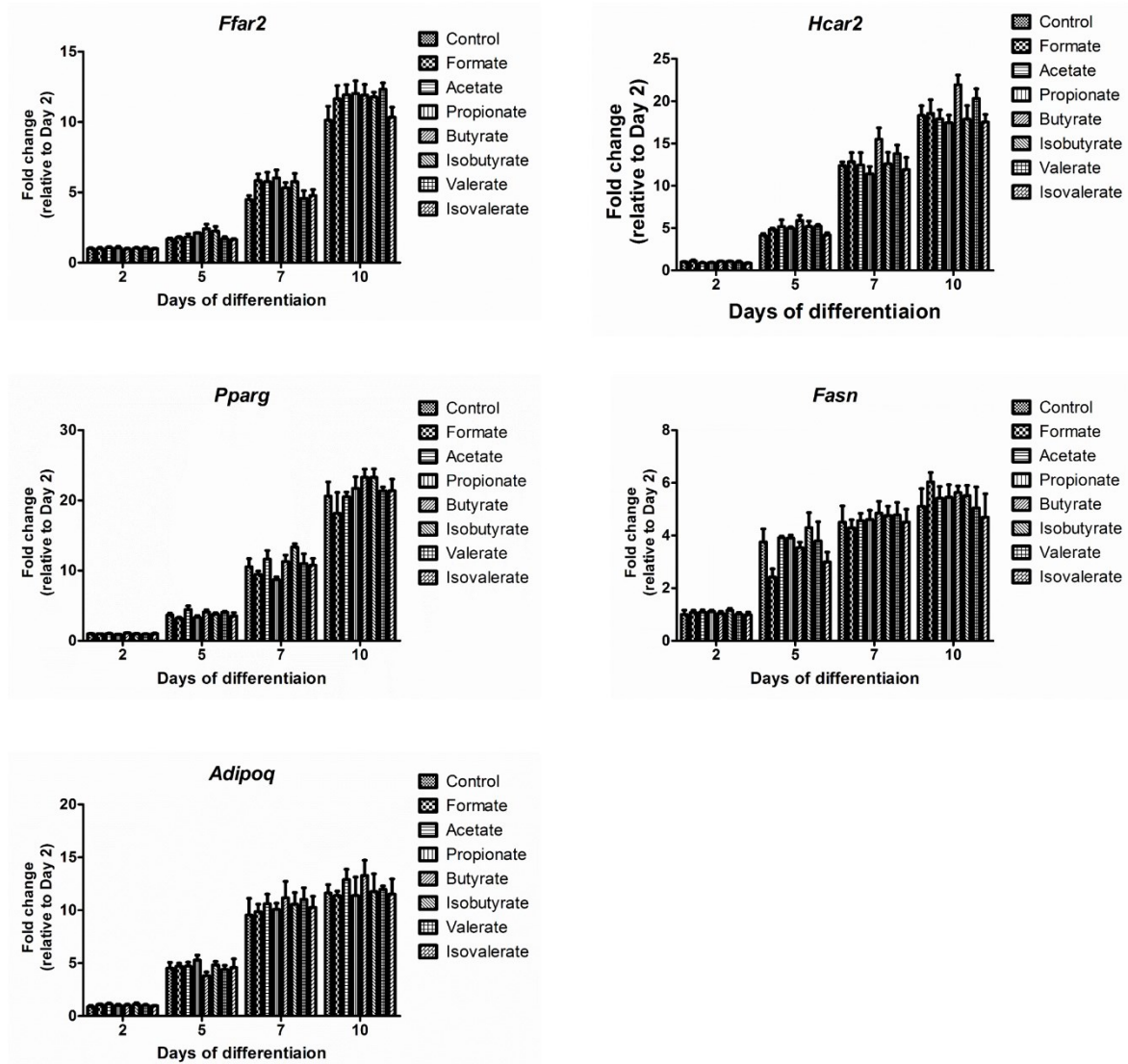


Figure S.2: RT-qPCR analysis of the gene expression during 3T3-L1 cell differentiation. The RT-qPCR results are expressed as fold change relative to control-treated group from day 2 samples.

Table S.3: *p*-values for the slope coefficient comparison between SCFAs-treated and control groups on the gene expression analysis.

	Formate	Acetate	Propionate	Butyrate	Isobutyrate	Valerate	Isovalerate
<i>Hcar2</i>	0.9335	0.9026	0.7496	0.0125	0.3869	0.0825	0.3196
<i>Fasn</i>	0.9936	0.9537	0.9347	0.7793	0.7829	0.1066	0.868

Supplementary data.

Table S.4: Minimum Essential Medium (MEM) formulation (ThermoFisher Scientific)

Components	Molecular Weight	Concentration (mg/L)	mM
Amino Acids			
L-Arginine hydrochloride	211.0	126.0	0.5971564
L-Cystine	240.0	24.0	0.1
L-Histidine hydrochloride-H ₂ O	210.0	42.0	0.2
L-Isoleucine	131.0	52.0	0.39694658
L-Leucine	131.0	52.0	0.39694658
L-Lysine hydrochloride	183.0	73.0	0.3989071
L-Methionine	149.0	15.0	0.10067114
L-Phenylalanine	165.0	32.0	0.19393939
L-Threonine	119.0	48.0	0.40336135
L-Tryptophan	204.0	10.0	0.04901961
L-Tyrosine	181.0	36.0	0.19889502
L-Valine	117.0	46.0	0.3931624
Vitamins			
Choline chloride	140.0	1.0	0.007142857
D-Calcium pantothenate	477.0	1.0	0.002096436
Folic Acid	441.0	1.0	0.0022675737
Niacinamide	122.0	1.0	0.008196721
Pyridoxal hydrochloride	204.0	1.0	0.004901961
Riboflavin	376.0	0.1	2.6595744E-4
Thiamine hydrochloride	337.0	1.0	0.002967359
i-Inositol	180.0	2.0	0.011111111
Inorganic Salts			
Calcium Chloride (CaCl ₂ -2H ₂ O)	147.0	264.0	1.7959183
Magnesium Sulfate (MgSO ₄ -7H ₂ O)	246.0	200.0	0.8130081
Potassium Chloride (KCl)	75.0	400.0	5.3333335
Sodium Bicarbonate (NaHCO ₃)	84.0	2200.0	26.190475
Sodium Chloride (NaCl)	58.0	6800.0	117.24138
Sodium Phosphate monobasic (NaH ₂ PO ₄ -2H ₂ O)	156.0	158.0	1.0128205
Other Components			
D-Glucose (Dextrose)	180.0	1000.0	5.5555553
Phenol Red	376.4	10.0	0.026567481



The microbiome and its pharmacological targets: therapeutic avenues in cardiometabolic diseases

Ana Luisa Neves¹, Julien Chilloux¹, Magali H Sarafian, Mohd Badrin Abdul Rahim, Claire L Boulangé² and Marc-Emmanuel Dumas

Consisting of trillions of non-pathogenic bacteria living in a symbiotic relationship with their mammalian host, the gut microbiota has emerged in the past decades as one of the key drivers for cardiometabolic diseases (CMD). By degrading dietary substrates, the gut microbiota produces several metabolites that bind human pharmacological targets, impact subsequent signalling networks and *in fine* modulate host's metabolism. In this review, we revisit the pharmacological relevance of four classes of gut microbial metabolites in CMD: short-chain fatty acids (SCFA), bile acids, methylamines and indoles. Unravelling the signalling mechanisms of the microbial–mammalian metabolic axis adds one more layer of complexity to the physiopathology of CMD and opens new avenues for the development of microbiota-based pharmacological therapies.

Address

Division of Computational and Systems Medicine, Department of Surgery and Cancer, Imperial College London, Exhibition Road, London SW7 2AZ, UK

Corresponding author: Dumas, Marc-Emmanuel (m.dumas@imperial.ac.uk)

¹ These authors contributed equally to this review.

² Current address: Metabotrix Ltd, Bio-incubator, Prince Consort Road, South Kensington, London SW7 2BP, UK.

Chemical compounds studied in this article

Acetate (PubChem CID: 176) Butyrate (PubChem CID: 264) Cholic acid (PubChem CID: 221493) Chenodeoxycholic acid (PubChem CID: 10133) Deoxycholic acid (PubChem CID: 222528) Indole-3-propionate (PubChem CID: 3744) 3-Indoxylsulfate (PubChem CID: 10258) Propionate (PubChem CID: 1032) Trimethylamine (PubChem CID: 1146) Trimethylamine-N-oxide (PubChem CID: 1145)

Current Opinion in Pharmacology 2015, **25**:36–44

This review comes from a themed issue on **Endocrine and metabolic diseases**

Edited by **Kevin G Murphy**

For a complete overview see the [Issue](#) and the [Editorial](#)

Available online 28th October 2015

<http://dx.doi.org/10.1016/j.coph.2015.09.013>

1471-4892/© 2015 Elsevier Ltd. All rights reserved.

Introduction

Cardiometabolic diseases (CMD) present a complex array of interrelated risk factors affecting more than one billion

people with a dramatic impact on mortality, morbidity and quality of life [1]. These factors (including impaired glucose tolerance, dyslipidemia, arterial hypertension, insulin resistance and central obesity) are epidemiologically clustered — the presence of at least three of five of these symptoms corresponding to the 'metabolic syndrome' clinical diagnosis [1]. Although many pharmacological mechanisms have been suggested, the underlying causes of CMD and its potential therapeutic avenues remain to be fully explored. With the advent of high-throughput methodologies (metagenomics, metabolomics), the gut microbiome emerged as one of the key drivers for CMD [2]. The gut ecosystem, as well as its individual members, was shown to contribute to the host metabolism [3*]. A lower bacterial gene count (LGC) is associated to increased adiposity, insulin resistance and dyslipidemia [4**] and dietary intervention can improve both bacterial gene richness and clinical metabolic outcomes [5**]. Patients with type 2 diabetes (T2D) also show specific compositional and functional changes in their metagenomes [6**].

With the increasing number of clinical studies reporting associations between the composition of the gut microbiota and CMD outcomes, one question arises — how are these changes in microbial ecology translated into pharmacological messages to the mammalian host? Consisting of trillions of non-pathogenic bacteria living in a symbiotic relationship with their host, gut microbiota produces several signalling molecules (e.g., LPS, peptidoglycans, but also metabolites) that bind host proteins and impact signalling networks, therefore playing a central role as chemical messengers in the microbial–mammalian crosstalk [7]. The identification of the pharmacological targets and signalling pathways of these metabolites is key to a better understanding the molecular crosstalk supporting the microbial–mammalian metabolic axis — and provides a suitable framework for the discovery of the mechanistic basis of these associations. In this context, fine mapping of the microbial signalling metabolome and its host molecular targets opens up novel pharmacological avenues for microbiome interventions.

The microbiome interacts with its host through microbial metabolites

In this review, we shall present four classes of gut microbial metabolites impacting host molecular mechanisms